INTERNATIONAL CENTER FOR AGGREGATES RESEARCH

ICAR

AN EVALUATION OF AUTOMATED DEVICES TO REPLACE AND AUGMENT MANUAL SIEVE ANALYSES IN DETERMINING AGGREGATE GRADATION

RESEARCH REPORT ICAR – 503-2

Sponsored by the
Aggregates Foundation
for Technology, Research and Education

Technical Report Documentation Page

1. Report No. ICAR 503-2	2. Government Accession No.	3. Recipient's Catalog No.
4. Title and Subtitle RAPID TEST TO ESTABLISH GRADING OF UNBOUND AGGREGATE PRODUCTS: An Evaluation of Automated Devices to Replace and Augment Manual Sieve Analyses in Determining Aggregate Gradation		5. Report Date February 2002 6. Performing Organization Code
7. Author(s) Alan F. Rauch, Carl T. Haas, and Craig Browne, and Hyoungkwan Kim		8. Performing Organization Report No. ICAR 503-2
9. Performing Organization Name and Address International Center for Aggregates Research The University of Texas at Austin Cockrell Hall 5.200 Austin, TX 78712-1076		10. Work Unit No. (TRAIS) 11. Contract or Grant No. Project No. ICAR-503
12. Sponsoring Agency Name and Address Aggregates Foundation for Technology, Research, and Education 1415 Elliott Place NW Washington, D.C. 20007		13. Type of Report and Period Covered Sept. 1, 1999 – Sept. 1, 2001 14. Sponsoring Agency Code
15. Supplementary Notes The final project report is Report No. ICAR 503-3		

16. ABSTRACT

Several automated devices are commercially available for measuring the gradation of unbound stone aggregates. These computerized machines, which provide a rapid alternative to manual sieving, capture and process two-dimensional digital images of aggregate particles to determine grain size distribution. Five of these automated gradation devices were evaluated for accuracy and performance. Fifteen aggregate test samples, with different size, shape, and mineral characteristics, were used in these tests. To quantify how well the machine results compare with data from standard sieve analyses, the CANWE statistic was developed and used. While the machine data did not match the sieve data exactly, the evaluated devices were found to provide good measures of particle gradation for most samples. These tests also indicate that some machines will give more repeatable results in multiple tests of a given material, while others yield better results when testing different materials. The methodology used in this study is suitable for objectively evaluating the accuracy of other rapid gradation machines for various applications.

ICAR Project 503 was undertaken to study rapid, automated methods of determining the grain size distribution of unbound aggregate products. Two technologies were studied in detail: digital image analysis and laser profiling. This report summarizes the evaluation of digital imaging devices, while the second part of the final project report describes the development of a laser scanning device for grading aggregates.

17. Key Words	18. Distribution Statement
grain size distribution, gradation, sieve analysis, digital image analysis, laboratory automation, rapid gradation test	No restrictions

19. Security Classif. (of report)	20. Security Classif. (of this page)	21. No. of pages	22. Price
Unclassified	Unclassified	146	

Form DOT F 1700.7 (8-72) Reproduction of completed page authorized

RAPID TEST TO ESTABLISH GRADING OF UNBOUND AGGREGATE PRODUCTS

An Evaluation of Automated Devices to Replace and Augment Manual Sieve Analyses in Determining Aggregate Gradation

by:

Alan F. Rauch
Carl T. Haas
Craig Browne
Hyoungkwan Kim

Department of Civil Engineering
The University of Texas at Austin
Austin, Texas

February 2002

Research Report ICAR 503-2

Research Project Number ICAR-503

Sponsored by the
Aggregates Foundation for Technology, Research, and Education

INTERNATIONAL CENTER FOR AGGREGATES RESEARCH
The University of Texas at Austin
Austin, Texas 78712
and
Texas A&M University
College Station, Texas 77843

DISCLAIMER

The contents of this report reflect the views of the authors who are responsible for the accuracy of the information presented herein. The contents do not necessarily reflect the official views of the International Center for Aggregates Research (ICAR). This report does not constitute a standard, specification, or regulation.

ACKNOWLEDGEMENTS

This is Part 1 of the final report from a study sponsored by the Aggregates Foundation for Technology, Research, and Education (AFTRE). The authors gratefully acknowledge the sponsorship of AFTRE.

This report summarizes data and conclusions from a series of evaluation tests conducted on five different test machines. The evaluation tests were greatly facilitated by the cooperation and assistance of the following individuals and organizations:

- Mr. Michael Strickland, Micromeritics Corporation, Norcross, Georgia.
- Mr. Brian Prowell, Virginia Transportation Research Council, Charlottesville, Virginia
- Mr. Delmer Dillon, John B. Long Co., Knoxville, Tennessee.
- Mr. Terry Reckart, W. S. Tyler, Mentor, Ohio.
- Dr. Dayakar Penumadu, Clarkson University, Potsdam, New York.

The assistance of Salavador Rodriguez in conducting these tests is also acknowledged.

Table of Contents

List of Tables

List of Figures

1. Introduction

1.1 Background

Engineers routinely use particle size distribution to characterize fine and coarse aggregates. Knowledge of material gradation can be beneficial for many reasons, such as helping to maintain proper mixing of aggregates and thus minimizing wasted material, ensuring that the aggregate meets specified standards for construction materials, and maximizing process efficiency by tracking changes in performance. Currently, the widely used industry standard for characterizing size distribution involves a sieving process such as that outlined in ASTM standard C 136a (ASTM 1999). However, with recent advances in technology, alternatives to the traditional sieve analysis are emerging that may expedite the grading of aggregates while offering additional characterization parameters.

Particle gradation plays a crucial role in the production of quality construction materials such as hot mix asphalt and Portland cement concrete. Recently, there has been increased emphasis on quality control and more rigorous material specifications. Some newer asphalt designs, such as the Superpave specification (Kennedy et al. 1994), specify aggregate shape parameters like flatness and elongation ratios as an additional design variable. The flatness and elongation test (ASTM D 4791) requires equipment different than that used for sieve analyses and is very time consuming and labor intensive.

Despite the relatively straightforward nature of the conventional sieve analysis, it has some drawbacks such as:

- Reduced efficiency and accuracy as the wire mesh deteriorates.
- Need for significant manual labor.
- Time consuming nature of the process, especially when frequent samples must be analyzed.
- Results are subject to human error.

- No capability to provide shape parameters.
- Square sieve openings may not yield the best measure of size for irregularly shaped particles.

In light of these problems, emerging technologies have been recently explored to develop an automated gradation process that minimizes or eliminates these and other drawbacks of the sieve analysis.

1.2 Automated Measurement of Particle Size

To conceptualize the context of an automated gradation measurement system, consider quality or process control in an aggregate production plant. Test samples can be acquired at material transfer locations, directly from a conveyor belt, or from stockpiles. For instance, crusher performance can be monitored by sampling material from the crusher discharge conveyor. Screening operations can be monitored by sampling the material produced on finished product belts.

To address the increased awareness for process control of various product parameters, more frequent samples are needed to perform timely analyses. Samples are typically acquired manually and taken to a laboratory where sieving and other analyses are performed, which provides a discrete measure of material gradation. Conversely, very frequent discrete sampling or continuous automated measurements can be implemented for on-line monitoring. Currently, on-line sampling and testing requires significant time and labor. In some cases, by the time a sieve analysis has been performed, the end product has already been mixed. In a fully automated situation, a variety of sampling techniques from belt sweep samplers to diversion chutes might be used to direct samples to a central analysis location or "grading station" (Kim et al. 2000) as depicted in Figure 1.1. In this configuration, the material stream can be monitored automatically or manually as frequently as desired. Figure 1.2 details different scanning configurations that might be used within a "grading station".

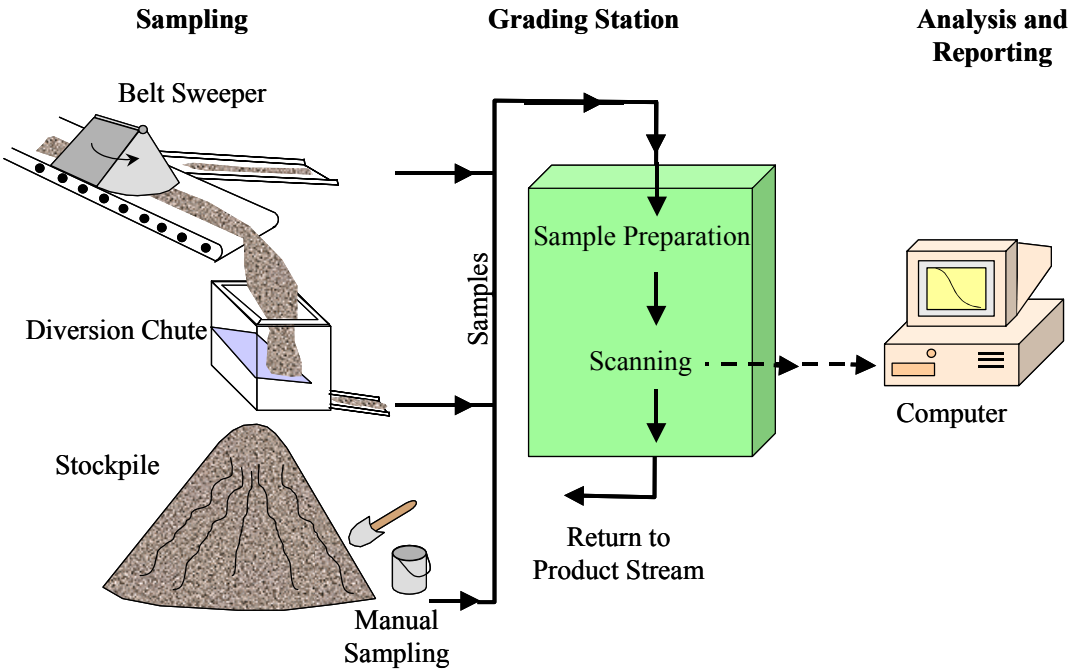

Figure 1.1 Context of "grading station" concept with different sampling schemes (from Kim et al. 2000).

Automating the gradation of aggregates offers several potential advantages over a conventional sieve analysis including:

- Accelerating the analysis to the point where real time changes in process control are feasible.
- Removing the need for human intervention to increase operator safety and avoid operator error and labor costs.
- Yielding increased precision in the measured size distribution curves (equivalent to an expanded sieve stack).
- Providing additional particle parameters such as shape and texture to complement the size distribution.

A variety of technologies could be used to construct automated machines for determining aggregate gradation. These techniques, which are briefly described below, include: automated sieve analysis, sedimentation, digital image analysis, and laser profiling.

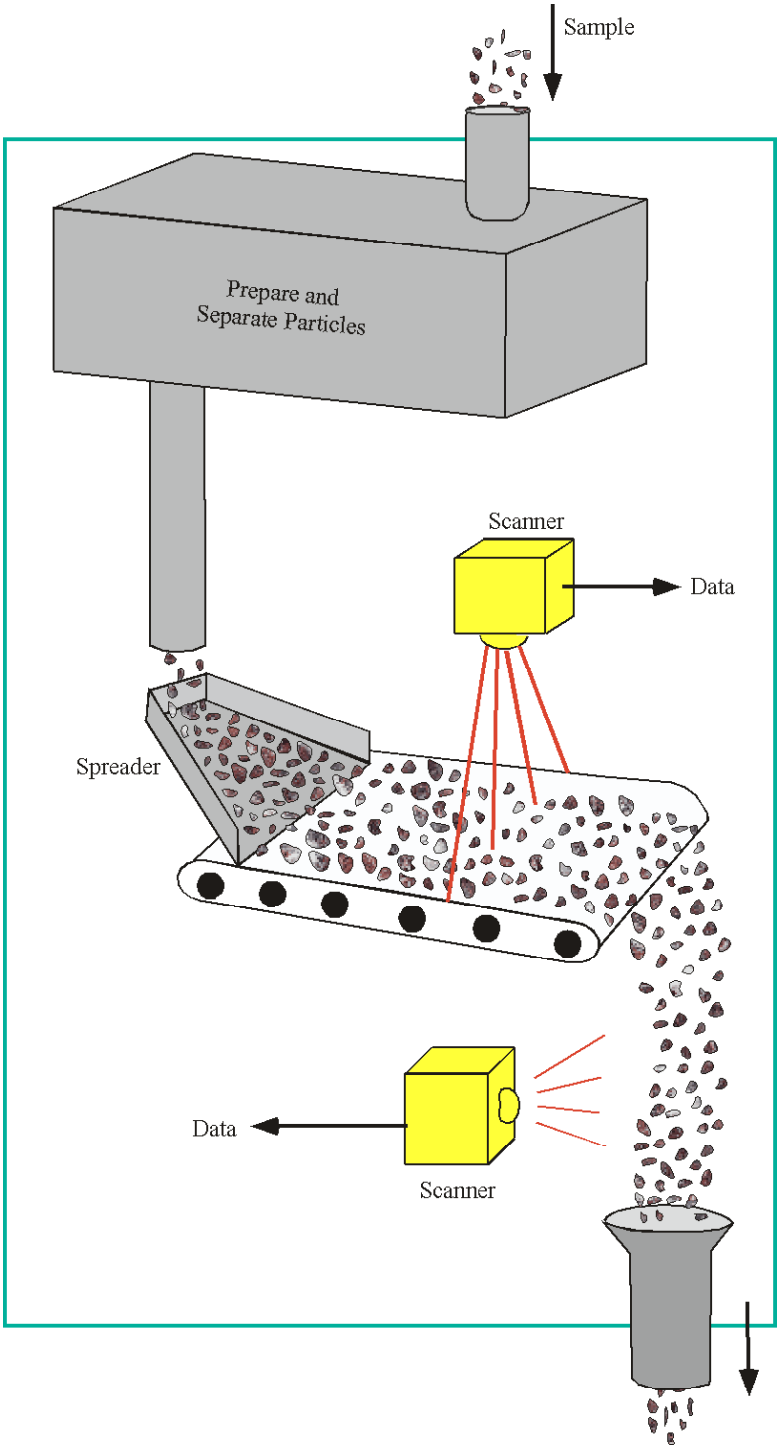

Figure 1.2 Detail of a "grading station" showing two potential scanning configurations (from Kim et al. 2000).

1.3 Technology Overview

Automated sieve analysis is the most straightforward technique as it simply performs a standard sieve test without manual intervention. From shaking of the sieve stack to weighing of the material retained on each sieve, the process is controlled by machine. The advantage to this approach is that it readily conforms to current standards for particle size distribution analysis. Automated sieve analysis is still subject to some of the limitations associated with manual analyses such as: no information on particle shape or surface texture is obtained, the technique is not well suited to continuous sampling and analysis of aggregates, and maintenance of moving parts and the sieves is a potential problem.

Sedimentation using a fractionating water column is used extensively to determine the particle size distribution of soil particles passing a No. 200 sieve. Unfortunately, hydraulic limitations prevent the accurate use of this technique for particles exceeding a size of about 2 mm. Beyond this size, particles begin to enter transitional or turbulent flow as their settling velocity yields Reynolds numbers greater than 2000. At this point, two unknowns, settling velocity and coefficient of drag, make it difficult to analytically interpret settling velocity to get particle size. The feasibility of using water sedimentation to rapidly size aggregates is discussed further in Appendix A.

Digital image analysis has recently garnered much interest, on both the research and commercial levels, as a method of rapidly assessing aggregate gradation. Kennedy and Mazzulo (1991) developed a semi-automatic image analysis sytem where the operator points to a particle on the computer monitor and its size is automatically determined. Although this technique is more accurate than a completely automated system, it is not practical in bulk analyses. Kemeny et al. (1993) used a video camera for image capture and a set of computer algorithms for processing the images. They used statistical procedures to account for fragment overlap, the two-dimensional nature of the images, and sample variability. Within the past decade, several devices using charge coupled device (CCD) cameras to capture

two-dimensional digital images of free-falling aggregate have been introduced commercially. Although this technology has made inroads towards industry acceptance, it is still in the development stages. Especially with aggregate material, the reliability of digital image analyzers has yet to be proven against conventional sieve techniques.

The most recent and perhaps most promising technology for this application is laser profiling. This method projects a laser stripe onto particles and a CCD array assigns a three-dimensional coordinate to a series of points along the stripe. Integrating the data from consecutive stripes yields a particle profile. Current work at the University of Texas at Austin is exploring the potential application of laser profiling to analyze aggregate particles. Aside from displaying encouraging gradation results, the technology has demonstrated the potential for providing shape and surface texture parameters (Kim et al. 2001).

Of the four technologies discussed, both digital image analysis and laser profiling appear to offer the greatest potential for analyzing aggregates ranging in size from the No. 200 mesh to 1.5 in (Rauch et al. 2000). As laser profiling is still in the early stages of development, digital image analysis is currently the most promising commercially available alternative to manual sieve analyses. Despite the appealing features of digital image analysis, devices incorporating this technology face three major obstacles in gaining wider industry acceptance. These include:

1. Lack of extensive performance data showing that the devices work well over a variety of aggregate material and size ranges.
2. No industry standard for aggregate gradation based on digital imaging data.
3. High initial costs.

In an effort to address issue 1, this work examines five commercially available 2D digital image-based devices. By comparing sieve data to machine generated gradation curves, the intent is to explore performance differences over a variety of different materials and particle size ranges.

1.4 Report Organization

Following this introductory section, this report is divided into five chapters. Chapter 2 provides general background on digital imaging and goes into further detail on the currently available commercial devices based on this technology. Particular attention is focused on the five devices that were evaluated in this study. Chapter 3 discusses the tests used to evaluate the devices. Information on the sample material and gradation as well as test procedures is included. Chapter 4 probes various techniques to analyze the test data. Both conventional test statistics and customized error ranking techniques are explored. Chapter 5 discusses the test results when analyzed using the test statistics described in Chapter 4. General trends and specific operational characteristics of each machine are highlighted to point out the relative merits of each implementation. Finally, Chapter 6 concludes with comments on the current state of automated particle size analysis and what the future holds for automated technology.

2. Digital Imaging-Based Technology for Characterizing Particle Size

In recent years, the rapid development, refinement, and decline in cost of charge coupled device (CCD) technology has made digital imaging analysis appealing to researchers developing automated methods for characterizing aggregate. Stemming from these research efforts, a number of digital imaging-based devices have become commercially available. Such devices are capable of performing automated operations such as gradation and shape analyses.

2.1 Digital Imaging Concept

In some fashion, all digital imaging-based devices utilize CCD cameras to analyze aggregate samples. The CCD captures two-dimensional images of particles as they are passed in front of the camera. By applying image transformation algorithms, information on particle size is obtained. To produce a gradation curve, volumetric information is also required. Unlike traditional sieve techniques, where the size fractions are based on weight, it is not possible to obtain weights when particles are imaged. Gradation curves from image analyzers thus compute size fractions based on volume. The underlying assumption is that the specific gravity of the particles is consistent across the entire sample.

All commercially available devices utilize one camera, so assumptions must be made to arrive at three-dimensional particulate information from a two-dimensional image. To more accurately characterize aggregate, researchers have developed systems employing two and even three CCD cameras. Maerz and Zhou (1999) developed a prototype imaging system that can provide particle size and shape information. Their research involved a small conveyor system to parade individual particles past two orthogonally oriented, synchronized cameras. Rao and Tutumluer's

(2000) research was similar, except that they used three orthogonal cameras to image particles. Rao and Tutumluer (2000) contend that relying on only two images could yield unacceptable errors in the determination of shape parameters. While both efforts were successful in capturing data on the three-dimensional shapes of particles, both systems were rather slow. The scanning rate was limited by the need to arrange the aggregate particles in a single line, so that a given particle could be imaged simultaneously by multiple cameras. Additional research efforts involving digital image analysis are summarized in Table 2.1.

Table 2.1 Summary of additional digital imaging research for particle size and shape analyses.

Source	Summary Points
Broyles et al. (1994)	• Employed two digital cameras and a stepped platform to simultaneously view aggregate particles from two directions at right angles from each other • Fast particle shape characterization was demonstrated, but the technique required a substantial component of human intervention to properly arrange the aggregate
Kuo et al. (1996;1998)	• Aggregates were attached to sample trays with two perpendicular faces. Two images, projections each face, of the particle were captured by rotating the sample tray 90 degrees • The width, thickness, and height were determined from the two images and provide direct measures of flatness and elongation • While providing detailed particle information, this method required significant manual involvement
Mora et al. (1998)	• Correlated imaging results based on area, rather than the more typical volume, to standard sieve analyses • Both corrected and uncorrected data compared to gradation curves from sieve results
Brzezicki et al. (1999)	• Used a special cylindrical tray with a system of parallel steps to utilize structured lighting (using shadows) to measure the three main dimensions of particles with a single camera and two light sources • Manual involvement was required to arrange particles properly on the tray prior to scanning
Maerz (1999)	• Discussed the use of high speed cameras to capture continuous material information (e.g. a stream of aggregate on a moving conveyor belt) • Presents case studies using the WipFrag II system to analyze material with particle sizes down to 1 mm
Kuo and Freeman (2000)	• Presented image indices for shape, roundness, and surface texture • Used 2D digital image analysis to determine these factors for 28 fine aggregate samples

2.2 Overview of Commercially Available Digital Imaging-Based Devices

While it is apparent that multiple camera systems can yield greater particle data than single camera setups, such systems are less practical. The equipment cost and device complexity is not justified in the current commercial market where particle size measurements are the primary concern. Indeed, the commercially available digital imaging-based devices all rely upon only a single CCD camera. In the following sections, detailed information is given on these machines. The first five units were evaluated further in this study as discussed in Chapters 3 through 5.

2.2.1 Micromeritics *OptiSizer PSDA^{TM} 5400*

The *OptiSizer* device was developed by the Danfoss-Videk company (now Videk, LLC), and is distributed in the U.S.A. by the Micromeritics Instrument Corporation. The device was initially developed for on-line applications (continuous scanning of a product stream), but can be modified for laboratory use (Strickland 2000). The *OptiSizer,* pictured in Figure 2.1, incorporates three main components. A vibrating feed system and backlight are mounted on a frame as seen to the left in Figure 2.1. A matrix CCD and processing unit, which is linked to a personal computer, are located in a sealed black box visible to the right in Figure 2.1. The test sample is placed into a feed cone that gradually deposits the material onto a vibrating channel, where it is dispersed and pushed to the end where the particles fall in front of a backlight. Manual adjustments to the vibratory feeder are made to ensure an optimum rate of particles is passing through the imaging plane. In the on-line version, a feedback loop automatically adjusts the feed rate.

The CCD camera captures two-dimensional images of groups of falling particles about twice per second. By imaging at this rate, only a fraction of the entire sample is captured and used in determining sample gradation. The *OptiSizer* device can process material from a No. 200 mesh sieve size (0.075 mm) up to at least 1.5 inch (38.1 mm). However, samples containing particles spanning this entire range

would have to be split into a fine and coarse fraction (at roughly the No. 4 sieve size) for proper analysis in two different runs through the machine. Analyses of fine aggregates (sand) are accomplished using a 3-inch feeder tray coupled with a red LED array backlight. An 8-inch vibratory feed tray and a xenon strobe backlight are used to analyze primarily coarse materials (gravel). Aside from changing the backlight and feeder for the different size ranges, the camera lens must be changed and the unit re-calibrated for optimal focus. In an on-line implementation, however, it would be feasible to have two *OptiSizer* analyzers working in tandem with the test samples split for optimal analysis over a wide size range.

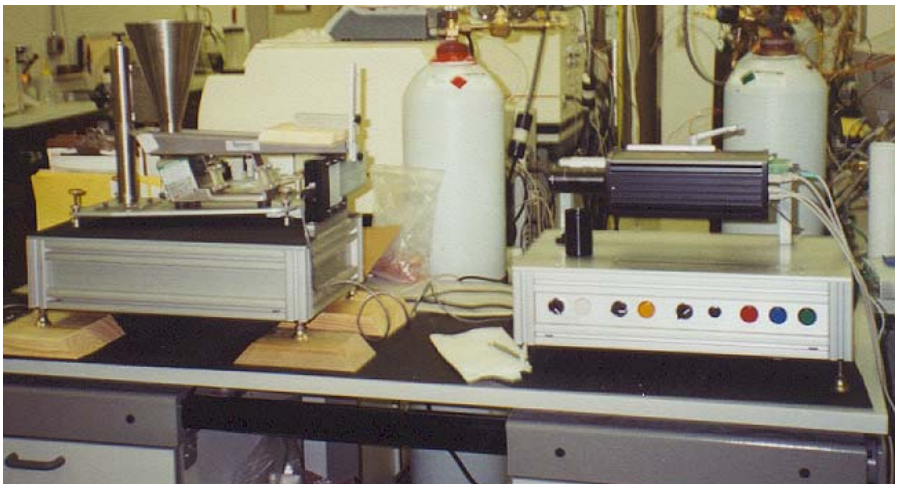

Figure 2.1 Micromeritics *OptiSizer PSDA™ 5400.*

An operator using the *OptiSizer* device can choose from a group of predefined analysis algorithms or specify a custom algorithm. During the author's *OptiSizer* evaluation, both the spherical and cubic analysis modes were utilized. In the spherical type analysis, each imaged particle profile area is converted into a circle of equivalent area. Volumetric information is then computed from the circle by taking a sphere of equivalent radius. Similarly, the cubic analysis converts particle profile area into a square of equivalent area. The volume is then computed from a cube with side dimensions equal to a side of the square (Strickland 2000).

The gradation process can be run using the setup shown in Figure 2.1 connected to a keyboard and monitor. However, in the evaluation configuration, a personal computer (PC) was also connected to the system. Data were transferred to the PC from the camera/processing unit via a serial (RS-232) connection. Using Microsoft Excel spreadsheet software, Micromeritics has developed a Visual Basic script to convert imported data into graphic and tabular report formats.

2.2.2 French LCPC *VDG-40 Videograder*

The *VDG-40* was developed by the French public works laboratory (LCPC) and is sold in the U.S.A. by Emaco. In addition to grain size, the device can simultaneously generate data on the flatness and elongation ratios for the test sample (Descantes et al. 2000; Prowell and Weingart 1999). The *VDG-40* device is pictured in Figure 2.2. The feed chute, to the right of the image, delivers aggregate onto a 5-inch wide manually controlled vibrating channel, which evenly feeds the particles onto a slowly revolving drum. The drum is designed to allow each particle to fall in an optimal orientation for imaging. The particles fall in a curtain from the drum and pass between a high intensity fluorescent backlight and a line-scan CCD camera. By merging data from successive line scans, the *VDG-40* can discern the outline of each particle in the aggregate sample. The *VDG-40* is capable of testing material ranging in size from a No. 16 mesh (1.18 mm) sieve to at least 1.5 inch (38.1 mm).

After merging individual line scans, the *VDG-40* unit goes on to perform image analyses on the resulting two-dimensional image. The longest dimension, or length, is first determined and becomes the major axis of an equivalent ellipse. The width, or greatest dimension perpendicular to the length, then becomes the minor axis of the equivalent ellipse. The width also corresponds to the size of aggregate used in computing the gradation curve. By revolving the ellipse about the major axis, an ellipsoid is created, the volume of which is assigned to the particle (Laboratoire Central des Ponts et Chaussees 1994).

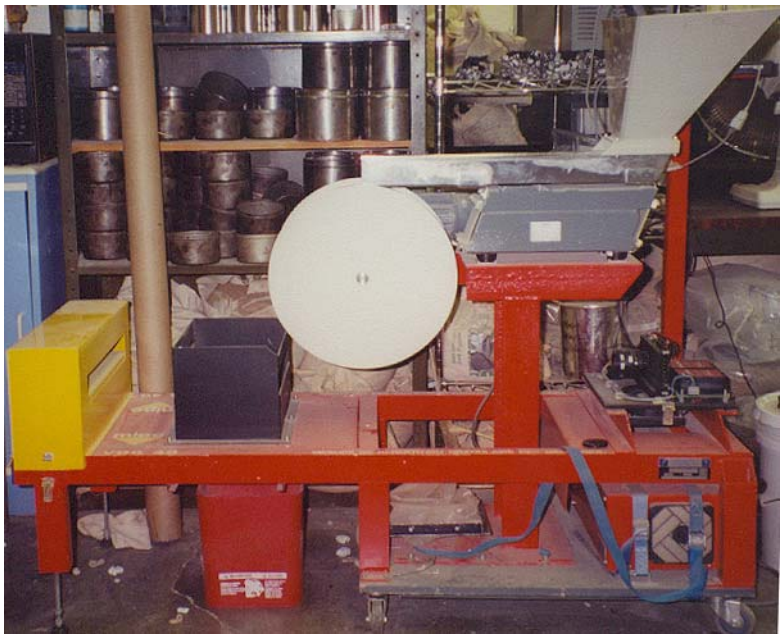

Figure 2.2 French LCPC *VDG-40 Videograder.*

The test data are acquired and analyzed on a personal computer, where a proprietary software package generates results and reports both gradation and flatness and elongation ratios.

2.2.3 John B. Long Company *Video Imaging System (VIS)*

The *Video Imaging System (VIS),* seen in Figure 2.3, was recently developed by the John B. Long Co. for on-line applications and is designed to work with the company's conveyor belt sweep samplers. The *VIS* machine is built around an adapted version of the *OptiSizer* described above. Aggregate samples are processed in the same general manner as in the *OptiSizer*, but on a much larger scale. The sample hopper can accommodate a very large quantity of aggregate that is fed onto a large vibrating chute (roughly 10 inches wide). Like the *OptiSizer*, the *VIS* system takes two-dimensional snapshots of the falling material with a matrix CCD. The images are analyzed in a fashion similar to the *OptiSizer*, expect that the transform algorithm was unknown and could not be changed in the evaluation tests. Currently, the system

has the capability to analyze particles from No. 16 mesh (1.18 mm) sieve to at least 1.5 inch (38.1 mm) (Dillon 2000).

Figure 2.3 John B. Long Company *Video Imaging System (VIS).*

The testing process is controlled via computer where a software package, implementing Microsoft Access, can generate reports. Feedback loops can be used to automatically adjust the feed rate based on the number of particles in a given image.

2.2.4 W.S. Tyler *Computerized Particle Analyzer (CPA)*

The *Computerized Particle Analyzer (CPA)* was commercially introduced in 1995 in Europe by W.S. Tyler's parent company, Haver & Boecker, and has been on the U.S. market since 1996 (Reckart 2001). The *CPA LAB* unit depicted in Figure 2.4, one of three *CPA* models available, can analyze material in the range of 0.1 mm to 12.5 mm or 0.2 mm to 36 mm, depending on the equipment settings (Tyler 2001). The *CPA 3-2* model (suited for either laboratory or on-line use) is equipped to handle

material ranging from 0.1 mm to 36 mm. The *CPA-4* is a custom unit that can be tailored to the user's needs. In past applications, the *CPA-4* has been configured to analyze material in an on-line setting up to 600 mm in size (Reckart 2001).

Tests begin with the operator filling the metal hopper, shown at the upper right of Figure 2.4, with a sample. The 3-inch vibratory feeder then evenly distributes the sample and transports it to the edge where it falls off in a curtain between the imaging device and backlight. Like the *VDG-40*, the *CPA* uses a line-scan CCD camera to image every particle in the sample as it falls in front of a backlight. The *CPA* line scan camera has a resolution of 2048 pixels (Reckart 2001).

Figure 2.4 W.S. Tyler *Computerized Particle Analyzer (CPA).*

The imaged particles can be processed in one of two ways. The size method takes the largest chord of a particle as its diameter. In the shape method, the perimeter of a particle becomes a circle of equivalent circumference (Reckart 2001). The diameter of this circle then becomes the particle size diameter. Results are then compiled by percent particle count for each of the specified size fractions. A generic correlation factor is then applied to give an approximate size distribution in terms of

percent volume for each size fraction. Ideally, a customized correlation is applied to the results to achieve a more accurate gradation for a given material.

All analysis and data reporting are performed in a custom software package. In addition to particle size information, the CPA software can compute various shape parameters including length to width ratios, maximum cut, and so on.

2.2.5 Buffalo Wire Works *Particle Size Distribution Analyzer (PSDA)*

Sponsored by Buffalo Wire Works Co., researchers at Clarkson University have developed the *Particle Size Distribution Analyzer (PSDA),* which is pictured in Figure 2.5. Like the devices described above, the *PSDA* uses a vibratory feeder to create a curtain of backlit, falling particles for imaging with a matrix CCD camera. Unlike the other systems, the *PSDA* uses a progressive scan CCD camera, with a resolution of 640 by 480 pixels, to achieve better clarity in the image of the falling particle (Penumadu 2001). A progressive scan camera captures a more accurate image of a falling particle since it scans every line sequentially. In an ordinary matrix-scan camera, the odd lines (or every other line) are scanned in the first pass and the even lines are scanned during the second pass. While the ordinary scanning method works adequately for static imaging, it introduces error when imaging falling particles. Like the *OptiSizer* and *VIS* units, the *PSDA* does not capture an image of every particle in the sample.

A distinct feature of the PSDA is the capability to automatically adjust the camera focus and optimize the backlight intensity based on pre-specified settings for different particle size ranges. The device is capable of analyzing particles ranging from the No. 200 sieve (0.075 mm) to at least 1.5 inch (38.1 mm). Like the *OptiSizer*, separate vibratory feed systems and backlights are required to scan fine and coarse samples. The machine has a dynamic range of roughly 12 times, meaning an accurate gradation could be determined for a sample containing material ranging from the No. 200 sieve size (0.075mm) up to roughly 0.9 mm (Penumadu 2001). If a sample exceeds this dynamic range (say the No. 200 to No. 4 sieve), it must be split

and run through the machine twice to determine a complete gradation.

Figure 2.5 Buffalo Wire Works *Particle Size Distribution Analyzer (PSDA).*

Once samples have been placed in the vibratory feeder, a PC controls the operation. One feature unique to this device is a convergence function that will automatically stop a test once sufficient data has been acquired to define a statistically correct gradation (Penumadu 2001). The *PSDA* device can also generate two-dimensional shape information including the shape factor defined by Kuo et al. (2000). Gradation and shape results are generated and reported using proprietary software.

2.2.6 Other Commercial Imaging Devices

At least three other digital imaging-based gradation units are commercially available, but were not evaluated in this study.

Scientific Industrial Automation Pty. Ltd., an Australian company, sells a device called the *Particle Parameter Measurement System (PPMS),* which is shown in Figure 2.6. Intended for on-line industrial applications, the *PPMS* is capable of analyzing particles from 1 to 100 mm (Bourke et al. 1997). However, a recent study

has shown the device has the ability, when properly configured, to measure fine material down to a No. 200 mesh (0.075 mm) sieve (Dumitru et al. 2000).

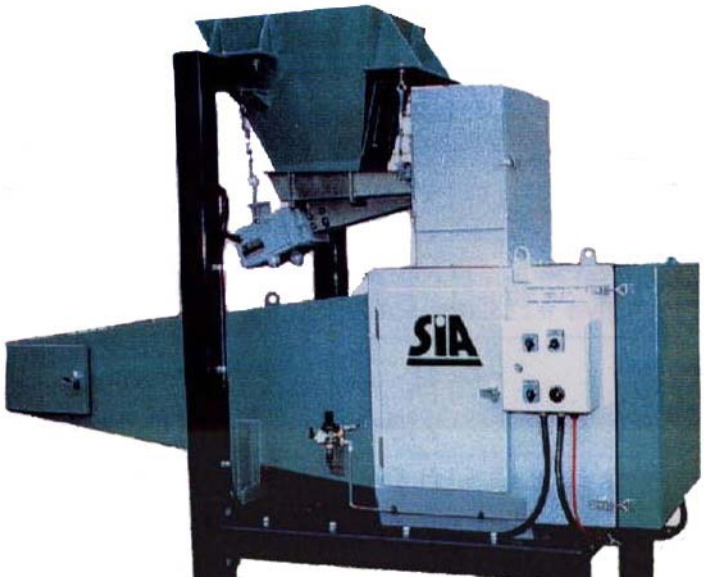

Figure 2.6 Scientific Industrial Automation *Particle Parameter Measurement System (PPMS)* (After Dumitru et al. 2000).

The *WipFrag* system, sold by WipWare Inc. (WipWare 2001), is designed to determine particle gradation from surface images of an aggregate pile, such as that produced from rock blasting. The *WipFrag System II* can employ up to 8 separate cameras at various locations along a conveyor belt to provide continuous analysis of the aggregate stream (WipWare 2001).

Split-Online® is a system similar to *WipFrag,* sold by Split Engineering LLC (Split 2001). It is designed to operate continuously, acquiring data from one or more distributed cameras, to monitor rock fragment size distribution (Split 2001).

3. Evaluation Tests of Automated Gradation Devices

To establish the validity of a new testing technology, the results must compare favorably with traditional testing techniques. In the evaluations presented here, results from the five automated digital imaging-based devices were compared to results obtained from standard sieve analyses (ASTM C 136a 1999) on a collection of samples spanning a range of sizes and material properties.

3.1 Sample Specifics

In order to present a diverse assortment of aggregates with different properties for the evaluation tests, a variety of aggregate sources were considered. Different materials were desired to represent an assortment of form (due to manufacturing process and source) as well as texture and color (inherent to mineralogy). Ideally, the same exact samples would be used in evaluating each device so that the highest consistency across tests could be obtained. Thus, aggregate materials that were resistant to breakdown over repeated testing were required.

Considering all requirements, the aggregate sources listed in Table 3.1 were chosen. Sample images of each aggregate source are given in Figures 3.1 and 3.2. From the five different sources, fifteen samples were prepared to six different gradations. The sample designations and details are given in Tables 3.2 and 3.3, respectively. These samples were obtained by sieving larger samples into distinct size ranges, then re-mixing to achieve the desired gradation. Sample weights were based on ASTM recommendations given in sieve standard C 136a (ASTM 1999).

Eight samples span the size range from No. 8 mesh to 1 inch. The four C-STD samples meet the criteria in the widely used AASHTO #57 specification (AASHTO M43 1995). The four C-SM samples have the same range in size, but

have a greater percentage of smaller particles and do not meet the AASHTO #57 specification on the No. 8 sieve size. Representing over half of the sample collection, the rationale for emphasizing this size range is that it is commonly produced by aggregate quarries and particularly for concrete production. In addition, by utilizing a standard specification to characterize these samples, a simple measure of test result quality can be taken. For instance, if a standard sieve determines a particular sample meets the specification, but the automated gradation unit does not, then there is a potential problem. Moreover, by analyzing results of four different sample materials while maintaining the same gradation, the significance of particle form, texture, and color on gradation results can be studied.

Table 3.1 Description of aggregate materials used to formulate test samples.

Aggregate Designation	Material Type	Particle Description	Source
CA	Granite	Angular, medium gray, white and black particles	Granite Rock - Wilson Quarry Aromas, California
GA	Granite	Light to dark gray angular sand	Vulcan Materials - Norcross Quarry Norcross, Georgia
TX	Natural River Gravel	Both rounded and angular particles of various minerals and colors	Capitol Aggregates - Bolm Road Plant Austin, Texas
VA	Traprock	Angular, dark gray diabase	Vulcan Materials - Manassas Quarry Manassas, Virginia
SD	Quartzite	Angular, very light red particles	L.G. Everist, Inc. Dell Rapids, South Dakota

Figure 3.1 Images of the three fine sample source materials.

Figure 3.2 Images of the four coarse sample source materials.

Table 3.2 Terminology used in gradation designations.

Designation	Description
C	Sample is primarily composed of coarse material (≥ No. 4 mesh)
F	Sample contains all fine material (< No. 4 mesh)
FTC	Samples contain a mix of both fine and coarse material
STD	Standard gradation
SM	Standard gradation weighted with smaller particles
LG	Sample includes larger particles up to 1.5 in
RND	Sample includes predominantly rounded particles up to 1.5 in

Table 3.3 Gradation of test samples.

Gradation Designation		C-STD	C-SM	C-LG	C-RND	FTC	F-STD
Material Source(s)		CA, SD, TX, VA	CA, SD, TX, VA	TX	TX	TX, VA	GA, TX, VA
Sample Mass (Kg)		6	6	15	15	2	0.5
US Stnd. Sieve	Opening Size (mm)	Percent Retained					
1.25 in	31.8	0.0	0.0	6.67	6.67	0.0	0.0
1 in	25.4	0.0	0.0	20.0	20.0	0.0	0.0
3/4 in	19.1	16.7	10.0	26.7	26.7	0.0	0.0
1/2 in	12.7	51.6	33.3	26.7	26.7	5.00	0.0
3/8 in	9.53	20.0	25.0	10.0	10.0	15.0	0.0
No. 4	4.75	10.0	25.0	6.67	6.67	30.0	0.0
No. 8	2.36	1.67	6.67	3.33	3.33	30.0	10.0
No. 16	1.18	0.0	0.0	0.0	0.0	20.0	20.0
No. 30	0.6	0.0	0.0	0.0	0.0	0.0	25.0
No. 50	0.3	0.0	0.0	0.0	0.0	0.0	25.0
No. 100	0.15	0.0	0.0	0.0	0.0	0.0	15.0
No. 200	0.075	0.0	0.0	0.0	0.0	0.0	5.0

The C-LG and C-RND samples contain larger particles, with a size range from the No. 8 to 1.5 in sieve sizes, and were selected to evaluate machine accuracy for materials with relatively large particles. Additionally, these samples serve to test the range over which the devices can accurately grade an aggregate sample. With identical gradations, the C-LG and C-RND samples consist of relatively angular and well-rounded particles, respectively. By using the same gradation and material source, the single effect of particle form on device results can be evaluated.

The two FTC samples were selected to test machine accuracy at a lower particle size of 1 mm. This type of sample is what may be found in a laboratory setting where a wide range of particle sizes might be tested. The FTC gradation provides insight into how well a device can simultaneously characterize both fine and coarse particles.

Finally, the three F-STD samples are uniformly graded particles meant to test the ability of some machines to analyze material down to a No. 200 sieve. Certain devices were unable to characterize aggregate smaller than 1 mm, which is the basis

for the FTC gradation lower limit. Devices that were capable of testing sub 1 mm size particles were included in the portion of the study involving the F-STD samples.

3.2 Testing Protocol

The author and an assistant conducted the evaluation tests by transporting the fifteen test samples to five laboratories around the country where the devices were available. The *OptiSizer*, *VIS*, and *CPA* were tested in the manufacturers' laboratories in Atlanta, Georgia, Knoxville, Tennessee, and Mentor, Ohio, respectively. The *VDG-40* was tested at the Virginia Transportation Research Council laboratory in Charlottesville, Virginia, while the *PSDA* was evaluated at Clarkson University in Potsdam, New York. The tests were conducted in July 2000 (OptiSizer, VIS, VDG-40) and January 2001 (CPA and PSDA).

At each location, the operator was given the test samples and asked to analyze them without prior knowledge of the grain size distribution or the opportunity to adjust any machine settings. Material-specific calibrations were not used. The samples were run through each device twice, unless a problem required a repeated run. One exception should be noted for the *PSDA* device. Due to optical limitations when analyzing the F-STD samples, the sample was first split at the No. 40 sieve and then each portion was run separately through the device. Only one complete test run on the *PSDA*, a composite of the two split portions, is reported for the F-STD samples.

Data from each device was collected either electronically or as report printouts for further analysis. Between tests with the different devices, the test samples, excluding the F-STD gradation, were sieved and re-mixed by hand to ensure the gradation met the sample specifications set forth in Table 3.2. Because of the inconvenience associated with re-sieving the F-STD samples between tests, entirely new samples (previously mixed to the target gradation) were used in the evaluations of each device.

4. Methodologies to Characterize Accuracy in Machine Evaluation Tests

Several statistical tools were considered to evaluate the device results. Aside from more conventional techniques, such as the Chi-square test statistic and average errors, some customized and less traditional methods were examined. Among the additional statistical tools considered was a Bayesian Approach (Ang 1975). This flexible technique has been used in several different applications and can be adapted for the evaluation of gradation results. The Bayesian Approach, detailed in Appendix B, is particularly useful when evaluating device results for a benchmark sieve that meets a given specification. While providing a comprehensive statistical analysis, the Bayesian Approach is rather complex and presents some challenging issues. The Bayesian approach was thus applied to only part of the test data, as described in Appendix B.

4.1 Introduction

A number of comparison tests were conducted wherein selected aggregate samples were processed through five different automated gradation machines. The test machines and samples are described in Chapters 2 and 3, respectively. The objective of these tests was to evaluate the accuracy of these machines, in comparison to conventional sieve analyses, in measuring the grain size distribution of the aggregate test samples.

In Figure 4.1, typical data from one of these tests is plotted as the cumulative distribution of percent passing by weight versus the logarithm of sieve opening size. Data from both a standard sieve test and the automated test machine are plotted here for comparison. While gradation data is conventionally plotted as a cumulative

distribution like that in Figure 1, it is easier to evaluate trends if the data is plotted as a histogram. Accordingly, the test data in Figure 1 are re-plotted in Figure 4.2 as a histogram, which more clearly shows the percentage of material retained within each specific size range.

Here, machine performance will be judged based on how well the automated test results compare with a standard sieve analysis over the full range of grain size in a given sample. The results from an ASTM C 136a standard sieve analysis (ASTM 1999) will be considered as the benchmark for this comparison. To objectively characterize the relative accuracy of the different rapid gradation analyzers, a method of quantifying the machine errors is needed. A machine that yields excellent accuracy will produce a close match (smaller error) between the histograms as plotted in Figure 4.2. Three different statistical measures of this error will be used to make these comparisons.

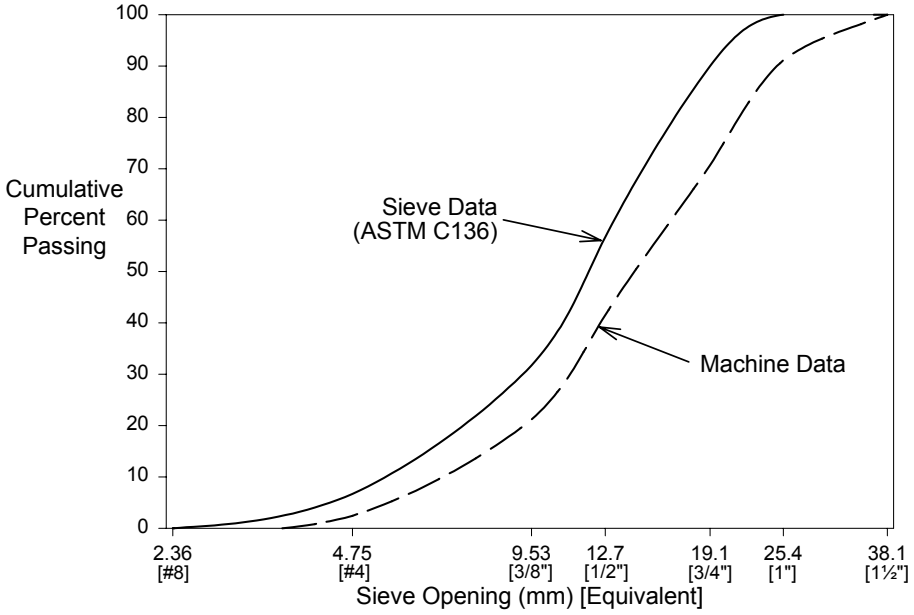

Figure 4.1 Example of test data plotted as cumulative percent passing.

Figure 4.3 shows hypothetical histograms comparing the data obtained from a rapid gradation machine with the benchmark sieve data. Each bar in the histogram is called a "bin". For the sieve data, the width of a bin represents the difference in the size of the mesh openings between adjacent sieves used in the stack. The height of a bin represents the percentage of material that passed the coarser sieve, but was

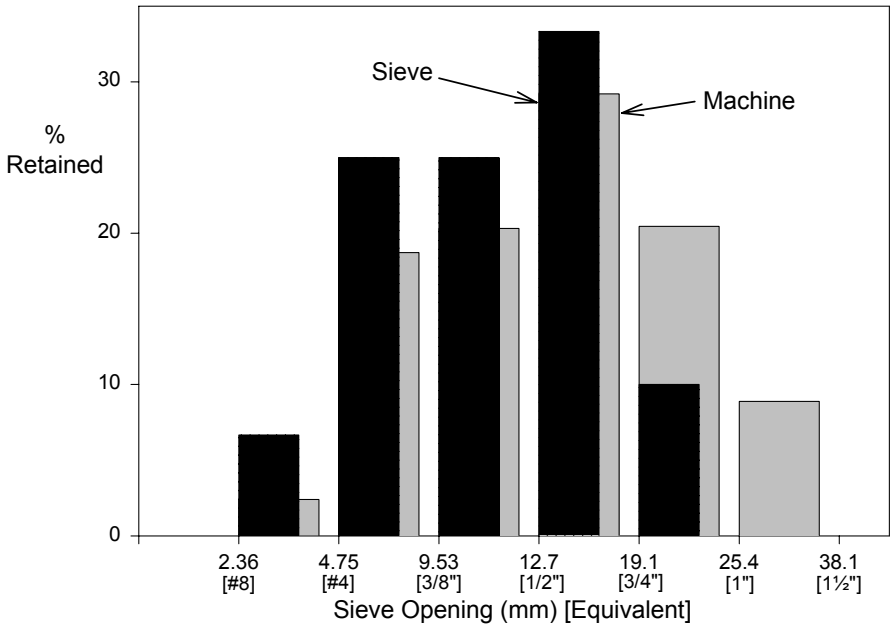

Figure 4.2 Example of test data plotted by individual percent retained.

retained on the finer sieve size, thereby defining the limits of the bin. The following symbols, indicated on Figure 4.3, are used in the discussions of various error statistics to follow:

N = number of bins or size groupings used in the analysis. For example, if a stack of five sieves are used in a conventional test, plus the pan used to retain any material passing the finest sieve, then N = 5 + 1 = 6.

For each bin in the histogram, the following are defined as indicated in Figure 4.3:

f_s = percent retained in the bin, as measured in the benchmark sieve test

f_m = percent retained in the bin, as measured by rapid gradation machine

n = equivalent number of uniform-sized particles in the bin

d_{min} = smallest sieve opening size corresponding to the lower limit of the bin

d_{max} = largest sieve opening size corresponding to the upper limit of the bin

d_{med} = median sieve opening size in the bin = $(d_{min} + d_{max})/2$

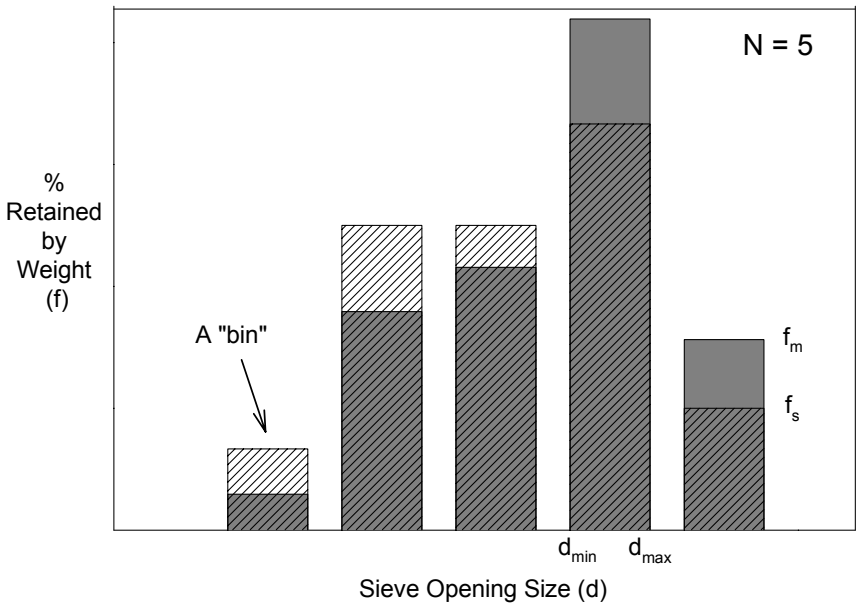

Figure 4.3 Illustration of terms used in characterizing device error.

Note that sieve test (benchmark) data are expressed in terms of percent retained by weight, but all of the automated devices tested actually measure the percent retained by volume. If one assumes that all particles in the sample have the same density, these two definitions are equivalent. However, given that aggregates are often comprised of rock fragments of varying mineral content, this assumption is not generally correct. While this introduces another source of error, the analysis that follows will assume that the machine results are equal to percent retained by weight, based on the assumption of a uniform particle density.

4.2 Chi-square (χ^2) Statistic

The Chi-square (χ^2) statistical test is commonly used to compare distributions of discrete data and can be applied to compare the gradation data as plotted in Figure 4.2. Chi-square is defined in the following manner:

$$\chi^2 = \sum_{i=1}^{N} \frac{(f_m - f_s)_i^2}{f_s} \tag{4-1}$$

Because a theoretical distribution for χ^2 is available, one can use the computed value of χ^2 to make probabilistic evaluations of machine quality. For example, based on the computed value of χ^2, one might be able to conclude that a given machine accurately characterized the sample gradation to within a 92% confidence level.

The major obstacle to the use of χ^2 occurs when a sieve test shows no particles in a given size range, but the automated machine incorrectly reports material in the same size range. That is, a problem arises if $f_m > 0$ for a given bin where the sieve test indicates $f_s = 0$. If any bin has $f_m > 0$ and $f_s = 0$, χ^2 becomes undefined. This problem appears frequently in the data to be analyzed, such as the data plotted in Figure 4.2 where $f_s = 0$ for the material retained on the 1 inch mesh sieve.

Another undesirable feature of the χ^2 statistic is that equal weight is given to the errors in all bin sizes. That is, the error in the 25.4 to 38.1 mm range is weighted equally in computing χ^2 as the error in the 1.18 to 2.38 mm size range, even though many more of the smaller particles might exist. Indeed, the value of χ^2 will depend on how the particle size data are grouped into bins. Despite these objections, χ^2 will be used in the analyses to follow as one measure of data accuracy.

4.3 Mean Error Statistic

It appears that no other commonly used statistic will give a satisfactory measure of quality for these data comparisons. Hence, new test statistics will be

defined to better quantify the accuracy of the rapid gradation machines with respect to standard sieve analyses.

Note that the χ^2 statistic is based on the square of the errors in each bin: $(f_m - f_m)^2$. Using the square of the errors eliminates a problem associated with using merely the errors, which have positive and negative values that would tend to cancel out in a simple summation. An alternative approach is to use the absolute value of the errors: $|f_m - f_m|$. This has the advantage of yielding an error statistic in the same units as the measurement (here, percent retained), instead of the square of the value.

In the simplest form, one could use a summation of the absolute value of the errors. Such a statistic would be defined for all bins even if f_s or f_m were zero, thereby avoiding the problem associated with χ^2. However, the computed error statistic would depend on the number of bins used in the analysis, indicating greater "error" when more bins (or sieves) are used. Hence, it is necessary to normalize the error statistic with respect to N, which gives the mean error (*MeanErr*) defined as:

$$MeanErr = \frac{\sum_{i=1}^{N} |f_m - f_s|_i}{N} \tag{4-2}$$

Despite its simplicity, the mean error statistic has an obvious deficiency. Like the χ^2 statistic, mean error gives equal weight to the errors associated with each bin, regardless of size range. In other words, a 5% error on the 1-inch sieve contributes the same weight to the value of *MeanErr* as 5% error on the No. 16 sieve. Depending on the application, measurement errors on the larger particles may be more or less important than the same relative errors at the smaller size ranges.

4.4 CANWE Statistic

In this section, a new test statistic is defined for characterizing the accuracy of a rapid gradation machine with respect to a standard sieve analysis. The statistic is developed based on the assumption that a weighted mean of the errors observed

across the full range of the sample particle size will give a better indication of data quality. That is, a meaningful and powerful measure of data quality can be obtained by defining a normalized, weighted error of the general form:

$$Err = \frac{\sum_{i=1}^{N} \left(\left| f_m - f_s \right|_i \cdot W_i \right)}{\sum_{i=1}^{N} W_i} \tag{4-3}$$

where W_i is a weighting factor that can be defined in a number of alternative ways, as discussed below.

The key is to now define a rational weighting factor for judging the performance of a rapid gradation machine. One problem in selecting the basis for the weights to use in Equation 4-3 is that these quantities may be determined differently in a machine or sieve test. For example, the weight of material in each bin is measured directly in a sieve test, but the automated machines actually determine the volume of the particles in a given bin. Also, while the machines might give a direct count of the number of particles analyzed in each bin, no such count is obtained in a sieve analysis.

4.4.1 Weighting factor based on bin size

An obvious choice to use in defining the weighting factor is to consider the range in particle size represented by a given bin. In equation form, the weighting factor for use in Equation 4-3 is then expressed as:

$$W_i = (d_{\max} - d_{\min})_i \tag{4-4}$$

where d_{max} - d_{min} represents the range in particle size for bin *i*. The idea is to give more weight to a 5% error in a bin representing particles from ¾ to 1 inch (span of 6.4 mm) than to a 5% error in the narrower range of a No. 16 to No. 8 mesh size

(span of 1.19 mm). As such, this formulation overcomes the problems associated with χ^2 and *MeanErr* as pointed out above.

The use of a weighting factor based on bin size will have some effects on the computed error statistic that are less obvious. First, in doing a conventional sieve test, the sieves used in the stack are generally selected to give a fairly uniform spacing in terms of the logarithm of mesh opening. Hence, the bins associated with this analysis tend to be wider for the larger particle sizes and more weight will therefore be placed on errors at the larger end of the gradation curve. This then may cause two side effects:

1. Because the resolution of the automated machines is usually some fixed value, larger relative errors will occur when sizing the smaller particles. For example, if the resolution is 0.25 mm, there will be approximately a 25% error on No. 16 mesh (1.19 mm) material, but only around 1.3% error for ¾ in (19.1 mm) material. Because errors in sizing larger particles will tend to get more weight, this effect will tend to cancel out. Thus, a weighting scheme based on bin size will tend to mask the effect of resolution error on grading smaller particles.
2. It has been shown that particle shape significantly influences standard sieve results (Fernlund 1997). In particular, as particle size increases, the effect of form also takes on greater significance. Thus, since these devices are approximating 3D shape based on 2D images, the errors inherent to their assumptions will be magnified as size increases. Thus, by increasing error weight with particle size, we should highlight the performance of the computational algorithm that transforms 2D images into 3D information and ultimately a sieve result.

4.4.2 Weighting factor based on the number of particles

Another weighting technique involves a weight factor based on the number of particles analyzed, regardless of size. In this scheme, the error associated with the measured percent retained for smaller particle sizes is given equal weight with that

associated with larger particles. From a statistical standpoint, one can expect that as the number of analyzed particles increases, the machine will tend to give a result that is closer to the overall sample gradation. This scheme gives more weight to errors associated with the measurement of more particles.

While an automated gradation device could be programmed to report the number of particles analyzed in each bin size, most commercial machines do not report this information. Hence, to define the desired weighting factors, an approximation of the number of particles analyzed must be used. To do this, the aggregate particles in each bin are approximated as spheres of uniform diameter equal to the median mesh size of each bin (d_{med}). The weighting factor is then derived by equating expressions for the mass of material in a given bin:

$$f_m \cdot Wt_{sample} = n \cdot \gamma_{particle} \cdot Vol_{particle} = n \cdot \gamma_{particle} \cdot \left[\frac{\pi}{8} (d_{med})^3 \right] \tag{4-5}$$

where Wt_{sample} is the total weight of the aggregate sample analyzed and $\gamma_{particle}$ is the average unit weight of the aggregate particles. Based on the assumption of uniform spherical particles in each size range, the number of particles scanned in each bin (n) is then approximately:

$$n = \frac{f_m}{(d_{med})^3} \cdot \frac{8 \cdot Wt_{sample}}{\pi \cdot \gamma_{particle}} \tag{4-6}$$

Hence, the number of particles in a given bin size will be approximately proportional to the fraction of material retained in that bin divided by the cube of the median grain size (n is proportional to f_m/d_{med}^3). That is, a weighting factor representing the number of particles in each bin could be computed as:

$$W_i = \left(\frac{f_m}{d_{med}^{\ 3}} \right)_i \tag{4-7}$$

Consider how error weighting by particle count would characterize the results in Figure 4.2. Particles in the 1 in range will be weighted less than an equivalent error in the No. 8 mesh sieve range. Since a few particles of large size may represent a significant percentage of the material in a given bin, it may take only a few erroneously categorized particles to significantly affect the machine-generated distribution. Comparatively, to achieve an equivalent error in the smaller size bins, significantly more particles would have to be incorrectly categorized. With the number of particles used as a weighting factor, a greater penalty is assessed for machine errors in the bins containing greater numbers of particles.

4.4.3 Other weighting schemes.

When evaluating the performance of aggregate materials, various weighting factors could be defined to represent the net mass, volume, or surface area of particles in a given bin. Weighting factors of this type might be defined as:

$$W_i = f_{mi} \cdot (\text{net mass of all particles in the test sample}) \quad (4\text{-}8)$$

$$W_i = f_{mi} \cdot (\text{net volume of all particles in the test sample}) \quad (4\text{-}9)$$

$$W_i = f_{mi} \cdot (\text{net surface area of all particles in the test sample}) \quad (4\text{-}10)$$

The net mass, volume, and surface area of the particles in the test sample are not readily available from typical rapid gradation test results, although a rapid gradation device could be configured to produce estimates of these quantities. However, each of the weighting factors (Equations 4-8 to 4-10) could be correlated to the number of particles in a given bin times a representative size of the particles in that bin. That is:

$$W_i = n \cdot (\text{representative size}) \quad (4\text{-}11)$$

Equation 4-11 suggests the form of another weighting factor, represented by a combination of the weighting factors defined earlier in Equations 4 and 7:

$$W_i = \left(\frac{f_m}{d_{med}^{\ 3}} \right)_i \cdot (d_{\max} - d_{\min})_i \quad (4\text{-}12)$$

As pointed out earlier, weighting the error statistic based on bin size alone (Equation 4-4) will tend to give more weight to errors in the larger size ranges, where the difference in opening size ($d_{max} - d_{min}$) tends to be larger. On the other hand, weighting based on particle counts in each bin (Equation 4-7) tends to give more weight to errors in the smaller size ranges. Multiplying the two weighting factors, as indicated in Equation 4-12, will thus tend to compensate for these effects at both ends of the sample size range. For these reasons, the weighting factor defined in Equation 4-12 was selected for this analysis.

4.4.4 Definition of the CANWE statistic

Using the weighting factor given in Equation 4-12, an error statistic can be defined according to Equation 4-3. This error statistic will be called the *CANWE* statistic, which stands for "Cumulative And Normalized Weighted Error". In equation form:

$$CANWE = \frac{\sum_{i=1}^{N}\left[\left|f_m - f_s\right|_i \cdot \left(\frac{f_m}{d_{med}^{\,3}}\right)_i \cdot (d_{\max} - d_{\min})_i\right]}{\sum_{i=1}^{N}\left[\left(\frac{f_m}{d_{med}^{\,3}}\right)_i \cdot (d_{\max} - d_{\min})_i\right]} \qquad (4\text{-}13)$$

Using this combined weighting approach, it is believed that differences between any two calculated *CANWE* values will most accurately represent differences in the quality of the data obtained from a given device.

4.5 Summary

Additional evaluation statistics could be selected or developed to express the accuracy of data obtained from a rapid gradation apparatus. However, the three test statistics defined above should provide adequate tools for comparing the accuracy of

the five test machines under consideration. The analyses to follow in Chapter 5 will thus rely on three statistical measures of quality:

- Chi-square (χ^2) statistic (Equation 4-1)
- Mean error statistic (Equation 4-2)
- CANWE statistic (Equation 4-13)

5. Test Results and Discussion

Combined, 135 test runs were conducted during the course of the five device evaluations. The gradation data from all test runs are presented graphically in Appendix C. In Figures 5.1 through 5.3, the results are plotted in terms of the three test statistics discussed in Chapter 4: Chi-square, MeanErr, and CANWE. Since all three analysis techniques yield similar trends, all observations regarding device performance will be based on the CANWE statistic. The similarities given by the three statistical tools are discussed in Section 5.1.

A number of aspects may be considered when characterizing the performance of rapid gradation devices. The primary use of the CANWE statistic is to identify the devices that produce gradation curves that more closely match a standard sieve gradation curve. However, CANWE results can also be used to evaluate repeatability between test runs and between different material types. Another important factor to consider is the time required to complete a test run. The speed at which these devices perform sieve analyses is a key advantage over the conventional sieving process, in addition to the potential for gathering data on particle shape.

5.1 Comparison of Results Given by the Three Statistical Methods

Each of the error statistics (chi-square, MeanErr, and CANWE) computed for all of the evaluation tests are plotted in Figures 5.1 through 5.3. For all three error statistics, smaller values indicate a closer match between the machine results and the benchmark sieve data over the full range of grain size in the test sample. That is, the machines giving the shortest bars in Figures 5.1 through 5.3 are the machines that gave the most accurate results for a particular test sample. Note that the magnitude of

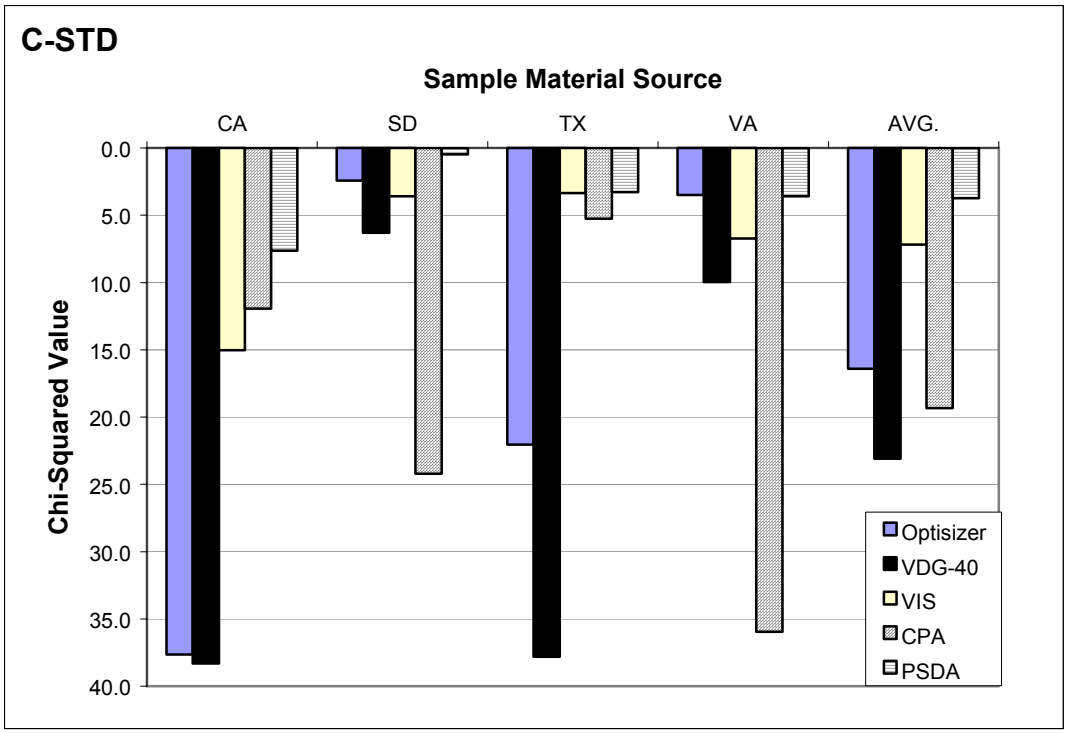

Figure 5.1a Comparison results with the Chi-square test statistic (C-STD).

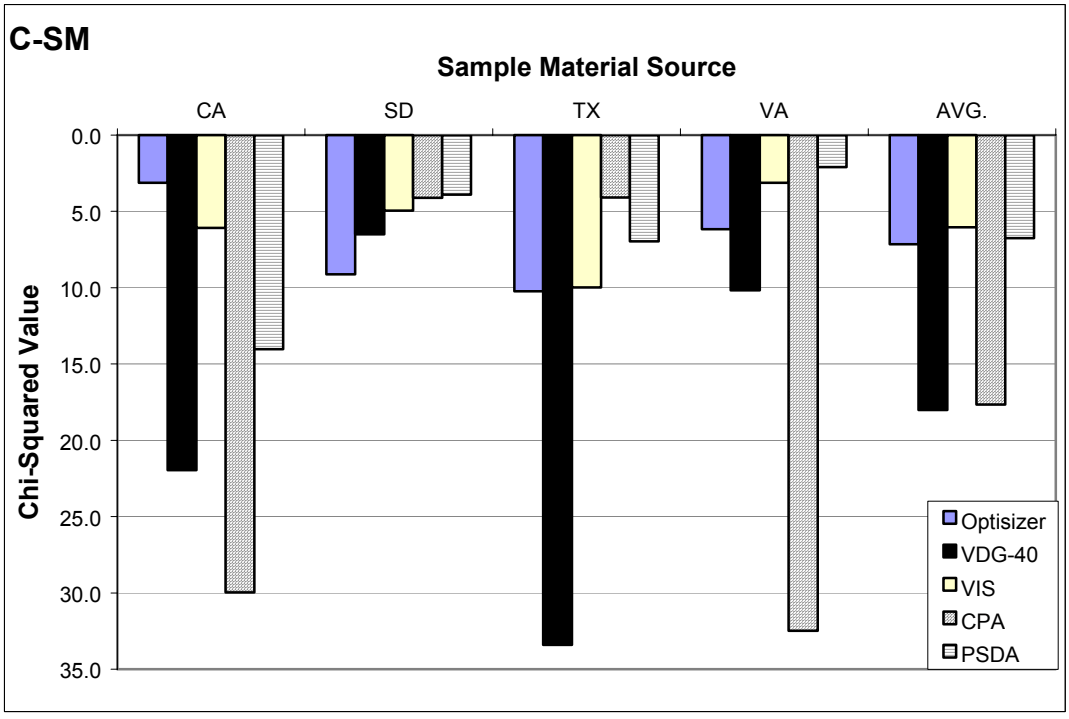

Figure 5.1b Comparison results with the Chi-square test statistic (C-SM).

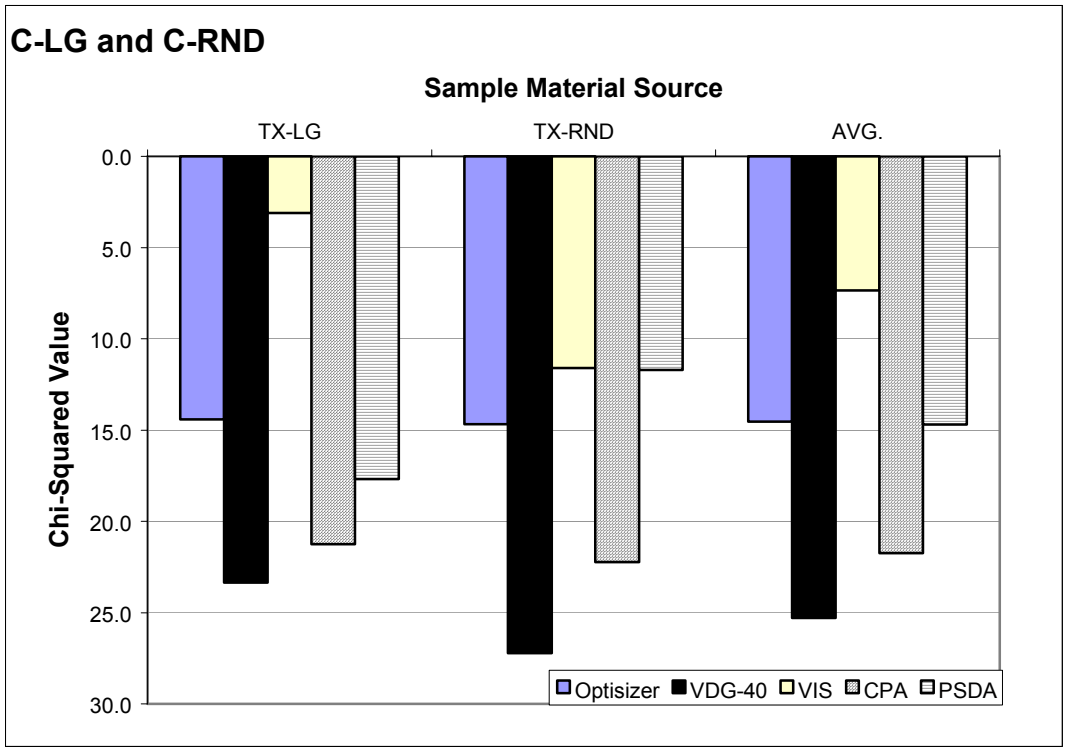

Figure 5.1c Comparison results with the Chi-square test statistic (C-LG, C-RND).

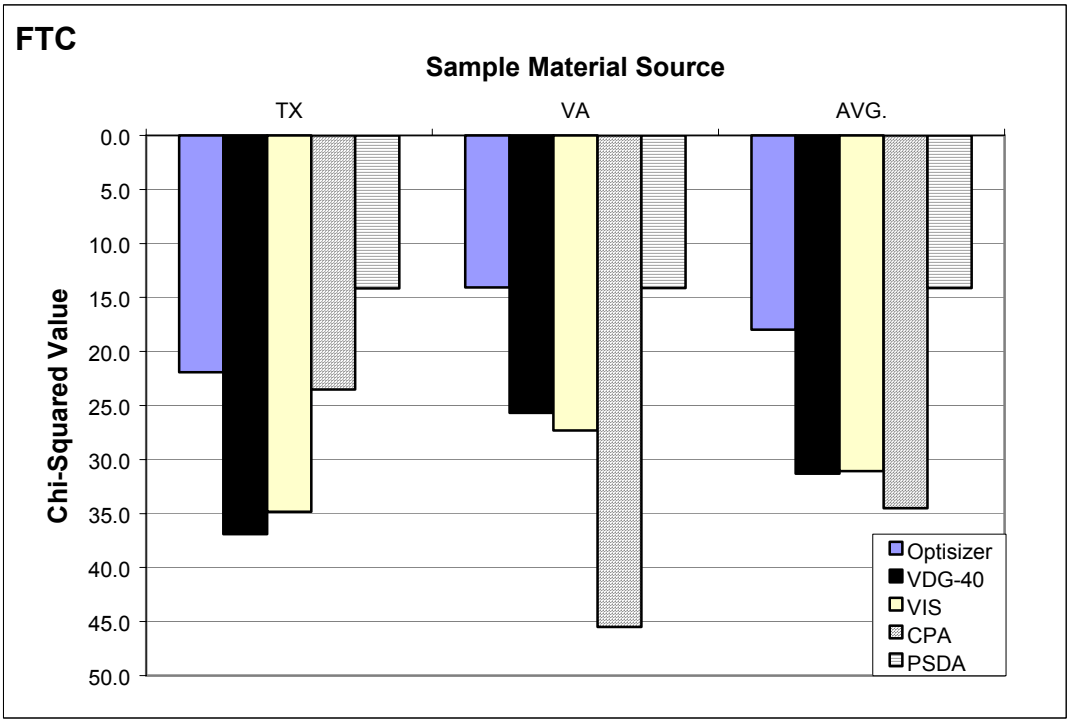

Figure 5.1d Comparison results with the Chi-square test statistic (FTC).

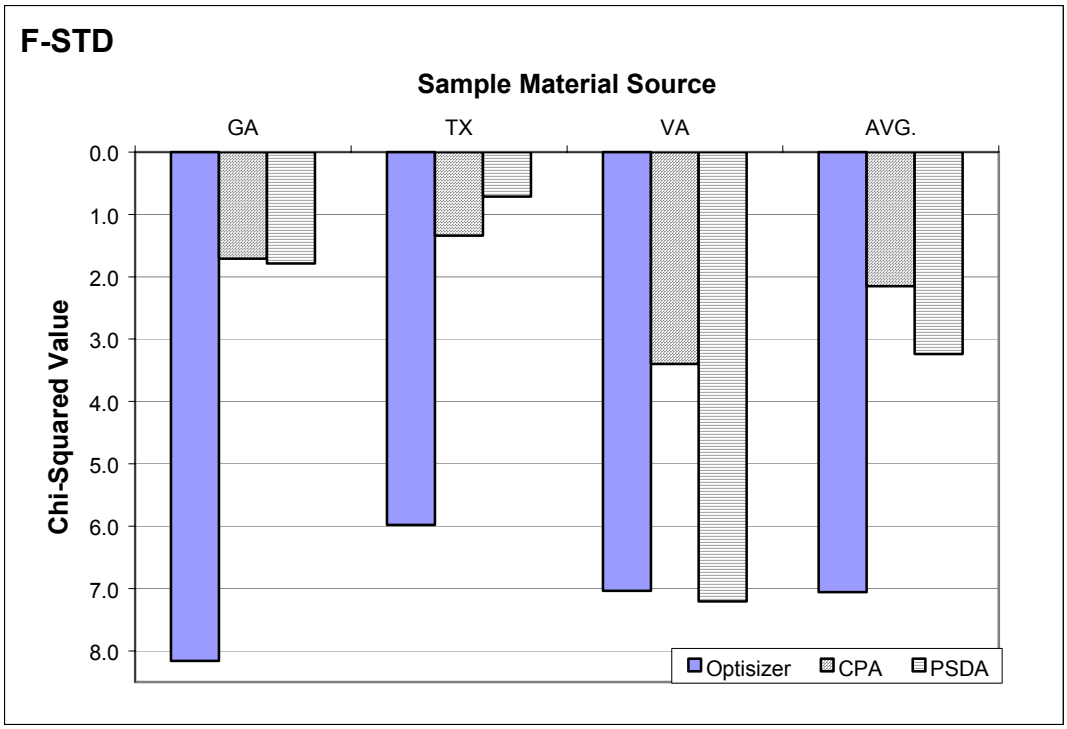

Figure 5.1e Comparison results with the MeanErr test statistic (F-STD).

the error statistic (height of bar) is plotted downward to reinforce the perception that longer bars indicate poorer machine performance. For example, consider Figure 5.1a. Based on the chi-square statistic, the PSDA device gave the closest match (shortest bar) to the sieve data for the CA-C-STD material, while the VDG-40 and OptiSizer gave almost equally poor results (longest bars) for this particular material.

From the data shown in Figures 5.1 through 5.3, the Chi-square, MeanErr, and CANWE test statistics show similar trends. Looking at Figures 5.1a, 5.2a, and 5.3a, the three test statistics show that the PSDA performs best overall on the C-STD material. The MeanErr statistic represents the only deviation from this trend for the C-STD material as it shows slightly more error for the CPA than the VDG-40 where Chi-square and CANWE showed the opposite. From Figures 5.1b, 5.2b, and 5.3b, the CANWE and MeanErr statistics show the PSDA to be the best overall performer for the C-SM material. The Chi-square and CANWE statistics show the VDG-40 and

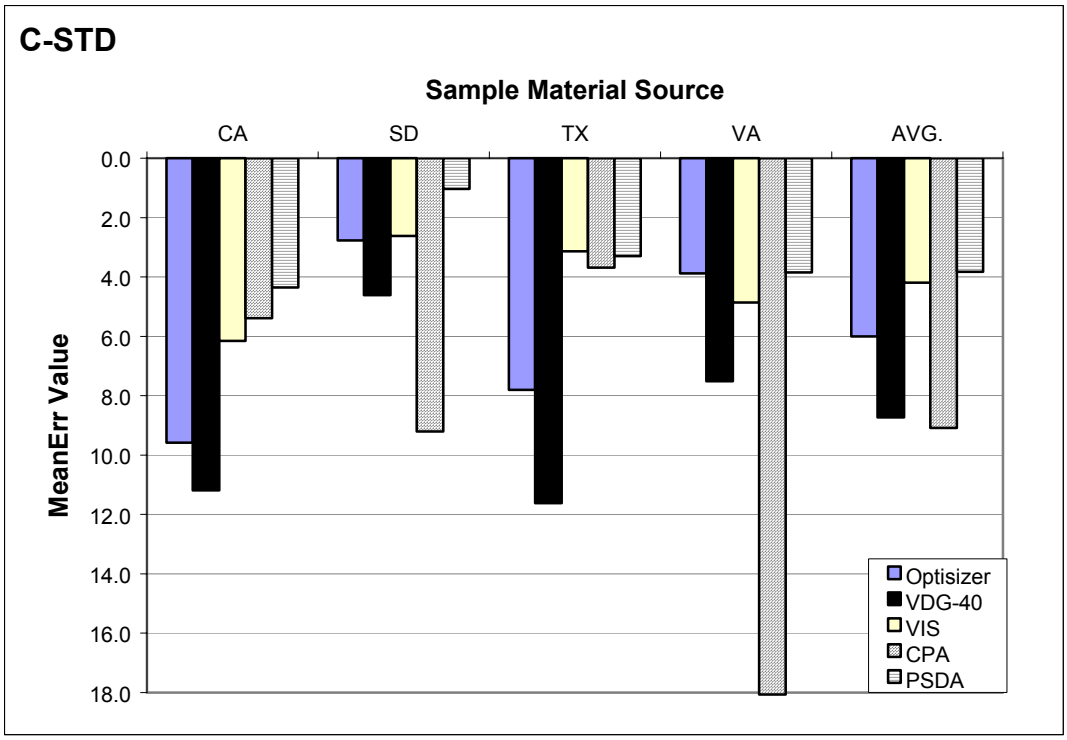

Figure 5.2a Comparison results with the MeanErr test statistic (C-STD).

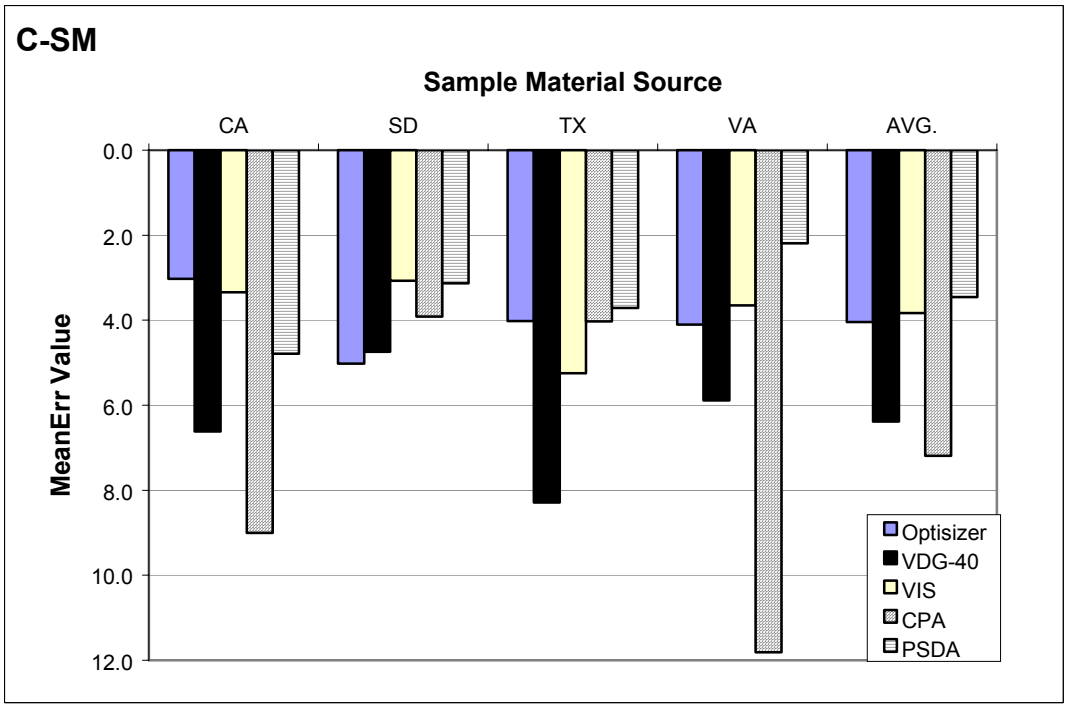

Figure 5.2b Comparison results with the MeanErr test statistic (C-SM).

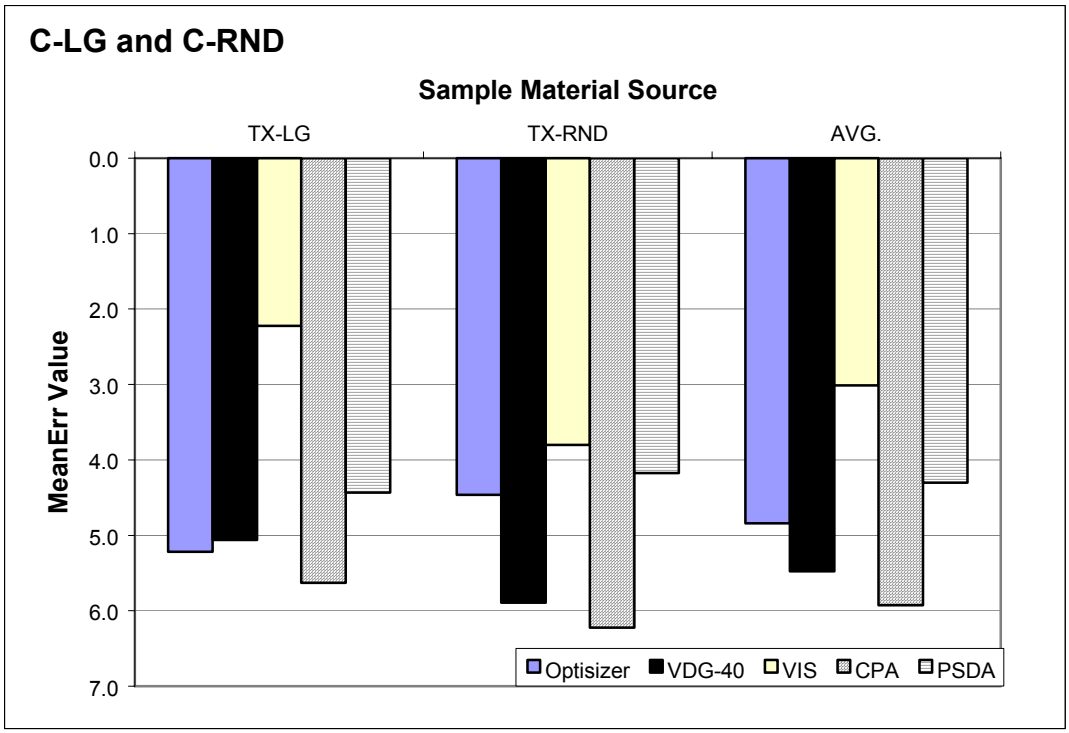

Figure 5.2c Comparison results with the MeanErr test statistic (C-LG, C-RND).

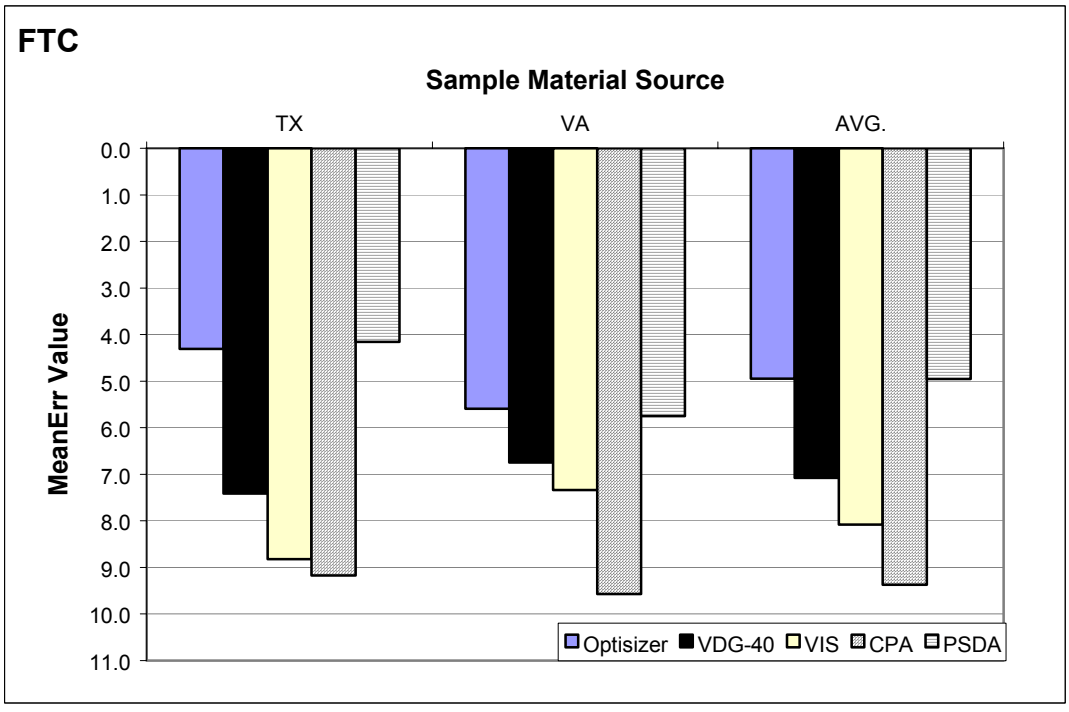

Figure 5.2d Comparison results with the MeanErr test statistic (FTC).

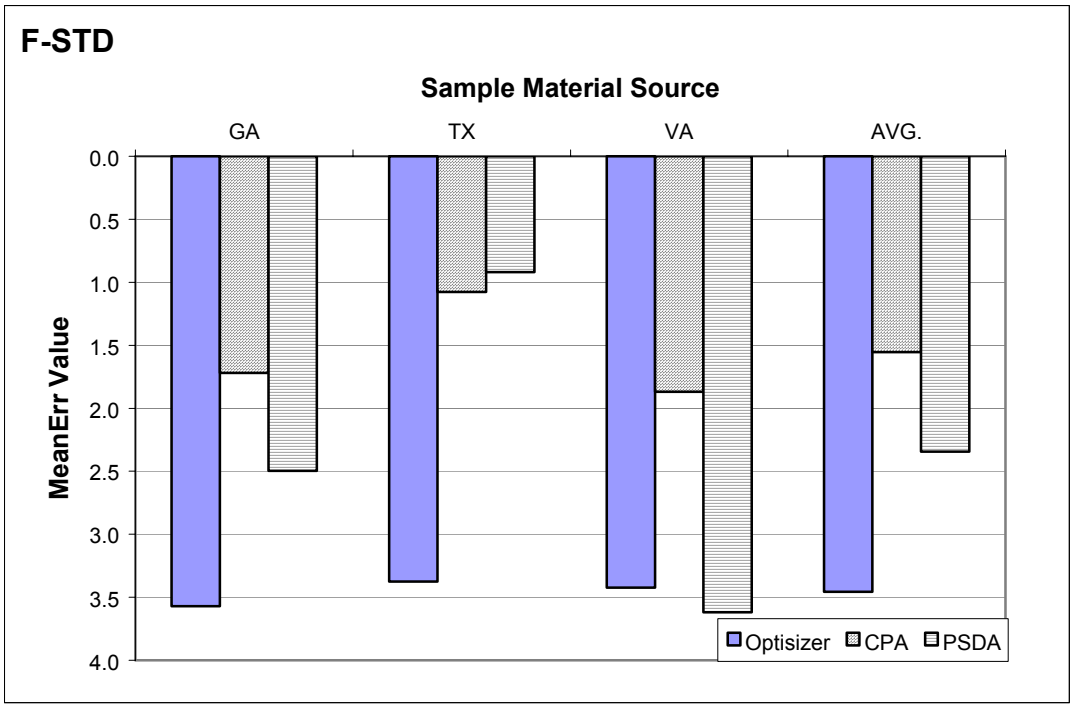

Figure 5.2e Comparison results with the MeanErr test statistic (F-STD).

and CPA to be the most error prone when evaluating the C-SM material. While the Chi-square and MeanErr statistics do not clearly differentiate performance for the OptiSizer, VIS, and PSDA, the CANWE statistic shows clear performance differences among these three devices. Regarding the C-LG and C-RND performance, Figures 5.1c, 5.2c, and 5.3c show that the VIS gives the smallest errors while the VDG-40 or CPA gives the greatest errors. Like with the C-STD material, the MeanErr shows the errors for the VDG-40 and CPA to be very close with the CPA having a slightly greater MeanErr value. For the FTC material (Figures 5.1d, 5.2d, and 5.3d) it is seen that all test statistics indicate the CPA gives the highest errors while MeanErr and CANWE indicate that the OptiSizer and PSDA are about equivalent in giving the least overall errors. Chi-square shows that PSDA performs with less error than the OptiSizer for the FTC material.

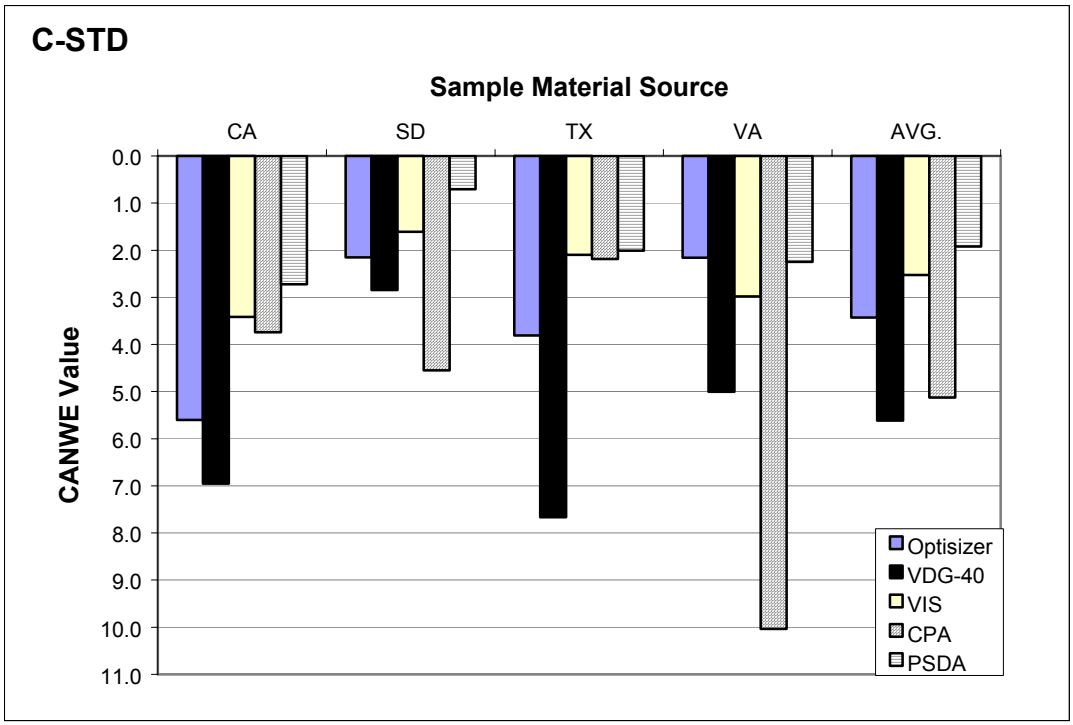

Figure 5.3a Comparison results with the CANWE test statistic (C-STD).

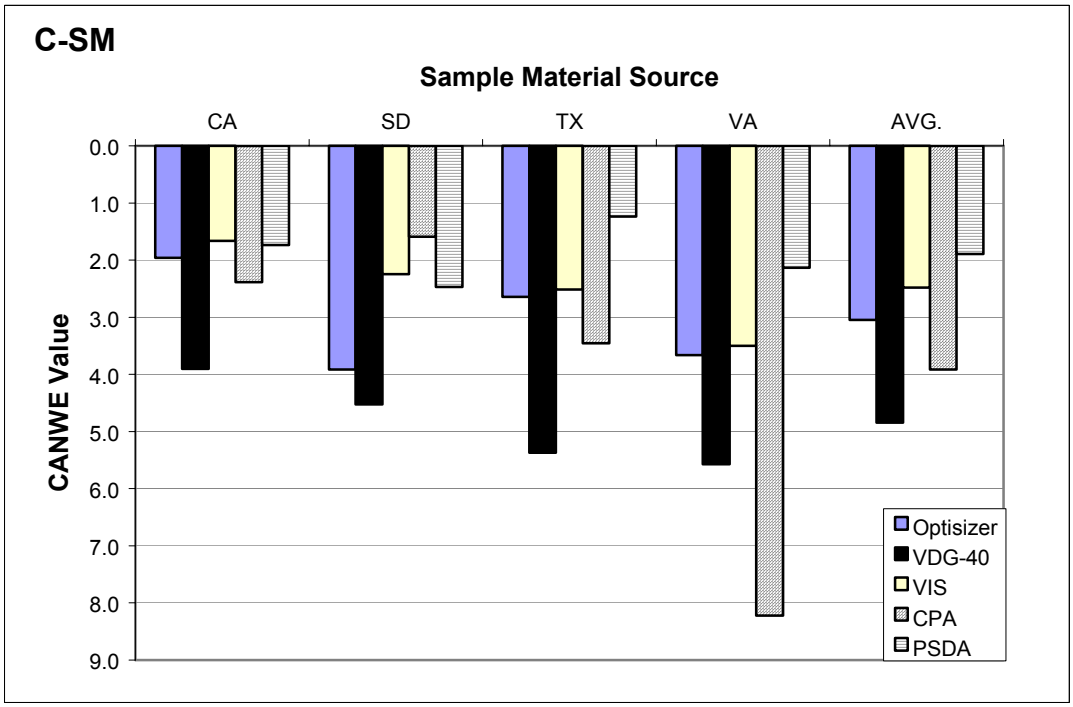

Figure 5.3b Comparison results with the CANWE test statistic (C-SM).

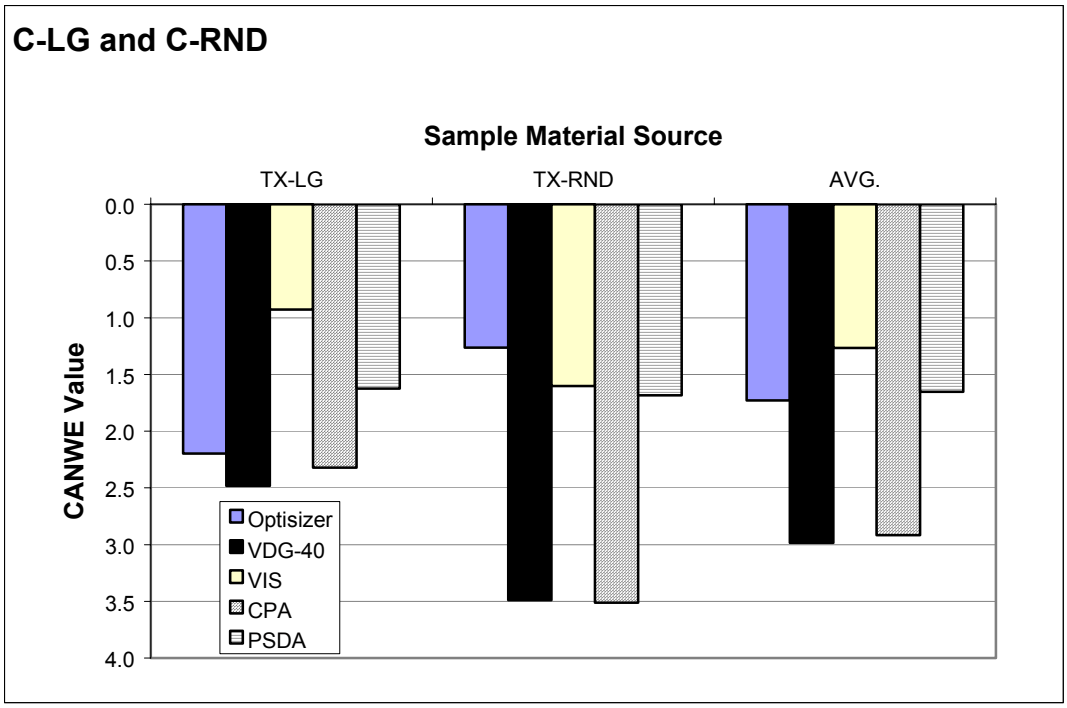

Figure 5.3c Comparison Results with the CANWE Test Statistic (C-LG, C-RND).

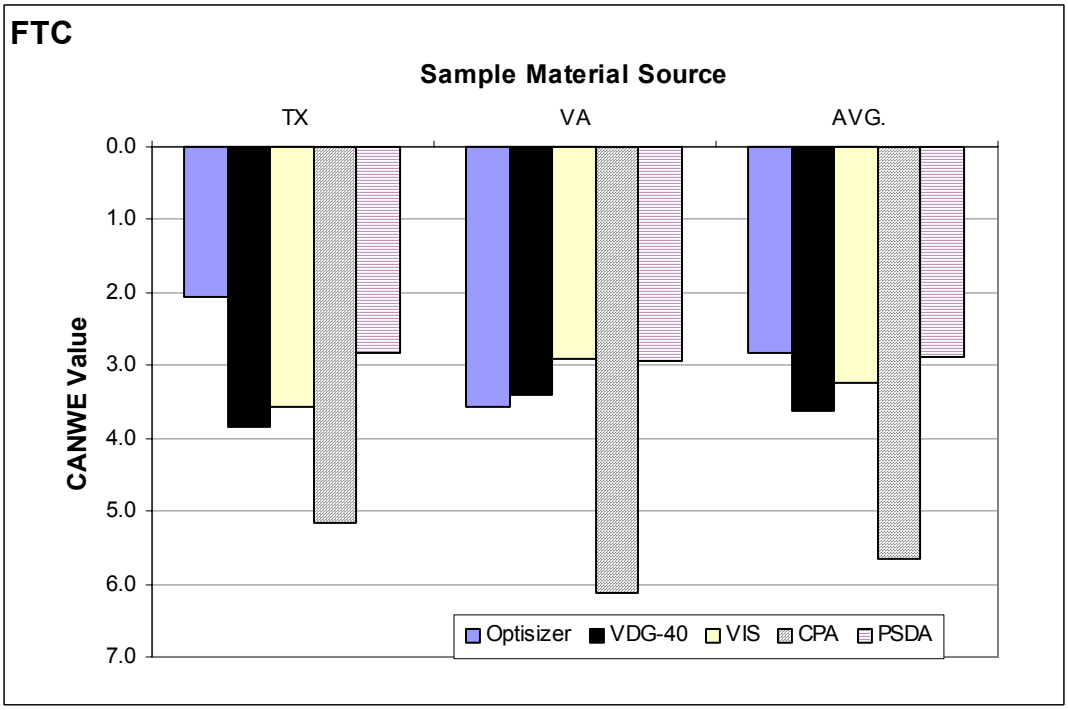

Figure 5.3d Comparison Results with the CANWE Test Statistic (FTC).

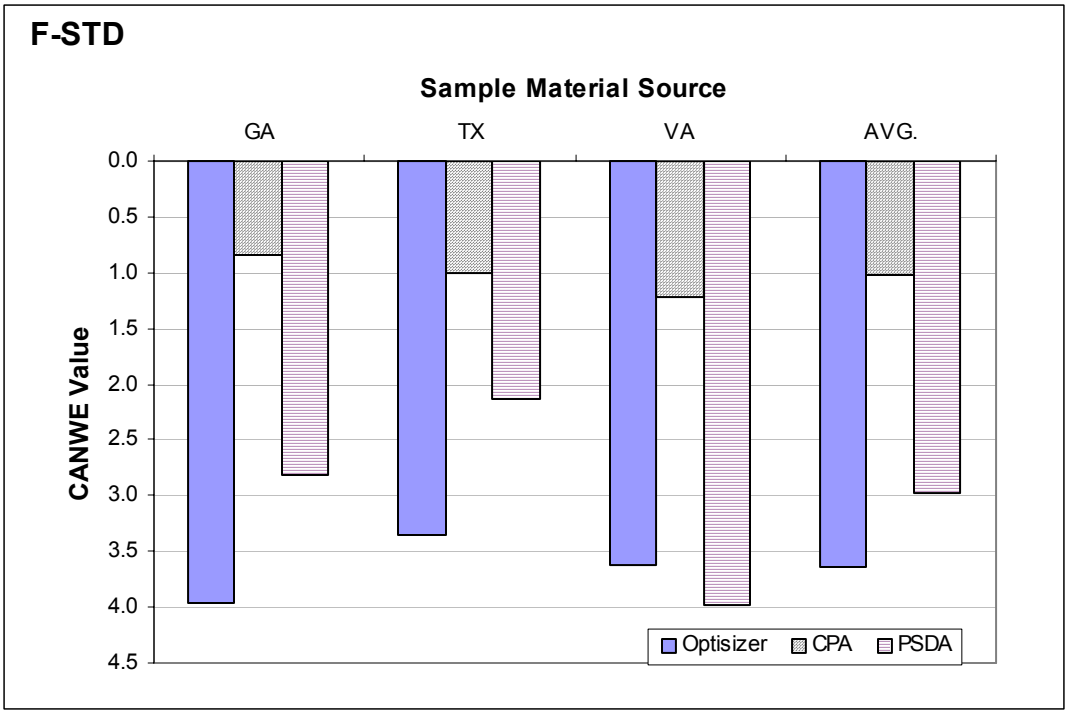

Figure 5.3e Comparison Results with the CANWE Test Statistic (F-STD).

In comparing the results for the F-STD material in Figures 5.1e, 5.2e, and 5.3e, an interesting observation is made. Since there were a relatively large number of particles captured during the analysis of the F-STD samples, the CANWE statistic weighting approach based on number of particles does not significantly affect results in comparison to the non-weighted approaches. Thus, it makes sense that all test statistics give the same trend with the CPA performing best and the OptiSizer giving the greatest performance errors.

Overall, the CANWE test statistic gives results in good agreement with both MeanErr and Chi-square in most cases. The CANWE thus seems to be a reasonable statistic upon which to characterize device performance. Moreover, more physical meaning behind the quantitative value of error can be derived from CANWE results than from the other two statistics. Hence, the CANWE statistic will be used as the basis for further examination of the test results.

5.2 General Performance Trends

The CANWE results for the samples containing coarse material, as plotted in Figure 5.3a through 5.3d, show that the PSDA and VIS usually give the best overall accuracy (smallest values of CANWE) when compared to the benchmark sieve. A notable exception to this trend is seen in Figure 5.3d for the FTC gradation. The VIS performs more poorly when analyzing this material, most likely due to the fixed feed rate used in the evaluation tests. The feed rate was optimized for a larger mean particle size than that found in the FTC samples. The larger amplitude vibratory motion used may have sent the smaller particles off the feeder edge too rapidly and in an overlapping fashion, resulting in poor presentation and in the capture of an insufficient number of aggregate particles. The camera focus may also be an issue with the smaller size particles. The focus may have been optimized for a larger mean particle size, which could lead to larger errors on the smaller particles.

The other exception to the trend noted above occurs with the C-LG and C-RND gradations, where the PSDA performs more poorly than the other devices. As with the VIS scan of the FTC material, the difficulty resulted from a feed rate that exceeded the camera's ability to capture a sufficient number of particles to accurately characterize the sample. Despite being the largest samples at 15 kg apiece, the C-LG and C-RND materials contain relatively fewer particles. Therefore, a statistically insufficient number of particles was probably imaged and used to define the gradation curve. This problem is common to some extent with the devices that use matrix-scan cameras. It is possible to minimize this problem in most cases through one of the following techniques:

1. Increase the total sample size.
2. Run the same sample through the machine multiple times.
3. Increase the rate at which images are captured.
4. Ensure the sample is homogeneously mixed

By taking measures similar to the four steps outlined above, test repeatability, discussed in further detail in the following section, may also be improved.

5.3 Repeatability of Results

Analyzing repeatability between successive machine runs reveals some important characteristics of the rapid gradation devices. First, the repeatability between different test runs of the same sample reflects the adequacy of the sampling technique. Secondly, the repeatability between different materials of the same gradation reflects both sampling technique and the effect of particle shape, which is related to the robustness of the 2D to 3D (image to volume) transformation algorithm used.

Table 5.1 shows the average difference in CANWE values between the test runs for a given gradation. For the C-STD samples, four difference values (CA, SD, TX, and VA materials) were averaged to obtain the value shown in Table 5.1, whereas the FTC value represents the average of two samples (TX and VA materials). Theoretically, if a device images the exact same particles each time a sample is analyzed, essentially identical results should be expected and there would be no difference in the CANWE values computed for the two runs. Indeed, the devices using line-scan cameras, which capture almost every particle in the sample, yield the smallest variation between test runs of the same sample. Since the units incorporating matrix-scan cameras will not capture the same fraction of the sample in each run, the results tend to differ more from one another. Again, this trend is observed in Table 5.1 with the OptiSizer, VIS, and PSDA results generally varying more than the VDG-40 and CPA results.

Table 5.1 Average difference in CANWE statistic between runs of a given sample gradation.

	Gradation Designation						
Device	**C-STD**	**C-SM**	**C-LG**	**C-RND**	**FTC**	**F-STD**	**AVG.**
OptiSizer	1.708	3.408	1.009	0.289	1.272	0.621	1.537
VDG-40	0.352	0.171	0.113	0.325	0.053	-	0.203
VIS	1.362	1.072	0.154	0.225	0.100	-	0.583
CPA	0.703	0.215	0.187	0.295	0.164	0.375	0.313
PSDA	0.692	0.660	0.036	0.394	0.211	-	0.399

There are instances, however, where the matrix-scan units yield better repeatability than the line-scan devices. For all of the devices, the methods and assumptions used to transform two-dimensional image to volumetric data may introduce additional error. Inconsistencies can be attributed, in part, to rotation of particles as they fall, which leads to variations in their presentation to the camera. Thus, a particle may be characterized differently if it is viewed parallel to its major axis (Profile A in Figure 5.4) as opposed to being viewed perpendicular to its major axis (Profile B in Figure 5.4). This effect may be more pronounced with the CPA device than the VDG-40, which employs a revolving drum to minimize particle rotation during free-fall. However, observations of the VDG-40's revolving drum during testing revealed another potential source of variation. Some particles tended to slide rapidly off the drum in such a way that they fell outside the main curtain of particles

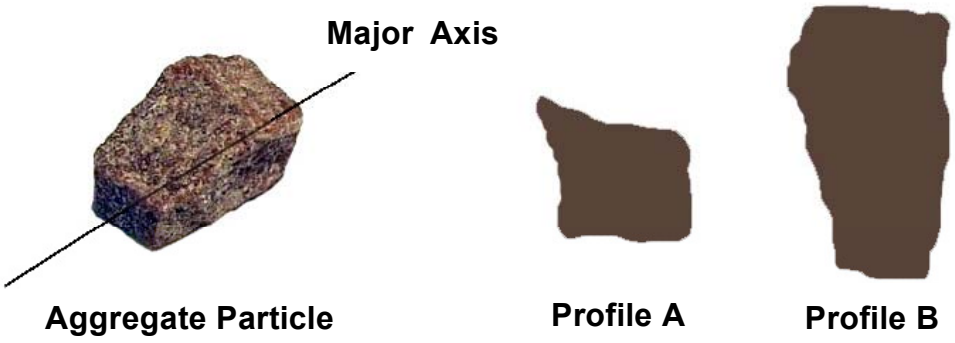

Figure 5.4 Illustration of Various Two-Dimensional Particle Profiles.

before the digital camera. It appears that this distance may be sufficient for some particles to be viewed outside the calibrated focal distance of the camera. These particles would then be categorized as smaller than they actually are, because they are further from the camera focal plane than is assumed. This problem was seen primarily with the larger particles and may explain why the VDG-40 yields average

differences higher than some matrix-scan units for the C-RND gradation. The rounded material also tended to roll off of the revolving drum, leading to increased horizontal velocity and more rotation.

Repeatability from material to material is indicative of the quality of transform algorithms used in converting two-dimensional image data into three-dimensional volumetric information. For a given gradation, a device that yields consistent results across all materials can be said to possess a robust transform technique that is valid for a wider range of particle shapes. Since it has been shown that shape also plays a role in sieve results (Fernlund 1997), a device that processes differing materials (and thus shapes) in a manner that yields results consistently similar to a sieve analysis is superior to a device that cannot account for assorted particle forms. Table 5.2 shows the standard deviation of results for each gradation. In this case, the C-LG and C-RND results are combined because it is not meaningful to assess the standard deviation of two values.

Table 5.2 Standard deviation of test runs on all materials.

	Gradation Designation					
Device	**C-STD**	**C-SM**	**C-LG/RND**	**FTC**	**F-STD**	**AVG.**
OptiSizer	1.819	2.032	0.688	1.161	0.448	1.425
VDG-40	2.017	0.724	0.598	0.267	-	0.902
VIS	1.178	0.992	0.405	0.386	-	0.740
CPA	3.197	2.754	0.701	0.574	0.271	1.806
PSDA	0.905	0.725	0.165	0.144	1.915	0.485

Table 5.2 indicates that the PSDA shows the lowest variation among results across different materials. This can be attributed to the PSDA's better use of particle shape in transforming two-dimensional data into volumetric information. The other devices use more generalized transforms as described in Chapter 3. Therefore, while generalized transforms may yield more rapid analysis, as required by the VDG-40 and CPA to analyze every particle, they are not necessarily optimized for any given material. Since shape is clearly a factor that affects sieve analysis, its use in

predicting volumetric information from two-dimensional images is beneficial. Shape effects appear to be less of a factor with smaller particle sizes as evidenced in the very low standard deviation of the CPA for the F-STD gradation. Although the VDG-40 and CPA do not take shape into consideration, calibration factors, discussed in the next section, that take advantage of their inter-test repeatability may be used to correct for shape effects.

The relatively weak repeatability of the OptiSizer, as evidenced by the high values in Table 5.1, may be attributed to two factors. First, like the other matrix-scan camera units, the sampling rate may be inadequate to properly scan a representative fraction of material each time it is run through the device. Thus, one would expect the results to vary if different particles are being imaged in each run. Furthermore, two different analysis algorithms were used in the two runs on the OptiSizer device, which introduces variability into the results in Table 5.2. It seems evident that depending on material type, the spheric or cubic algorithms may be more suitable. Since an operator may not know which algorithm is best suited to a particular material before running a test, the observed variability is potentially representative of the variation in results given from the OptiSizer.

5.4 Calibration Factors

Although the VDG-40 and CPA did not perform as accurately as the other devices, their high repeatability can be used to advantage. Consider an online application where a relatively uniform stream of aggregate will be analyzed. If the device consistently gives the same gradation curve for similar material, then a correlation or calibration factor can be used to obtain the "correct" sieve curve.

In fact, assumed calibration factors were used by the CPA in these evaluation tests. Part of the reason the CPA performed relatively poorly relates to the need for an ideal calibration factor to analyze the raw data. This factor varies from material to material and even from gradation to gradation for the same material. For instance, the same calibration factor is not equally suited for use with both the TX F-STD and TX

C-LG gradations. In a laboratory setting where several small samples of diverse materials are being tested, an operator would need to select appropriate calibration factors for each.

In an online application, the accumulation of sieve data over time would allow for selecting appropriate calibration factors. Initially, the device and sieving operations could occur simultaneously to develop a calibration factor that best suits the automated aggregate analyzer. Once a factor has been established, periodic verification by means of a conventional sieve test would be required to ensure the device continues to yield appropriate results.

The use of calibration factors is not limited to the line-scan units, but can be used with any of the five devices in this evaluation. However, the variability seen in the results from the matrix-scan devices makes it more difficult to establish calibration factors. Again, this variability can be reduced by any of the methods suggested in Section 5.1.

5.5 Time to Complete Test Runs

A key advantage of the automated gradation devices over traditional sieve tests is their ability to perform analyses in very short periods of time, providing essentially "real-time" data to an operational monitor. So that particles do not agglomerate, all of the five devices evaluated require dry test samples. Therefore, sample preparation must be considered in total processing cycle times. With larger particles, say greater than No. 4 mesh size, moisture content will not significantly affect the agglomeration of particles and minimal preparation is usually required. Sands, on the other hand, must be dried sufficiently to prevent particle clustering. Furthermore, the fines or minus No. 200 fraction must be measured by conventional means (wash sieving), if needed. The processing times shown in Table 5.3 are valid for pre-dried samples and represent the time from when the sample is deposited in the device to the point when all material has been processed and gradation results are reported.

Table 5.3 Approximate testing durations for the five rapid gradation devices.

Device Name	Range in Testing Duration per 1 kg of Sample	
	Coarse Samples	**Fine Samples (F-STD)**
OptiSizer	40 seconds to 5.5 minutes	50 minutes
VDG-40	1 to 6 minutes	*
VIS	15 to 30 seconds	*
CPA	1 to 3.5 minutes	40 minutes
PSDA	5 seconds to 2.5 minutes	36 minutes

* Cannot measure gradation of fine samples

It can be seen that testing times for certain devices vary considerably more than for others. Recall that for some devices, the feed rate was controlled manually, which partially contributed to a range in test times. Also, consider a 1 kg sample of 1 in particles versus the same mass of No. 4 mesh particles. Clearly, the sample of No. 4 mesh material will take longer to process because a larger number of particles must be analyzed in any given image. To prevent the systems from becoming overloaded, the feed rate must be slowed so that an optimum number of particles are processed in any given time interval. Therefore, the testing time will vary depending on grain size distribution. For example, the C-SM samples tended to take slightly longer to process than the C-STD samples because they contained a higher fraction of smaller particles. Likewise, the FTC samples, while weighing 3 kg less than the C-SM or C-STD samples, often took as long or even longer to process.

It can be seen that times for scanning the fine materials are considerably longer than those for the coarse samples. This phenomenon again relates to the total number of particles in each sample. If an equivalent number of particles were examined in each case (smaller total weight for fine materials relative to coarse materials), analysis times would likely be almost equivalent. Therefore, when considering total test time, sample quantity must be considered.

The VIS exhibits faster processing rates than all other machines primarily due to the large capacity vibratory feeder and large backlight. More material is in the field of view at any time, thus more material is imaged in a given snapshot. Since the camera is configured to capture a wide field of particles, it is able to capture more

information at a time. A drawback to this technique may lie in the VIS's lower detection limit of 1mm diameter particles. In addition, since the field of view is so large, the camera's focus cannot cover the entire range from No. 200 mesh material to 1.5 in size without modifications to the camera's focus.

While all devices test fine material at comparable rates, the CPA scans a larger total number of particles with its line-scan camera configuration. In conjunction with the analysis rates shown in Table 5.3, the analysis time per particle for the CPA is very short. Although the per-kilogram rate indicates the CPA to be slower than the PSDA and the OptiSizer, it may be capturing more than enough particles to accurately characterize a fine material. Thus, the analysis time shown in Table 5.3 must be closely evaluated if it is a critical feature. The PSDA shows a slightly faster ability to characterize fine material. The PSDA incorporates a function that determines the point where a statistically sufficient quantity of material has been processed. This is a somewhat subjective threshold, but it occurs at a time when the cumulative gradation curve does not vary significantly (as defined in the software) with additional data. Incidentally, while the automatic cutoff was reached on the fine specimens in these evaluation tests, the device did not automatically shut off when the C-LG and C-RND samples were processed. This may indicate the need for larger quantities of coarse material to provide statistically correct particle size distributions.

5.6 Cost

Although not performance related, the initial cost of a rapid gradation device is an important consideration for potential implementation. In some cases, it may be cost that dictates feasibility. Table 5.3 summarizes the approximate purchase price of each device.

Table 5.4 Device Costs.

Device Name	Approximate Cost
OptiSizer	$40,000 for fine particle setup – additional cost for larger coarse material feeder and backlight
VDG-40	$50,000
VIS	$60,000
CPA	$23,500 for CPA LAB and $40,000 for CPA 3-2
PSDA	Not Available

In general, the costs for digital image-based devices remain relatively close to one another. The one exception is the CPA LAB at $23,500. The VIS is the most expensive at $60,000, primarily because the VIS implements a much larger material feeding system than the other devices. The PSDA was not yet on the market at the time it was reviewed and the cost was not available. It is expected that as technology advances and these devices are implemented on a wider basis, the prices may gradually decline. However, as of this writing, these prices are approximately what should be expected.

5.7 Summary by Device

Micromeritics *OptiSizer PSDA™ 5400***.** The OptiSizer device has been commercially available for a relatively long time. To date, it has seen significant usage in the sugar, fertilizer and plastics industries. Since aggregate is a highly variable material, the matrix-scan sampling technique of this device places it at somewhat of a disadvantage compared to the line-scan units. However, this difficulty can be overcome by any of the techniques outlined in Section 5.2. A combination of sampling technique and processing algorithm leads to more variable gradation results compared to the other devices. The variation can be attributed partially to the use of two different transformation techniques (cubic vs. spherical models) during these evaluation tests. However, since it is not clear which technique actually yields more appropriate results for a given material, this variation may in fact be experienced in real-life applications, especially in the laboratory.

French LCPC *VDG-40 Videograder*. More widely used in Europe, a few VDG-40 units have been sold in the US. The strength of the VDG-40 is the ability to produce very repeatable results for any given sample. Since it employs a line-scan camera, it has the ability to scan almost every particle in a sample for a gradation analysis. In addition, given sample weight, it generates flatness and elongation data. Since less attention has been spent researching the validity of these shape results, it is unclear whether or not the assumptions made from a two-dimensional image are valid for estimating such three dimensional parameters. Despite the strong correlation between results for the same sample, relatively high variation was seen between different materials of the same gradation. This indicates the algorithm used in transforming the two-dimensional images into volumetric information may not be as robust as that used in the other devices. Because the VDG-40 is designed for laboratory applications, where very different materials are routinely tested, this variation is a potential concern.

John B. Long Company *Video Imagining System (VIS)*. The VIS machine is a scaled-up design built around a matrix-scan system. In the online situation, when coupled with a belt sweep sampler, the VIS is an effective tool for continuously monitoring material on conveyor belts. The large capacity setup enables this device to analyze a given quantity of aggregate faster than the other devices. At the same time, the VIS was seen to have some difficulty assessing samples containing particles down to 1 mm (No. 8 mesh material) in the evaluation tests. This could be due to factors such as sample size, fixed feed rate, and resolution of the camera.

W.S. Tyler *Computerized Particle Analyzer (CPA)*. The CPA is similar to the VDG-40 in a number of ways. It was developed in Europe and is based on line-scan technology. Unlike the other devices, it requires a specific correlation file for each sample. While this is a drawback in the laboratory setting, the high repeatability between results of a given sample could be utilized to obtain a suitable correlation factor to monitor a relatively consistent material stream in an online setting. Unlike

the VDG-40, the CPA is capable of processing fine material down to the No. 200 mesh size.

Buffalo Wire Works *Particle Size Distribution Analyzer (PSDA).* The PSDA incorporates some unique features in its implementation of digital imaging. When the particle size range of interest is known before hand, the PSDA can automatically select an appropriate calibration. Furthermore, it has the ability to detect when a statistically sufficient quantity of material has been analyzed. In this study, it was found that a relatively large quantity of coarse particulate material is required to achieve this level of statistically correct results. Moreover, this device utilizes particle shape in determining gradation. This is an important consideration as shape affects sieve results. The robust PSDA algorithm is reflected in the high levels of repeatability observed across differing materials and size ranges. The limited dynamic range of this device is seen as an inconvenience when analyzing material encompassing a wide size range, such as the F-STD samples. Currently the device requires such samples to be split in half and run through the device with separate settings. Knowing the weight of each fraction allows the two individual results to be combined into a composite gradation curve.

While each device has distinct advantages over the rest, no device seems to be the complete solution for any given application (e.g., online versus laboratory). Once the unique features found in each device are more widely known, the resulting wealth of knowledge could lead to extremely flexible solutions. As additional testing proceeds and as these devices find more common use in the field, further adjustments in software processing and improvements in technology should enhance convenience, speed, accuracy and reliability.

6. Conclusion

Five rapid aggregate analyzers were reviewed and evaluated. While other machines are commercially available to perform similar gradation operations, this group of devices represents the automated gradation equipment currently on the market. Digital imaging technology is core to all five of these devices. Although other technologies, such as laser profiling, posses great potential in this application, they are still being developed and are likely to be more costly.

6.1 Obstacles to Industry Acceptance

While this report has shown that certain automated devices are capable of measuring particle gradation, they have not yet been widely implemented in the aggregate materials industries. To date, these devices have been used primarily in applications such as plastics, peaning, sugar, and fertilizer manufacturing. Typically, these applications are in large manufacturing facilities, in contrast to typically small aggregate operations. Obviously, a larger facility can realize the savings needed to justify the greater capital expense for implementing automated devices. The lack of awareness of the capabilities of automated devices among aggregate producers and related industries, combined with high price tags, has resulted in continued reliance on the tried and true manual sieve analyses.

Automated devices may be seen primarily as sieve-replacement technology in the aggregates industry, whereas their main advantage over sieving is continuous or very frequent sample stream monitoring. While certain devices can replace a stack of sieves in a laboratory, they seem more ideally suited to continuous operation on the production line. In addition, with increasing demand for particle parameters other than size, such as flatness and elongation ratios, these devices appear to be a viable solution to laborious manual tests to perform such shape analyses.

6.2 Application of Devices in Industry

While digital imaging-based technology is being developed and sold by a number of companies, a buyer of such technology must clearly identify and understand their own particular needs. The five devices evaluated here have unique strengths that may make them more suitable than others in any given application.

6.2.1 Laboratory Environment

Certain characteristics make a rapid gradation device well suited to tests run in a laboratory environment. Here, it is assumed that several small batches of various materials and size ranges will be routinely tested. In the context of the digital imaging devices, some features are essential to laboratory type testing. These features include:

- Capability to image entire sample. The CPA and VDG-40 devices, both based on line-scan technology, have the advantage of including nearly every particle in a sample in the gradation results. This advantage may be less pronounced with fine aggregates where a relatively large number of particles is analyzed. However, the CPA exhibited the best correlation with the sieve results for the F-STD materials. Although certain materials can be run through the matrix-scan devices multiple times to achieve a larger effective sample size, errors could be introduced with fragile materials that tend to break down from handling during testing.
- Capability to process a wide range of particle sizes. Devices such as the VIS and VDG-40 are at a disadvantage in this respect because their lower detection limit is 1 mm. The CPA is convenient for testing samples with a wide range of particle size because it does not require any hardware changes or focus adjustments to analyze particles ranging in size from a No. 200 mesh up to 1.5 in. While the PSDA requires some adjustments to analyze the various size ranges, the focus and backlight intensity are automatically

adjusted, given the approximate size range of interest. The OptiSizer requires the most manual adjustments in going from primarily coarse to fine material, because it requires a different lens and manual focus changes. In addition, the PSDA, OptiSizer, and CPA require a different feed unit to effectively process the larger materials. Although the same feed unit (3 in width) was used in the CPA evaluation, it was not very practical for testing the coarse samples. Both the OptiSizer and PSDA required a different feed and backlight setup for the coarse and fine materials.

- Robust transform algorithm. Because the use of calibration factors is not practical when testing several different materials and size ranges, the grading device should either not use calibration factors or be programmed to make adjustments without operator intervention. Also, the PSDA exhibited the best ability to produce gradation curves that were in close agreement with the benchmark sieve data. The success of the PSDA may be attributable to its use of shape in determining gradation.

6.2.2 Online Environment

In an online situation, such as monitoring a conveyor belt of material coming out of a rock crusher, nearly continuous data is desired to monitor process changes. In this application, the emphasis is more on changes in material gradation rather than the actual gradation itself. Therefore, material- and size-specific calibrations may be appropriate given enough historical sieve data. In addition, since large quantities of material will be scanned in this setting, many of the requirements that apply to laboratory devices are not needed for online implementations. The following outline the key elements for online monitoring systems:

- Ability to process large quantities of material. Either matrix-scan or line-scan digital technology should work well in this respect. Matrix-scan units tend to have an advantage over the line-scanners because they can theoretically

process a given quantity of material faster. The VIS had the ideal configuration for handling large batches of material with a high capacity feed hopper and feed tray.

- Simple and rapid, yet consistent processing algorithms. The key to process control is identifying changes as quickly as possible; thus, a device that can process large quantities of material in short time periods is ideal. The VIS was the clear leader in this category as it gave the shortest analysis times while providing relatively consistent gradation curves.
- Ability to optimize analysis of specific particle size ranges and materials. Because the particle size range of interest in many online applications is known, certain devices can be optimized to scan only that range of particle sizes. The PSDA and OptiSizer allowed for optimizations of this nature, with the advantage lying in the PSDA's ability to automatically adjust focus and backlight intensity. The other devices could be optimized as well, but would require a greater understanding of the hardware to perform such changes. Since material in an online application is likely to be relatively consistent, calibration factors may be appropriate to adjust machine-generated results to known sieve results. Quality control sieve testing would still be required on a regular basis to ensure that the device is producing accurate gradation results.
- Ability to be networked and operate remotely. Most likely, analysis of material in an online application will occur at a location separated from the process control center. Thus, it is necessary for the device to transmit data rapidly to a remote location. All devices evaluated operate in conjunction with a personal computer, so this consideration is not a deciding factor. Furthermore, all devices were capable of incorporating feedback loops to monitor the quantity of material falling in the imaging field and automatically adjust and optimize feed rate.

Currently, none of the five devices evaluated offers an ideal solution for laboratory use. The PSDA comes closest to meeting the requirements set forth above, but falls short in analyzing only a portion of the test sample. While this may not pose a significant problem when large sample quantities are available or when fine material is processed, smaller sample quantities may pose problems if multiple runs are required to achieve a statistically correct gradation curve.

In contrast, all devices except for the VDG-40, which was intended solely for laboratory applications, could be used with success in an online situation. However, the VIS seems most suited to this environment given its large size and robust construction. The one drawback is the VIS machine's inability to analyze aggregate containing material smaller than 1 mm.

6.3 The Future of Rapid Gradation Technology

Although the devices evaluated in this study had their drawbacks, as technology advances and insight is gained about their performance, the future appears promising for these machines. If these devices are intended primarily as process control tools or purely gradation analyzers, a single camera may prove sufficient. However, assumptions required to process two-dimensional images to estimate three-dimensional shape have a limiting accuracy. The only way to acquire true three-dimensional particulate data through digital imaging is to utilize multiple cameras in the image acquisition phase. Additional cameras add expense, increase complexity, and inevitably lead to slower test times.

The future of both gradation and shape analyses may in fact belong to laser scanning devices. Current research at the University of Texas at Austin is showing positive results with a laser profiler to acquire aggregate data. However, this technology is in the very early stages of research and development. Within the next decade, progress with this form of particle analysis may produce a more advanced group of rapid gradation and shape analyzers than those available today.

Appendix A: Fractionating Water Column

One method of determining particle size distribution involves differentiating between settling times, assuming that larger particles have proportionally larger mass. This concept forms the basis of the hydrometer analysis routinely used by geotechnical engineers to measure gradation of soil particles passing a No. 200 sieve. The basis for a fractionating water column is that particles will reach a terminal settling velocity in a medium (generally water) as the force due to their weight is counteracted by the force due to drag on the particle surface. Force due to weight is proportional to diameter cubed, whereas the force due to drag is proportional to diameter squared. Thus as particle size increases, the settling velocity increases.

An automated version of the hydrometer has been developed by Micromeritics Corporation and is called the SediGraph. The SediGraph is capable of performing a hydrometer analysis in less than ten minutes for particle sizes as small as 0.1 μm (Coakley and Syvitski 1991). The SediGraph machine utilizes X-rays to detect the changing concentration with time of fine particles settling in an aqueous suspension. Analysis time is reduced through a controlled upward movement of the X-ray detector with time (Coakley and Syvitski 1991). This device is capable of determining grain size distributions for particles between 0.1 and 300 μm.

Apparently, no commercial fractionating water column equipment is available to test soil mixtures containing particle sizes larger than 0.3 mm. A fractionating water column prototype built by Aljassar et al. (1993) utilized a 5 ft tall clear sedimentation cylinder with light sensing photocells to measure light blockage due to settling particles. The prototype was designed to determine gradations of particles ranging from .075mm (No. 200 sieve) to 2.38mm (No. 8 sieve) (Aljassar et al., 1993). After making empirical correlations to calibrate their setup, Aljassar et al.

(1993) had a device that could measure a grain size distribution that very closely matched a conventional sieve analyses.

To explore the idea of using a fractionating water column for much larger particles, preliminary analyses and experiments were conducted. Analytical predictions of settling velocity assume the particles in suspension are smooth spheres. For particles less than about 2.4 mm, the relationship between settling velocity and drag coefficient is linear and modeled by Stoke's Law (Aljassar et al. 1993). Beyond a size of 2.4 mm particles begin to enter transitional or turbulent flow as their settling velocity yields Reynolds numbers greater than 2000 and Stoke's Law is no longer valid. For particles greater than 2.4 mm, two unknowns, settling velocity and coefficient of drag, make analytical prediction of settling velocity more difficult as an iterative technique is required to arrive at a correct value.

The variability in settling velocities of aggregate is illustrated in Figure A.1. The calculated values are based on assuming smooth spheres with a specific gravity equal to 2.67 (roughly that of the tested aggregate). The grid-filled boxes represent the range of settling velocity measured for the test aggregate particles. The deviation from the predicted model is primarily due to irregular particle shape and surface texture of the aggregate particles. Note the data from Aljassar et al. (1993) plotted at the lower left corner of Figure A.1. This data follows a relatively linear trend as predicted and discussed above.

While an analytical model can account for the effects of turbulent drag on large particles, no such procedure exists for modeling the effects of irregular particle shapes on hydrodynamic drag. Hence, considerable experimental calibration would be needed to develop an empirical model of the settling velocity of large, non-spherical aggregates. From a theoretical standpoint, this makes a fractionating water column an unattractive approach for grading coarse aggregates.

A possible implementation of the fractionating water column in the field would require automatic handling of aggregate samples and measurement of settling velocity. Samples could be taken off of a conveyor belt using a sweep sampler and

transported to a bucket near the top of the water column. The bucket could be equipped with an opening bottom that could be first lowered into the water and then opened to release the aggregate in a semi-controlled manner into the column. The necessary measurements could be obtained with either a photocell to measure light blockage (concentration) versus time or a scale at the bottom of the column to measure cumulative settled weight over time.

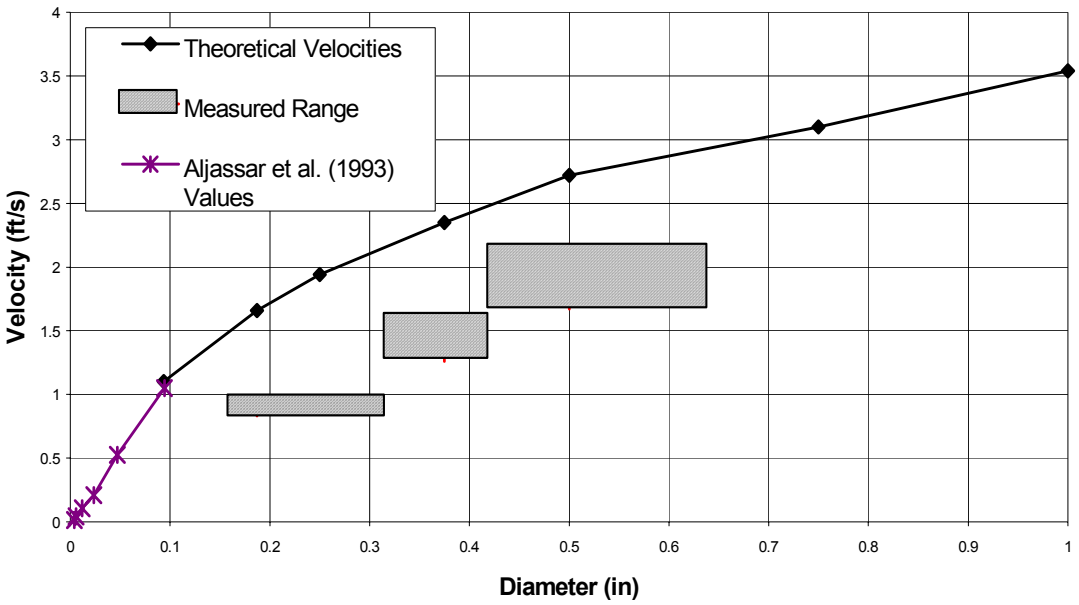

Figure A.1 Terminal settling velocities over laminar to turbulent flow conditions.

Aside from difficulties in modeling the effects of particle shape and turbulent drag, large-scale fractionating water columns would suffer from other difficulties if implemented in the field environment:

- Hydrodynamic drag varies with water viscosity, and therefore with temperature. To accurately measure settling velocity, a homogeneous and constant temperature must be maintained or measured in the water column

- Settling velocity is a function of specific gravity in a given particle. A possible sensitivity to aggregate specific gravity may lead to variations in gradation results
- When sizable batches of aggregate are introduced into a water column the effects of interference between adjacent settling particles are unknown and clearly random.
- No quantitative information on aggregate shape or surface texture can be extracted from water column analyses, without extensive laboratory testing to derive empirical relations between settling time and particle shape.
- Each implementation of the water column would need to be calibrated with local conditions and monitored throughout its operational lifetime to adjust for variations in the aggregate being processed.
- In cold climates, freezing of the column media (most likely water) poses a problem. Additional equipment such as heaters or an indoor housing unit would be required to eliminate this difficulty.
- The water in the column will get cloudy and will need to be changed regularly. While the disposal of this water would not be a major issue in a typical production plant, this would require a water source and drain, adding to the cost of equipment and maintenance.

Given all of these considerations, a fractionating water column is not a practical approach for automating the determination of aggregate grain size distribution.

Appendix B: Bayesian Approach

Statistical methods of evaluating machine accuracy are discussed in Chapter 4. In this appendix, another technique is suggested for analyzing the results of an automated gradation device. The Bayesian approach as described was applied to analyze only some of the test data on three gradation machines. Hence, the results of this analysis are somewhat incomplete

The Bayesian Approach (Ang 1975) is based on Bayes Theorem as expressed below:

$$P(B_j \mid A) = \frac{P(A \mid B_j)P(B_j)}{\sum_{i=1}^{n} P(A \mid B_i)P(B_j)} \qquad \text{(B.1)}$$

Where:

$P(B_j)$ = prior probability

$P(A|B_j)$= new information

$P(B_j|A)$= posterior probability

Essentially, the Bayesian Approach works by taking any quantity of experimental data (in this case the sieve results for 15 samples and device data for those samples) and using it to predict future performance trends, given the data collected. One appealing aspect of this approach is that it can be updated continuously with new data to produce a more refined model.

As a starting point for the analysis of the gradation devices, consider the percent of material retained on the ½ in sieve for any sample. We can say that, on average, the machine will give a result that is equal to a scaled value of the benchmark sieve value plus an error term (B.2). The standard deviation for the device (B.3) can be modeled in a similar fashion as shown below:

$$\mu_{f^*} = \theta_1 \cdot f + \theta_2 \qquad \text{(B.2)}$$

$$\sigma_{f^*} = \theta_3 \cdot \mu_{f^*} + \theta_4 \qquad \text{(B.3)}$$

Where:

μ_{f^*} = average machine result (fraction of sample retained)

σ_{f^*} = standard deviation of machine result

f = measurement made by a standard sieve, and

$\theta_1, \theta_2, \theta_3, \theta_4$ are the model parameters for a particular sieve size

The Bayesian Approach was selected to determine the expected model parameters given the data collected. Because no prior information on the likely combination of model parameters was known, all combinations of θ_i were given an equal probability of occurrence in the ensuing Bayesian analyses [$P(B_j)$ = constant]. Thus, finding the combination of parameters that best "fit" the observed data became a matter of maximizing the likelihood function, L(f*), for all data points. The likelihood function is expressed as:

$$L(f^*) = \prod_{i=1}^{n} \frac{1}{\sqrt{2\pi}\sigma_{f^*}} e^{-\frac{1}{2}\left(\frac{f^* - \mu_{f^*}}{\sigma_{f^*}}\right)^2} df^* \qquad \text{(B.4)}$$

Where: n = number of data records on a given sieve fraction

The likelihood function is represented in Equation B.1 as $P(A|B_j)$, or the new information that in this case is the machine generated gradation curves. In this case, f and f^* are modeled as a normal variates. Using the "Solver" add-in with Microsoft Excel, the values of θ_i that maximized the likelihood function were established. An example of the maximized values and corresponding calculations are found at the end of this appendix in Table B.3a. In addition, the Second-Moment Bayesian Method (Gilbert 2000) was employed to determine the confidence in the model parameter estimates. Table B.3b shows the calculations behind the determination of model parameter confidence. Essentially what is shown here is determination of curvature at the local maxima as defined by the model parameters found in Table B.3a. A pointed peak indicates higher confidence than a gradually sloping crest.

Prior to discussing the comparative results, there is one important item to note. Data for the 1 in sieve size could not be modeled since the benchmark sieve value in this situation was 0%. In other words, no unique solution for the model parameters could be found. With this in mind, the following tables summarize the results of this analysis. Table B.1 presents the expected value for all model parameters and their estimated uncertainties. Based on the expected values for the model parameters, Table B.2 shows the probability that each machine would produce results falling within the AASHTO #57 specification given a sieve test that indicates it either should or should not fall within the specified range.

Table B.1 Expected model parameters for various particle sizes.

1/2" Sieve

Device	Param.	E(θi)	Std.Dev(θi)	δ
Optisizer	θ_1	1.00727	0.19339	0.1920
	θ_2	0.01345	0.11303	8.4071
	θ_3	-0.03020	0.05535	-1.8324
	θ_4	0.06929	0.03127	0.4514
VDG-40	θ_1	0.72427	0.04631	0.0639
	θ_2	0.23390	0.02602	0.1112
	θ_3	0.00904	0.02713	3.0014
	θ_4	0.01957	0.01723	0.8806
VIS	θ_1	0.98474	0.11932	0.1212
	θ_2	0.03366	0.06891	2.0471
	θ_3	-0.01431	0.04336	-3.0301
	θ_4	0.05005	0.02486	0.4966

#4 Mesh Sieve

	Param.	E(θi)	Std.Dev(θi)	δ
Optisizer	θ_1	1.11132	0.23578	0.2122
	θ_2	-0.08221	0.10095	-1.2279
	θ_3	-0.05182	0.07387	-1.4255
	θ_4	0.07171	0.02711	0.3781
VDG-40	θ_1	0.94791	0.06983	0.0737
	θ_2	-0.09105	0.02717	-0.2984
	θ_3	0.03862	0.04760	1.2325
	θ_4	0.01881	0.01319	0.7013
VIS	θ_1	1.07249	0.10312	0.0962
	θ_2	-0.05081	0.04121	-0.8111
	θ_3	0.02670	0.05807	2.1754
	θ_4	0.03380	0.02171	0.6422

#8 Mesh Sieve

	Param.	E(θi)	Std.Dev(θi)	δ
Optisizer	θ_1	0.84263	0.15465	0.1835
	θ_2	0.00585	0.00367	0.6265
	θ_3	0.43912	0.15132	0.3446
	θ_4	-0.00230	0.00377	-1.6417
VDG-40	θ_1	0.59565	0.02893	0.0486
	θ_2	0.00133	0.00061	0.4558
	θ_3	0.12702	0.03635	0.2862
	θ_4	-0.00051	0.00049	-0.9652
VIS	θ_1	0.73000	0.04193	0.0574
	θ_2	0.00283	0.00104	0.3687
	θ_3	0.11783	0.04064	0.3449
	θ_4	0.00004	0.00084	23.7220

From the results in Table B.2, it is clear that the VDG-40 is less likely than the other devices to properly characterize aggregates. All devices tend to have the most difficulty in correctly characterizing the smaller, No. 8 material. However, the 0.97 probability that the VDG-40 identifies out of specification No. 8 material as "in-spec" stands out. Both the OptiSizer and VIS have considerable difficulty on the No. 8 sieve, but not to the same degree as the VDG-40. The likely source of problems with smaller material is the device's resolution. For these machines the resolution is generally 1mm, thus the percent error on smaller particles will be larger than on larger particles. However, two phenomena occur as particle size increases that introduce two additional sources of error. For one, there are fewer particles for the device to analyze. For the VIS and OptiSizer this becomes a very important problem since they only sample (with sequential "snapshots" of falling material) the sample. What occurs is essentially improper sampling if the device fails to capture a representative number of particles from each size range. The VDG-40, on the other hand, scans every single particle, thus giving a perfect sample of the initial sample. For this reason, the VDG-40 gives highly repeatable results as reflected in the relatively small standard deviations for all model parameters in Table B.1. The second issue with increasing particle size is related to the error inherent to estimation of particle volume. As previously discussed, these devices can only approximate particle volume, a process that can lead to increasing magnitude of error as particle size increases. Larger particles tend to be less uniform in shape than smaller particles, thus making volume estimation more difficult. Add to the potential sources of error discussed above, the fact that the output from these devices is based on volume and not weight (like used in standard sieve analyses) and one can expect automated machine-based results would not exactly match sieve results.

Table B.2 Likelihood that devices will give "correct" results for an AASHTO #57 blend.

Sieve Size	Device Name	P(35<f*<75|μ=68.33)	P(35<f*<75|μ=43.33)
1/2"	Optisizer	0.8423	0.9636
	VDG-40	0.7913	1.0000
	VIS	0.8618	0.9944
Sieve Size	**Device Name**	**P(15<f*<60|μ=30)**	**P(15<f*<60|μ=50)**
#4	Optisizer	0.9576	0.9963
	VDG-40	0.9504	1.0000
	VIS	0.9984	0.9929
Sieve Size	**Device Name**	**P(0<f*<5|μ=1.667)**	**P(0<f*<5|μ=6.667)**
#8	Optisizer	0.9990	0.3083
	VDG-40	1.0000	0.9716
	VIS	1.0000	0.4029

While the VDG-40 gave the lowest probabilities of correctly characterizing aggregates, it is interesting to note that it had the least variability in terms of the model parameters. Based on the fact that it accounts for every particle, one would expect consistent results. Indeed, consistent results are seen in the data found in Appendix C. By comparison, the VIS and OptiSizer tend to have higher levels of uncertainty in their model parameters. Clearly, the VIS and OptiSizer are better suited to an on-line application, where they scan large amounts of material, rather than the laboratory. Possibly, had the VDG-40 been better calibrated, it would have given superior results.

One last issue that should be addressed is the testing performed on the OptiSizer. Unlike the VIS or VDG-40, the OptiSizer allows the user to select the computational algorithm to analyze the sample. For example, we chose to perform on each sample one run using the spheric model and another run using the cubic model. In other words, we assumed that we had no knowledge of which model would give better results. Therefore, the probabilities put forth in Table B.2 should be considered as laboratory type results where one will analyze several small batches of various different materials. However, in an on-line application, the material being analyzed will often be relatively consistent. Significant performance data from past sieve

analyses would be available to permit optimization of the computational algorithm. Therefore, less variability would likely be encountered in these results, had an "optimized" transform model been used. For instance, the Texas material was generally quite rounded, thus the spheric model proved to give more accurate results than the cubic model. Still, a major problem detracting from the accuracy of the OptiSizer in the laboratory is its relatively poor repeatability.

The scope of this effort was limited to only 8 aggregate samples out of 15 total. However, the framework has been established to accommodate additional data from the remaining samples as well as any further test data acquired from these devices. Clearly, more data will always give higher confidence in probabilities that may be calculated.

Table B.3a Example of OptiSizer 1/2 in data analysis using C-STD and C-SM gradation data.

θ_1=	1.0073
θ_2=	0.0134451
θ_3=	-0.0302039
θ_4=	0.0692858

Optimized Model Parameters

F (benchmark)	f* (device value)	μ(f*)	σ(f*)	Likelihood Function, L(f*)	ln(L)
0.6833	0.6665	0.7017123	0.04809135	6.342	1.847
0.6833	0.6524	0.7017123	0.04809135	4.904	1.590
0.6833	0.7423	0.7017123	0.04809135	5.806	1.759
0.6833	0.6566	0.7017123	0.04809135	5.341	1.675
0.6833	0.7353	0.7017123	0.04809135	6.499	1.872
0.6833	0.7138	0.7017123	0.04809135	8.036	2.084
0.6833	0.7902	0.7017123	0.04809135	1.527	0.423
0.6833	0.6566	0.7017123	0.04809135	5.341	1.675
0.4333	0.4012	0.4498949	0.05569722	4.885	1.586
0.4333	0.4117	0.4498949	0.05569722	5.659	1.733
0.4333	0.4397	0.4498949	0.05569722	7.043	1.952
0.4333	0.4966	0.4498949	0.05569722	5.041	1.618
0.4333	0.4474	0.4498949	0.05569722	7.155	1.968
0.4333	0.4030	0.4498949	0.05569722	5.023	1.614
0.4333	0.5757	0.4498949	0.05569722	0.559	-0.581
0.4333	0.4240	0.4498949	0.05569722	6.432	1.861
		Minimized Product:		5.212E+10	24.67684

Table B.3b Calculations to determine uncertainty in model parameters found in Table 5.3a.

i=1;j=1

thetai	thetaj	ln(L)	□	$\delta^2 g/(\delta\theta_i \delta\theta_j)$
0.9972	1.0073	24.57096	10.512	-2103.123
1.0072694	1.0073	24.67684		
1.0173421	1.0073	24.56934	-10.672	

i=2;j=2

thetai	thetaj	ln(L)	□	$\delta^2 g/(\delta\theta_i \delta\theta_j)$
0.0133	0.0134	24.67679	0.409	-6048.9
0.0134451	0.01345	24.67684		
0.0135795	0.0134	24.67679	-0.4043	

i=3;j=3

thetai	thetaj	ln(L)	□	$\delta^2 g/(\delta\theta_i \delta\theta_j)$
-0.0299	-0.0302	24.67664	-0.6685	-4450.5
-0.030204	-0.0302	24.67684		
-0.030506	-0.0302	24.67664	0.6757	

i=4;j=4

thetai	thetaj	ln(L)	□	$\delta^2 g/(\delta\theta_i \delta\theta_j)$
0.0686	0.0693	24.67388	4.2783	-12080.7
0.0692858	0.06929	24.67684		
0.0699787	0.0693	24.67401	-4.0919	

g = ln(L)	$d^2g/d\theta id\theta j$

i=1;j=4

thetai	thetaj	ln(L)	□	$\delta^2 g/(\delta\theta_i \delta\theta_j)$
1.007269	0.06929	24.67684	-4.0919	627.0
1.007269	0.06998	24.67401		
1.017342	0.06929	24.56934	2.2236	
1.017342	0.06998	24.57088		

i=1;j=2

thetai	thetaj	ln(L)	□	$\delta^2 g/(\delta\theta_i \delta\theta_j)$
1.0072694	0.0134451	24.676844	-0.40425	-3527.1
1.0072694	0.0135795	24.67679		
1.0173421	0.0134451	24.569343	-35.9319	
1.0173421	0.0135795	24.564512		

i=2;j=3

thetai	thetaj	ln(L)	□	$\delta^2 g/(\delta\theta_i \delta\theta_j)$
0.0134451	-0.0302039	24.676844	0.675744	230.6
0.0134451	-0.0305060	24.67664		
0.0135795	-0.0302039	24.67679	0.706752	
0.0135795	-0.0305060	24.676576		

i=3;j=4

thetai	thetaj	ln(L)	□	$\delta^2 g/(\delta\theta_i \delta\theta_j)$
-0.030204	0.0692858	24.676844	-4.09191	-6999.5
-0.030204	0.0699787	24.674009		
-0.030506	0.0692858	24.67664	-1.97779	
-0.030506	0.0699787	24.67527		

i=1;j=3

thetai	thetaj	ln(L)	□	$\delta^2 g/(\delta\theta_i \delta\theta_j)$
1.0072694	-0.0302039	24.676844	0.675744	420.4
1.0072694	-0.0305060	24.67664		
1.0173421	-0.0302039	24.569343	4.910425	
1.0173421	-0.0305060	24.56786		

i=2;j=4

thetai	thetaj	ln(L)	□	$\delta^2 g/(\delta\theta_i \delta\theta_j)$
0.0134451	0.0692858	24.676844	-4.09191	368.2
0.0134451	0.0699787	24.674009		
0.0135795	0.0692858	24.67679	-4.04241	
0.0135795	0.0699787	24.673989		

"-G"	2103.12
"[-G"]-1	0.00048
Var(q1)	0.00048
Std.Dev1	0.02181
lower95	0.96453
upper95	1.05001

[G]

-2103	-3527	420	627
-3527	-6049	231	368
420	231	-4451	-6999
627	368	-6999	-12081

[-G]-1

3.7401E-02	-2.172E-02	4.459E-03	-1.3042E-03
-2.1718E-02	1.278E-02	-2.58E-03	7.5819E-04
4.4588E-03	-2.582E-03	3.063E-03	-1.6220E-03
-1.3042E-03	7.582E-04	-1.62E-03	9.7800E-04

Std.Devθ_1	0.19339	Std.Devθ_2	0.11303	Std.Devθ_3	0.055345	Std.Devθ_4	0.031273
lower95	0.62822	lower95	-0.2081	lower95	-0.138681	lower95	0.007991
upper95	1.38632	upper95	0.23499	upper95	0.078273	upper95	0.130581

Appendix C: Evaluation Test Data

Sample: Texas C-LG Test Machine: Optisizer

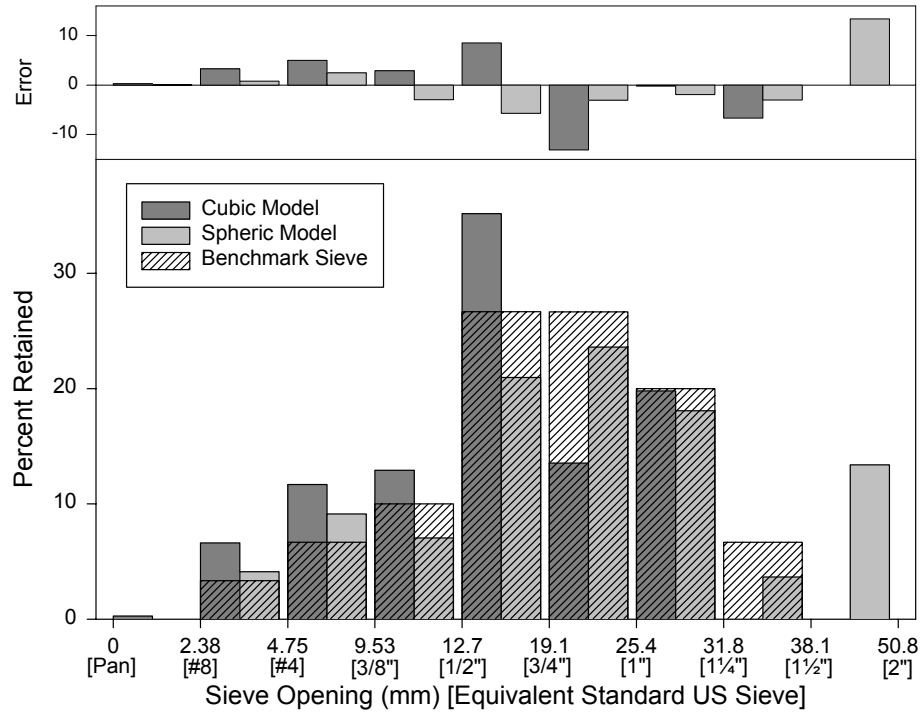

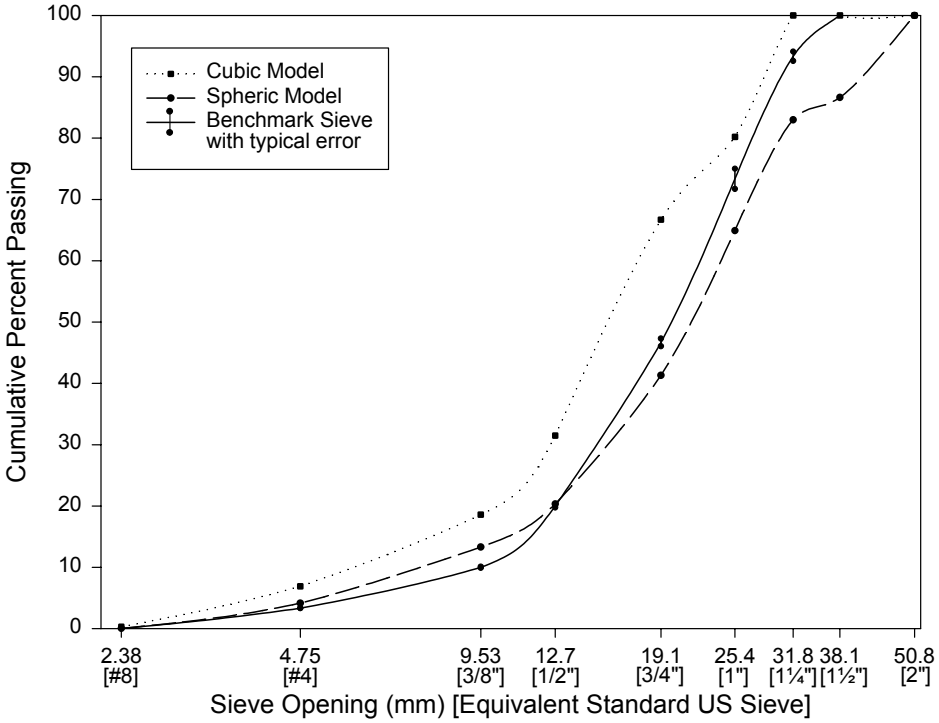

Sample: Texas C-RND	Test Machine: Optisizer

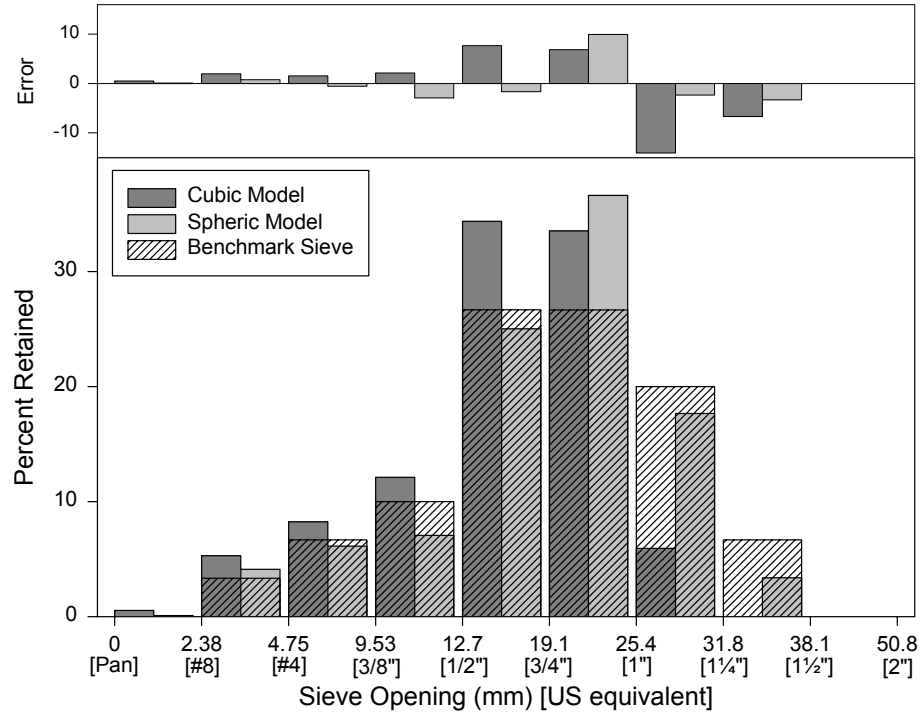

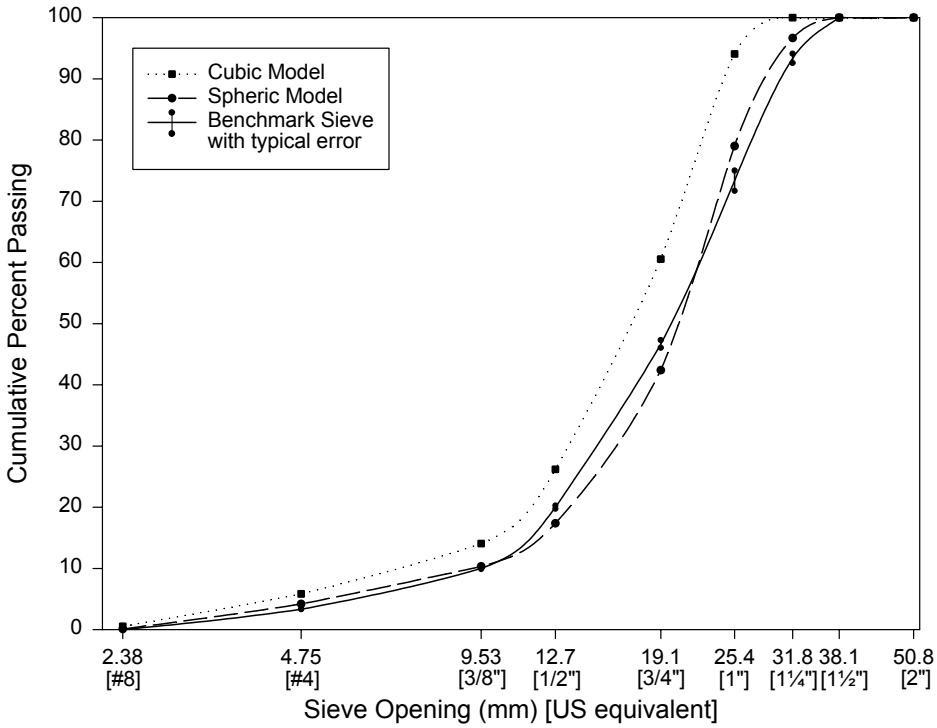

Sample: CA-C-SM	Test Machine: Optisizer

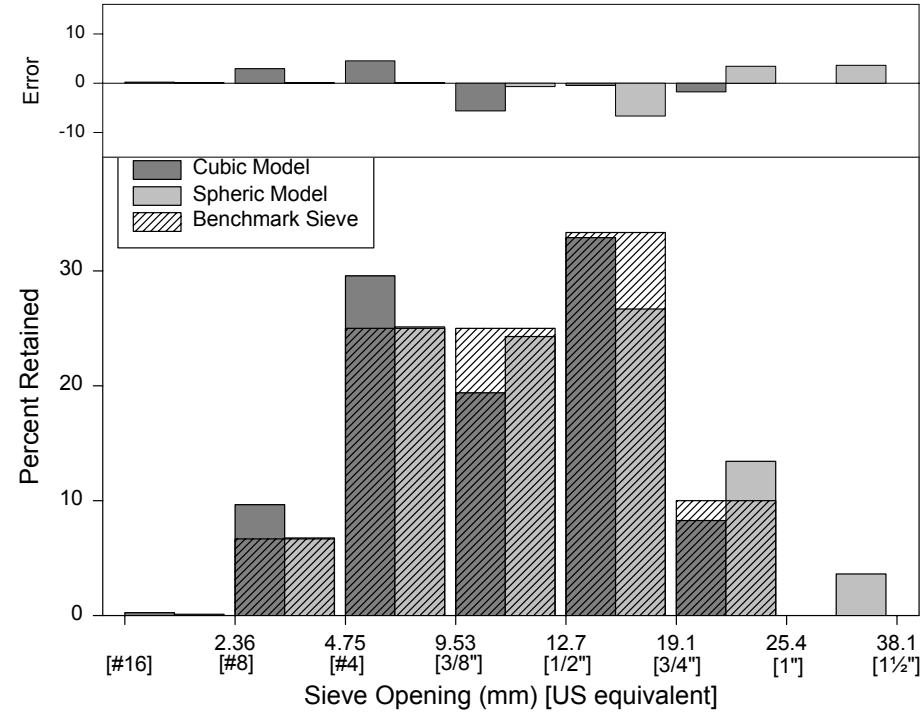

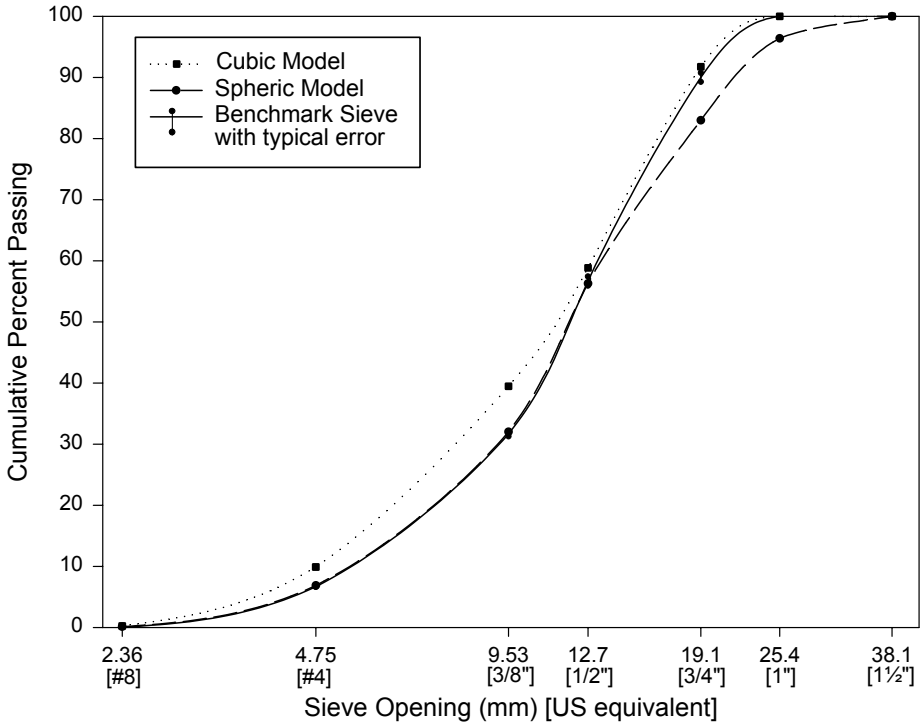

Sample: SD-C-SM Test Machine: Optisizer

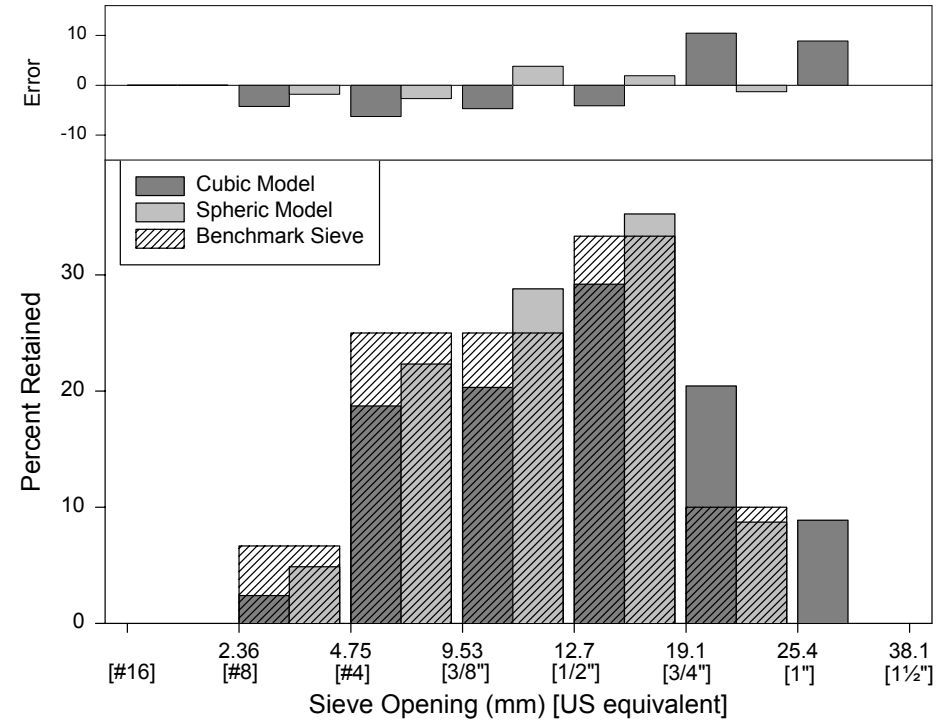

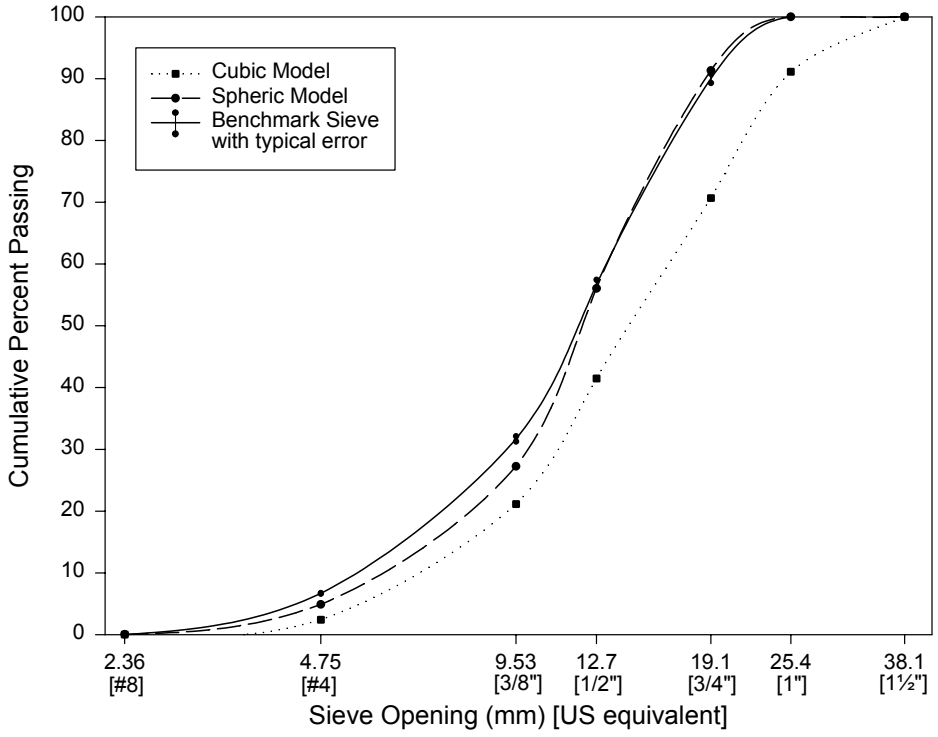

Sample: TX-C-SM	Test Machine: Optisizer

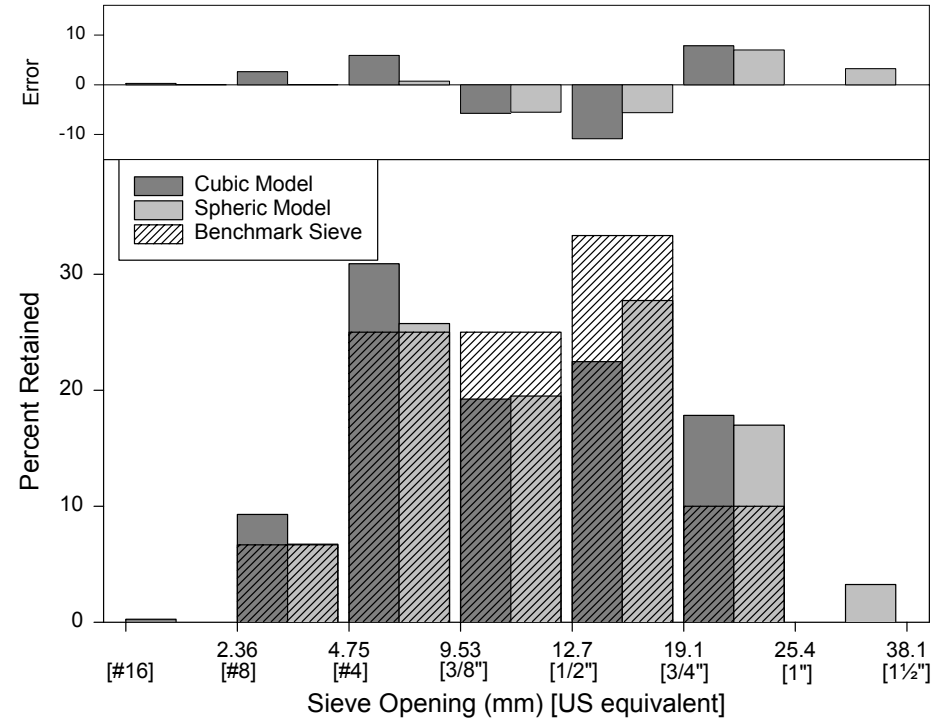

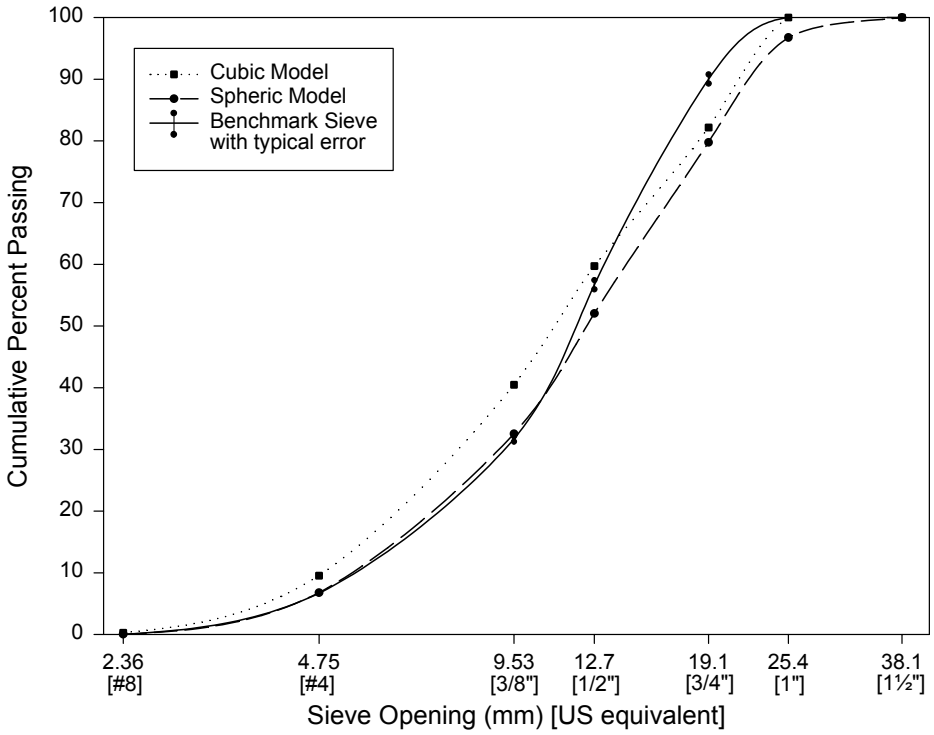

Sample: VA-C-SM	Test Machine: Optisizer

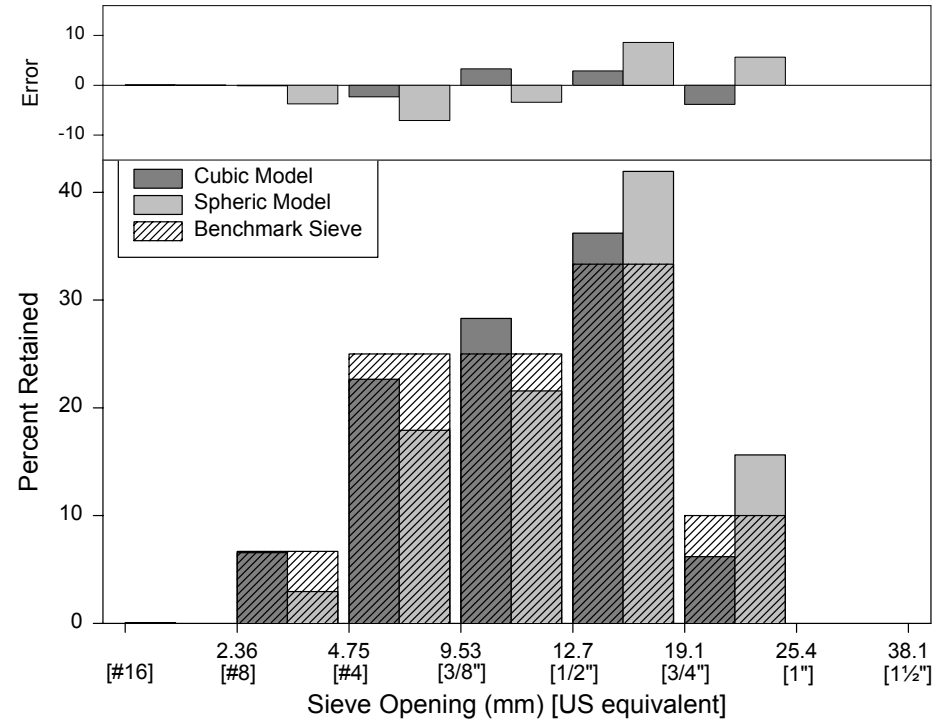

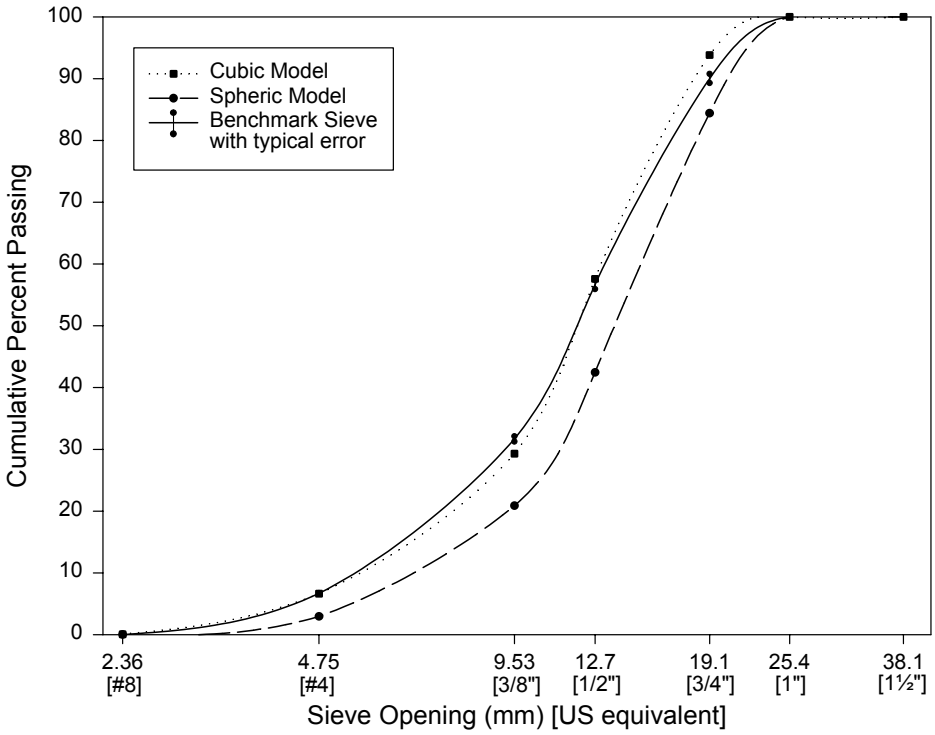

Sample: CA-C-STD	Test Machine: Optisizer

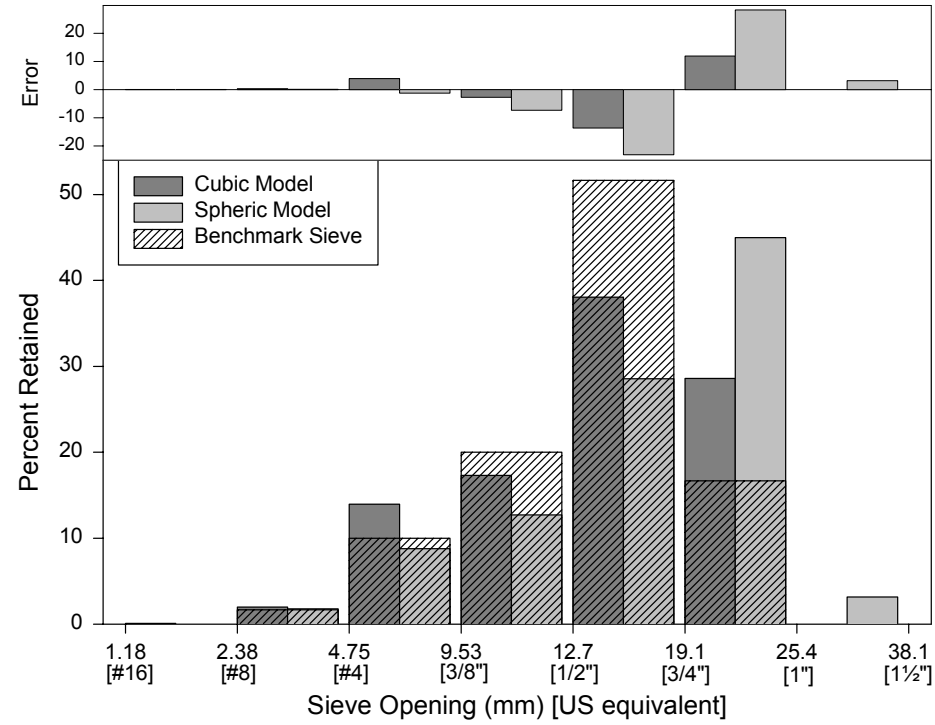

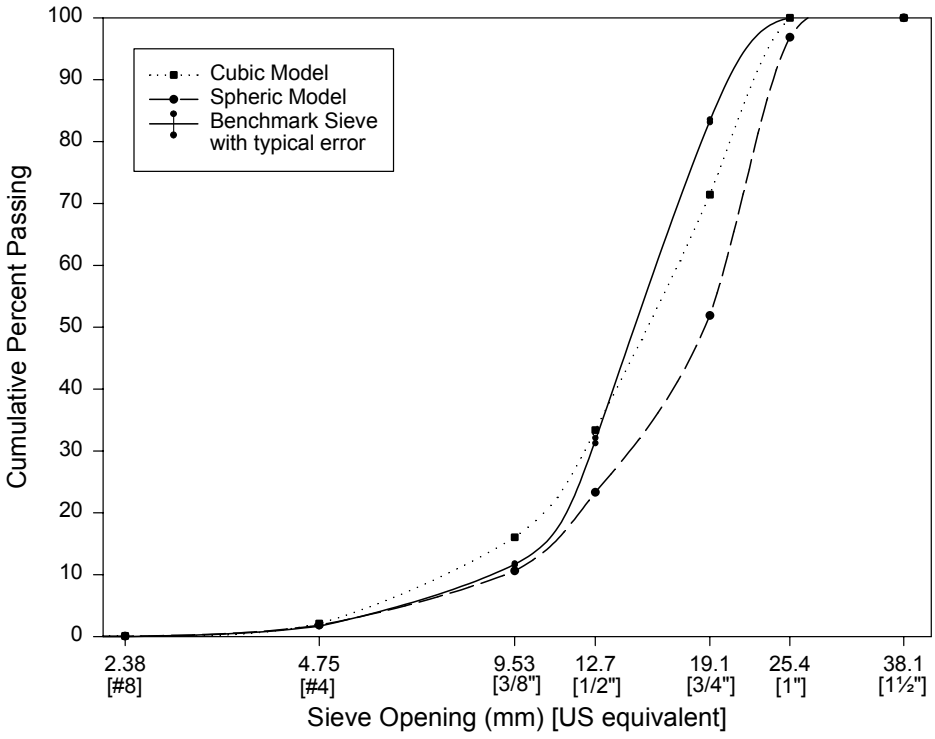

Sample: SD-C-STD	Test Machine: Optisizer

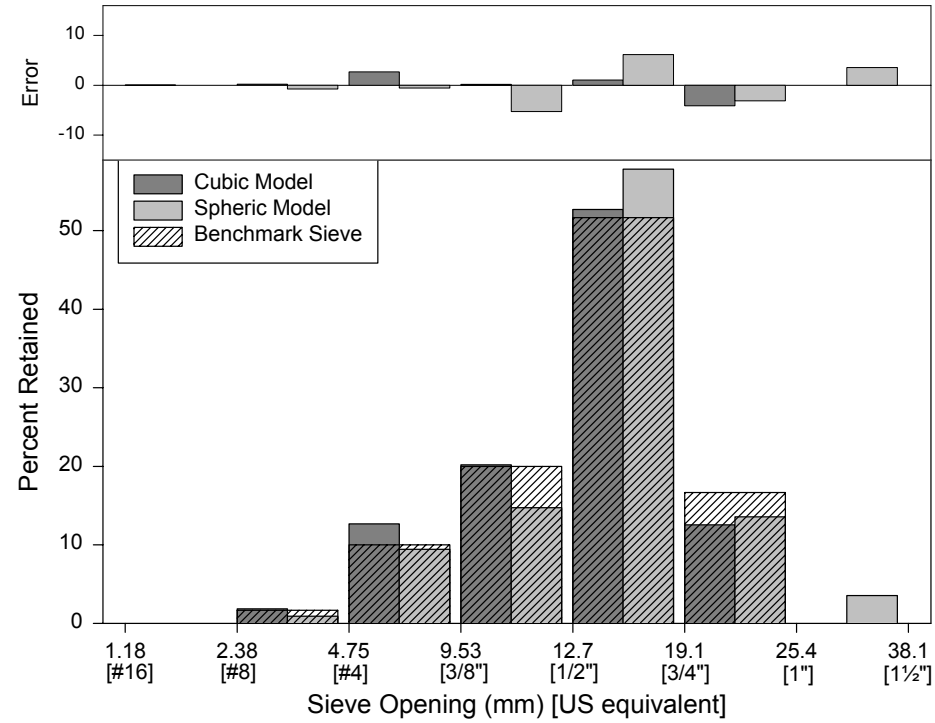

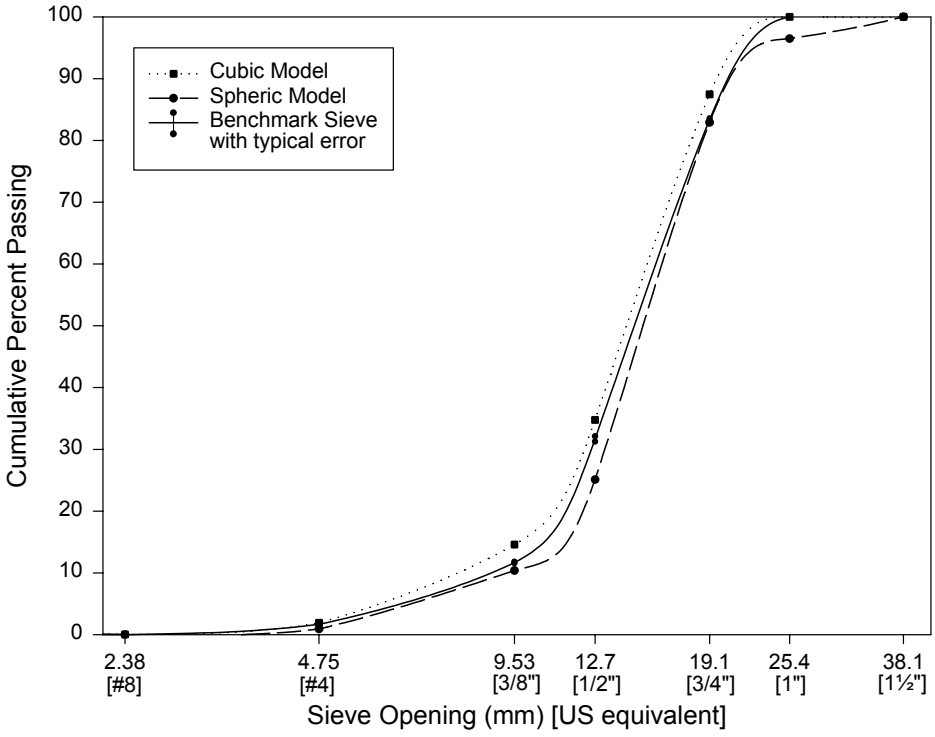

Sample: TX-C-STD	Test Machine: Optisizer

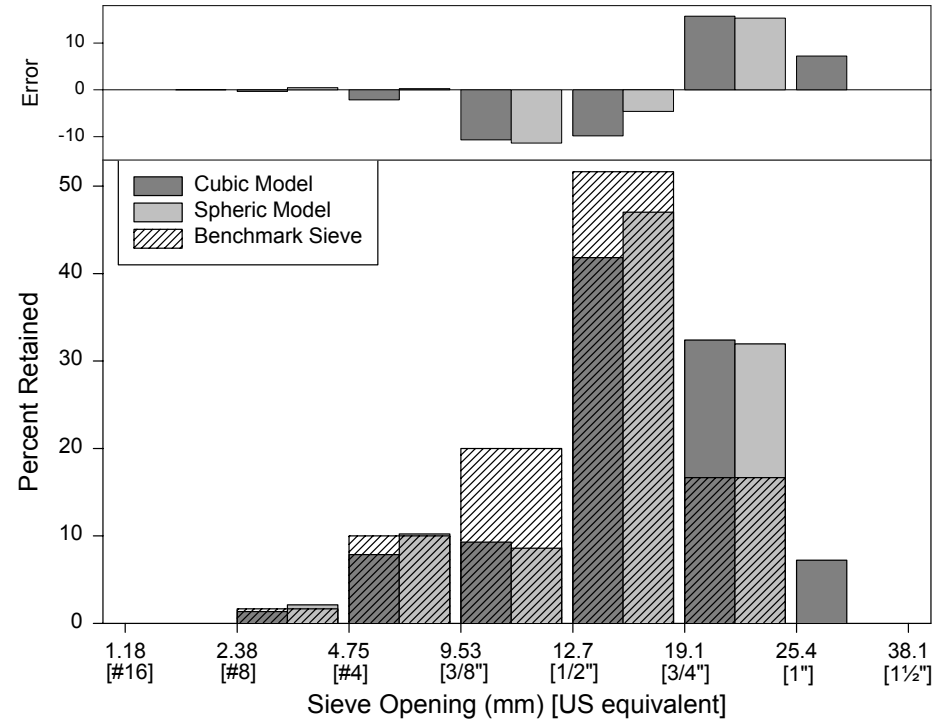

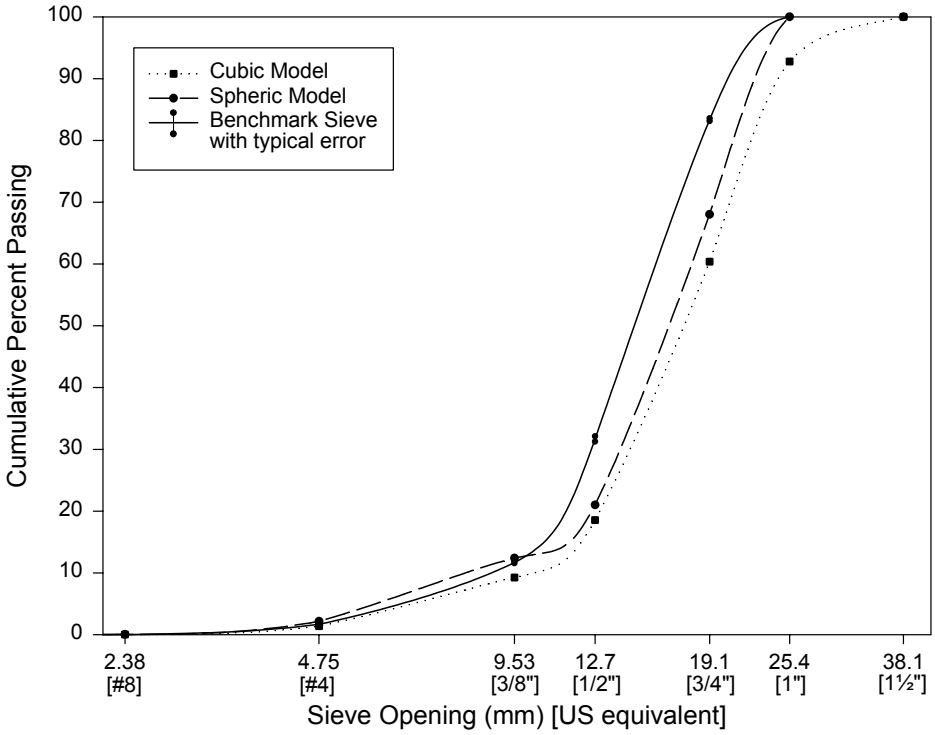

Sample: VA-C-STD	Test Machine: Optisizer

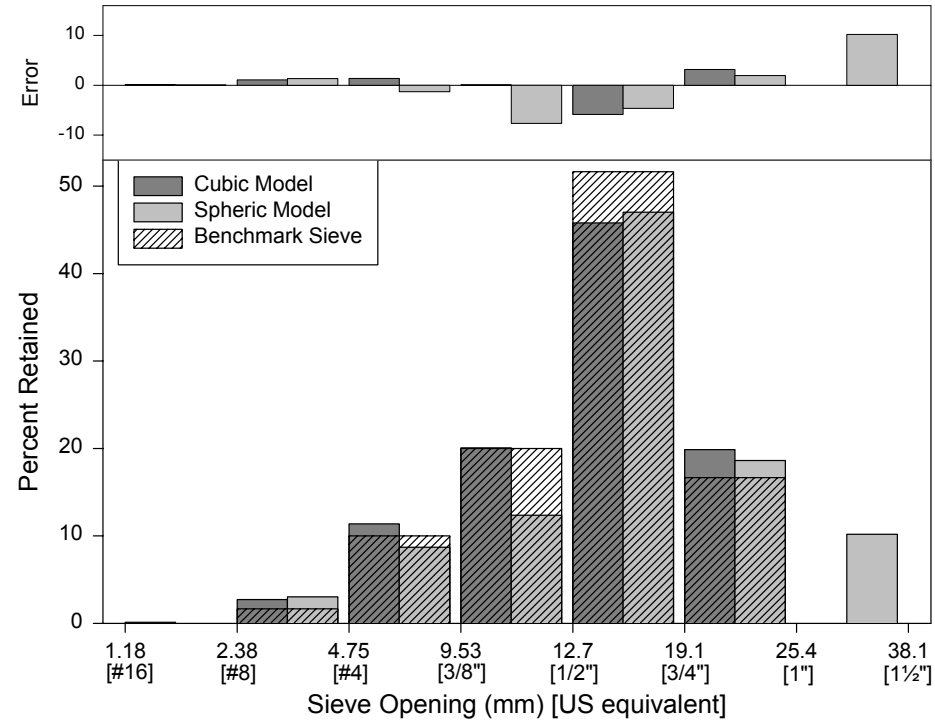

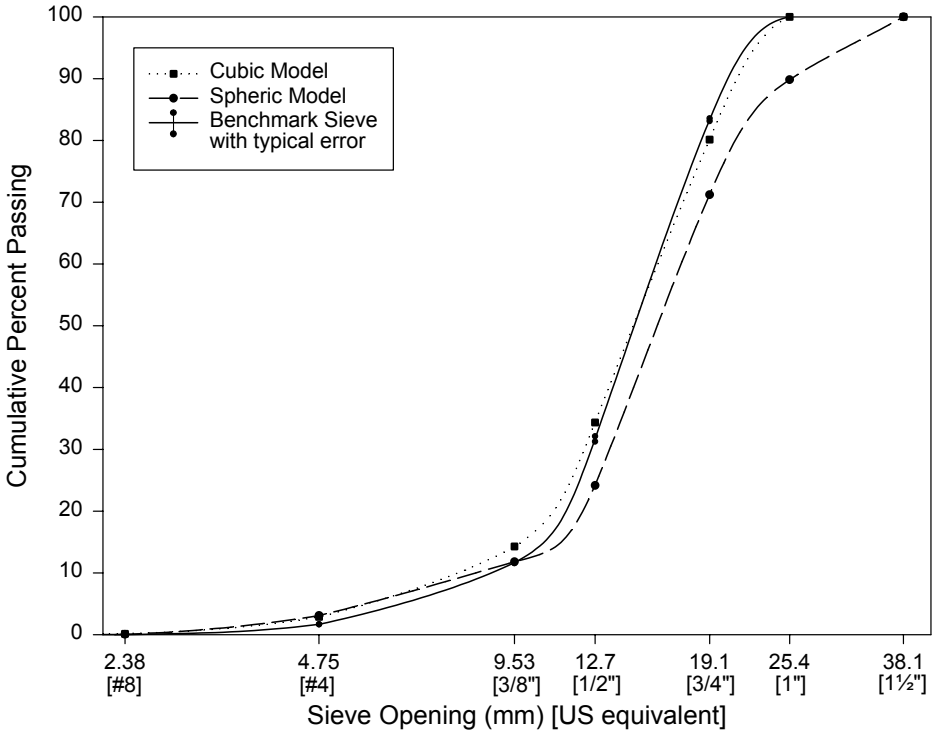

Sample: TX-F-FTC	Test Machine: Optisizer

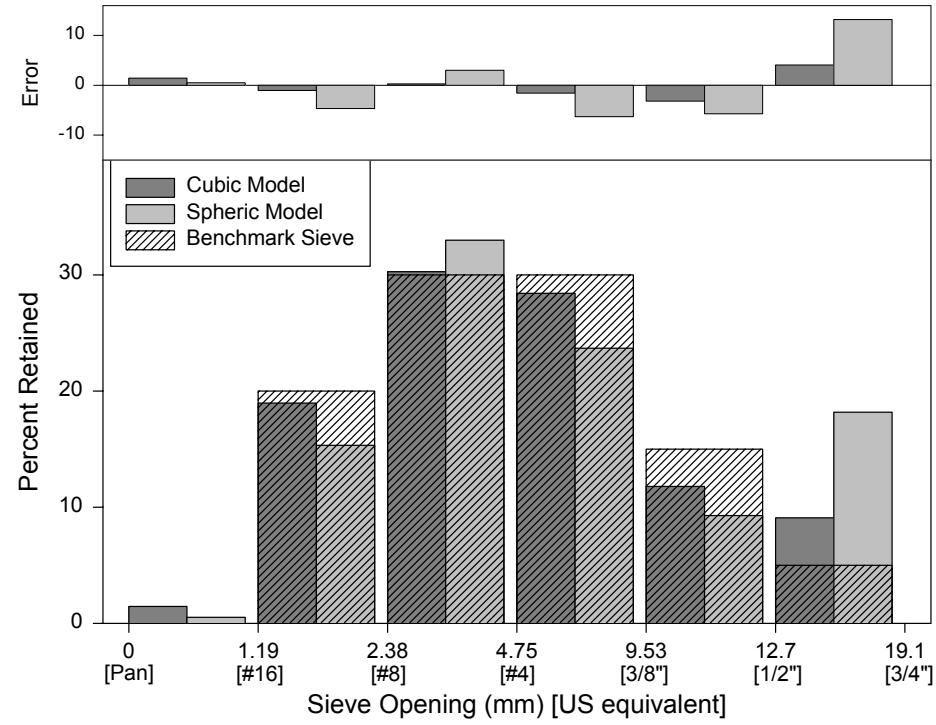

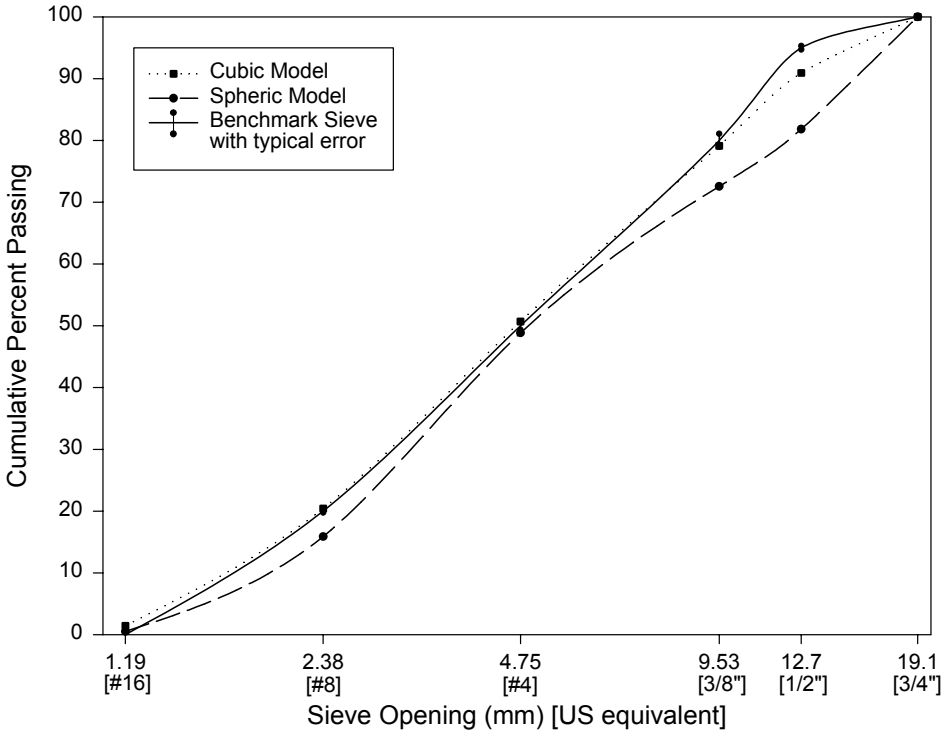

Sample: VA-F-FTC Test Machine: Optisizer

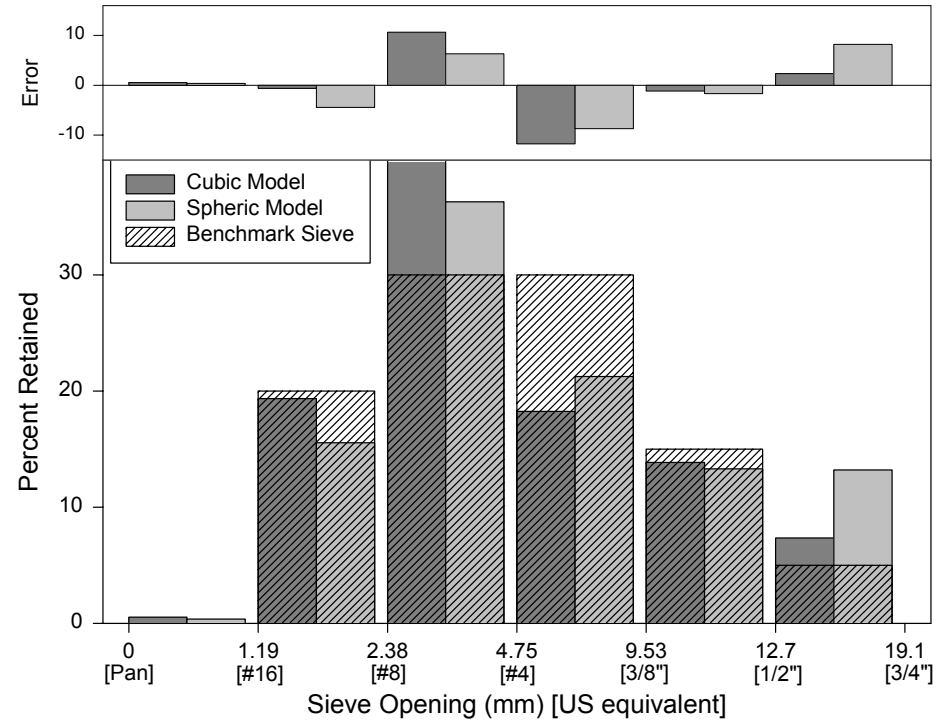

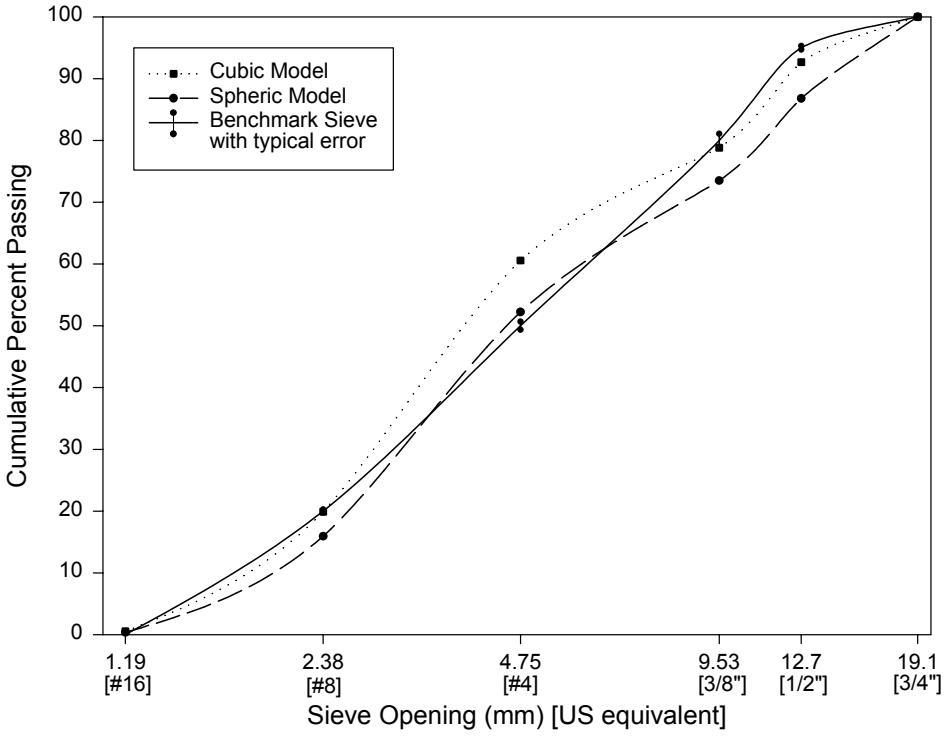

Sample: GA-F-STD Test Machine: Optisizer

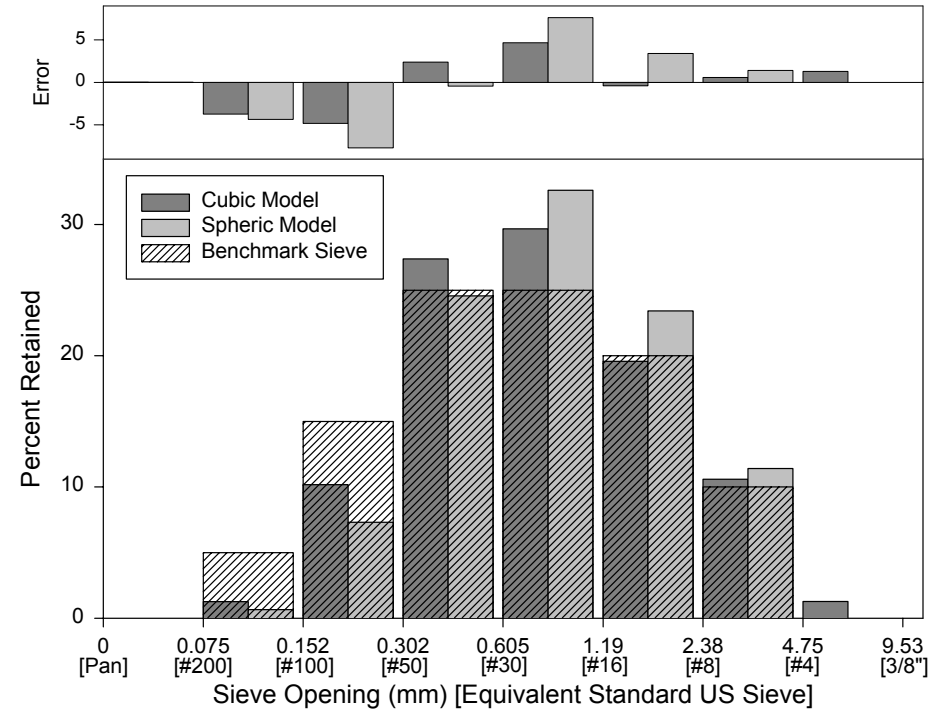

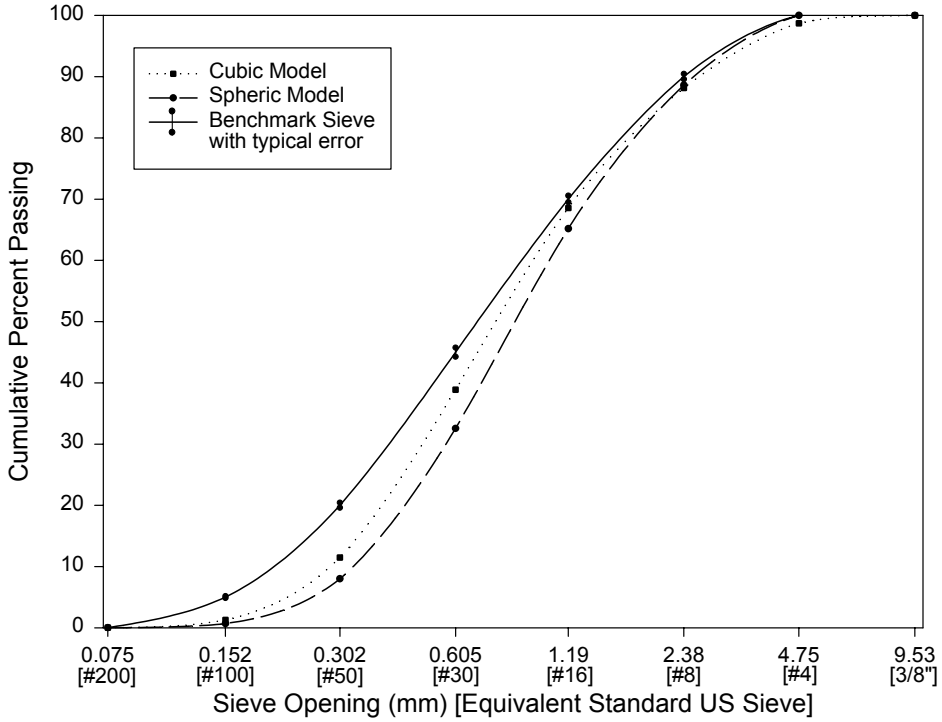

Sample: TX-F-STD Test Machine: Optisizer

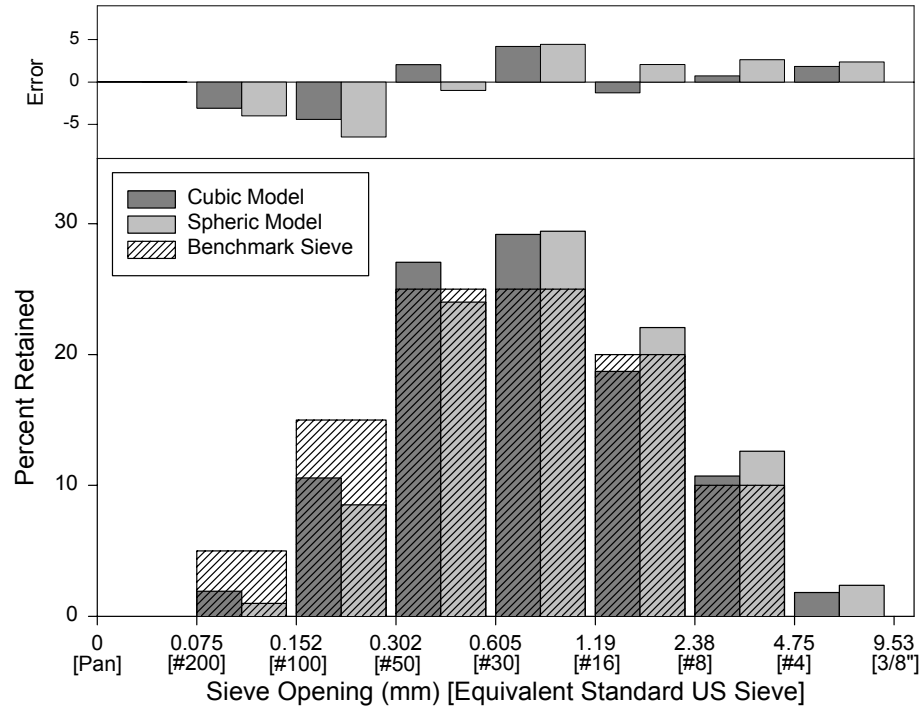

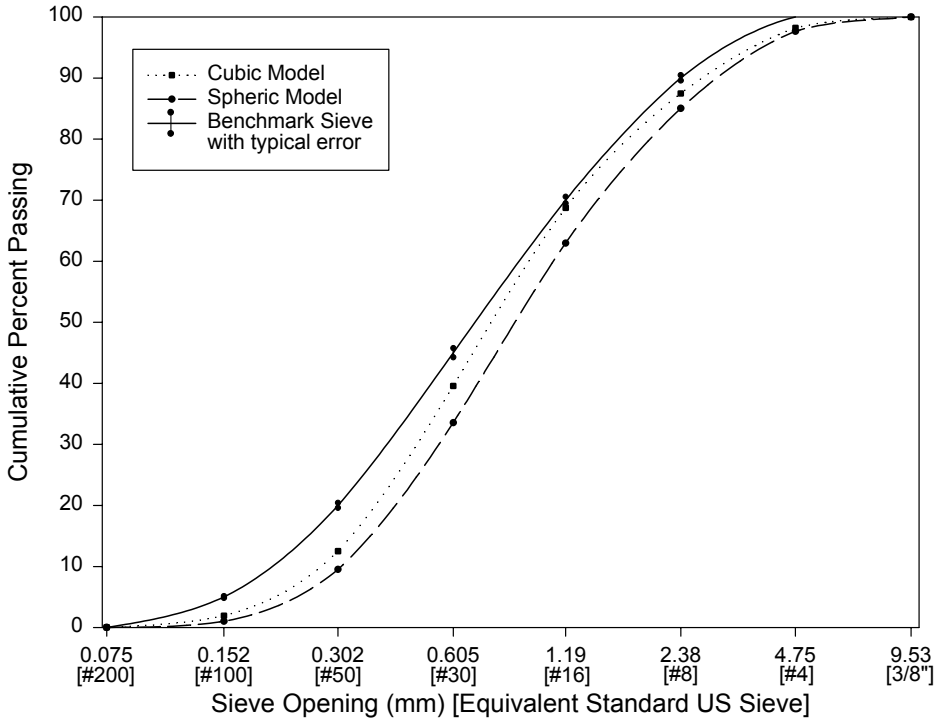

Sample: VA-F-STD Test Machine: Optisizer

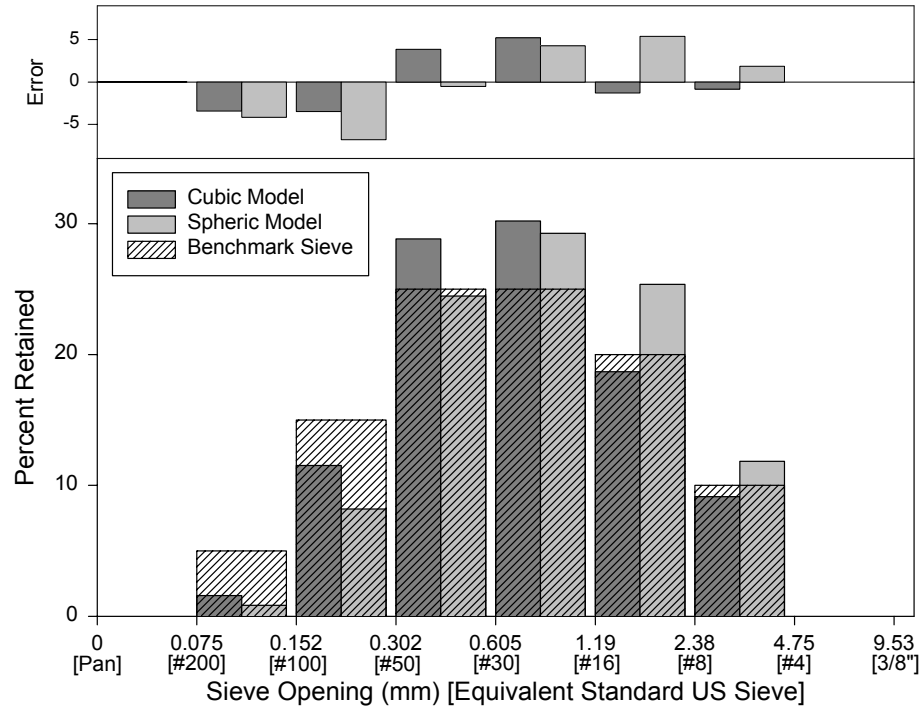

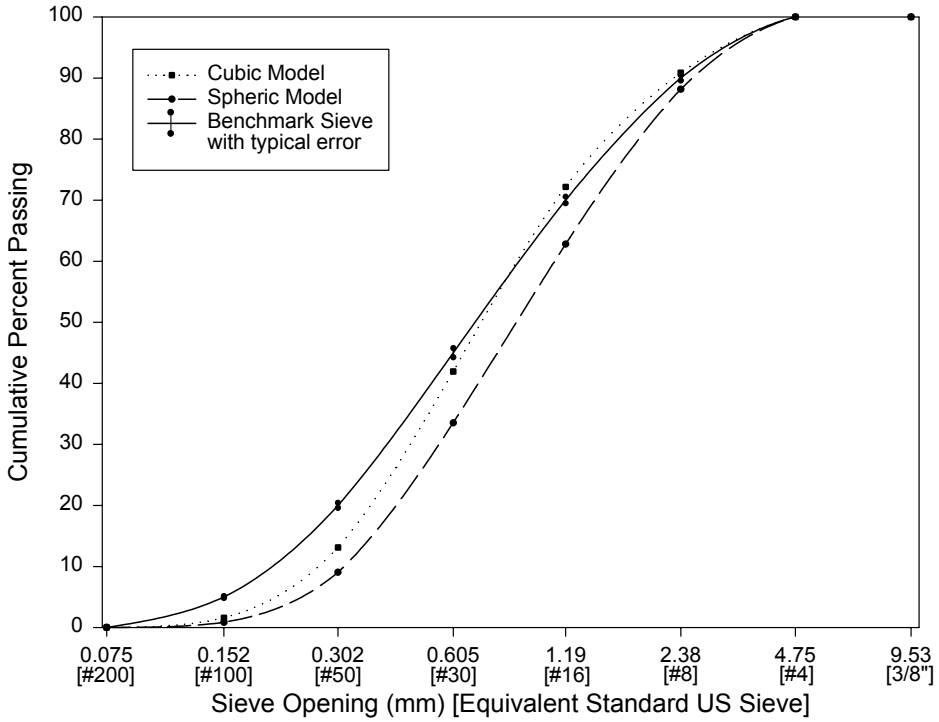

Sample: Texas C-LG Test Machine: VDG-40

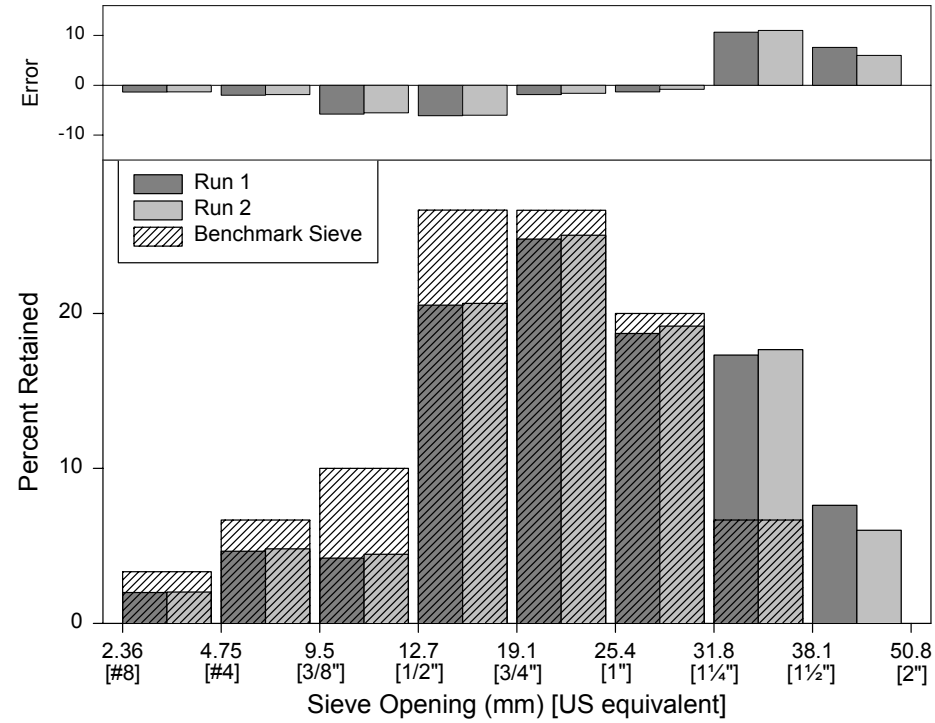

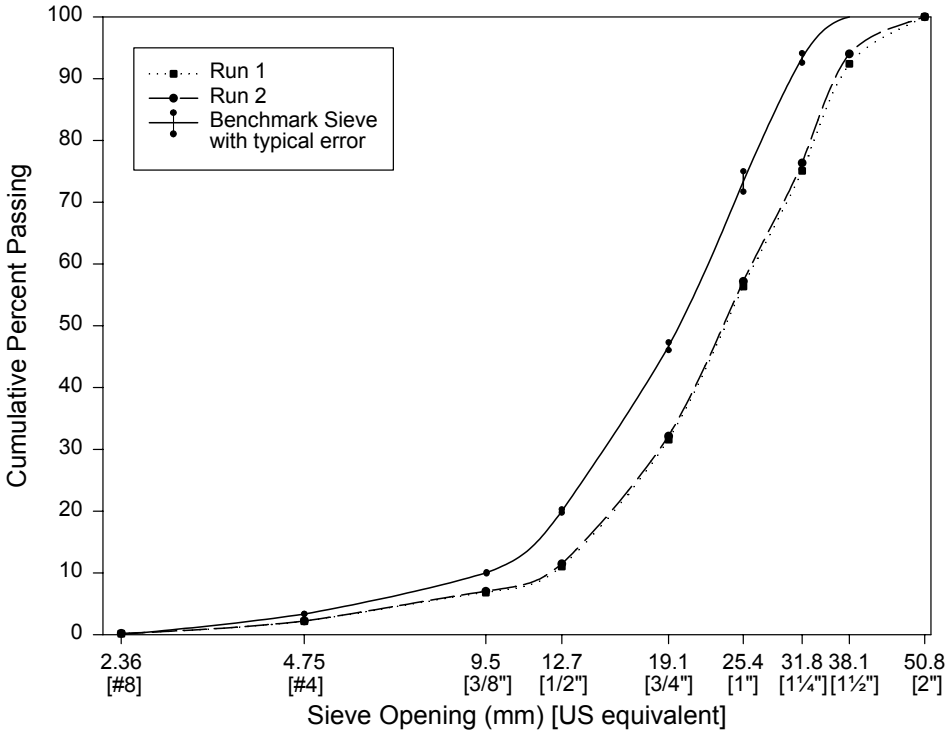

Sample: Texas C-RND Test Machine: VDG-40

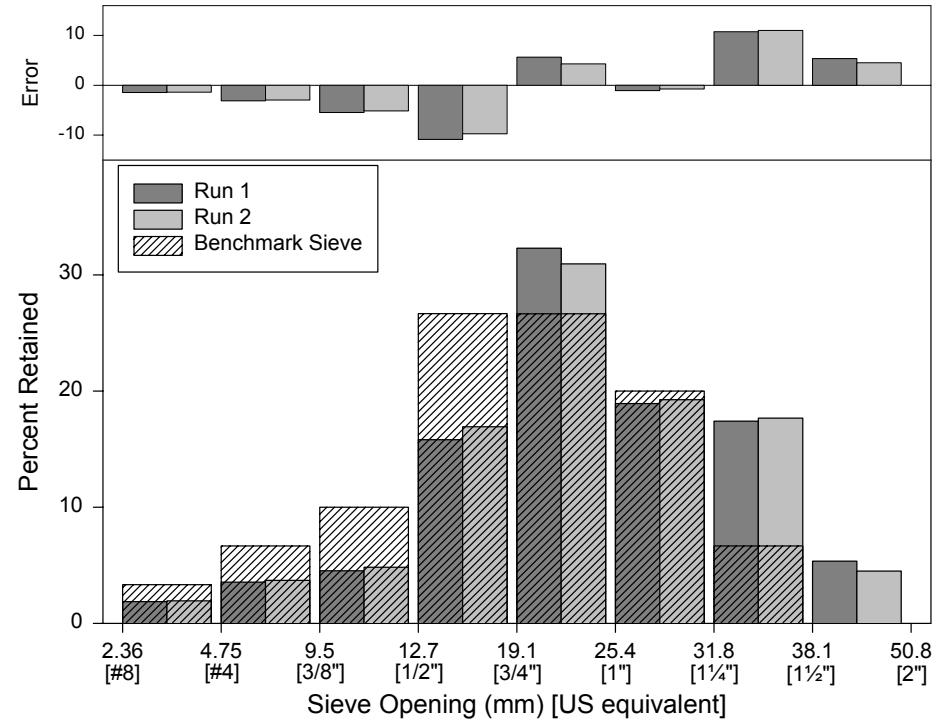

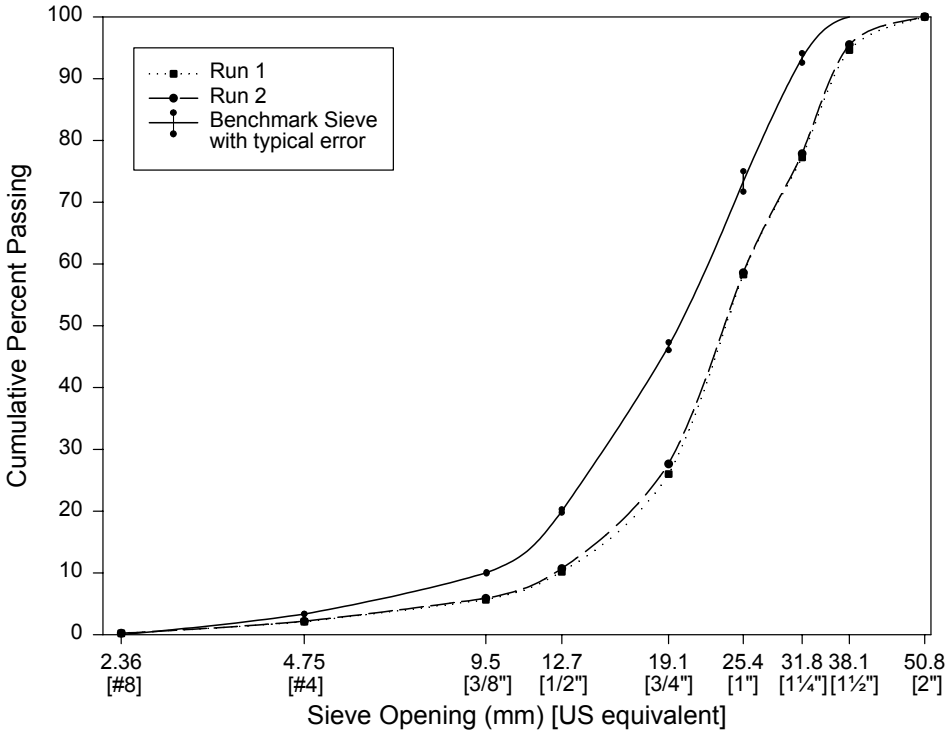

Sample: CA-C-SM	Test Machine: VDG-40

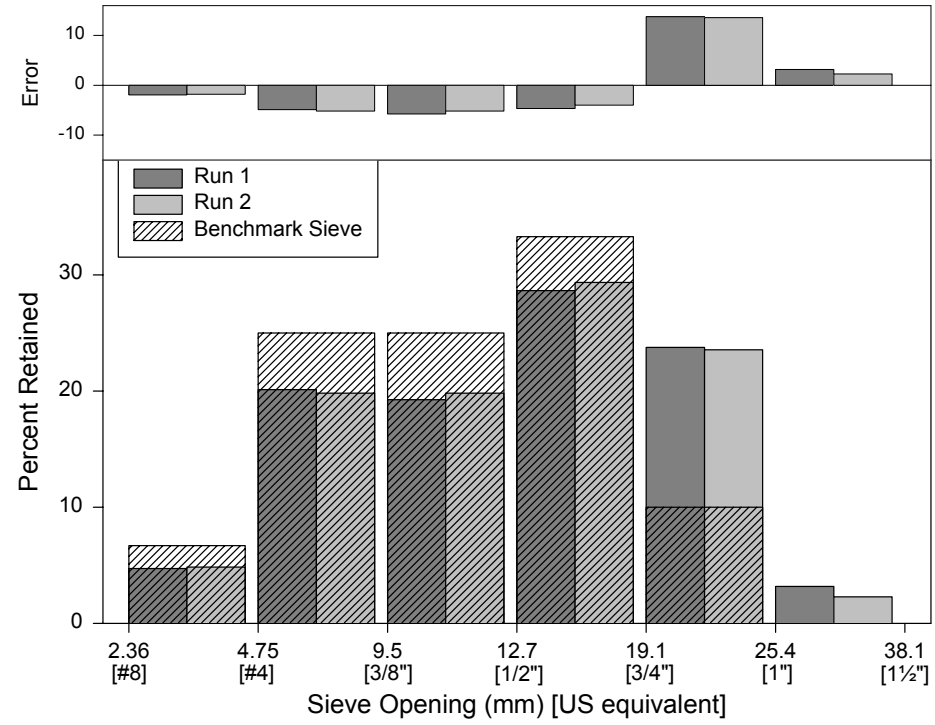

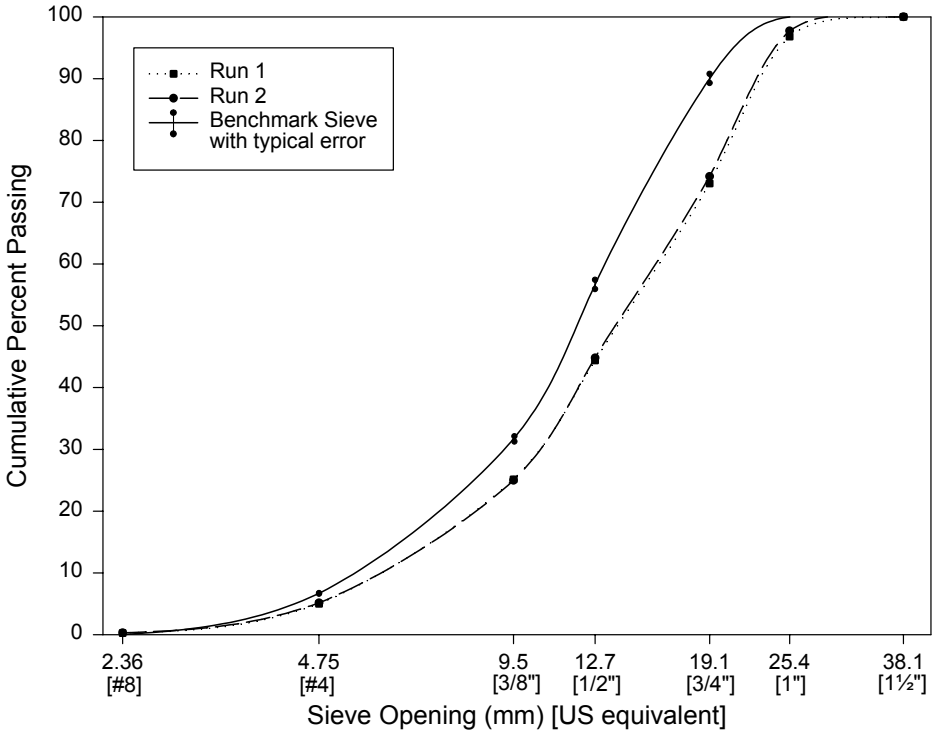

Sample: SD-C-SM	Test Machine: VDG-40

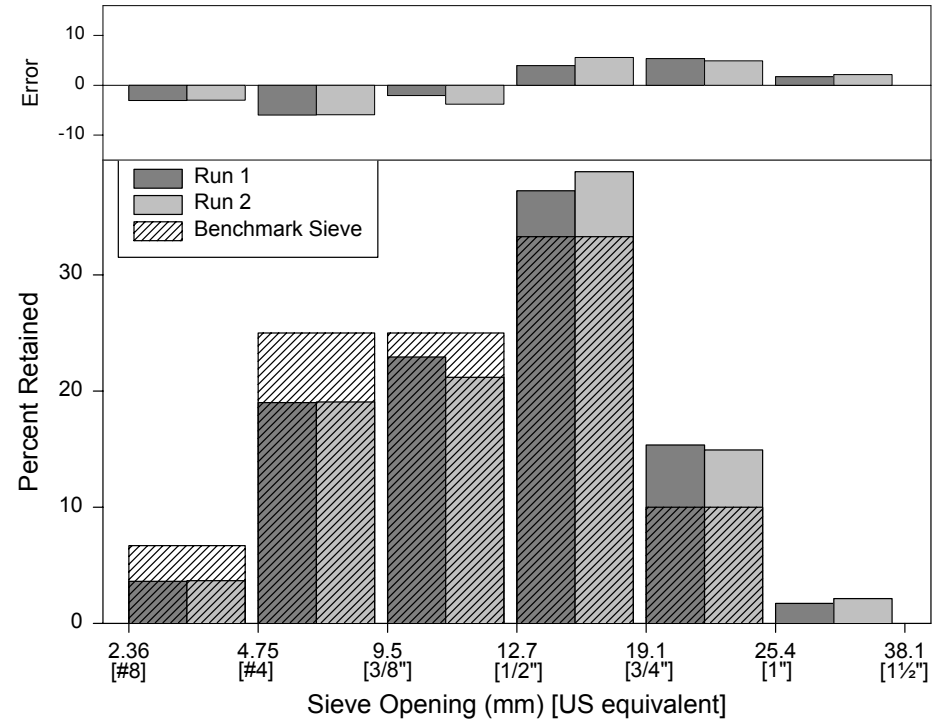

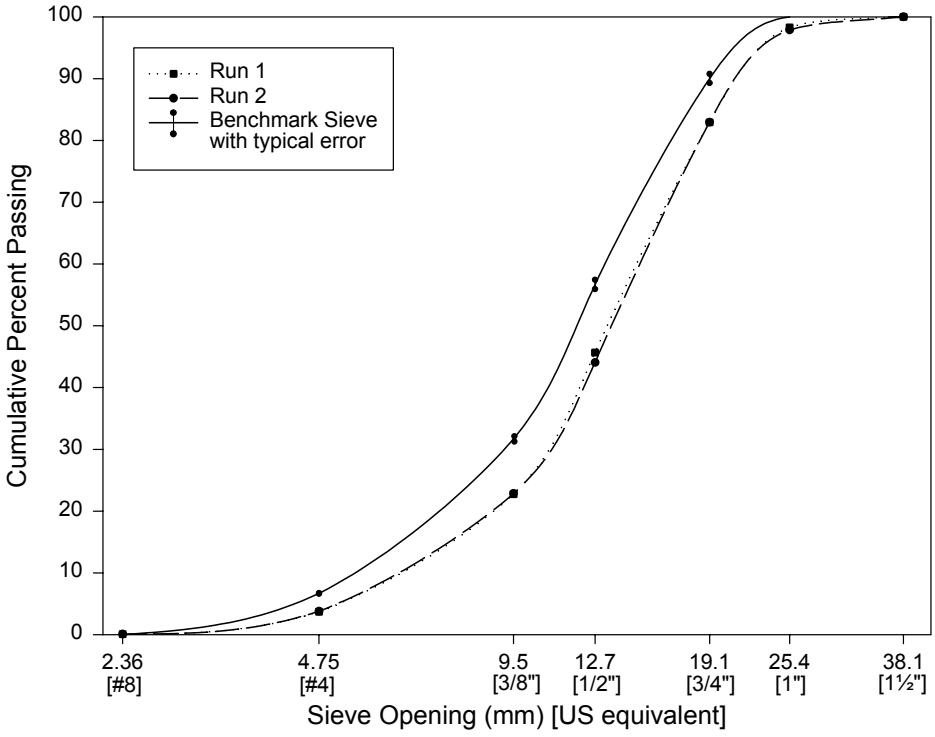

Sample: TX-C-SM Test Machine: VDG-40

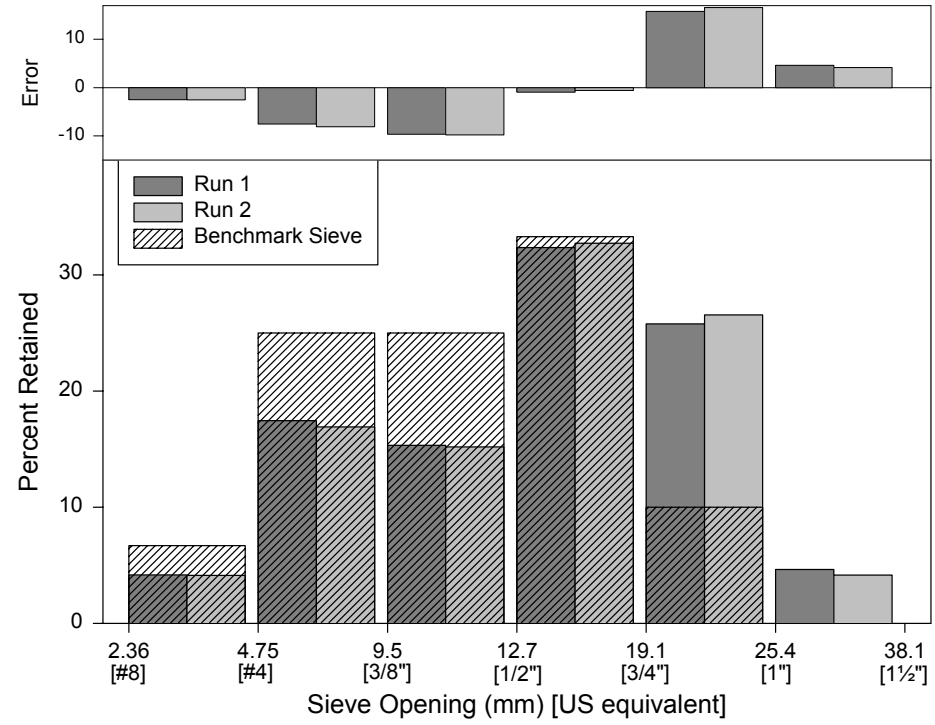

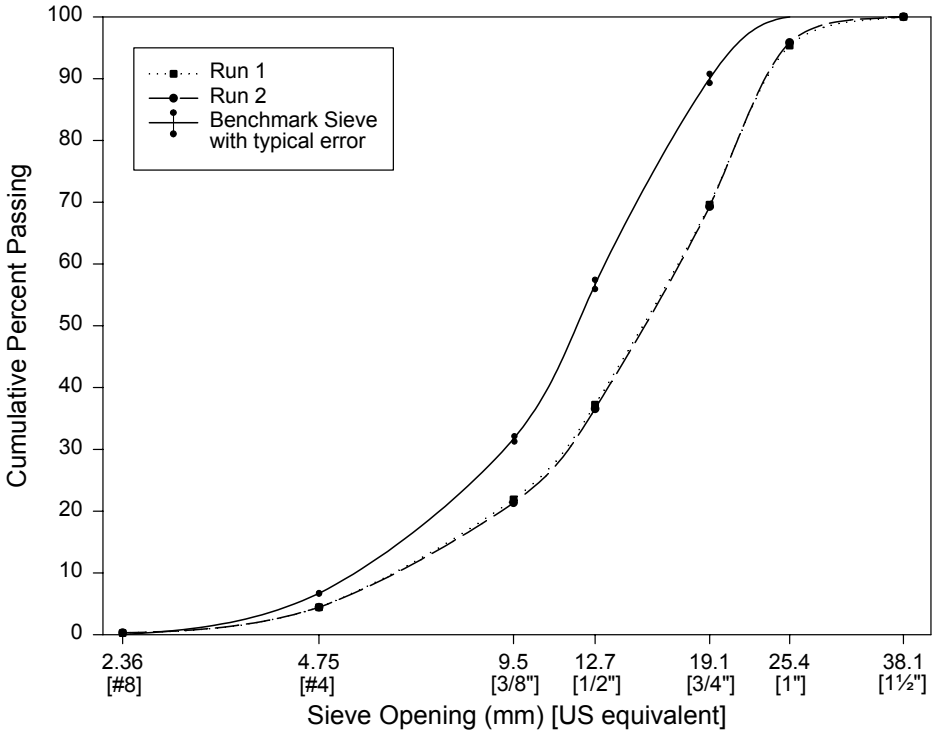

Sample: VA-C-SM	Test Machine: VDG-40

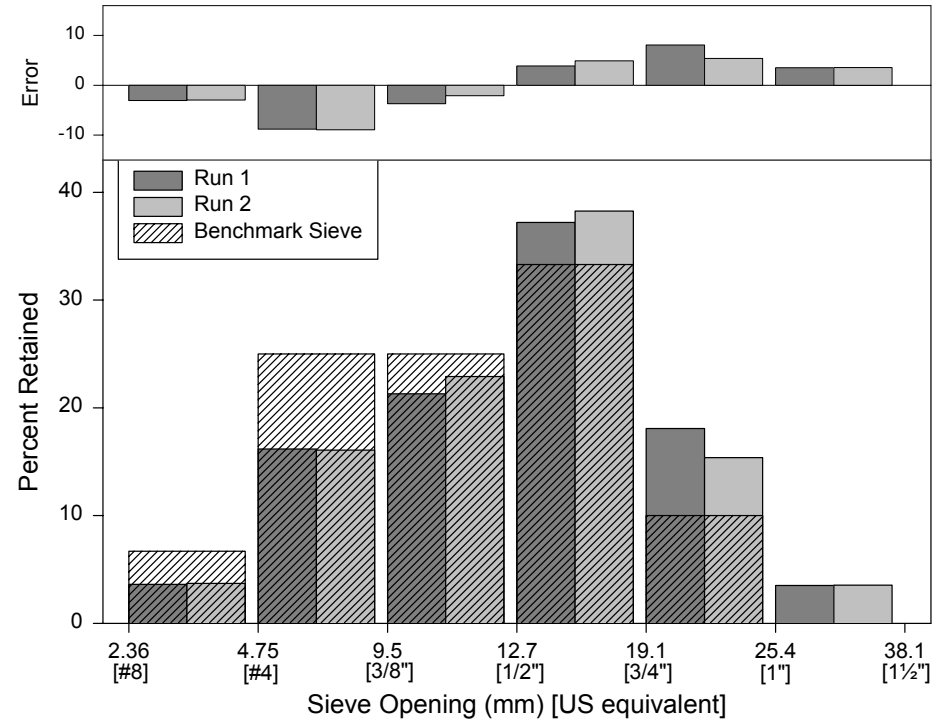

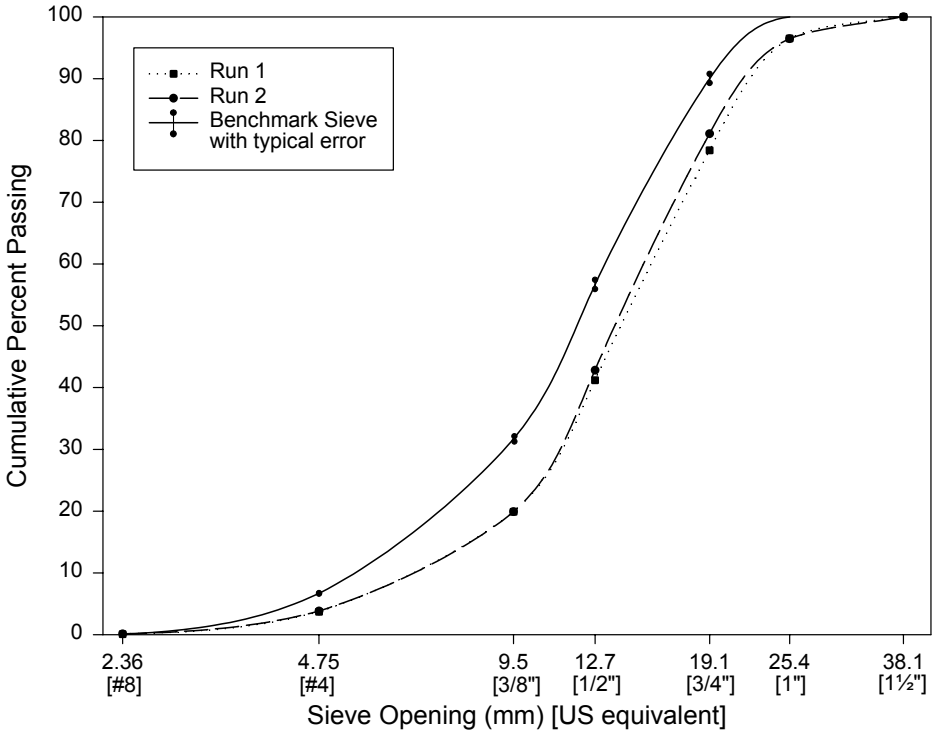

Sample: CA-C-STD	Test Machine: VDG-40

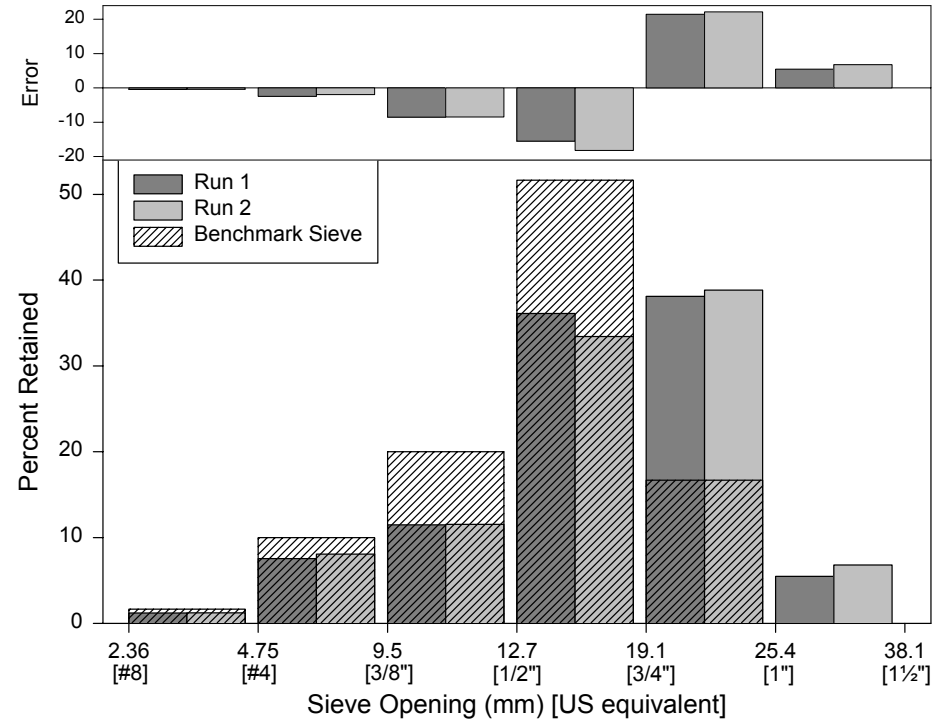

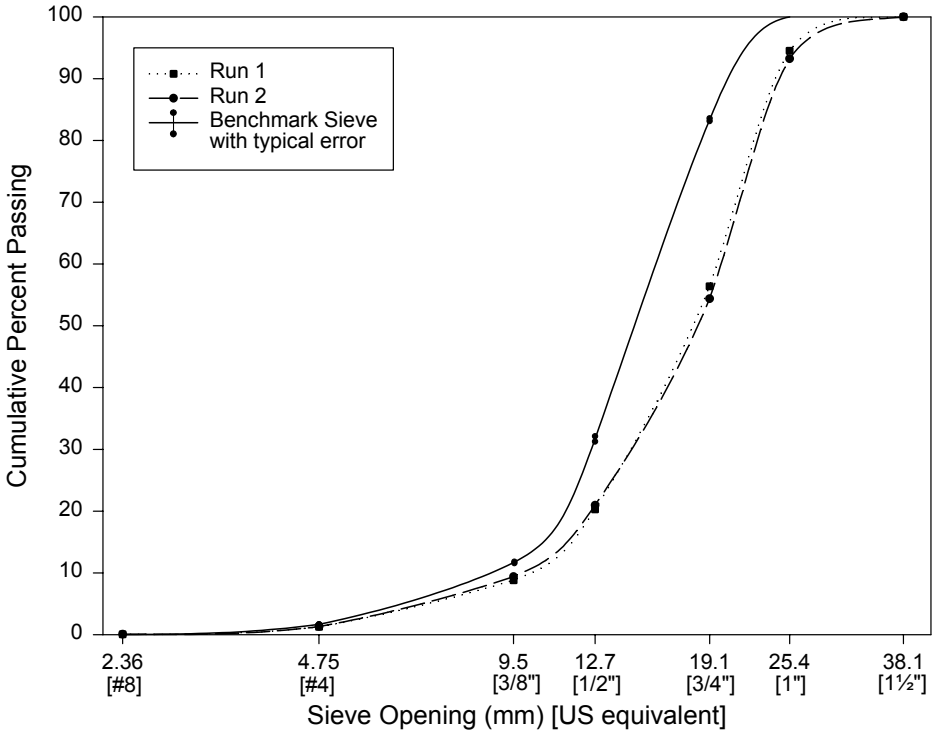

Sample: SD-C-STD	Test Machine: VDG-40

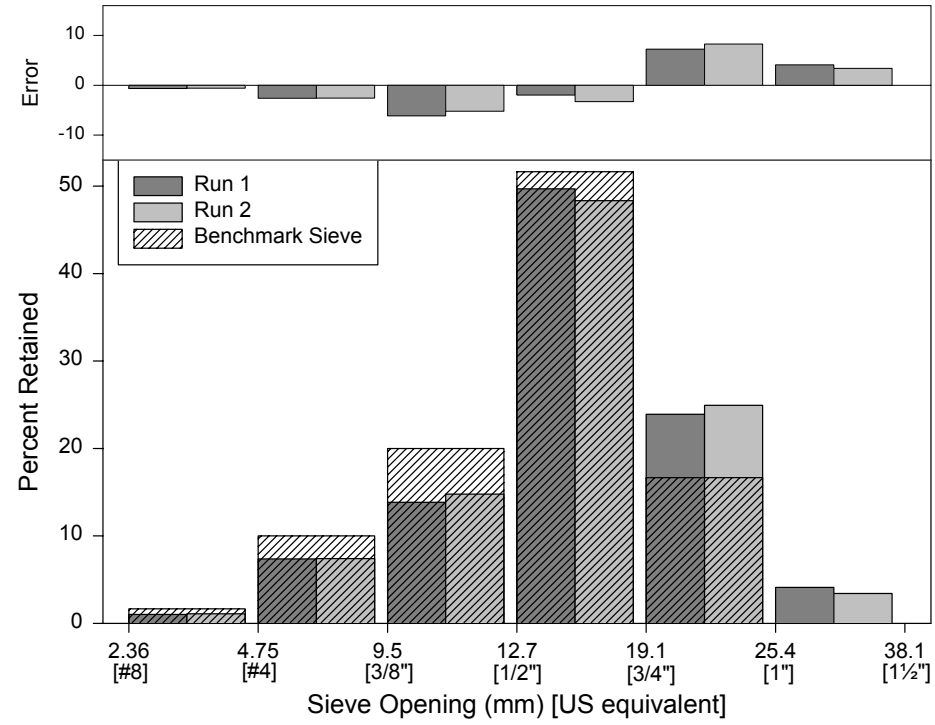

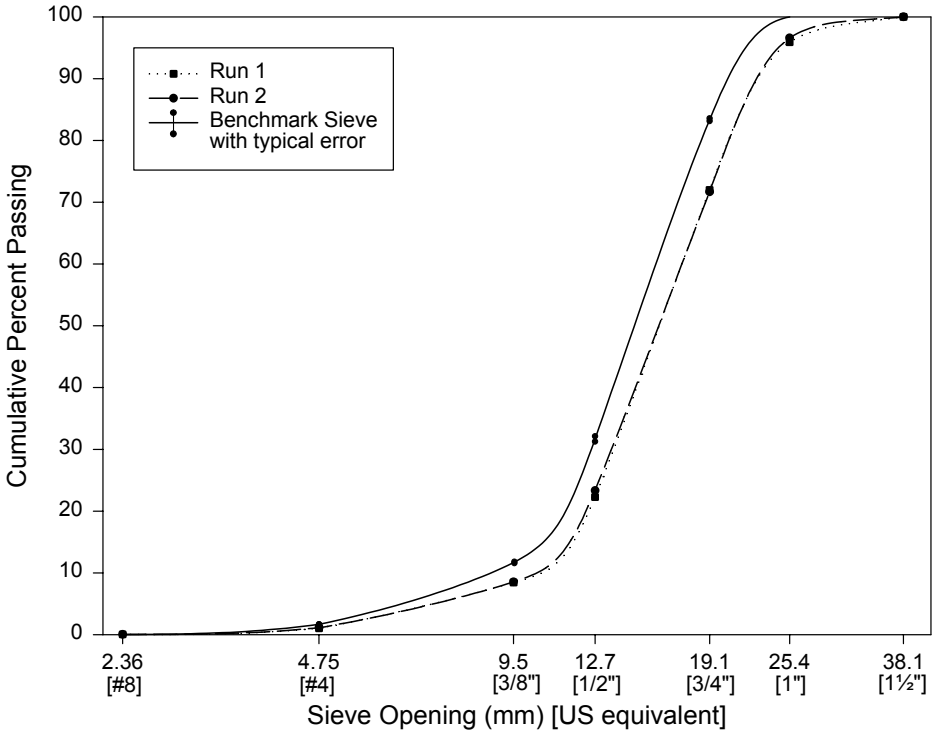

Sample: TX-C-STD	Test Machine: VDG-40

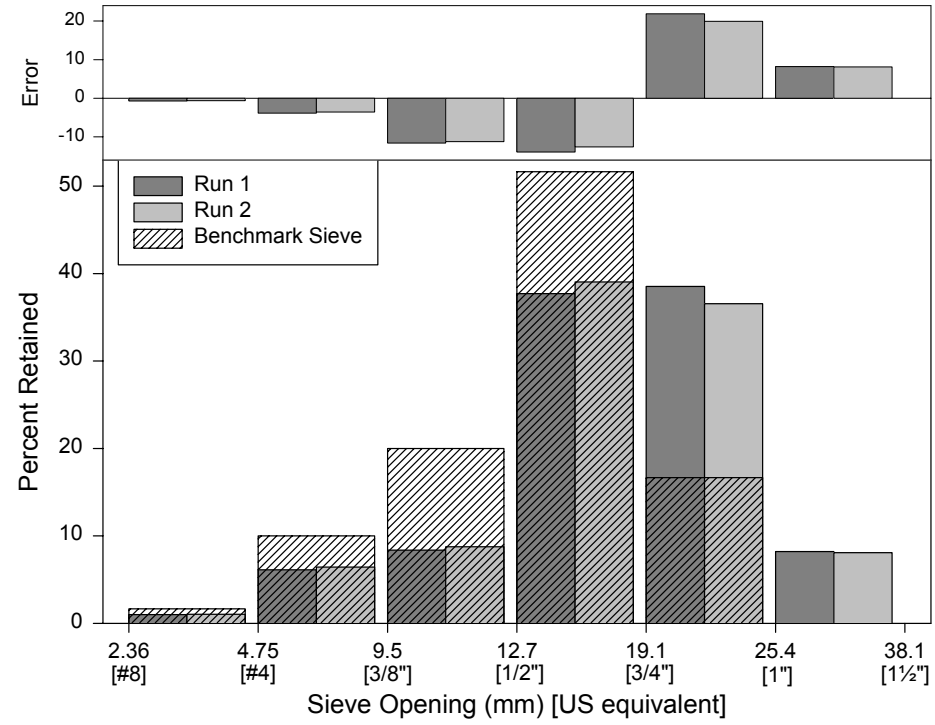

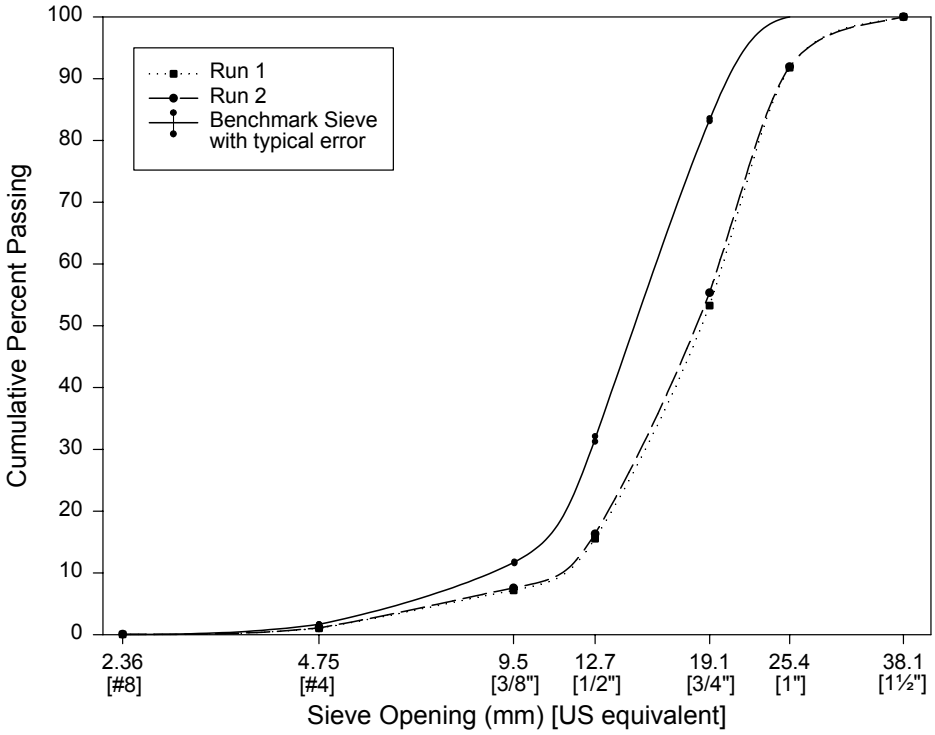

Sample: VA-C-STD	Test Machine: VDG-40

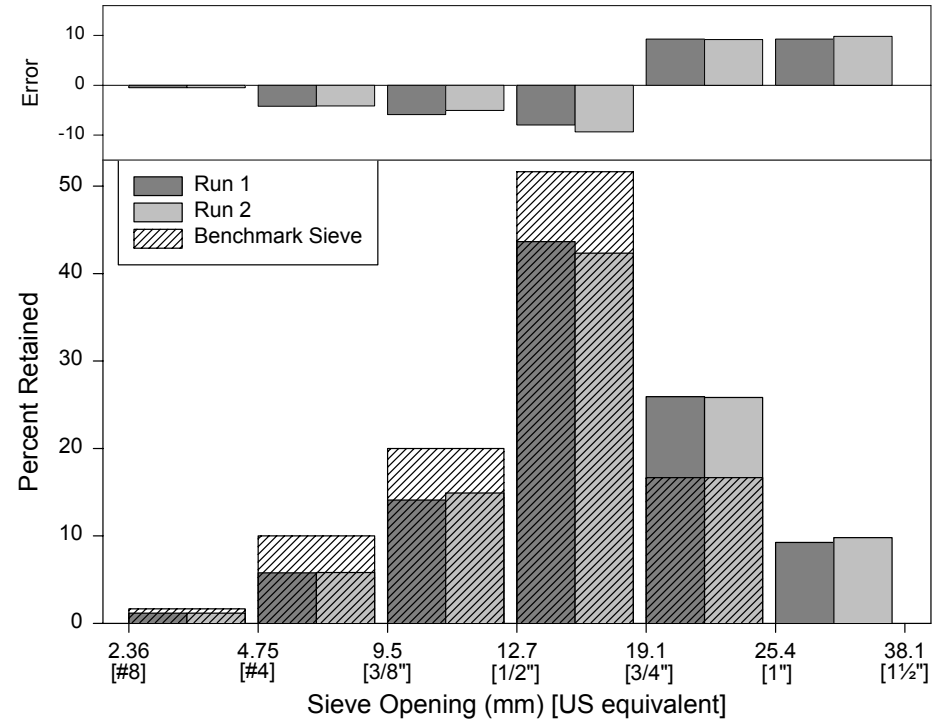

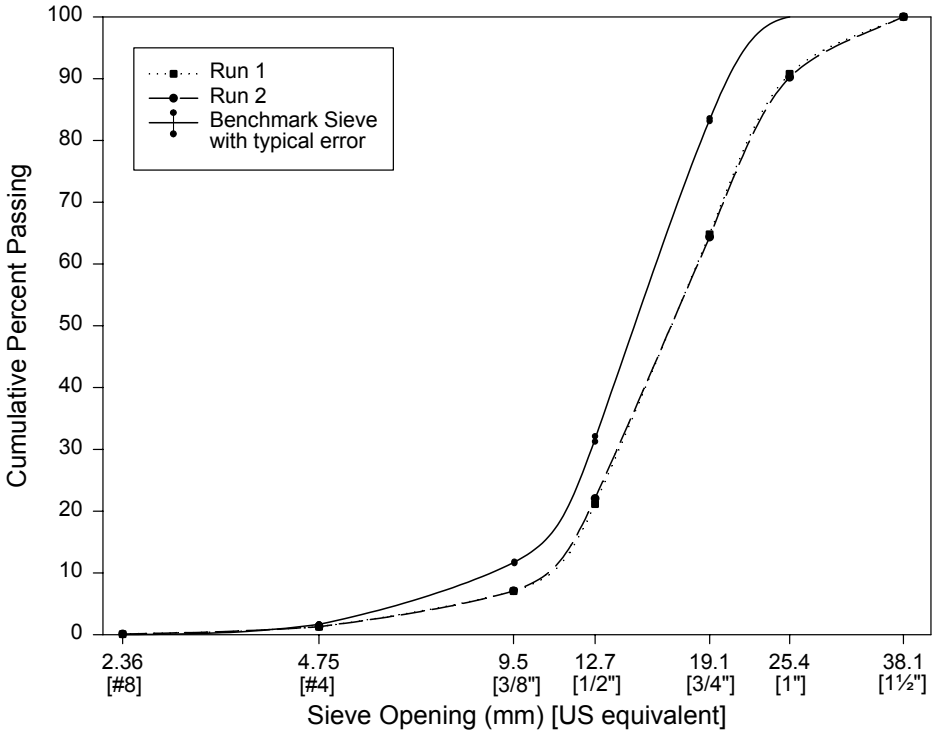

Sample: TX-F-FTC	Test Machine: VDG-40

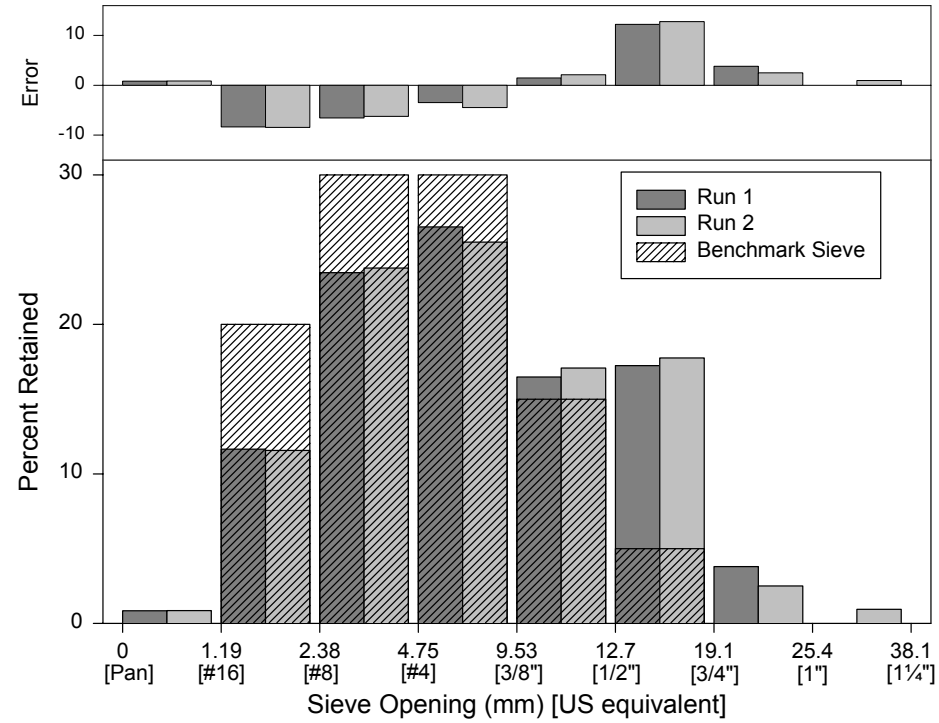

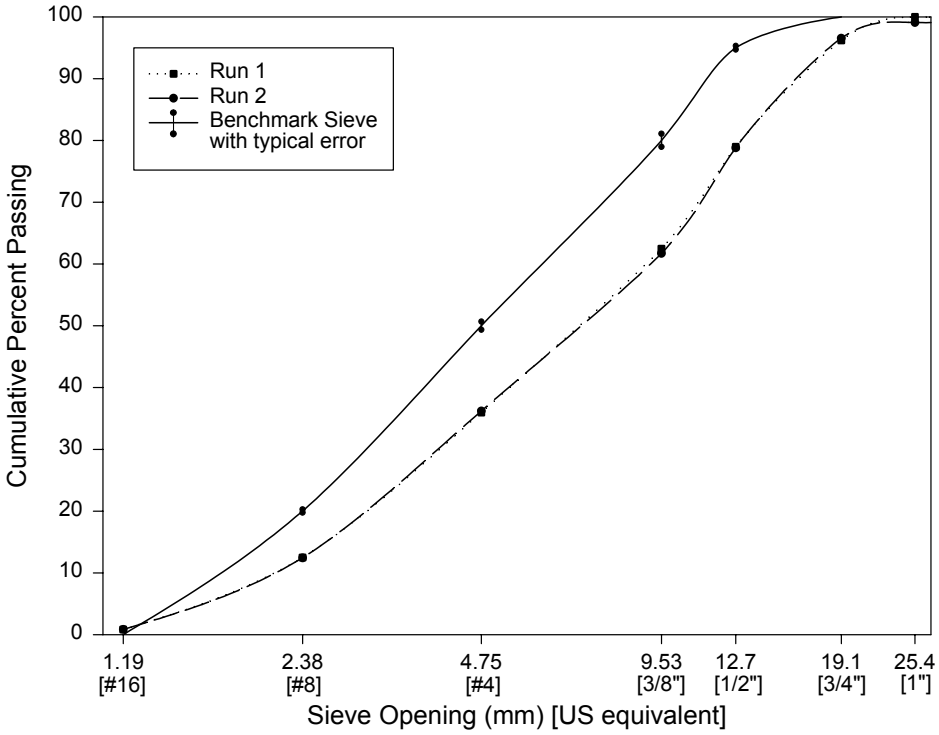

Sample: VA-F-FTC	Test Machine: VDG-40

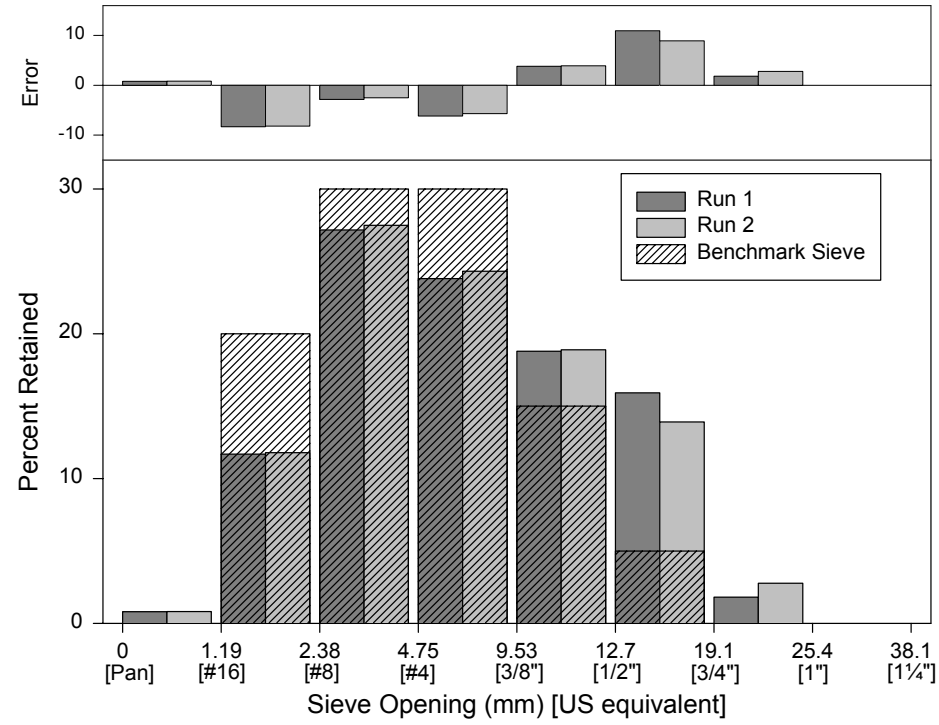

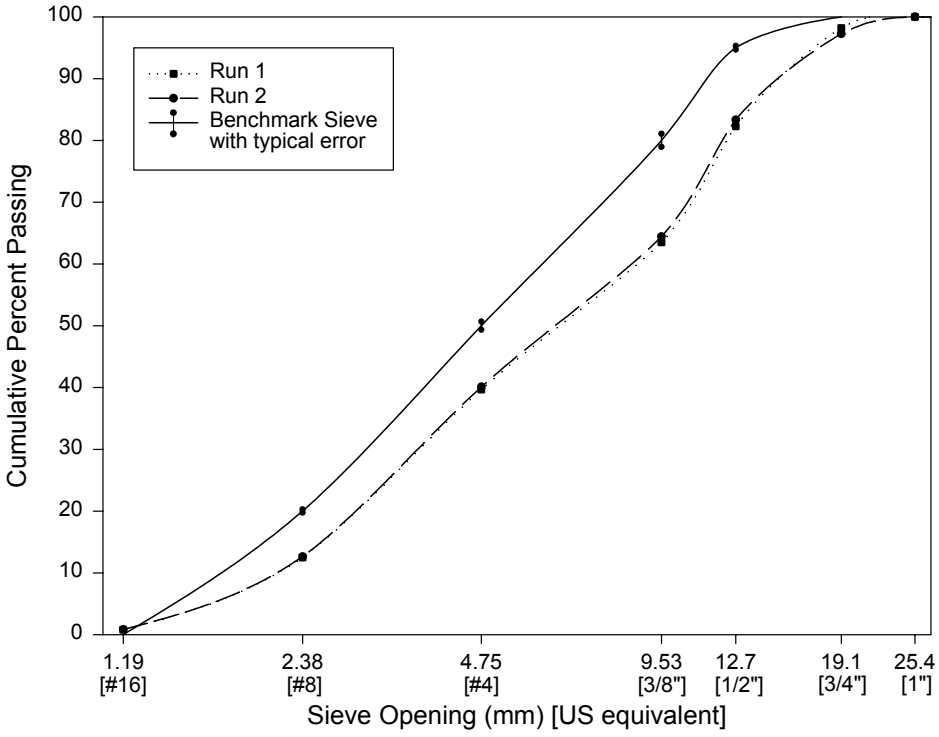

Sample: Texas C-LG	Test Machine: VIS

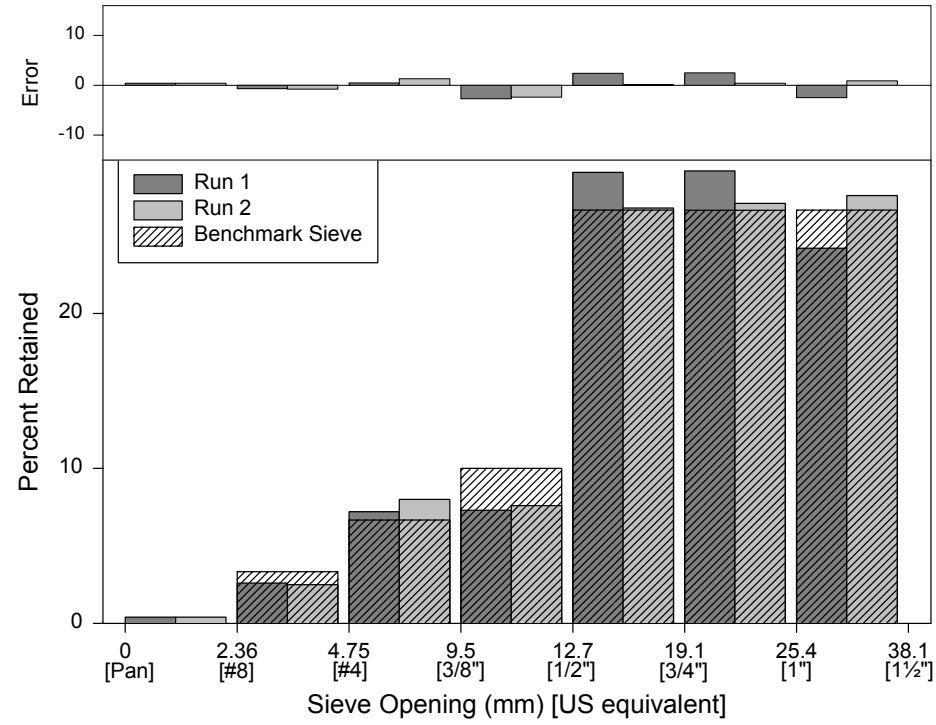

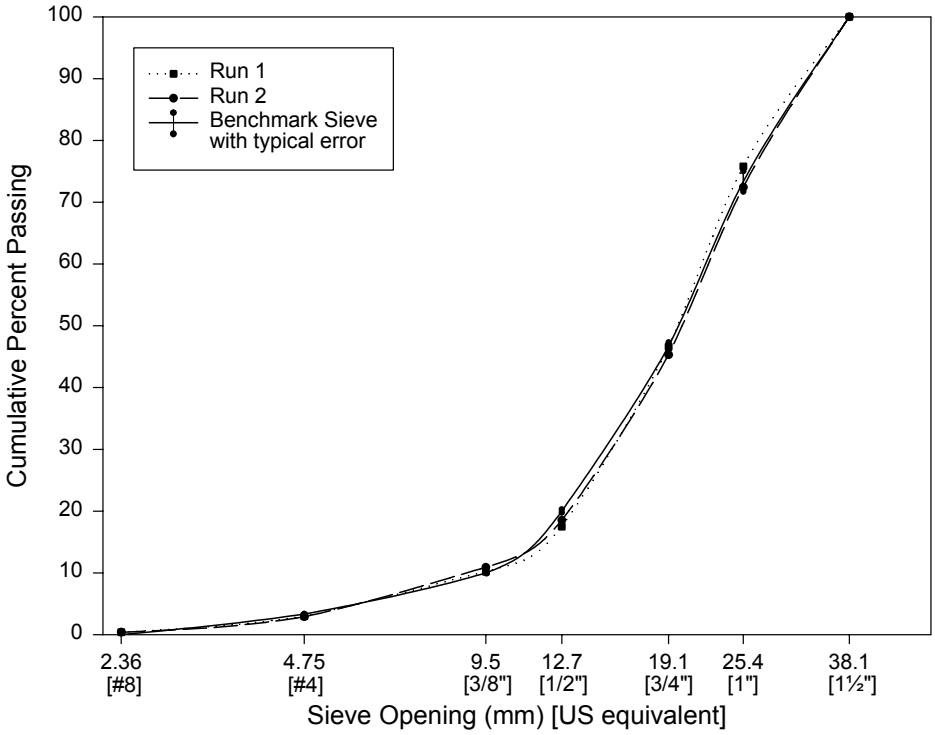

Sample: Texas C-RND	Test Machine: VIS

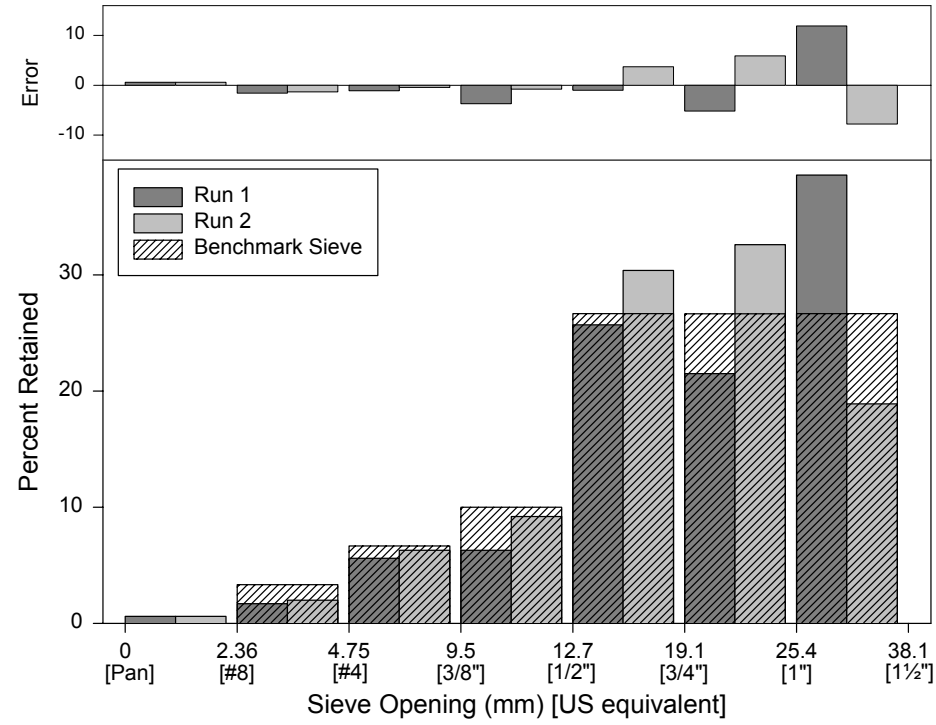

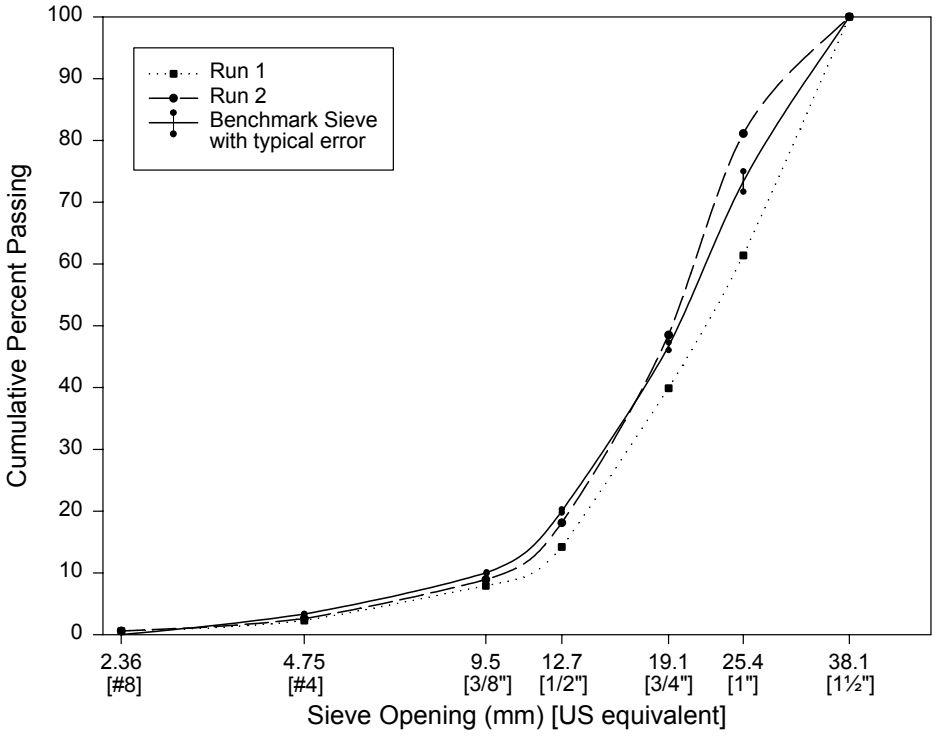

Sample: CA-C-SM	Test Machine: VIS

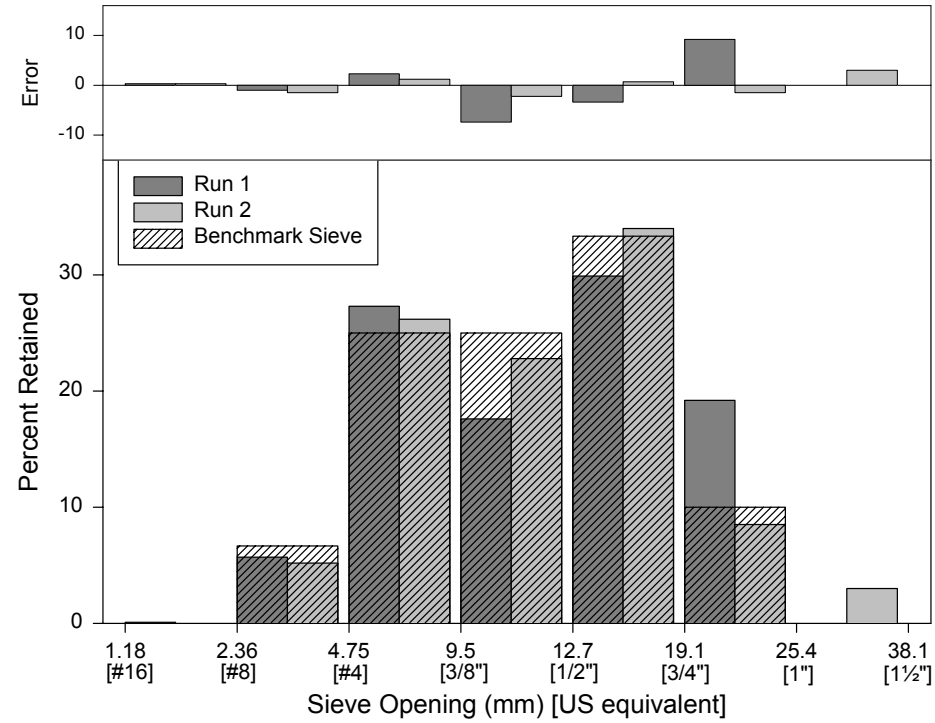

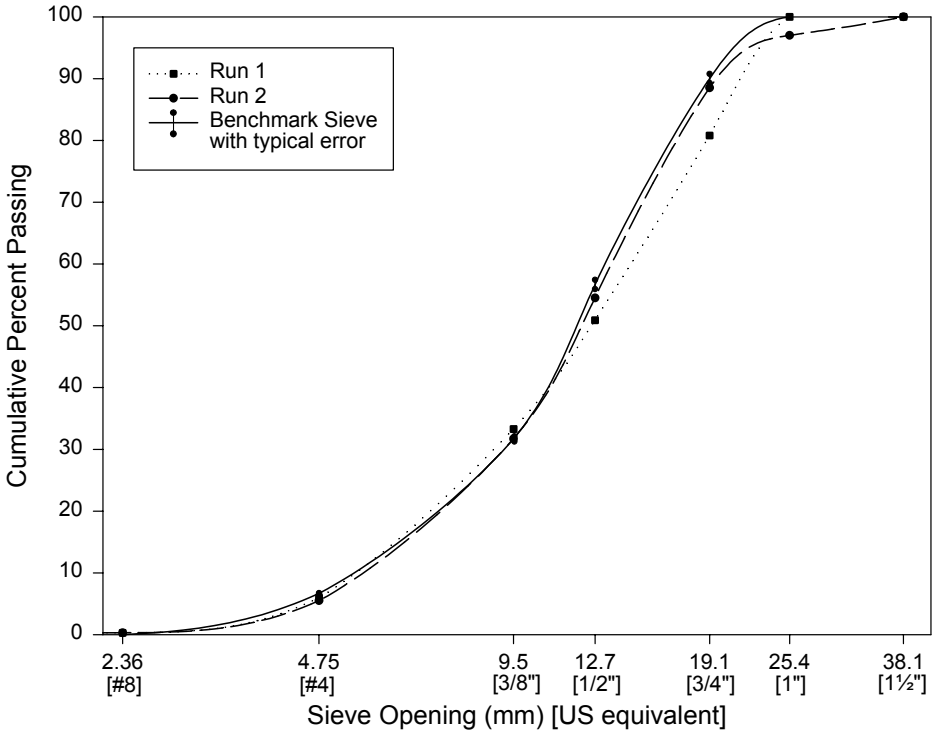

Sample: SD-C-SM	Test Machine: VIS

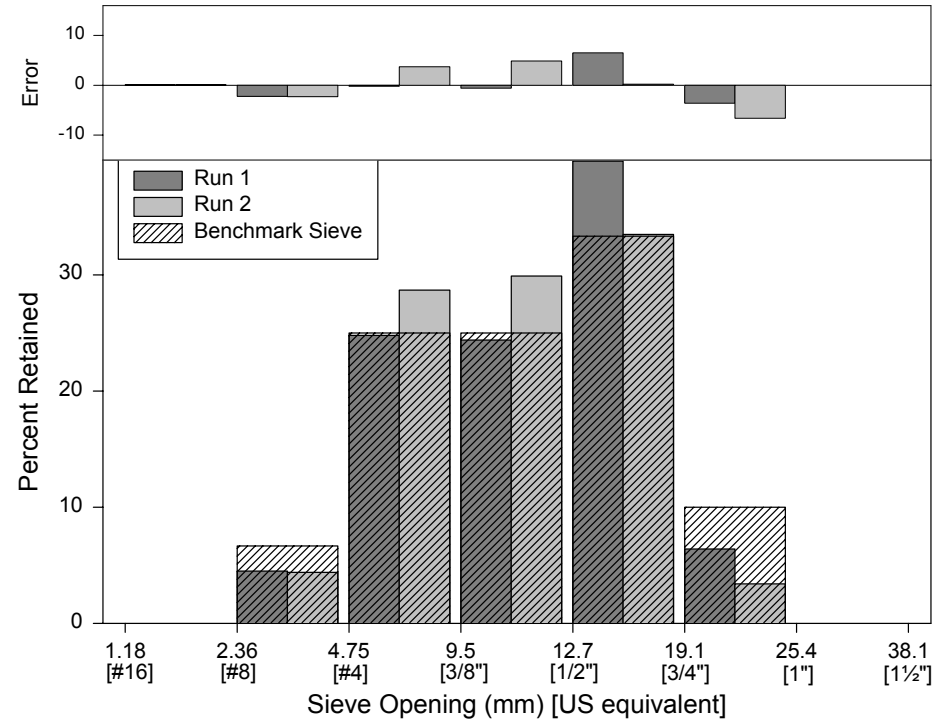

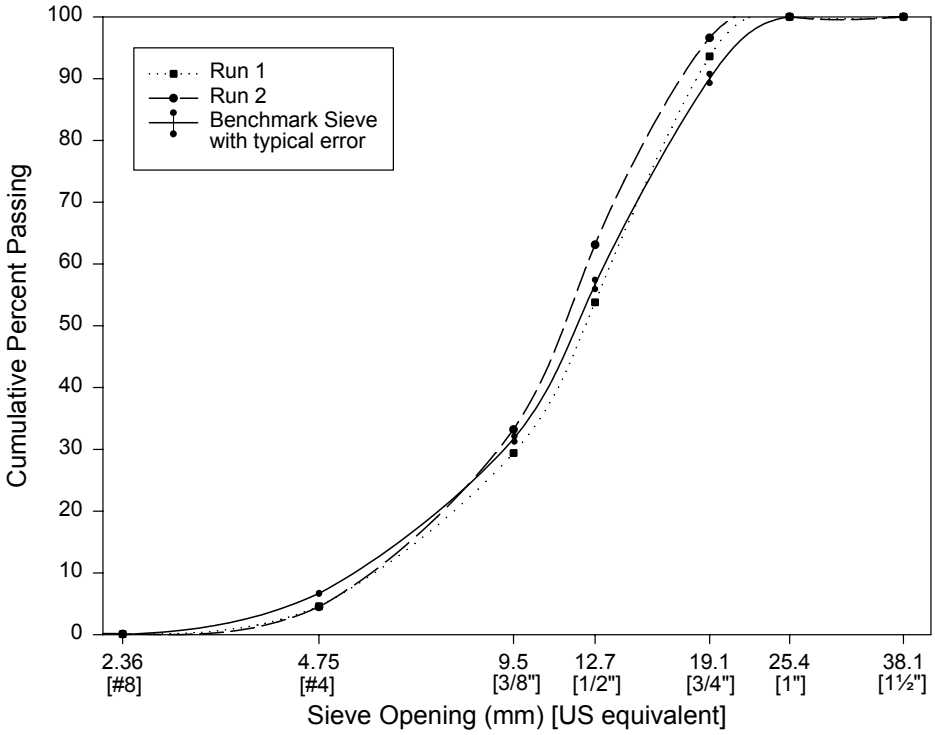

Sample: TX-C-SM	Test Machine: VIS

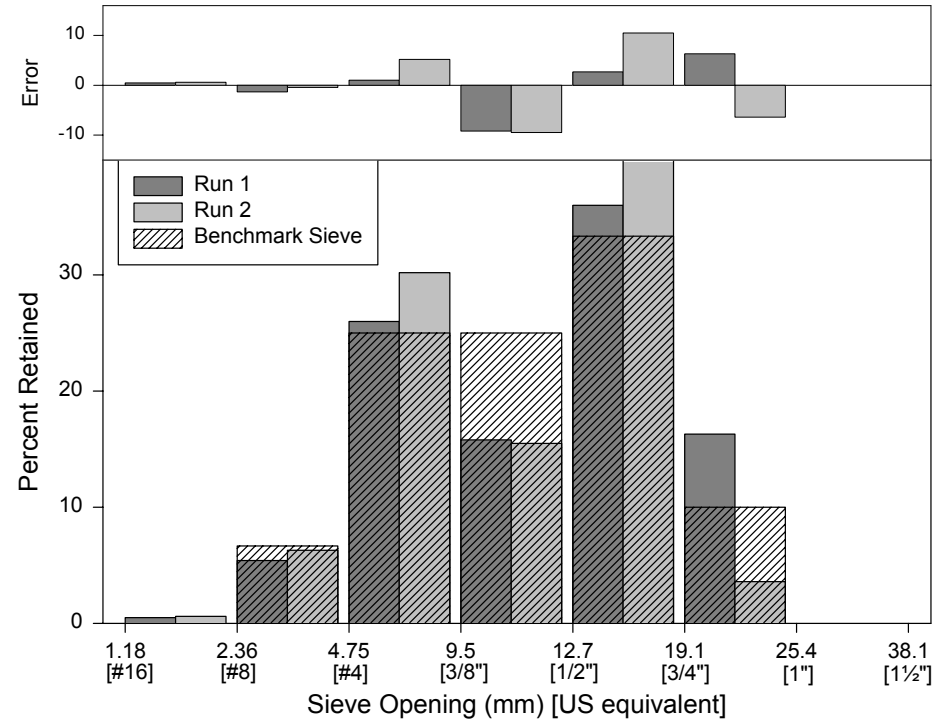

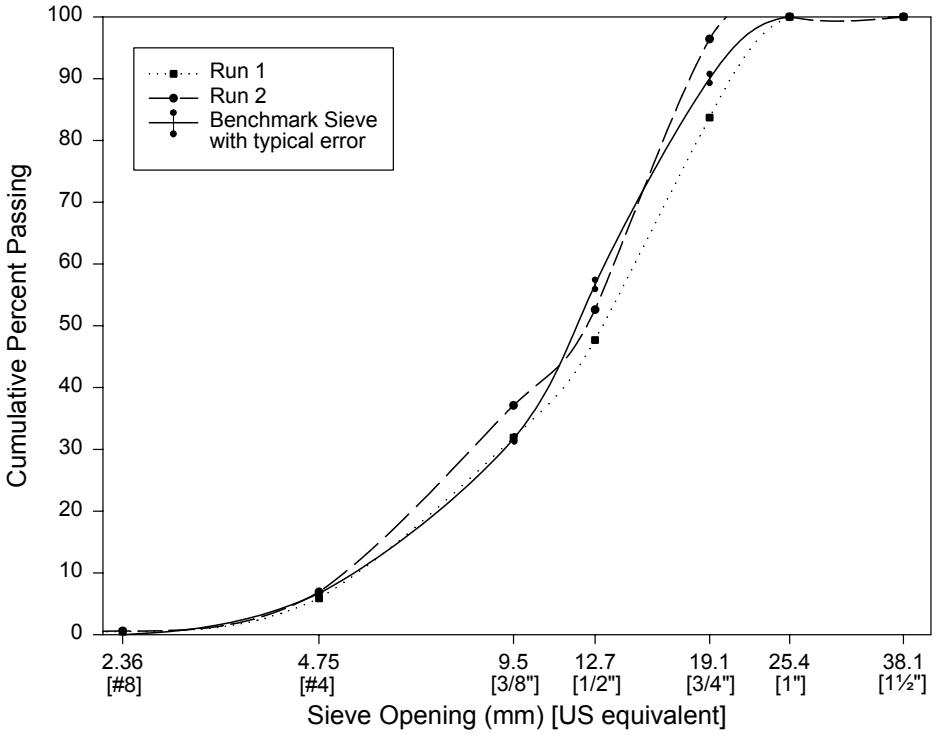

Sample: VA-C-SM	Test Machine: VIS

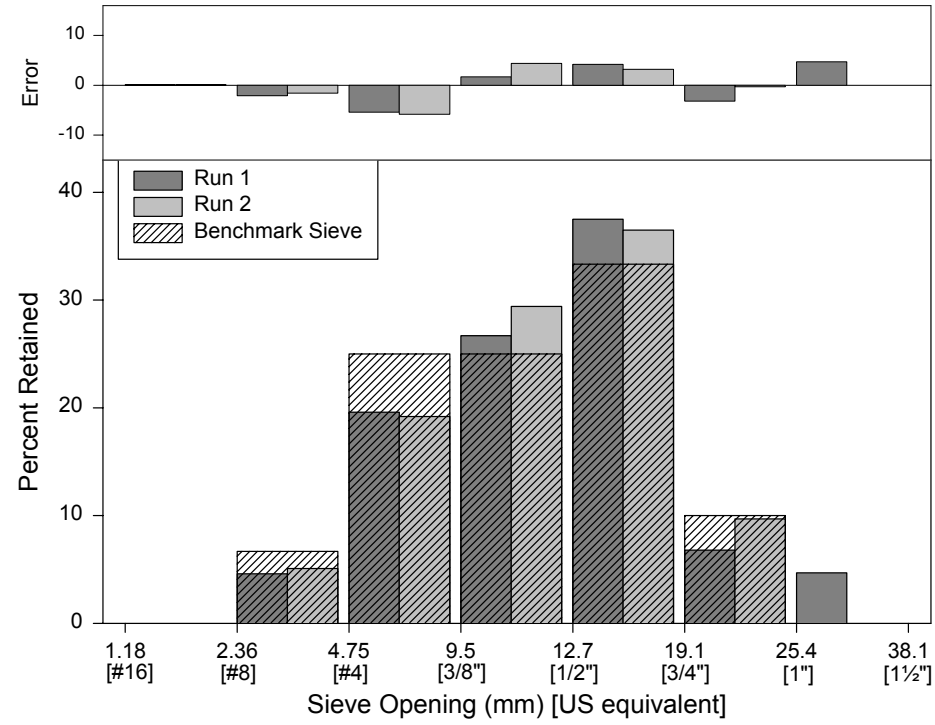

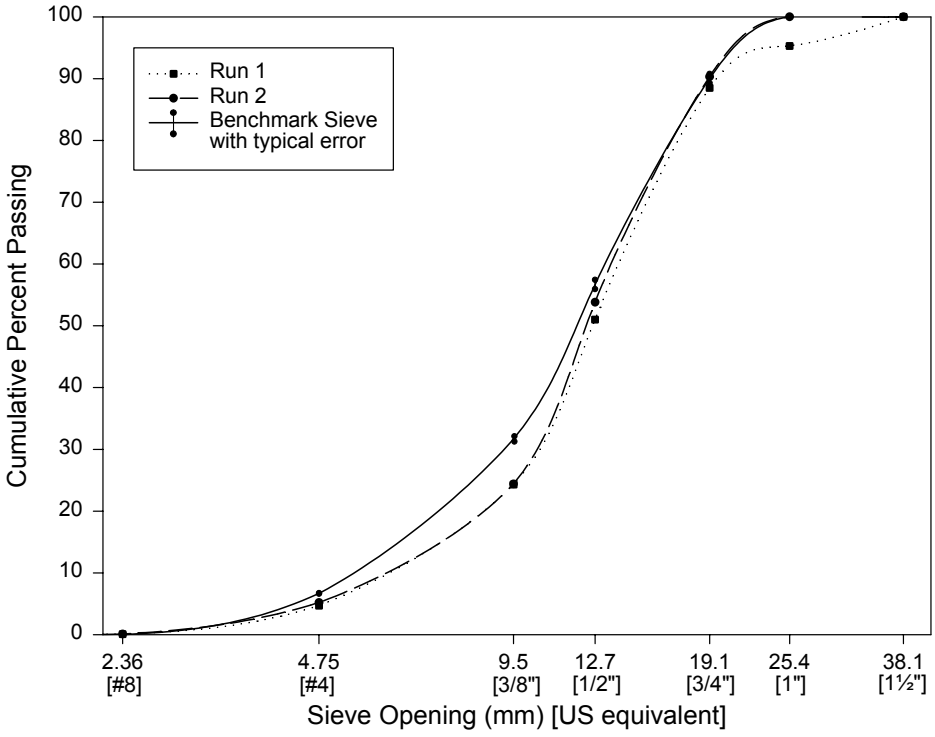

Sample: CA-C-STD	Test Machine: VIS

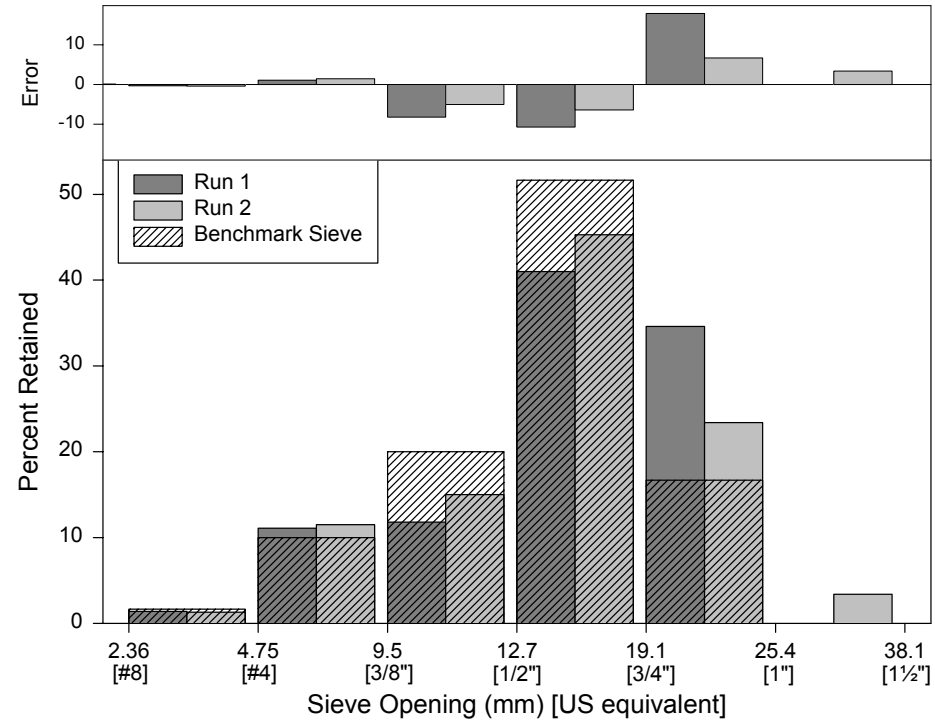

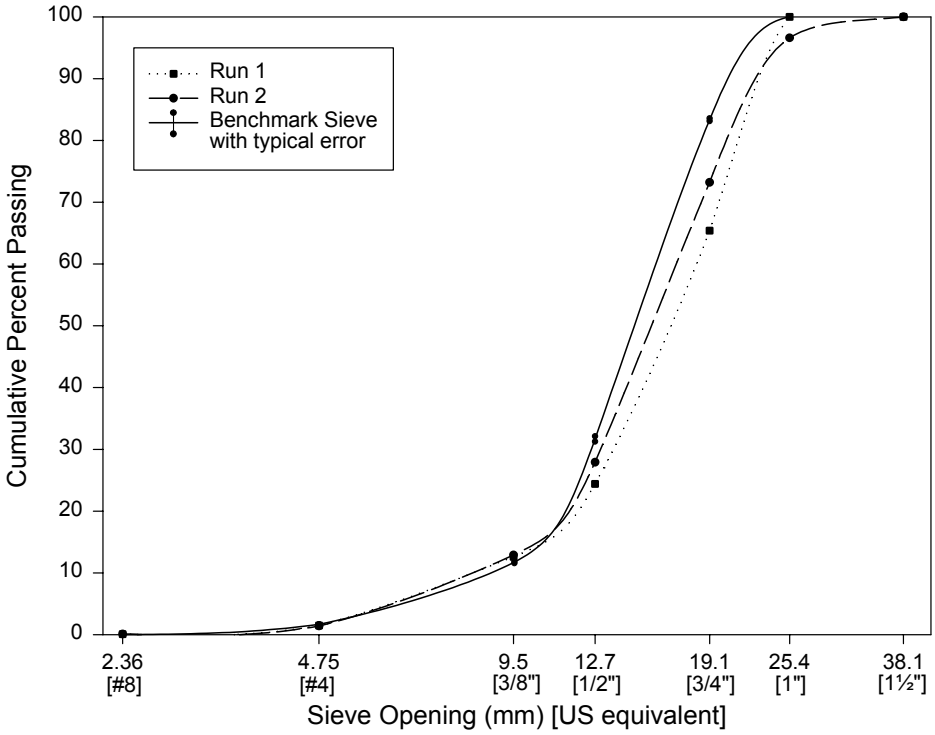

Sample: SD-C-STD	Test Machine: VIS

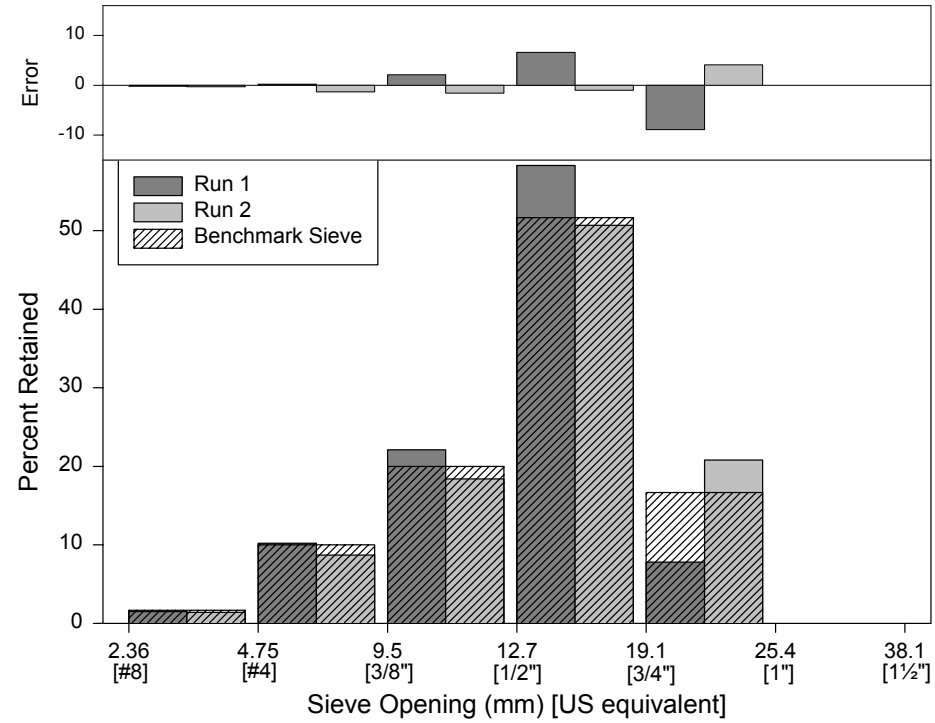

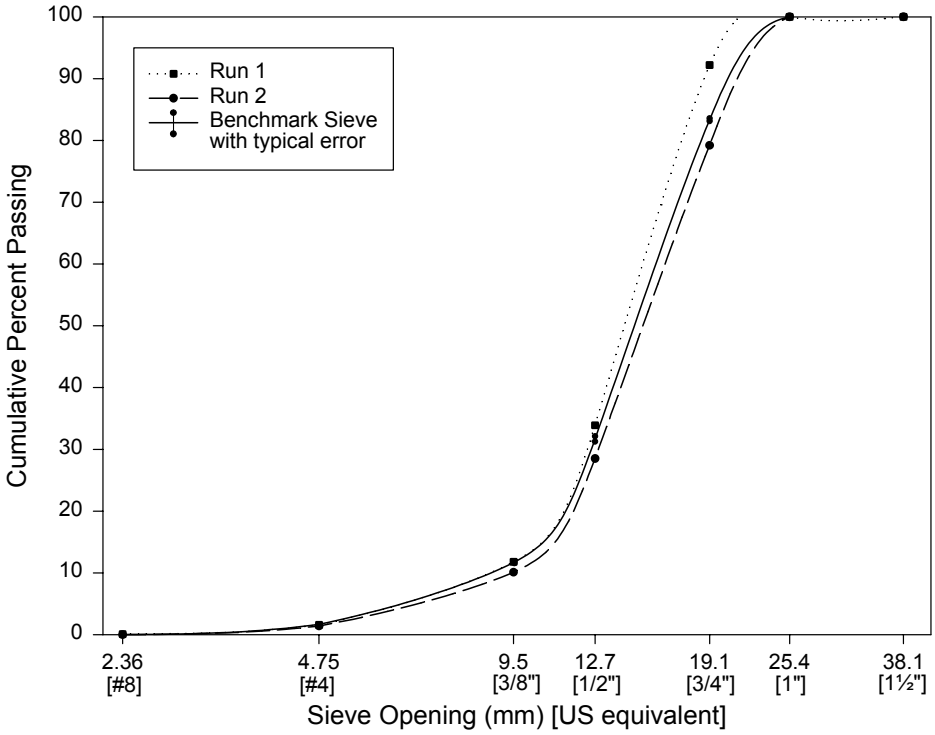

Sample: TX-C-STD	Test Machine: VIS

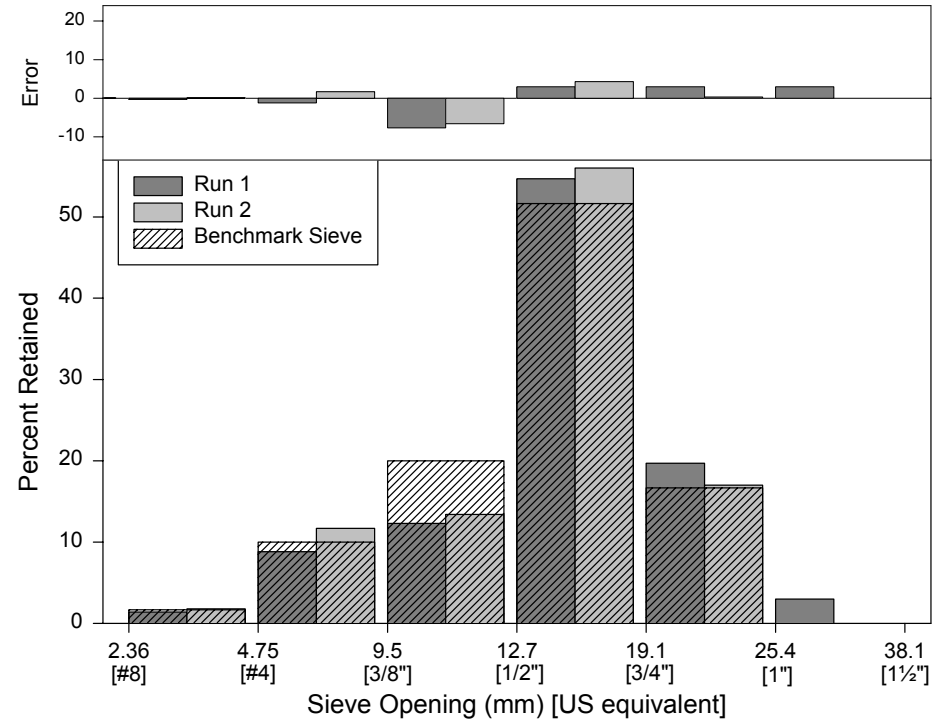

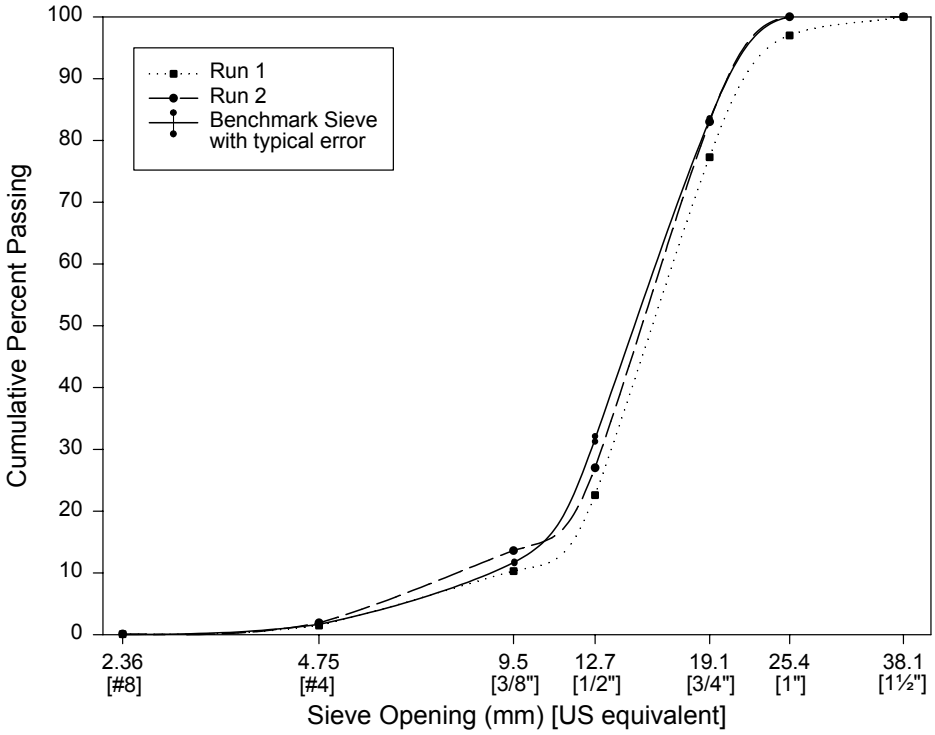

Sample: VA-C-STD	Test Machine: VIS

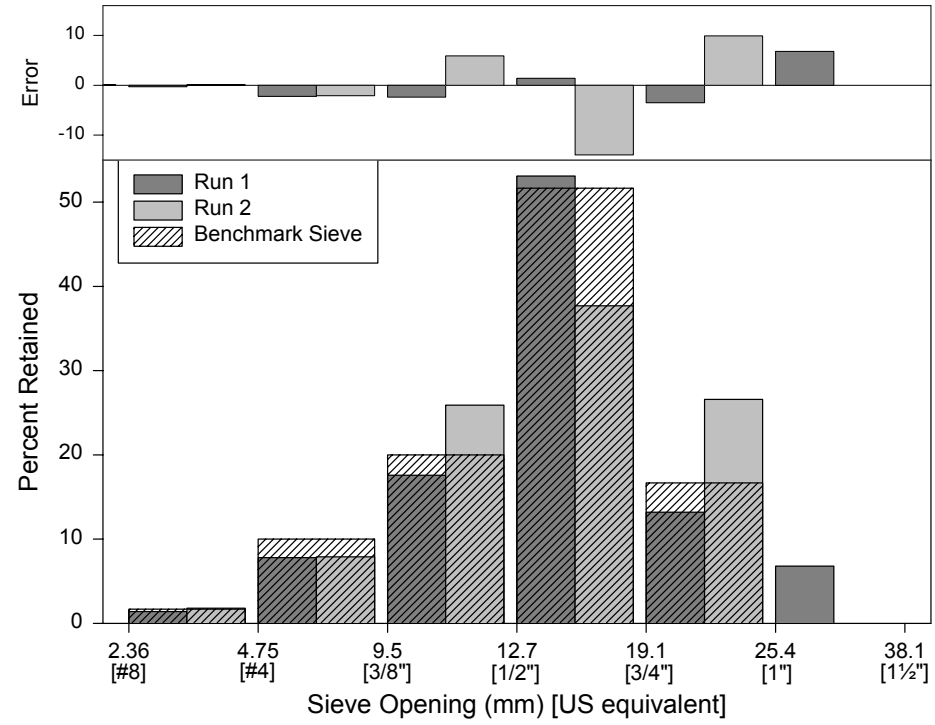

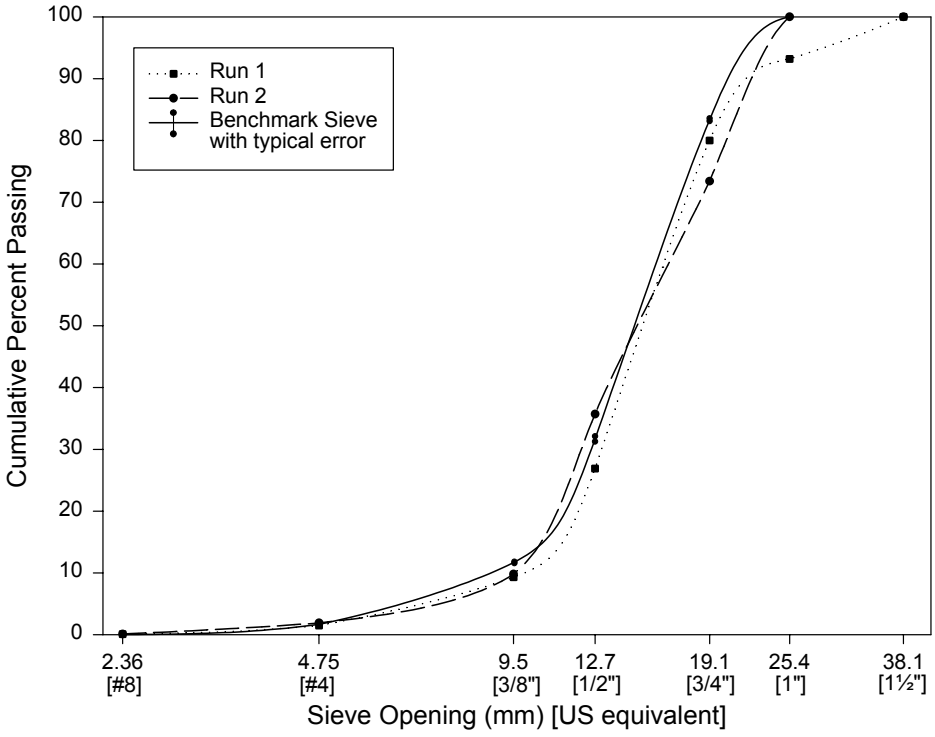

Sample: TX-F-FTC	Test Machine: VIS

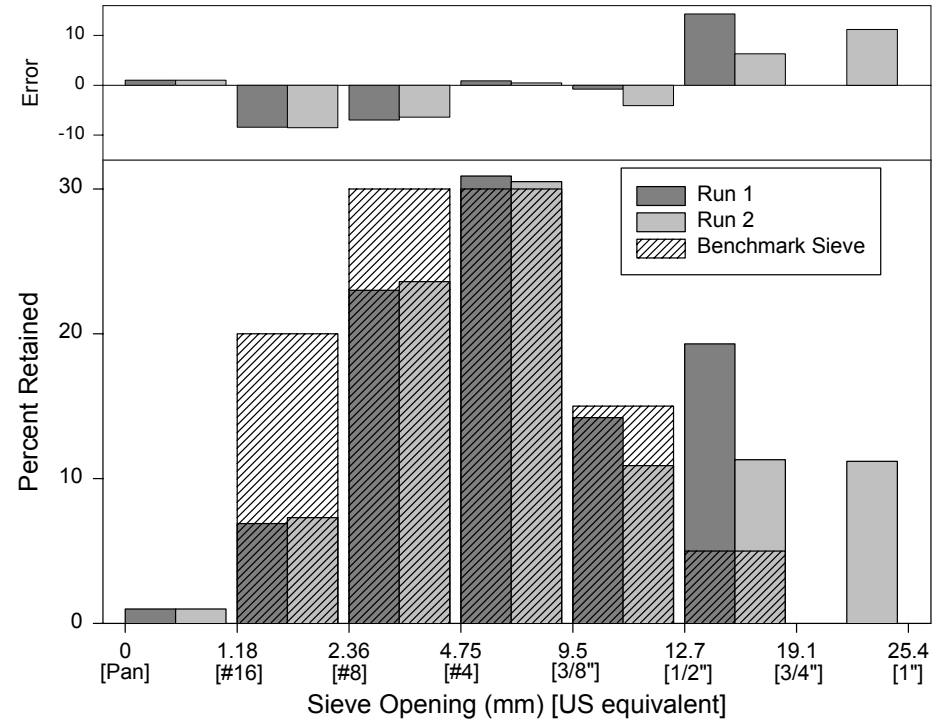

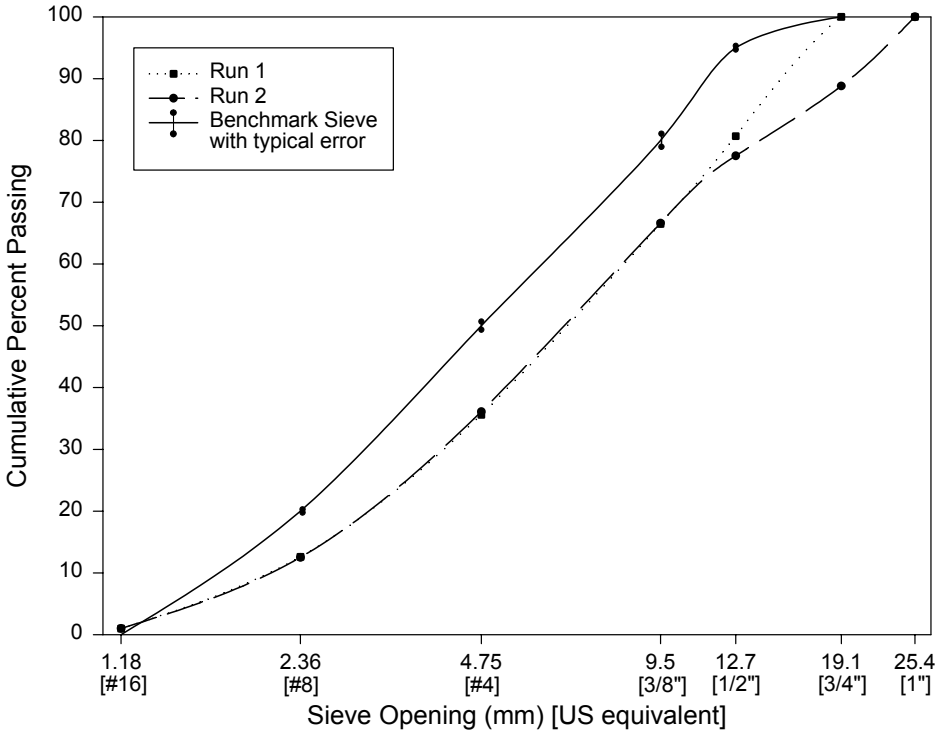

Sample: VA-F-FTC	Test Machine: VIS

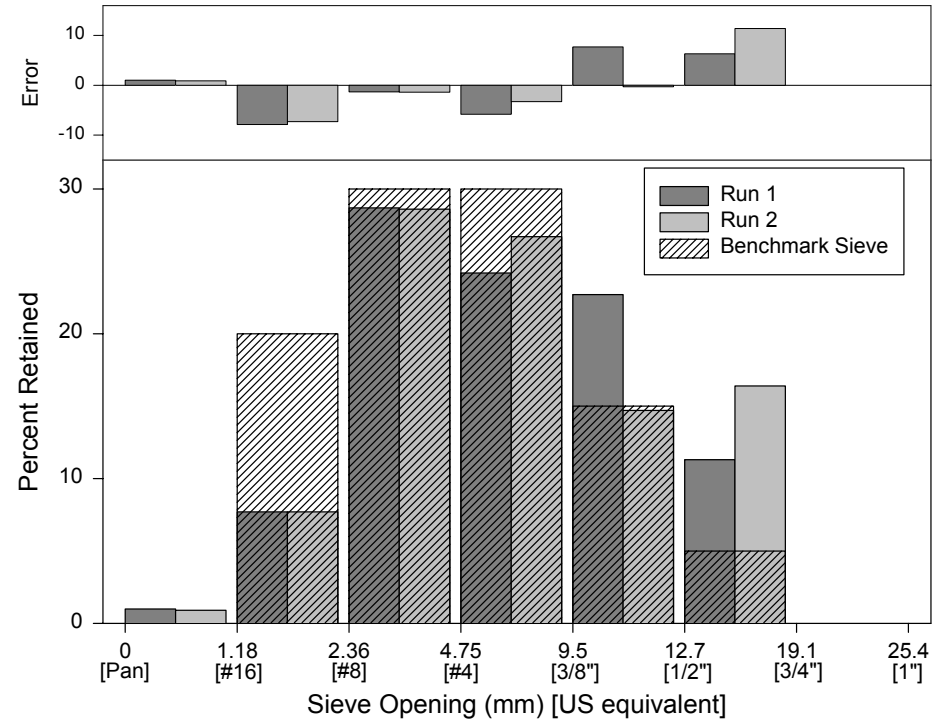

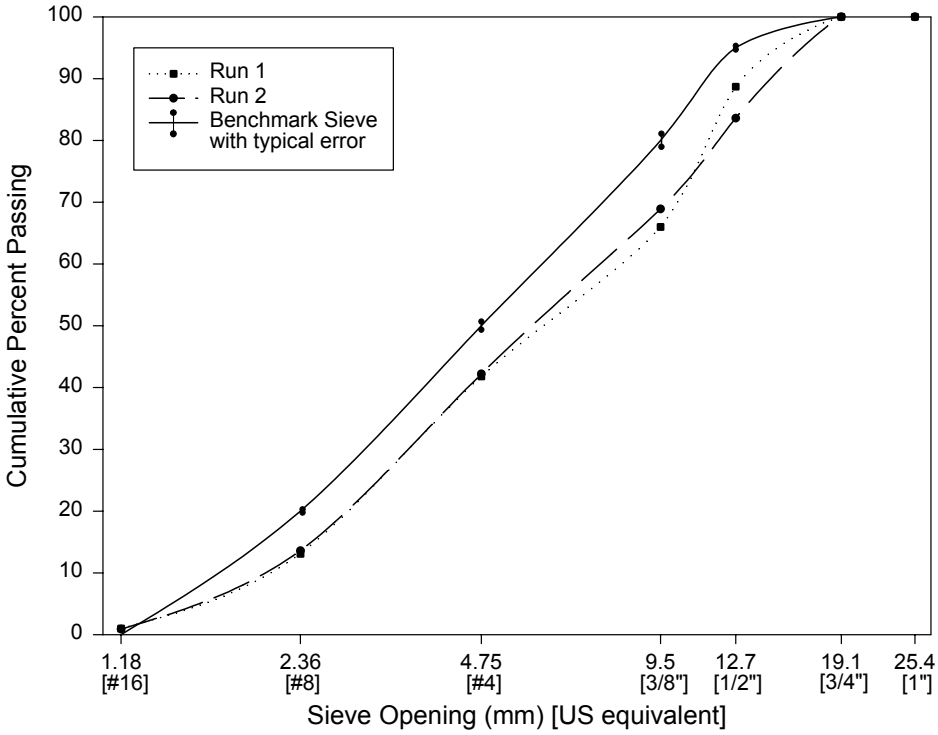

Sample: Texas C-LG Test Machine: CPA

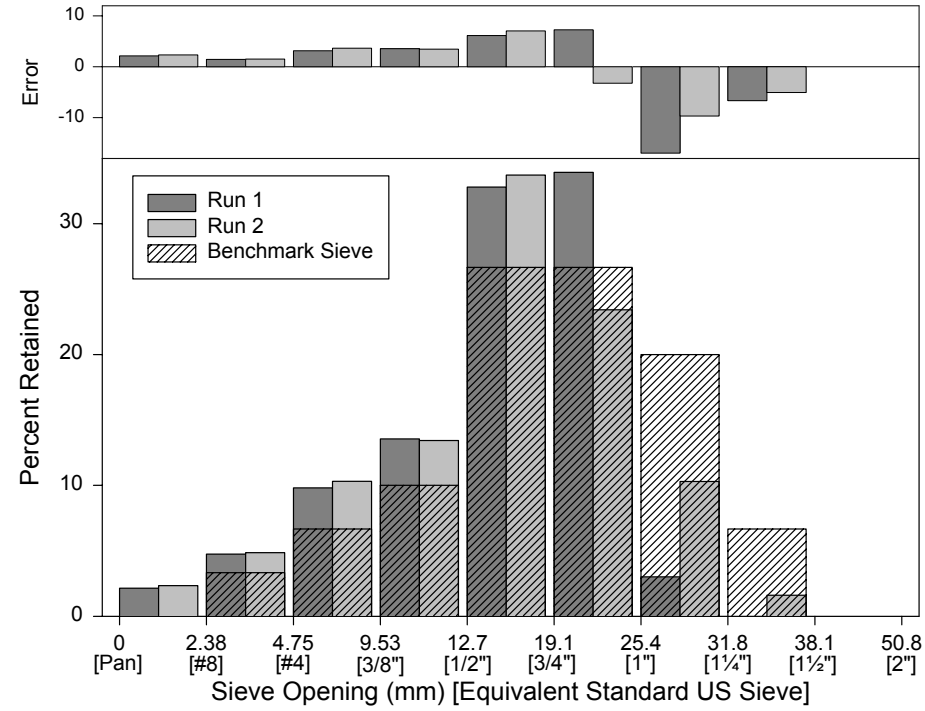

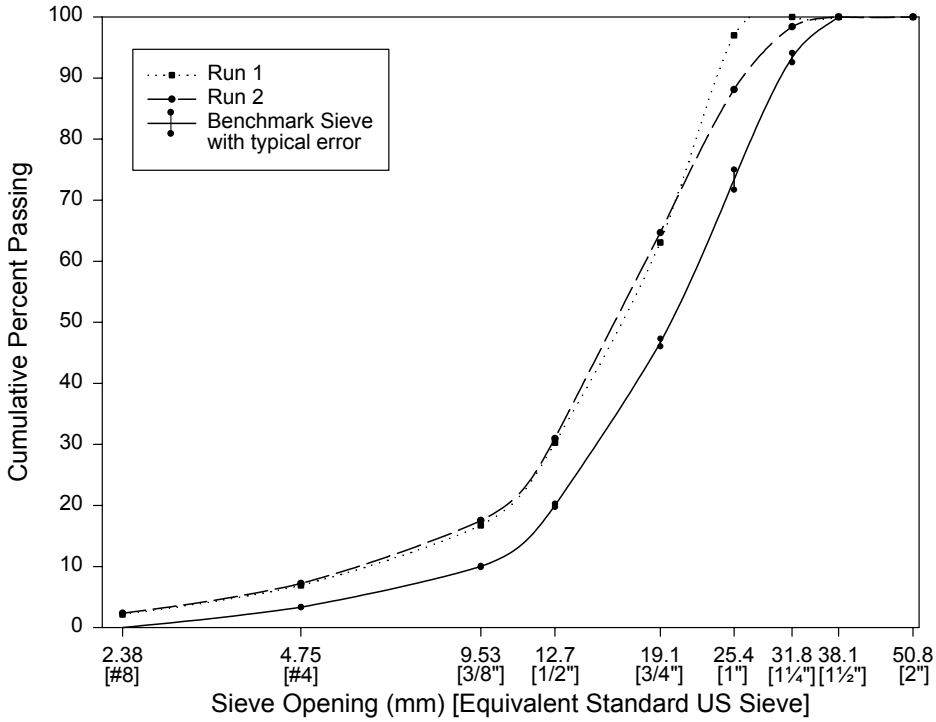

Sample: Texas C-RND	Test Machine: CPA

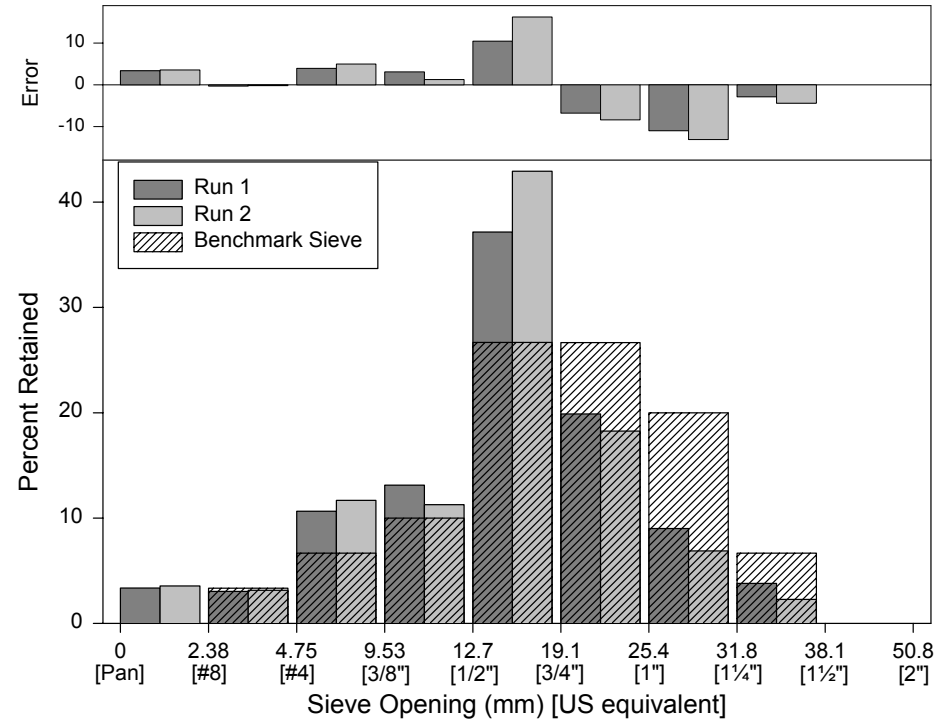

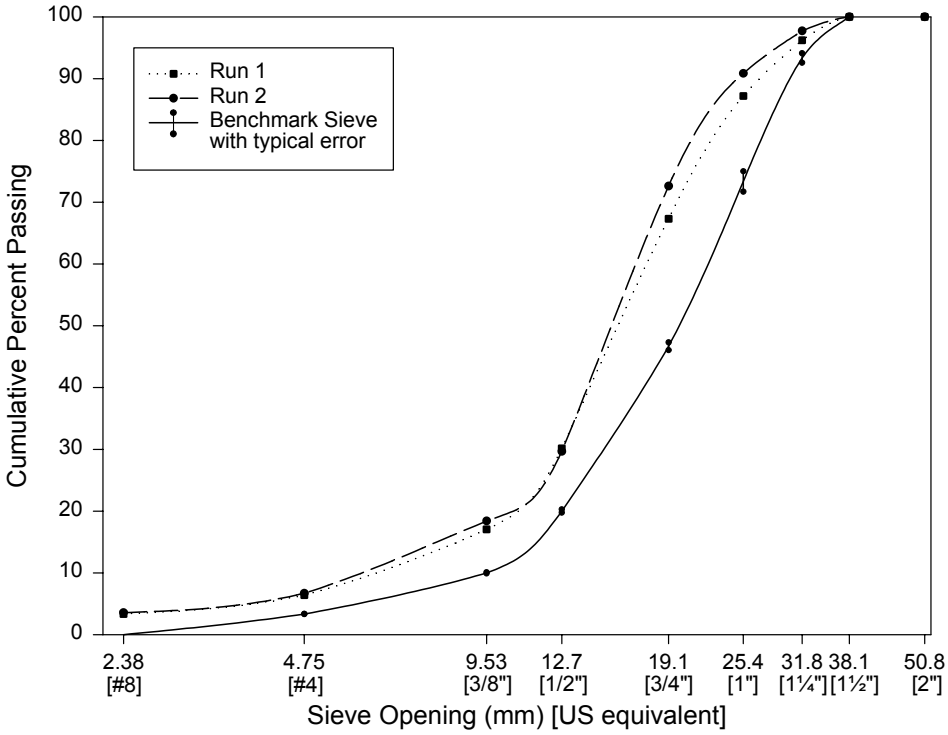

Sample: CA-C-SM	Test Machine: CPA

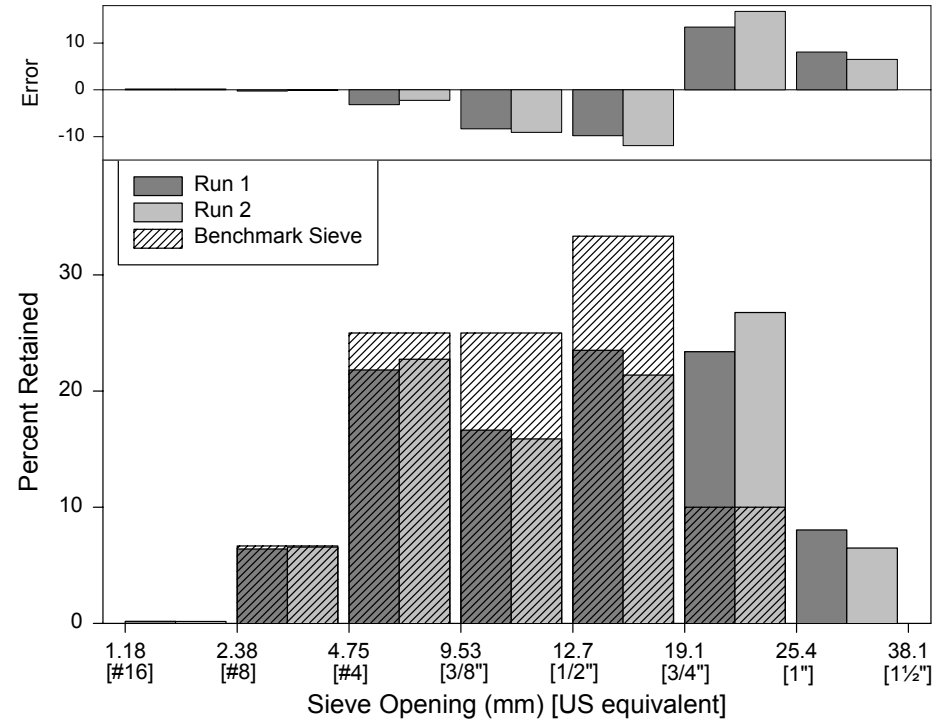

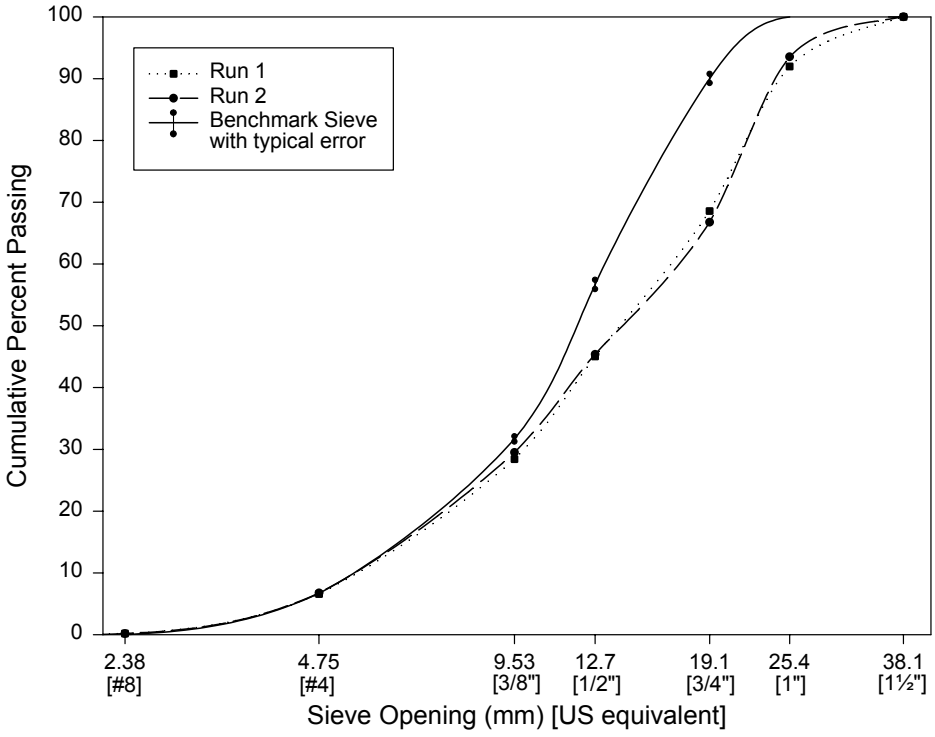

Sample: SD-C-SM	Test Machine: CPA

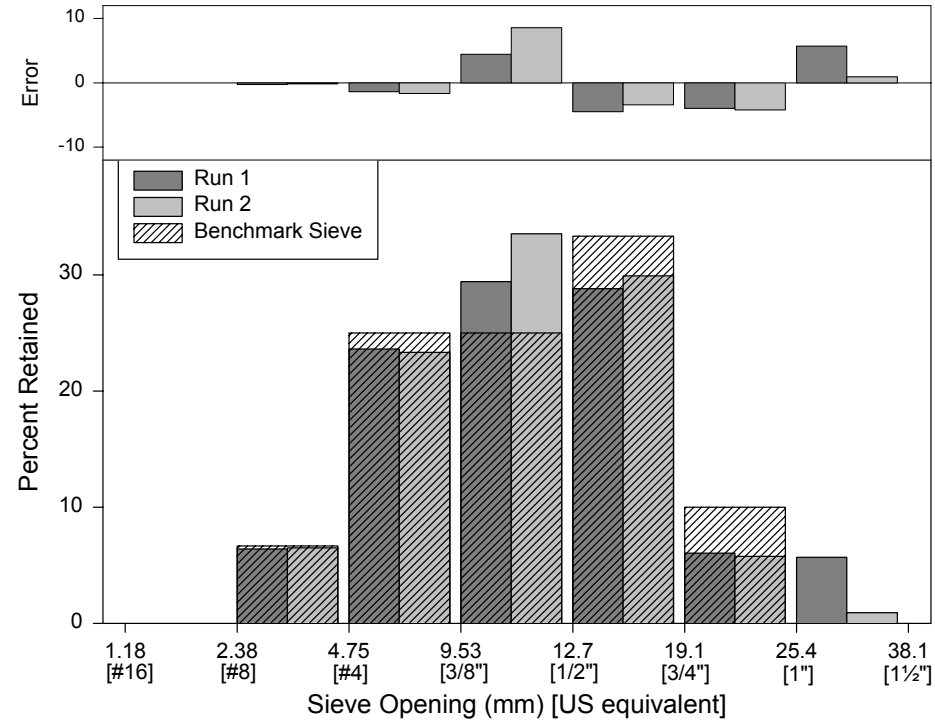

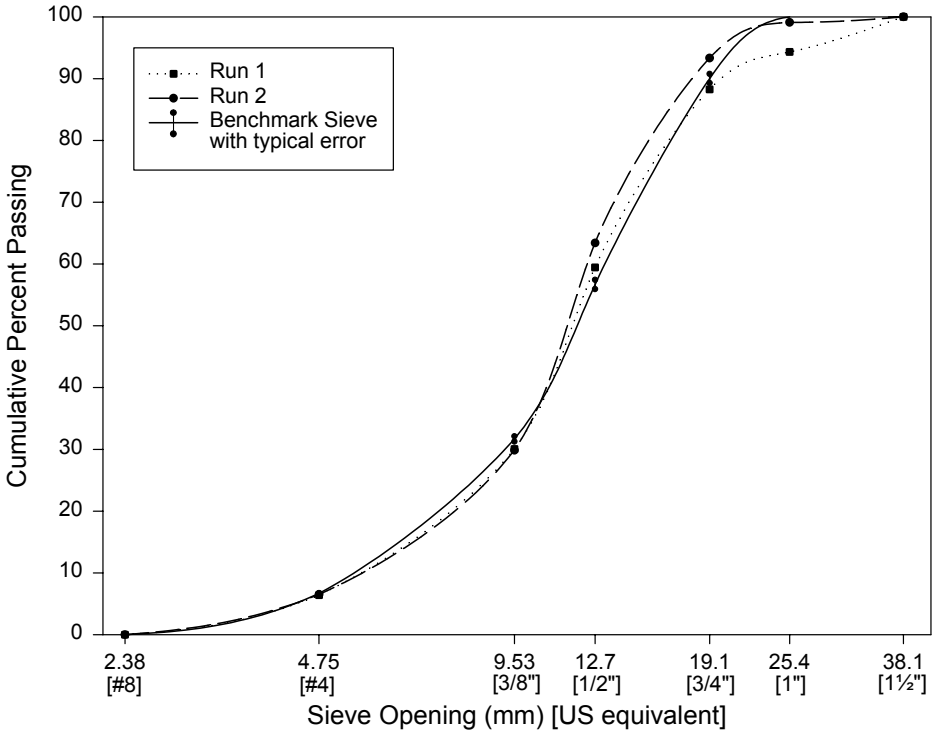

Sample: TX-C-SM	Test Machine: CPA

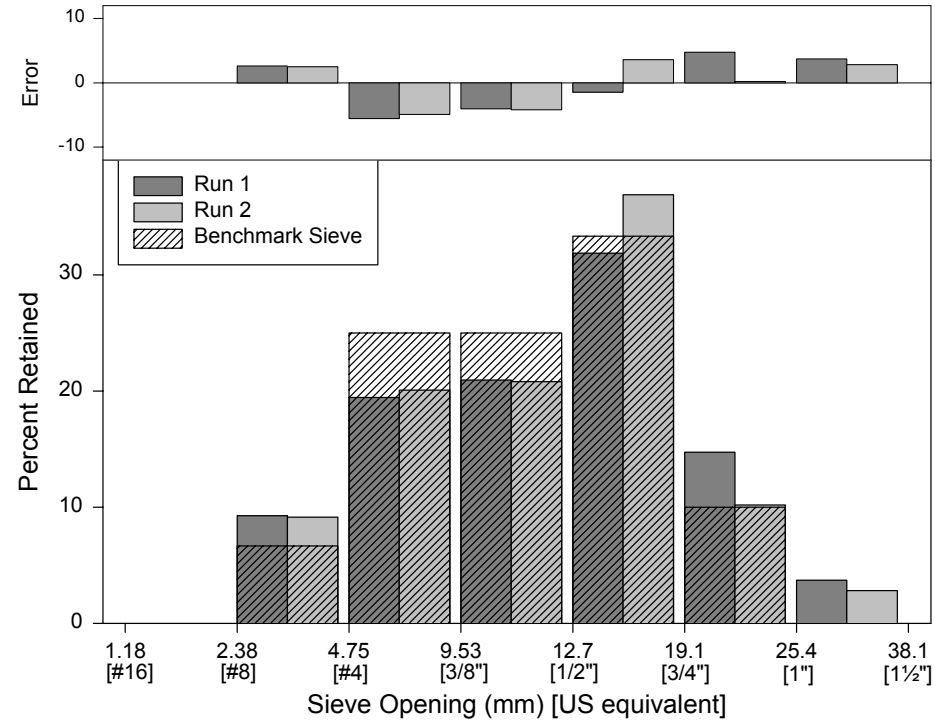

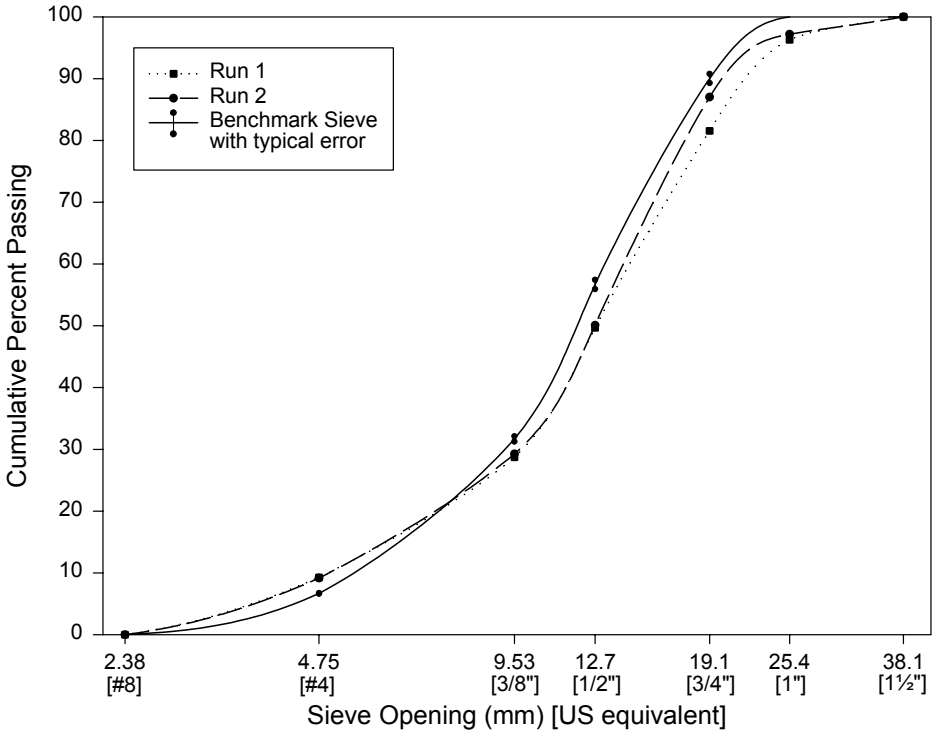

Sample: VA-C-SM	Test Machine: CPA

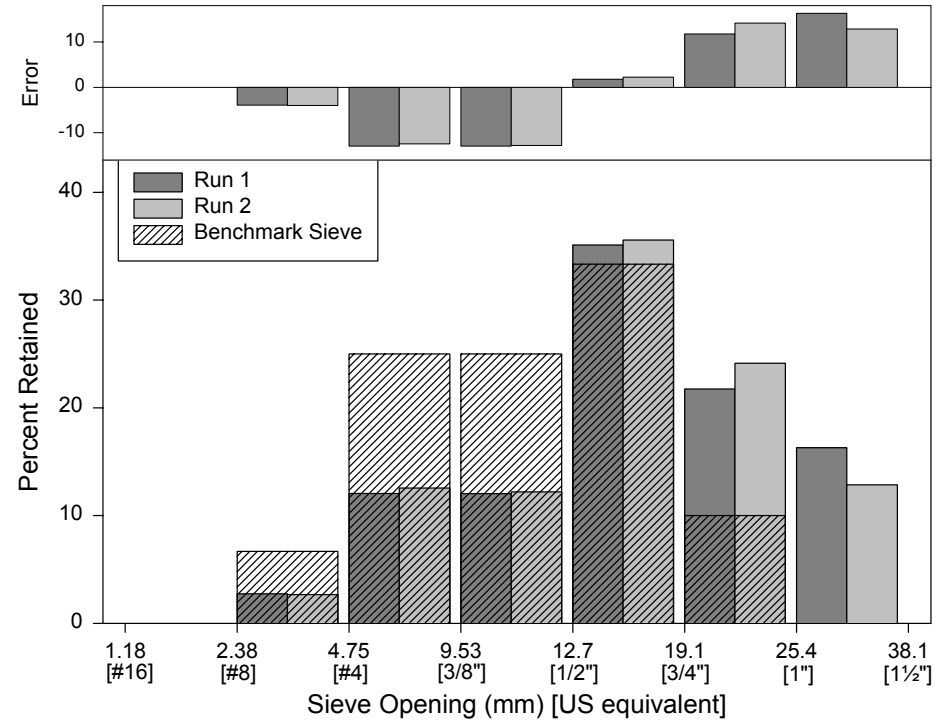

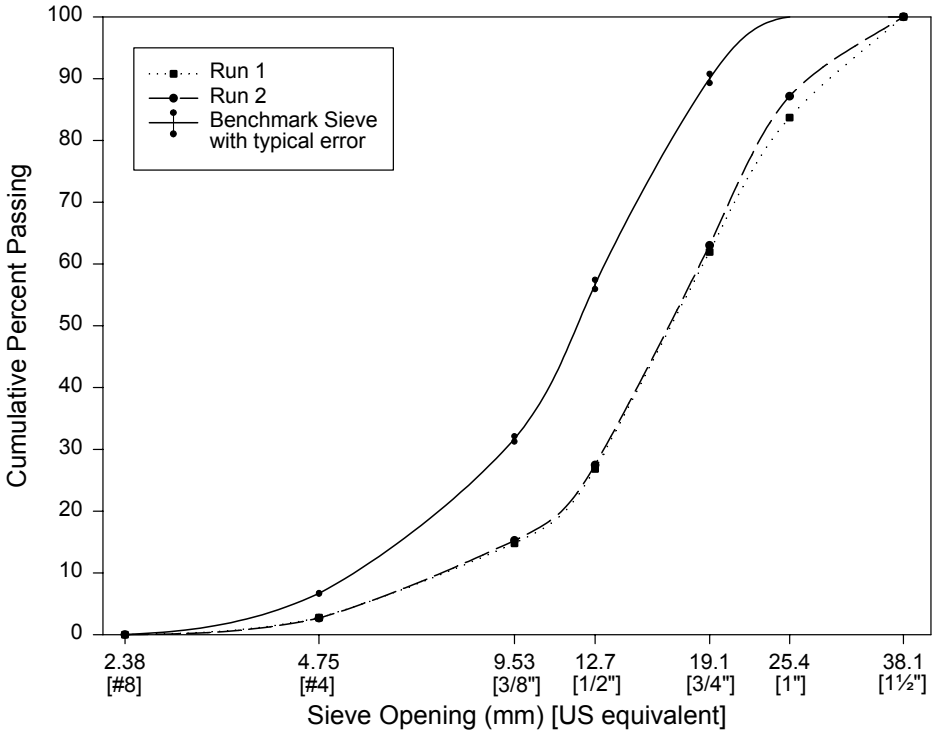

Sample: CA-C-STD	Test Machine: CPA

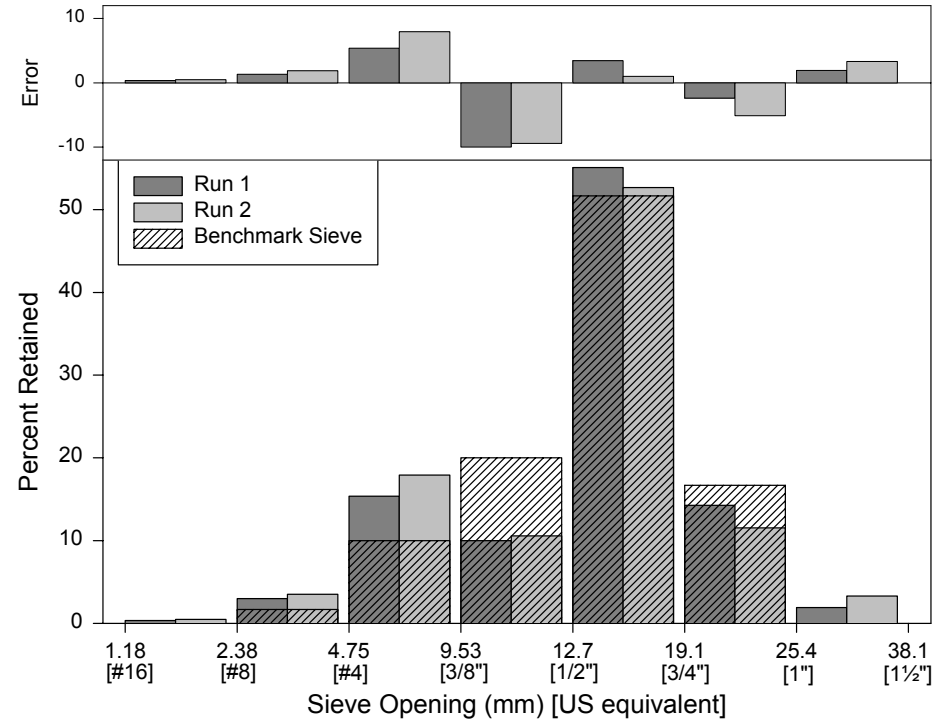

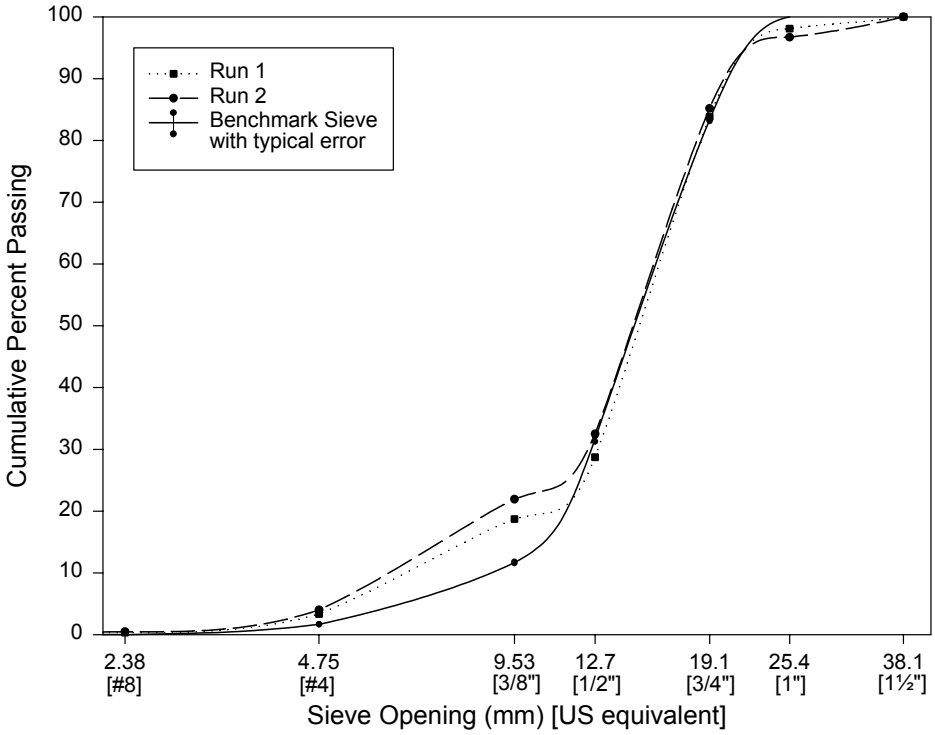

Sample: SD-C-STD	Test Machine: CPA

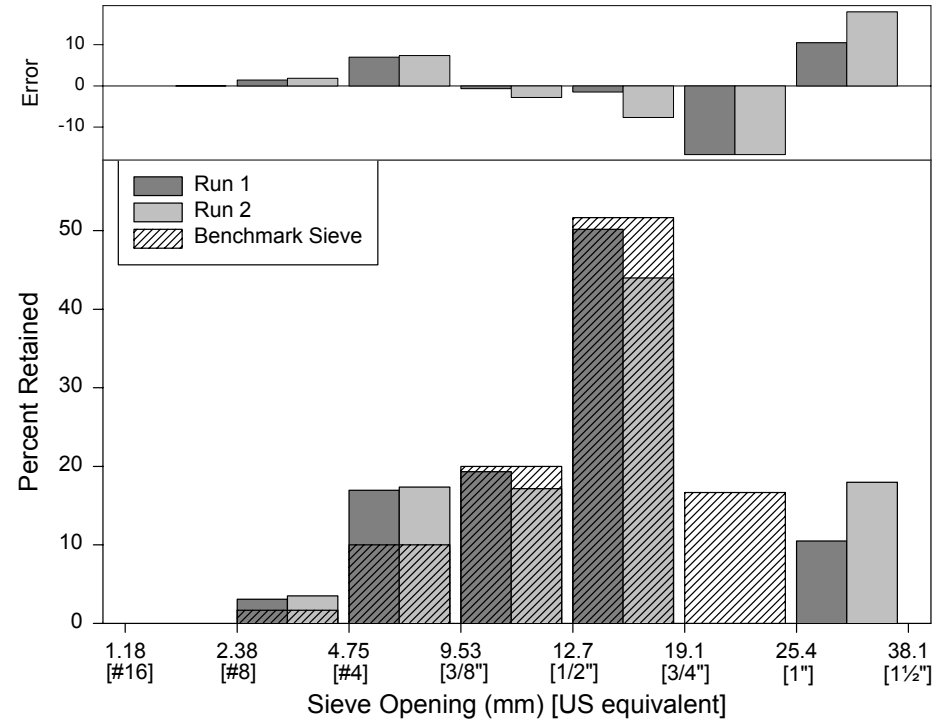

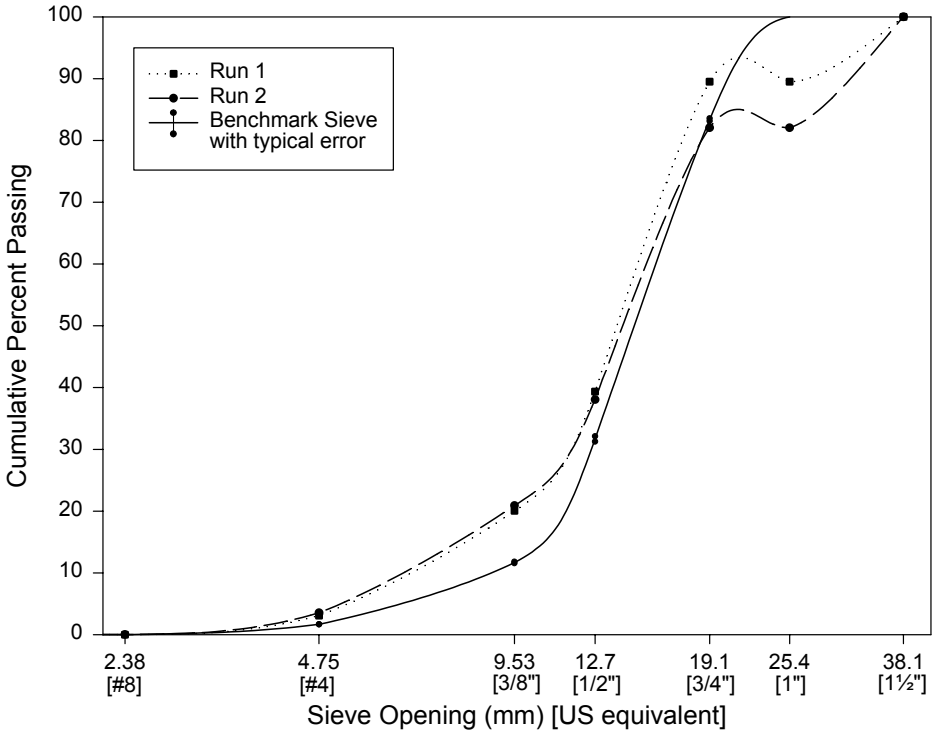

Sample: TX-C-STD	Test Machine: CPA

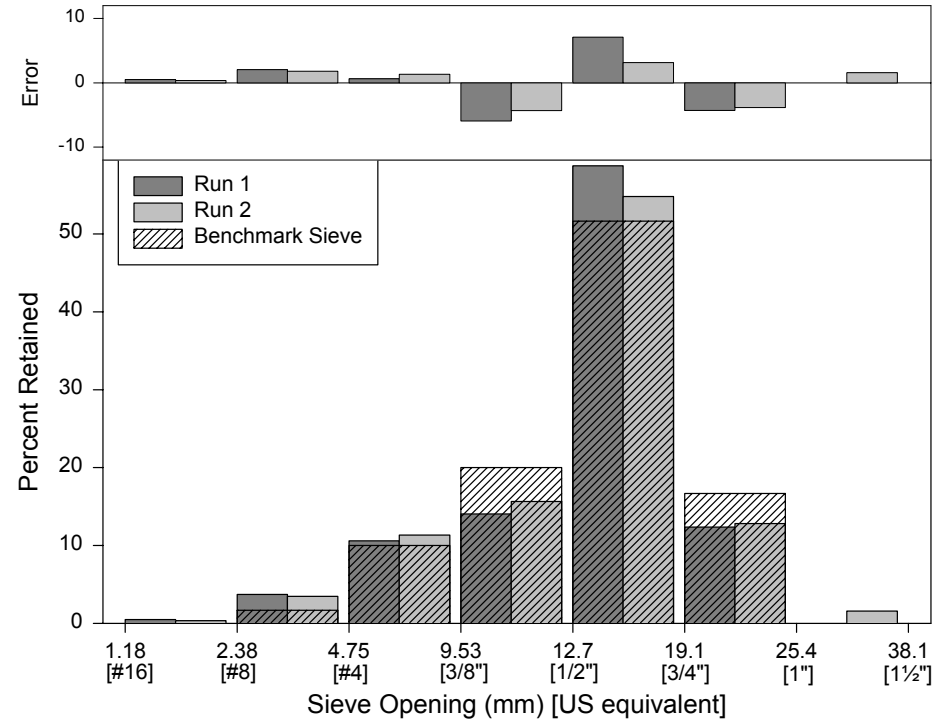

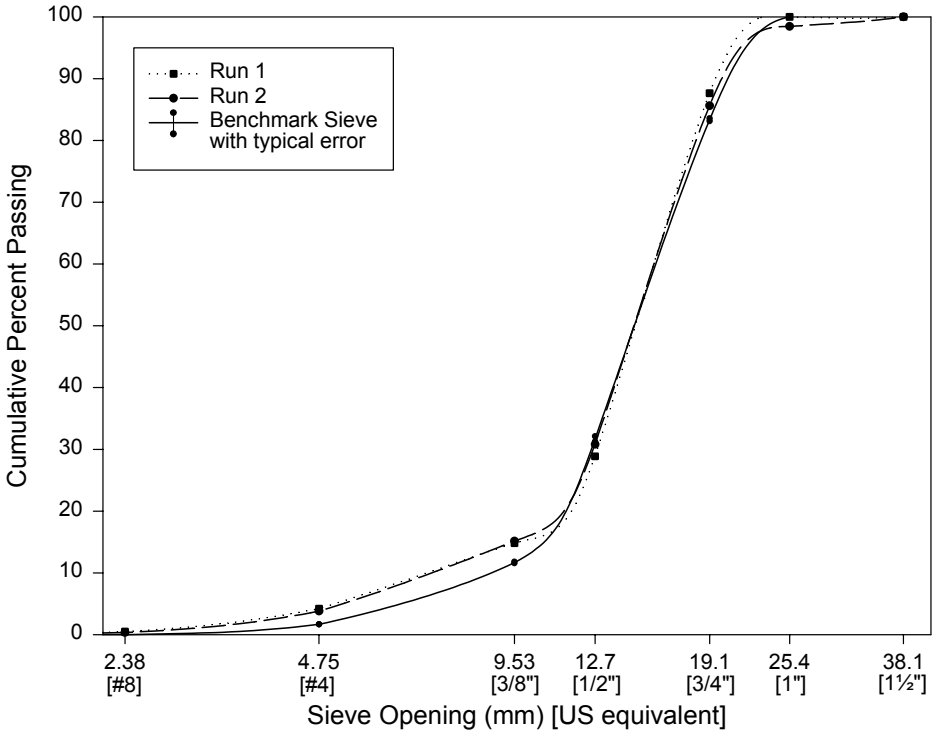

Sample: VA-C-STD	Test Machine: CPA

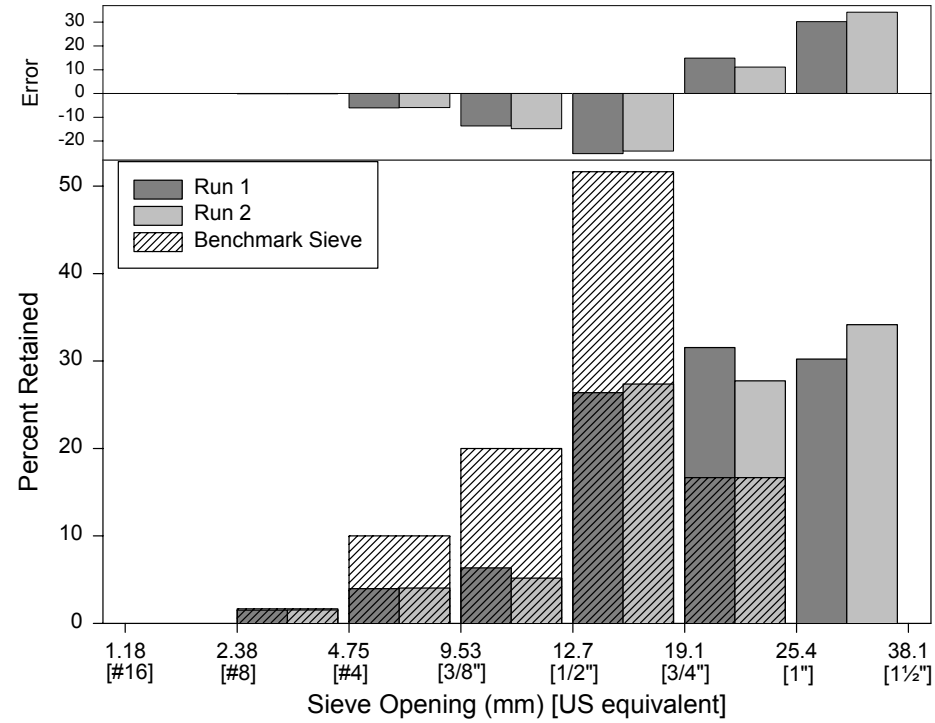

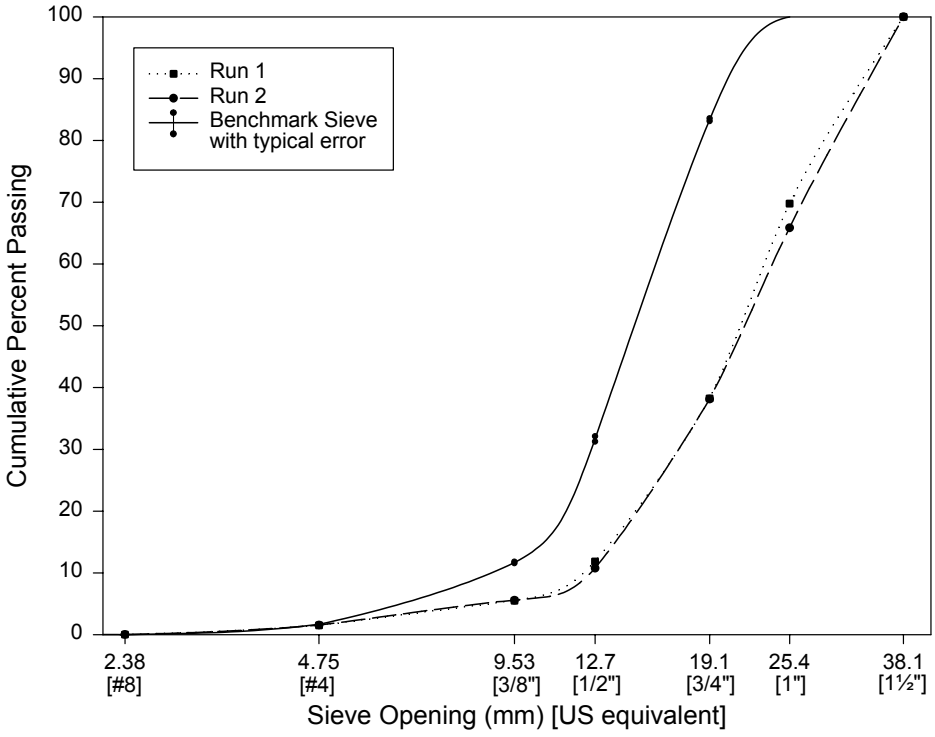

Sample: TX-F-FTC	Test Machine: CPA

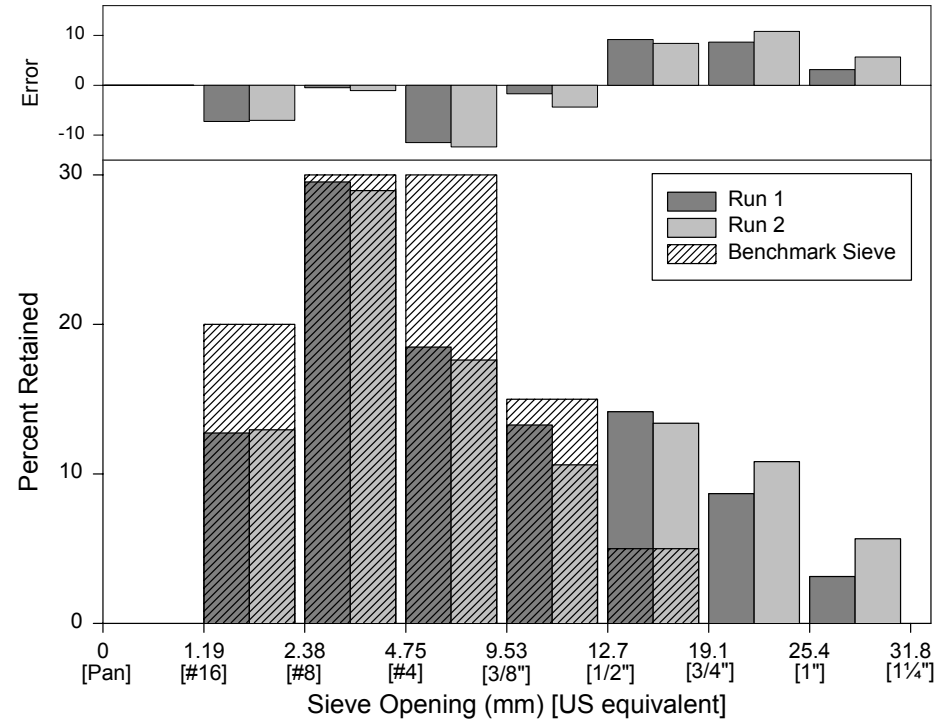

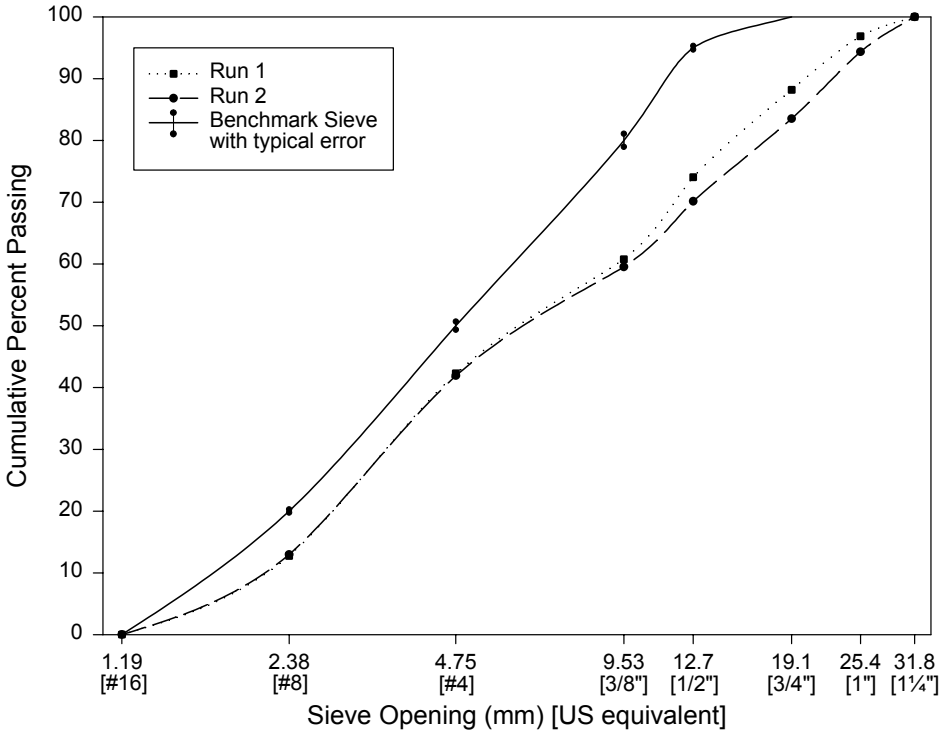

Sample: VA-F-FTC	Test Machine: CPA

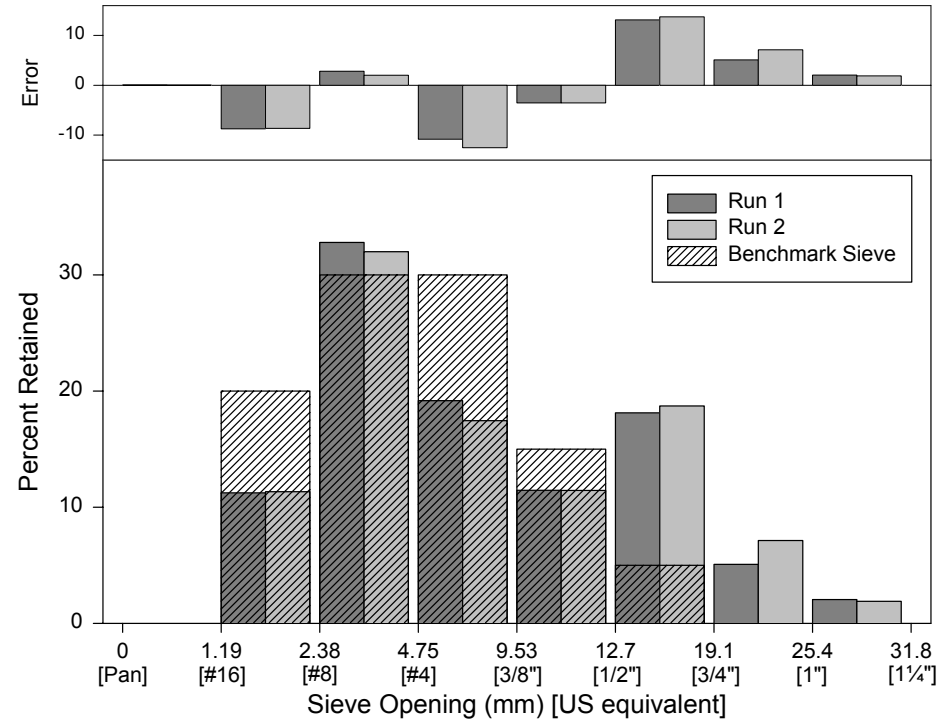

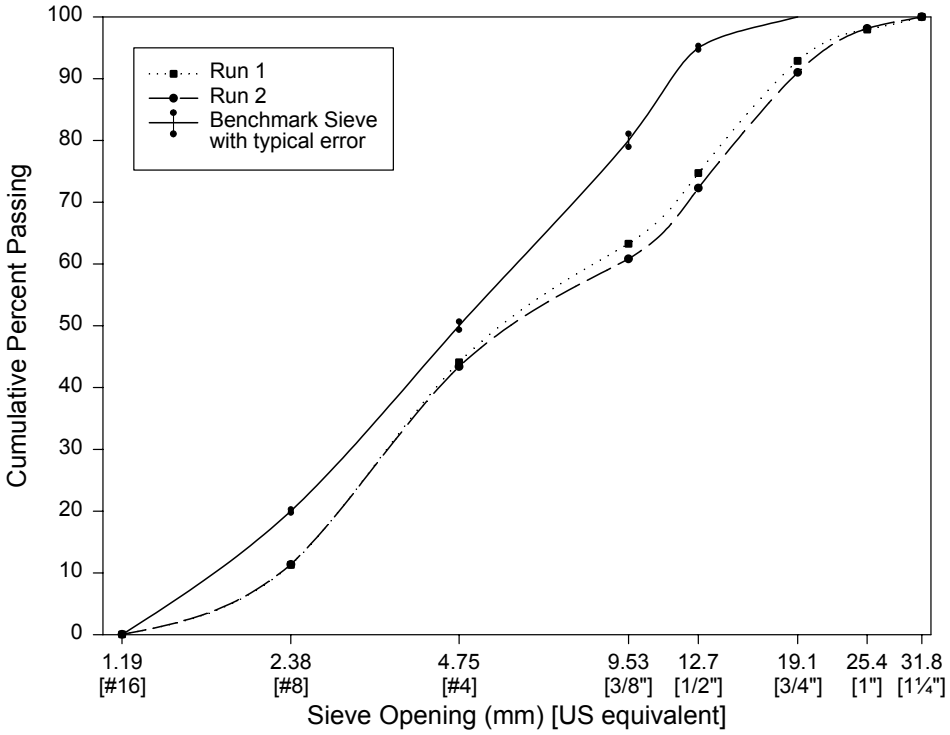

Sample: GA-F-STD	Test Machine: CPA

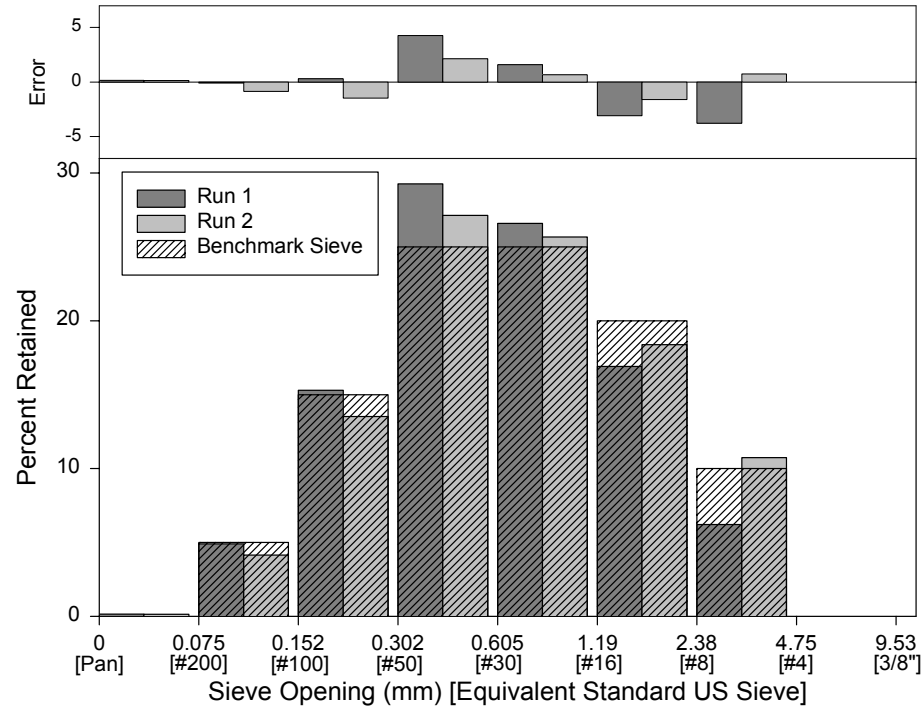

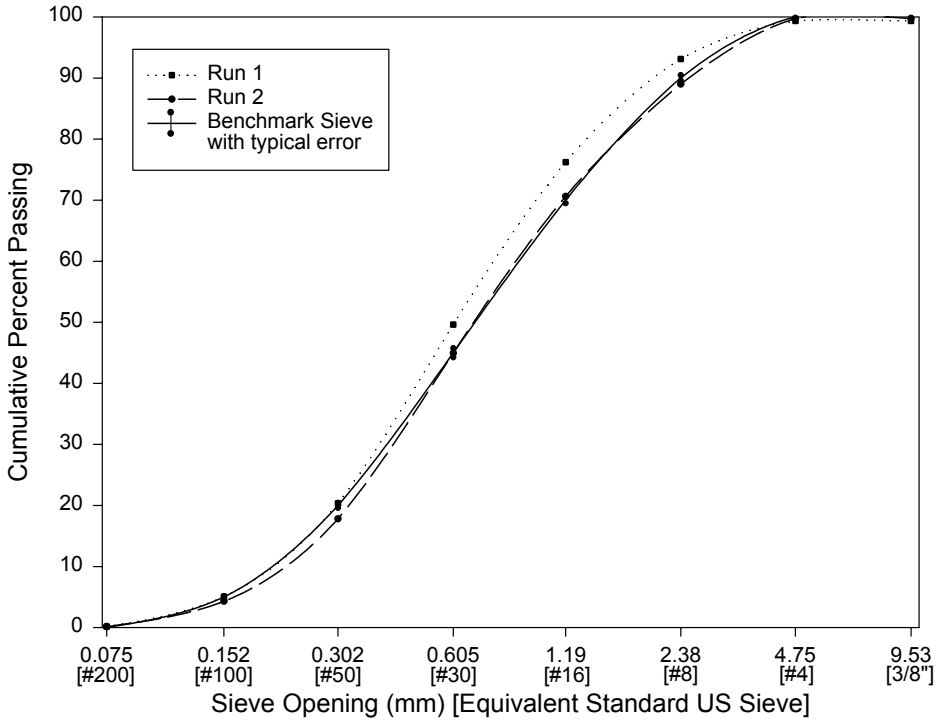

Sample: TX-F-STD	Test Machine: CPA

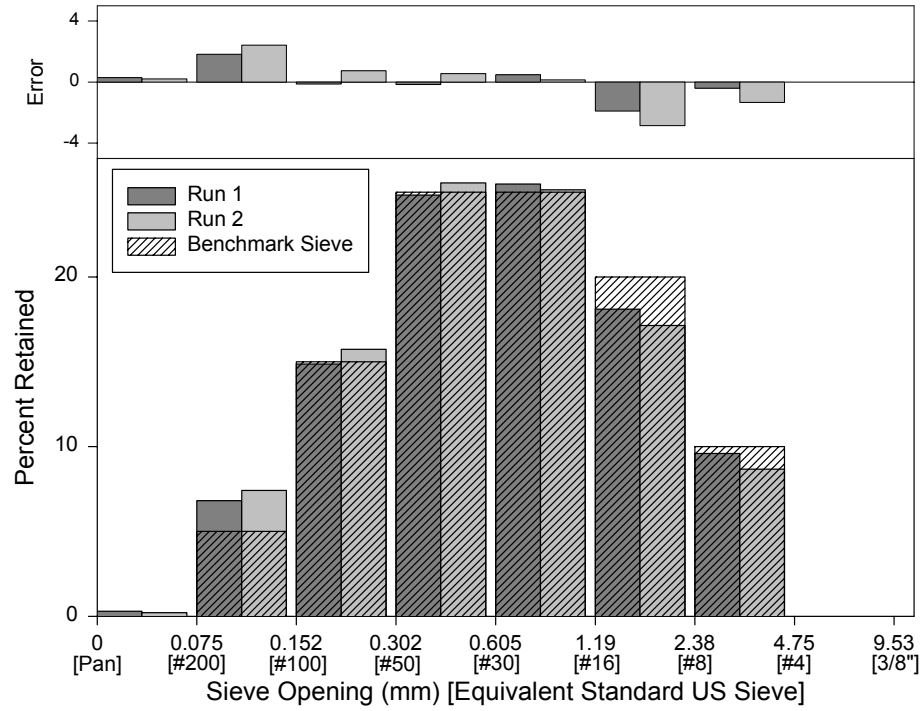

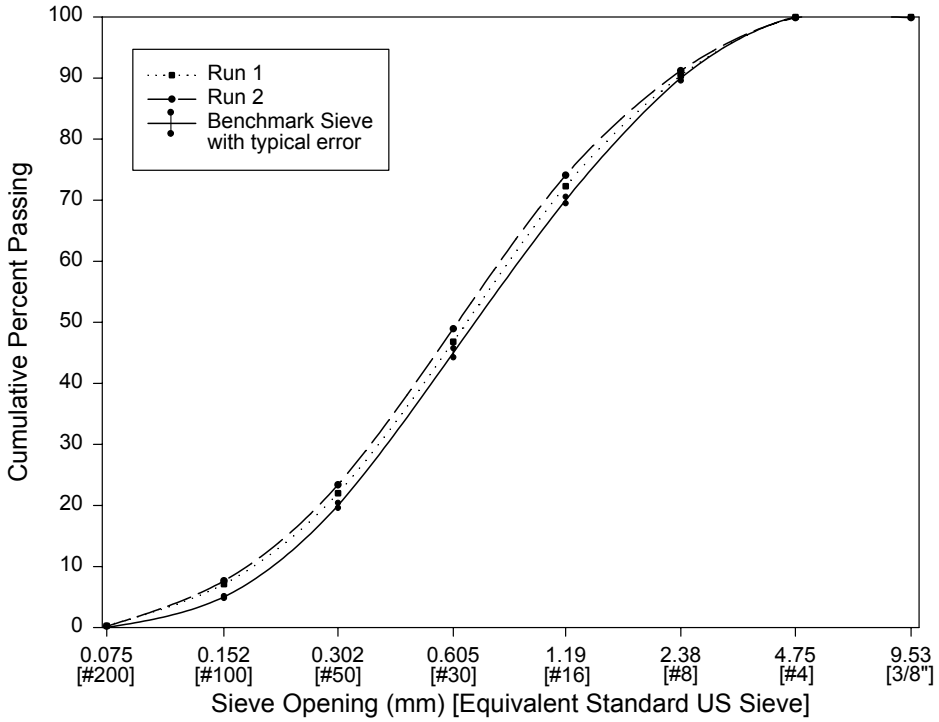

Sample: VA-F-STD Test Machine: CPA

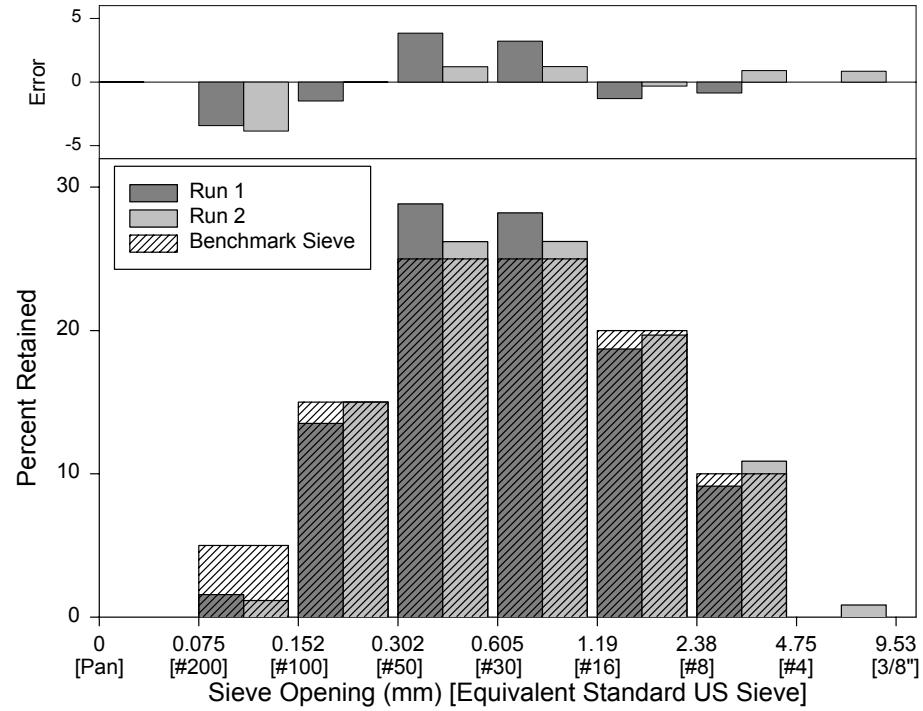

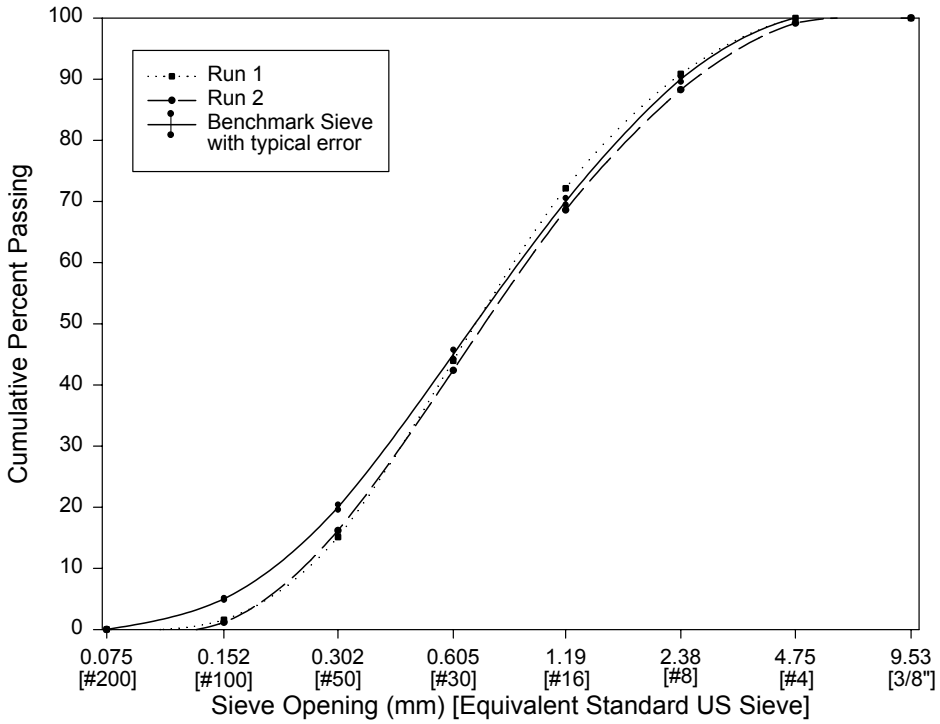

Sample: Texas C-LG	Test Machine: PSDA

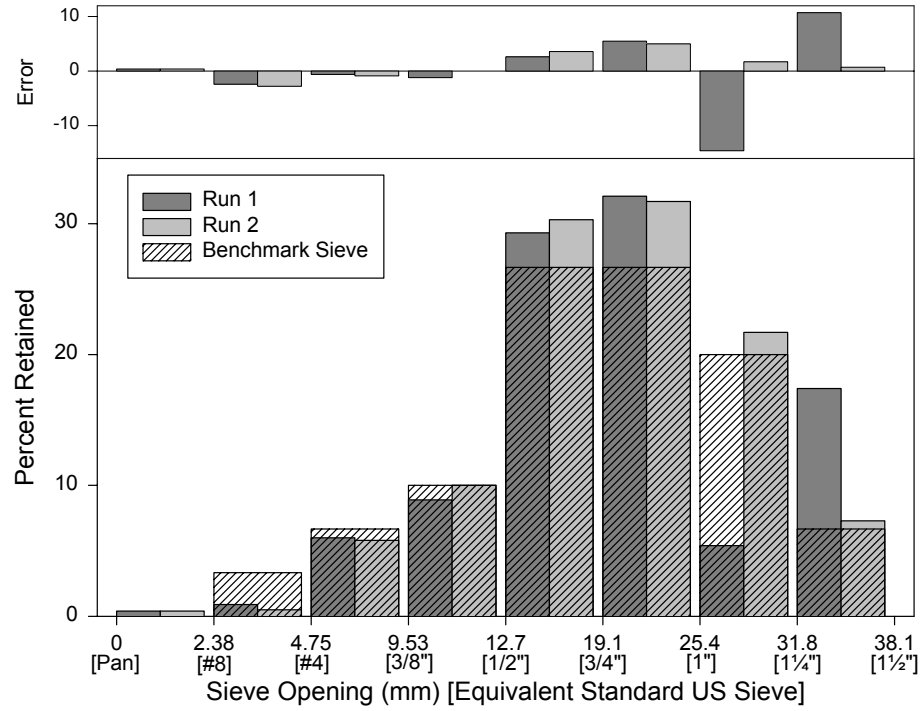

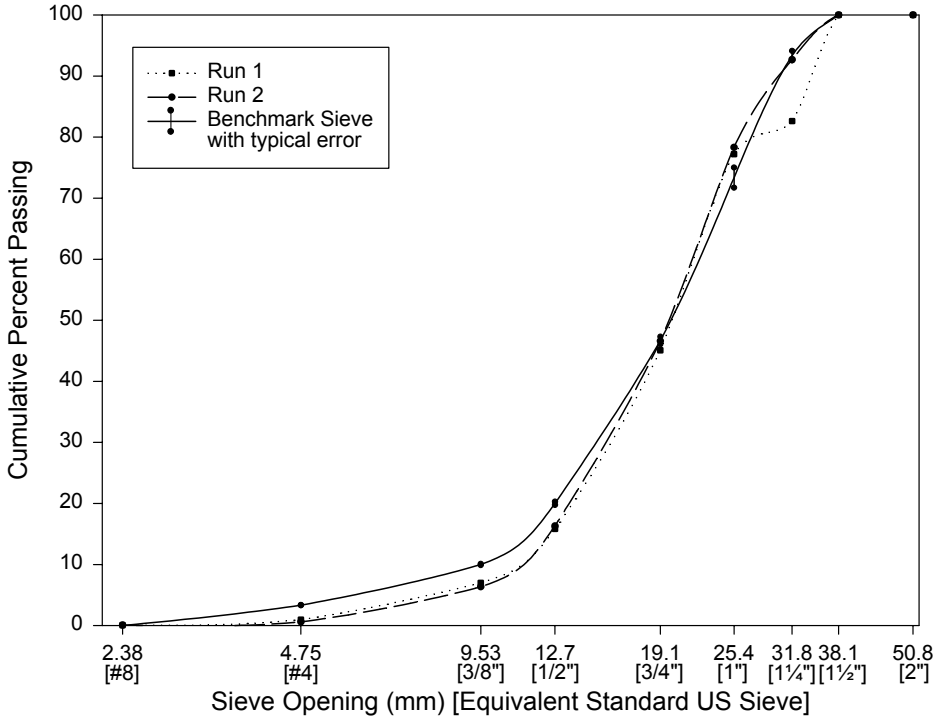

Sample: Texas C-RND	Test Machine: PSDA

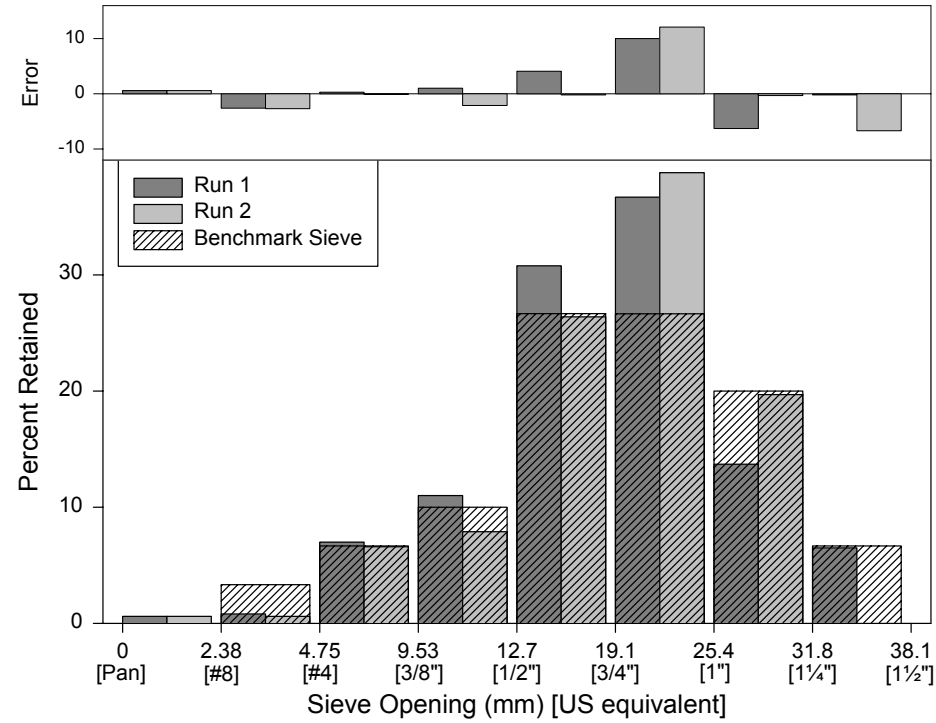

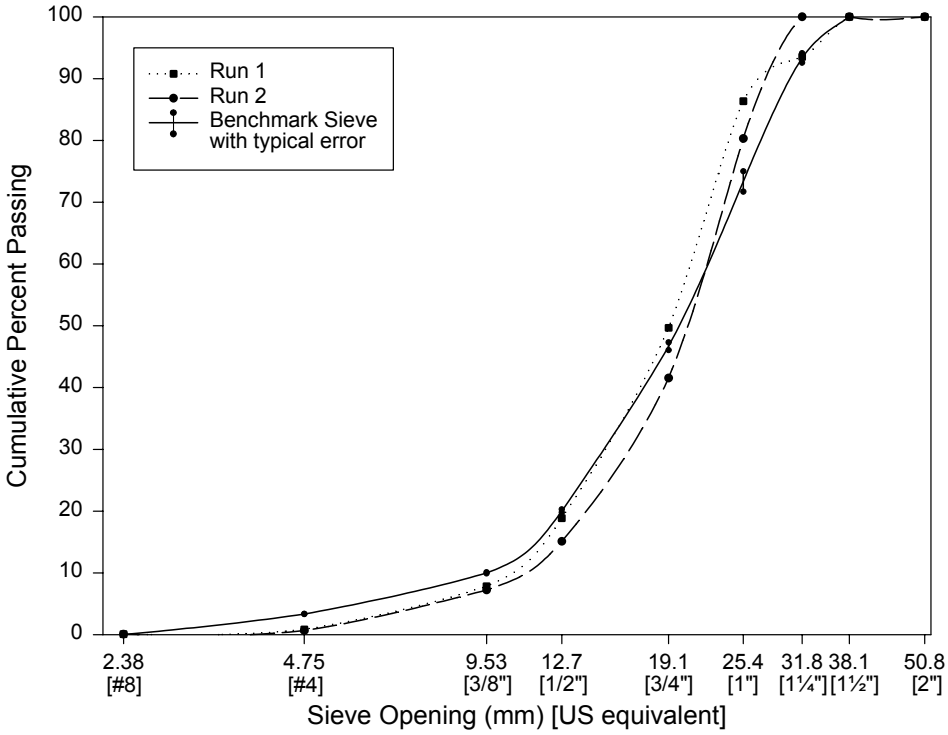

Sample: CA-C-SM	Test Machine: PSDA

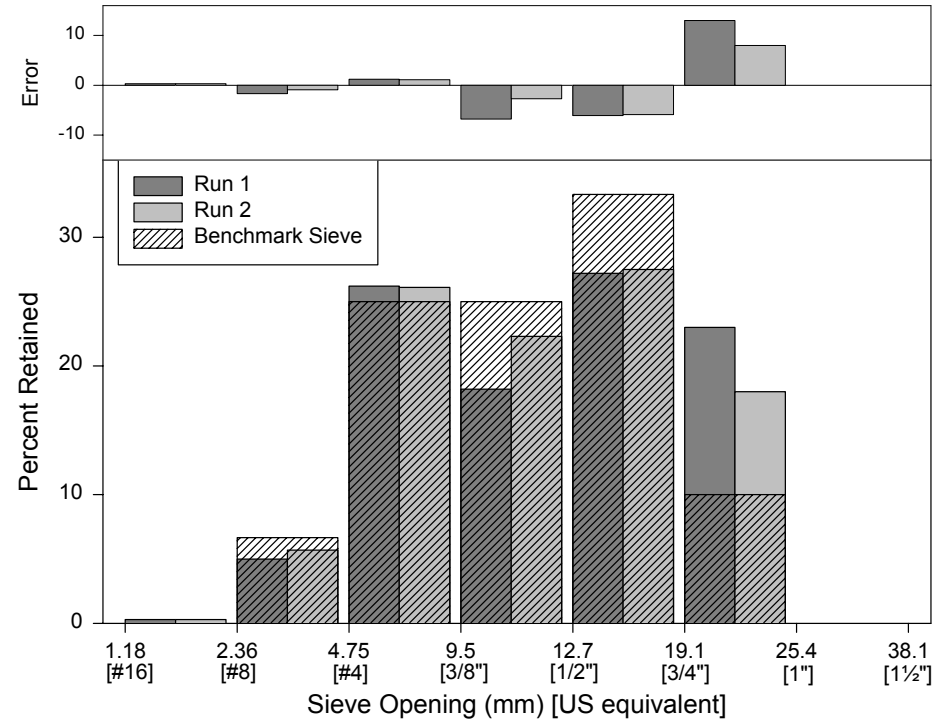

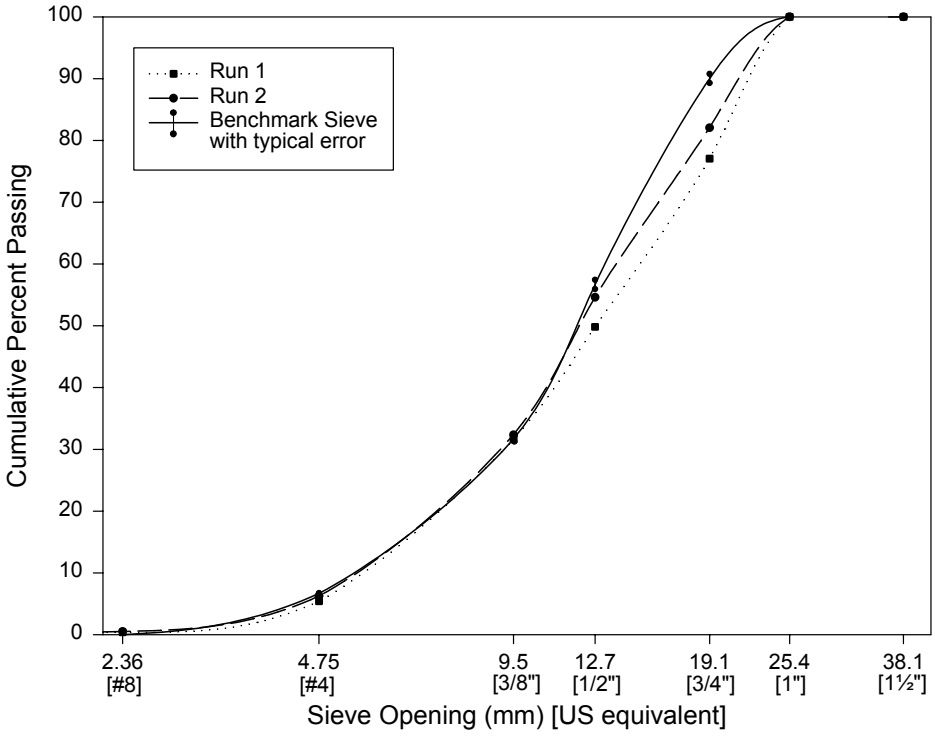

Sample: SD-C-SM	Test Machine: PSDA

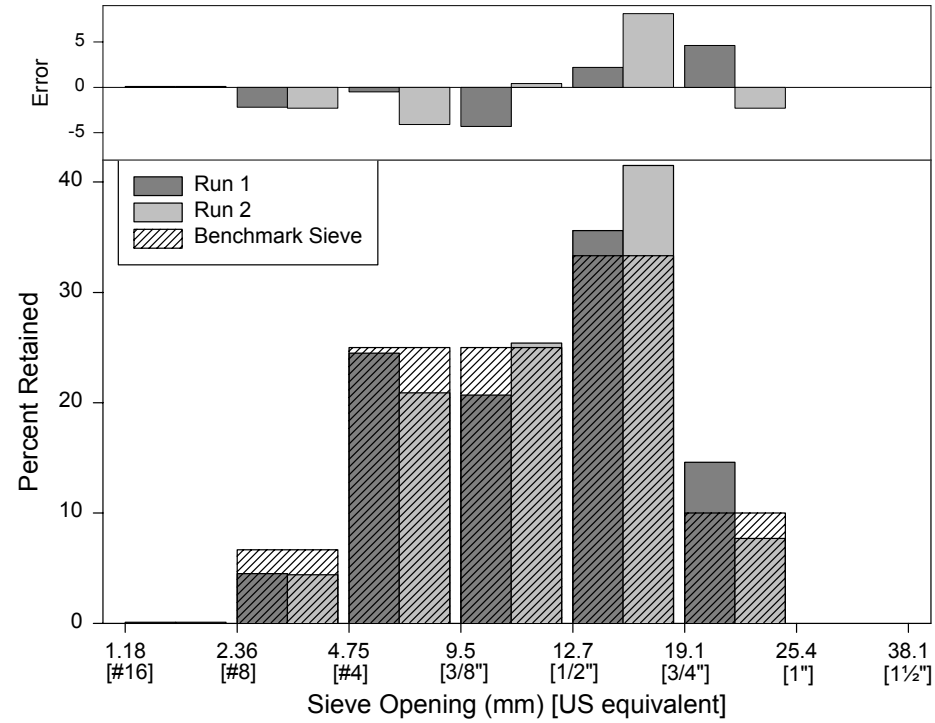

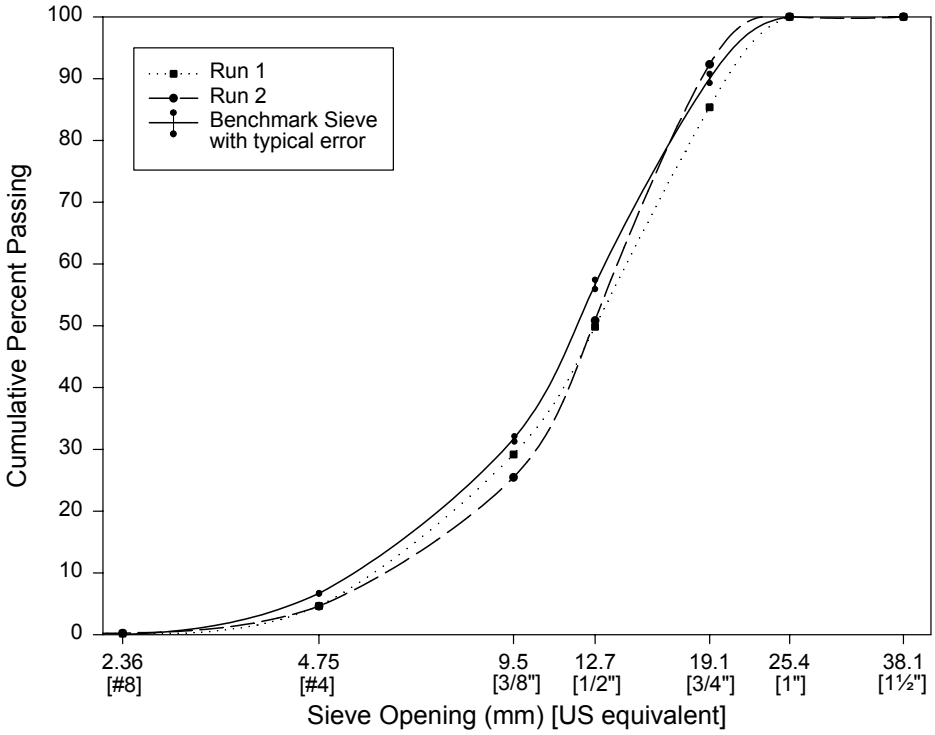

Sample: TX-C-SM	Test Machine: PSDA

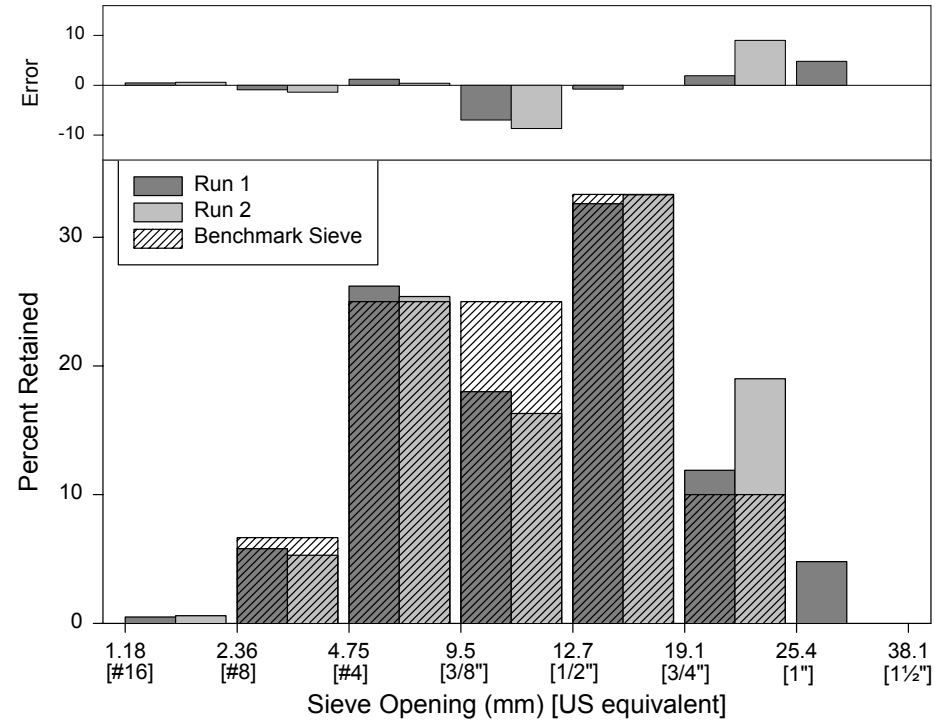

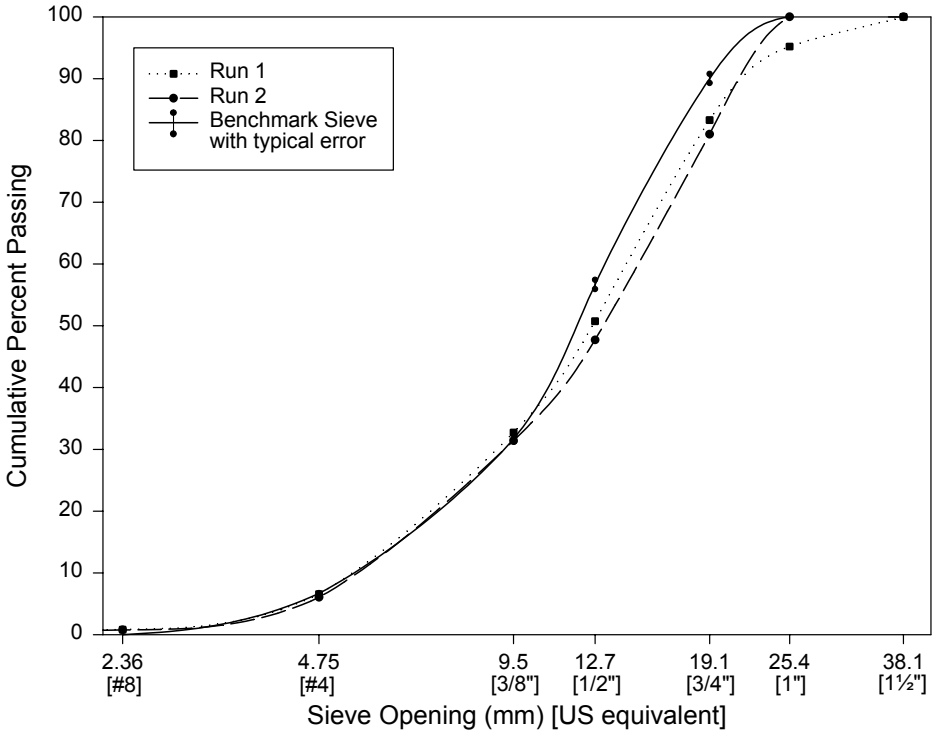

Sample: VA-C-SM	Test Machine: PSDA

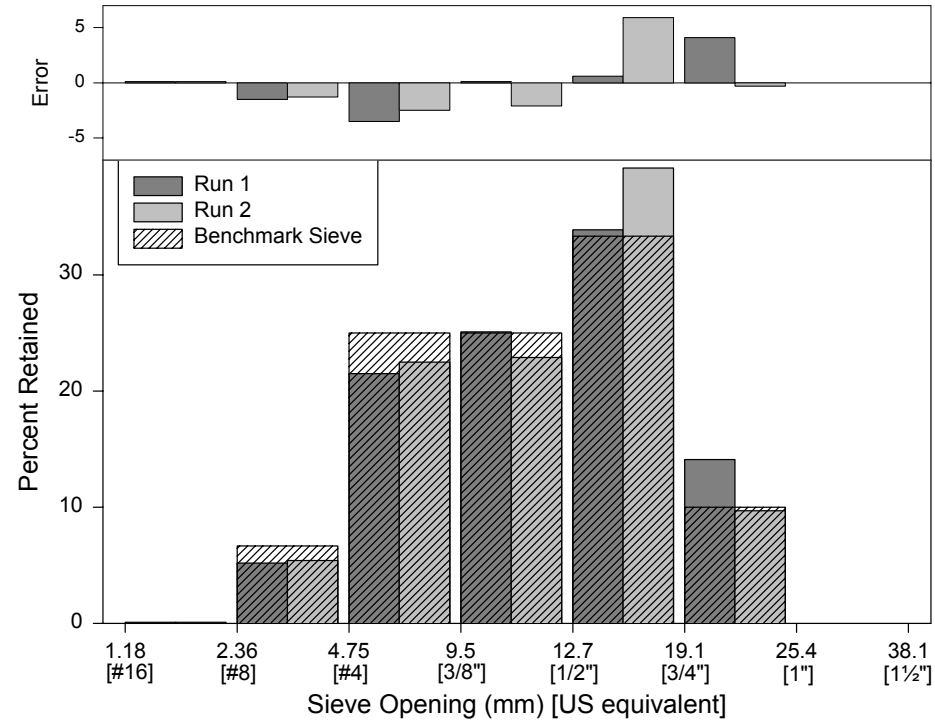

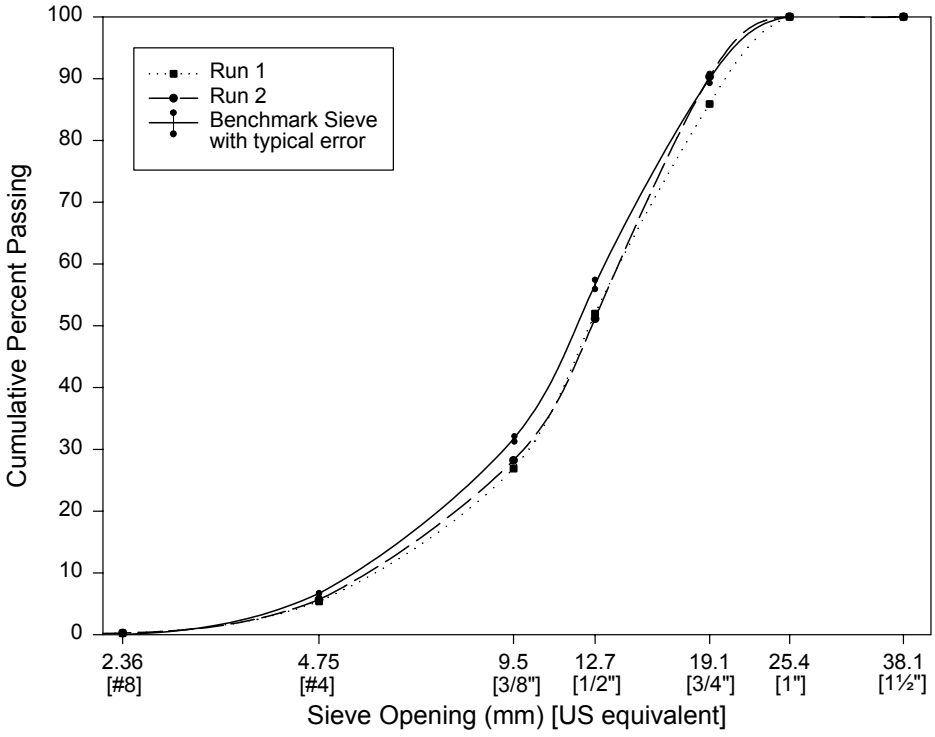

Sample: CA-C-STD	Test Machine: PSDA

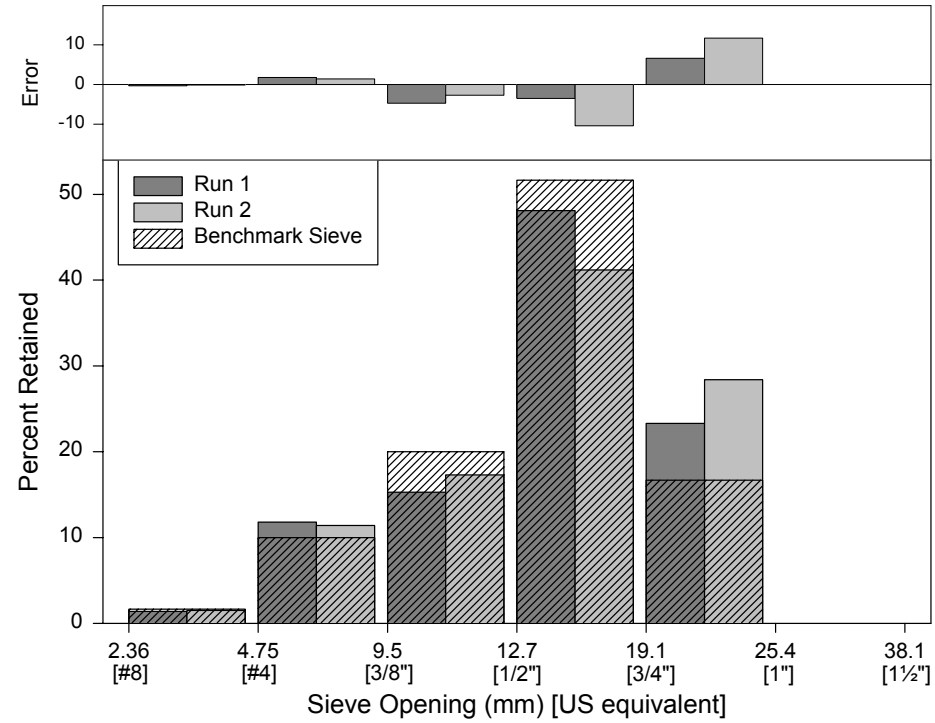

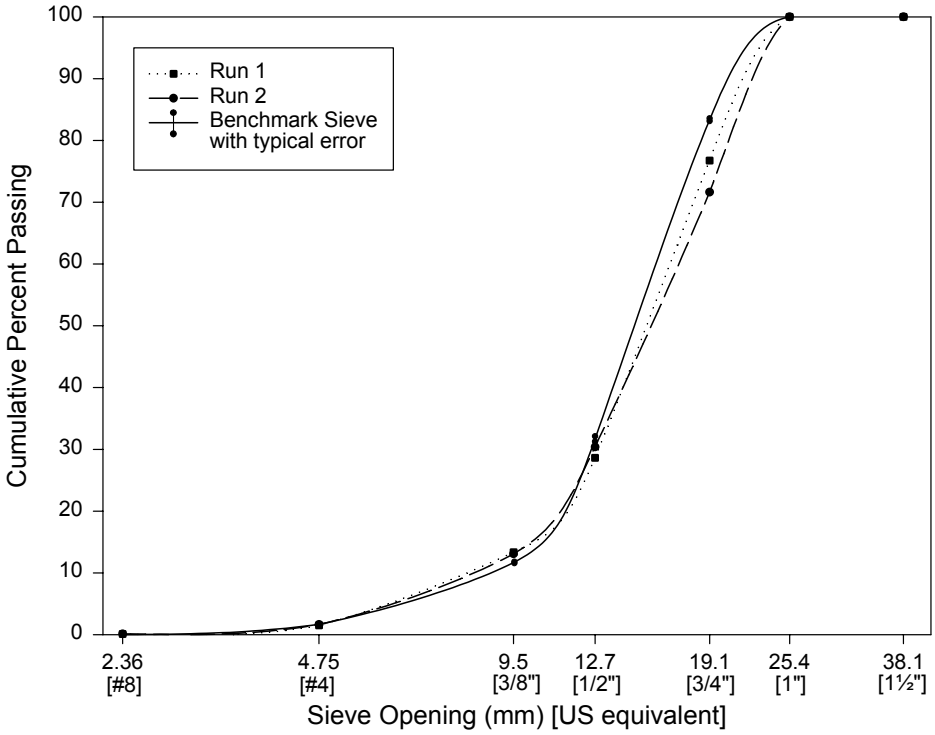

Sample: SD-C-STD	Test Machine: PSDA

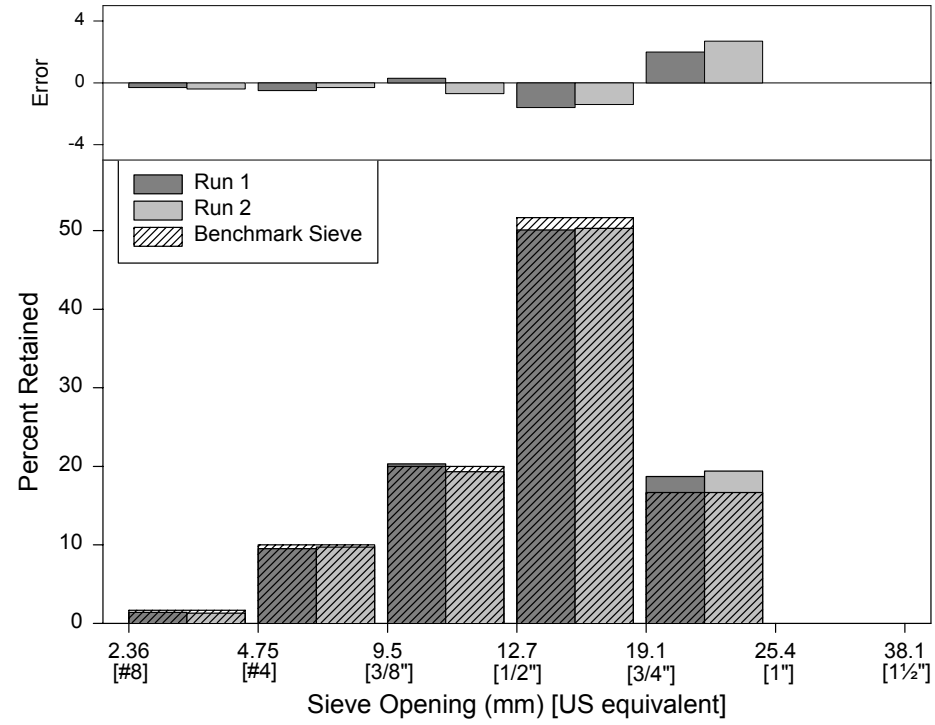

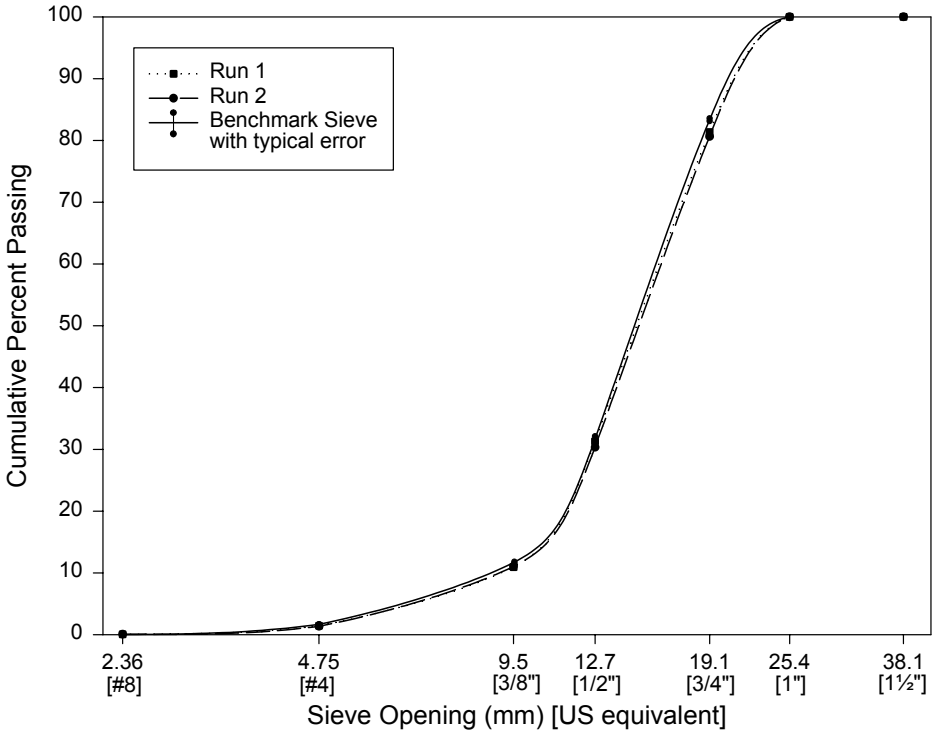

Sample: TX-C-STD	Test Machine: PSDA

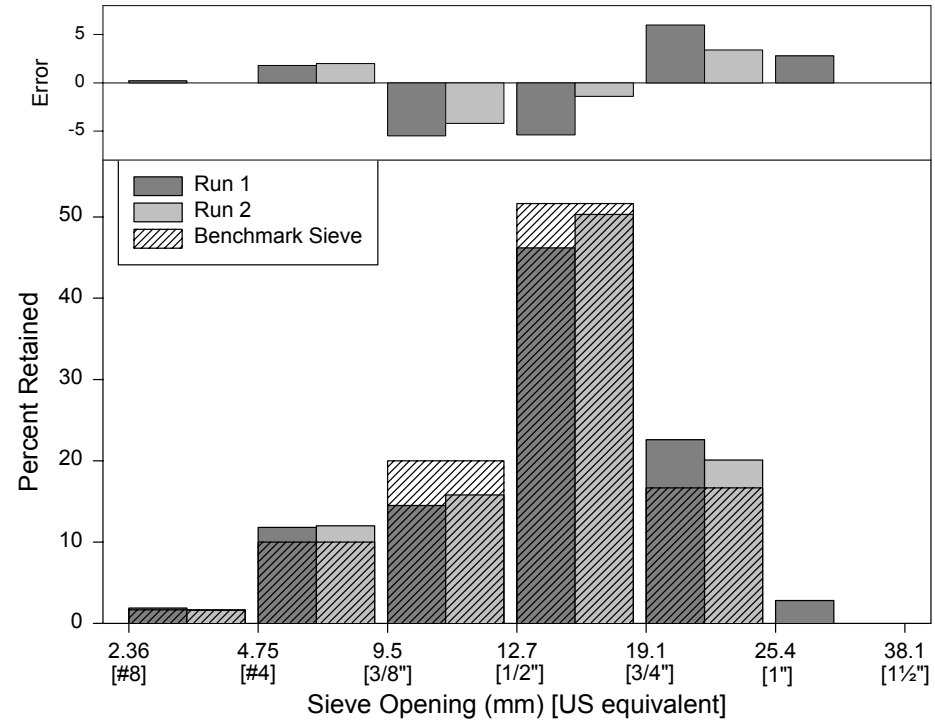

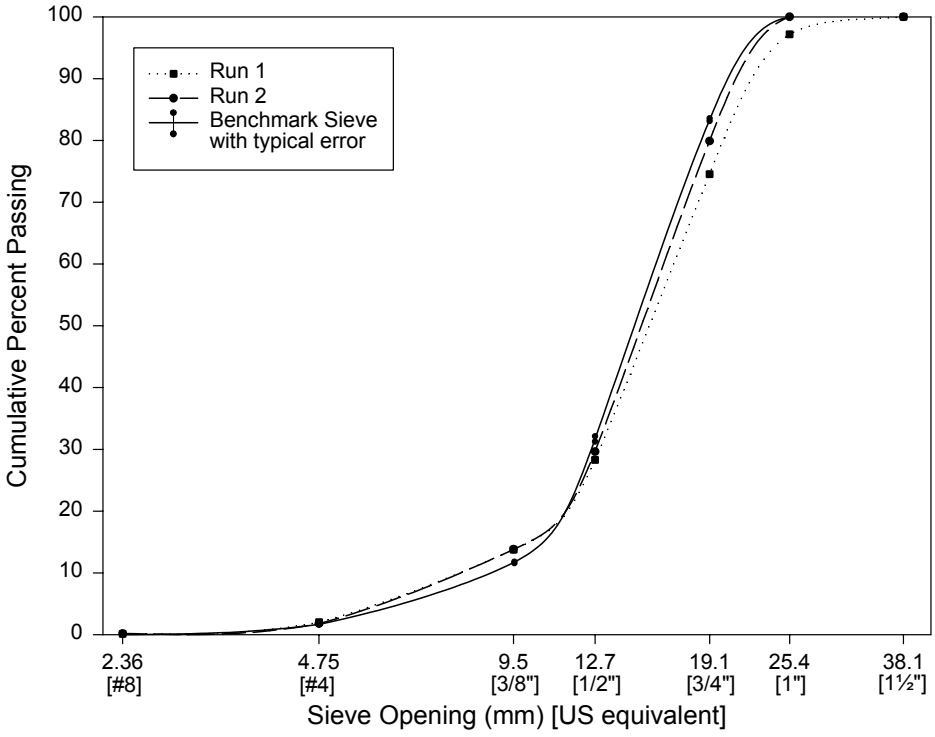

Sample: VA-C-STD	Test Machine: PSDA

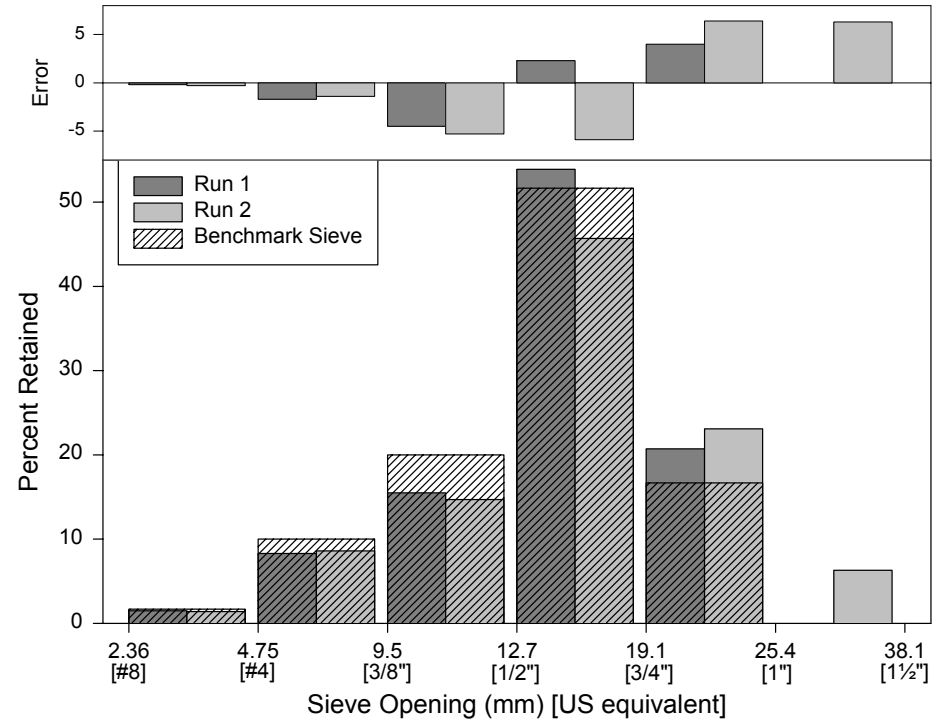

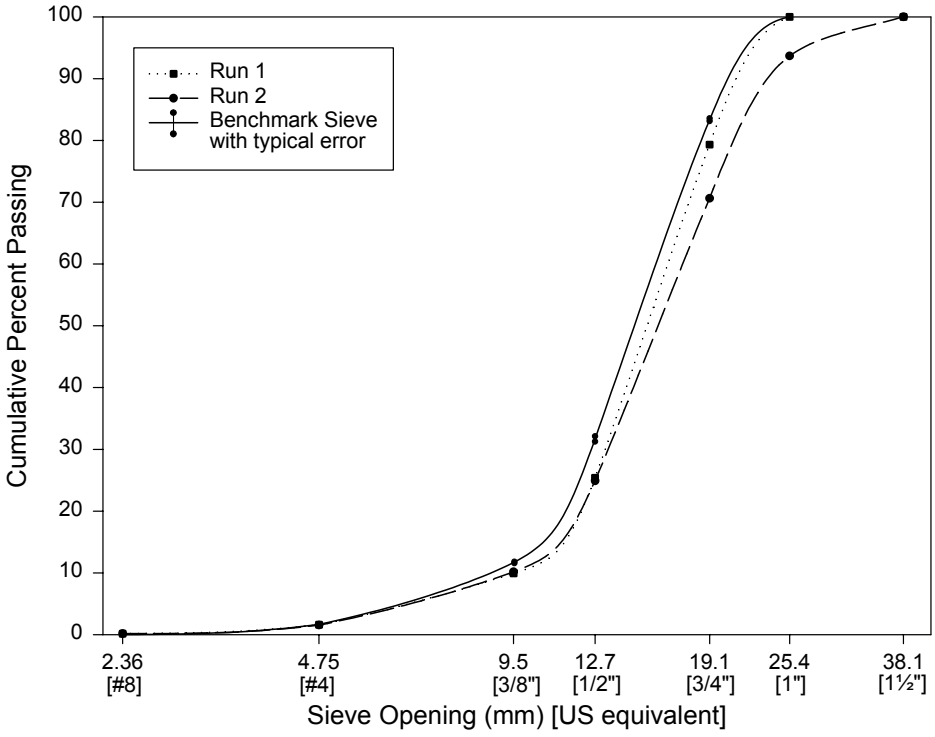

Sample: TX-F-FTC	Test Machine: PSDA

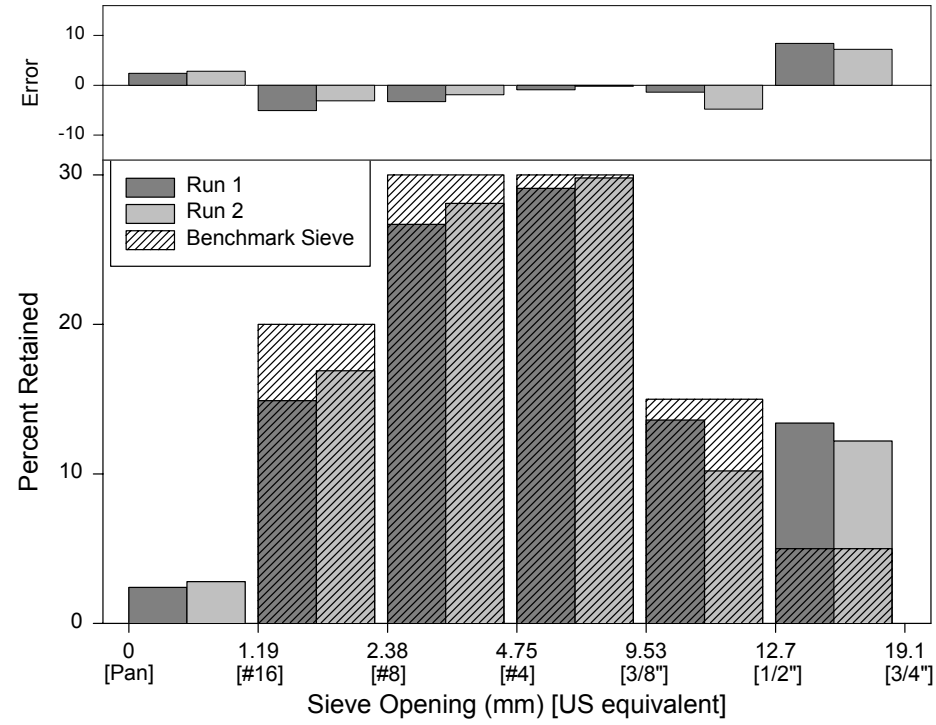

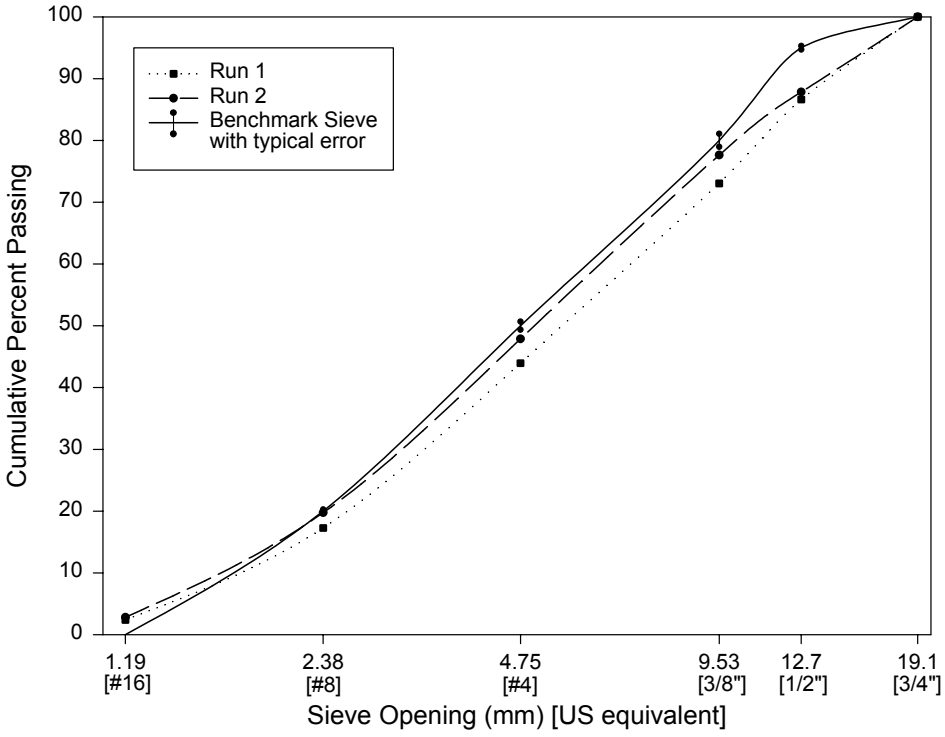

Sample: VA-F-FTC	Test Machine: PSDA

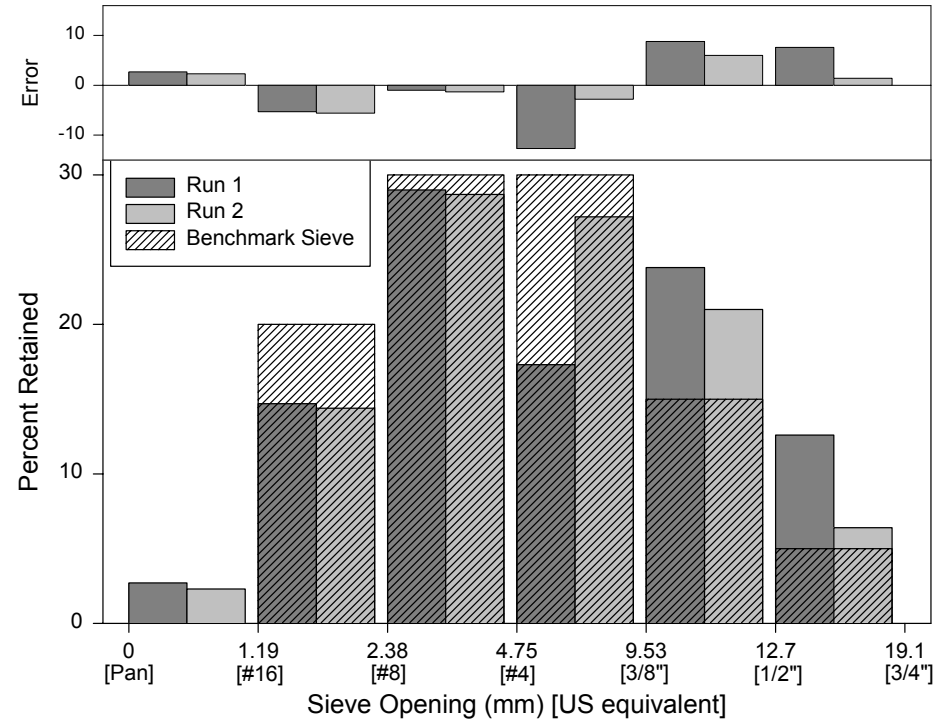

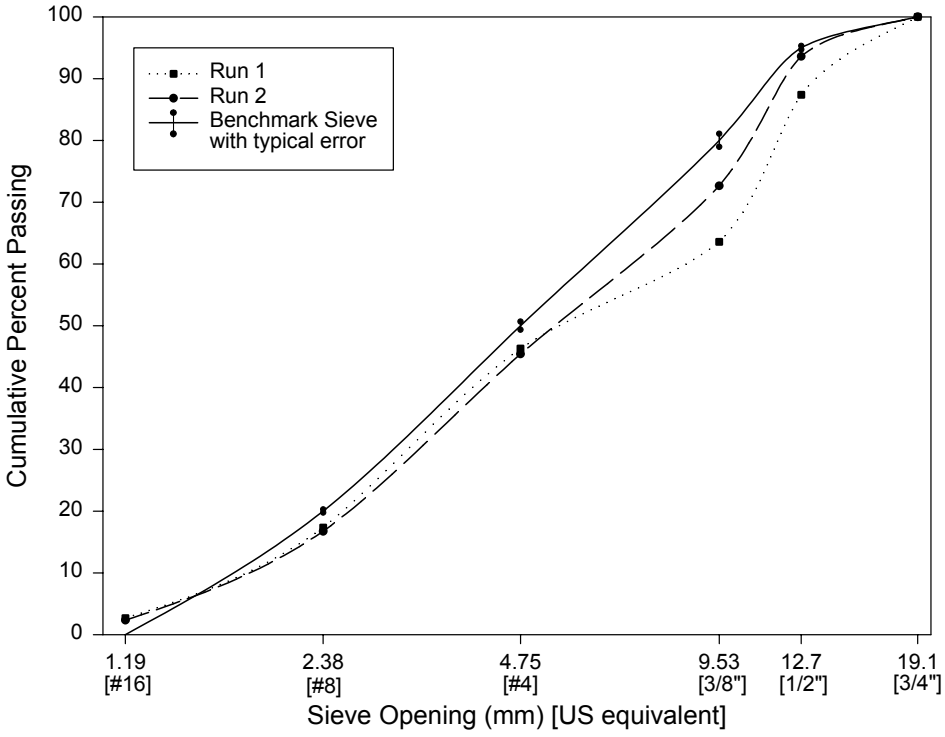

Sample: GA-F-STD	Test Machine: PSDA

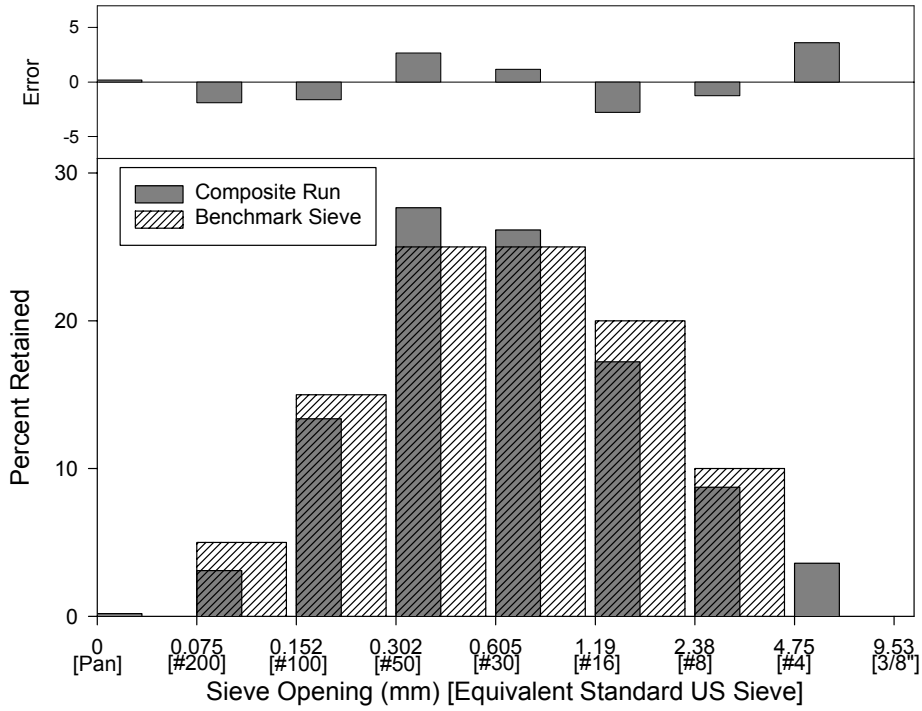

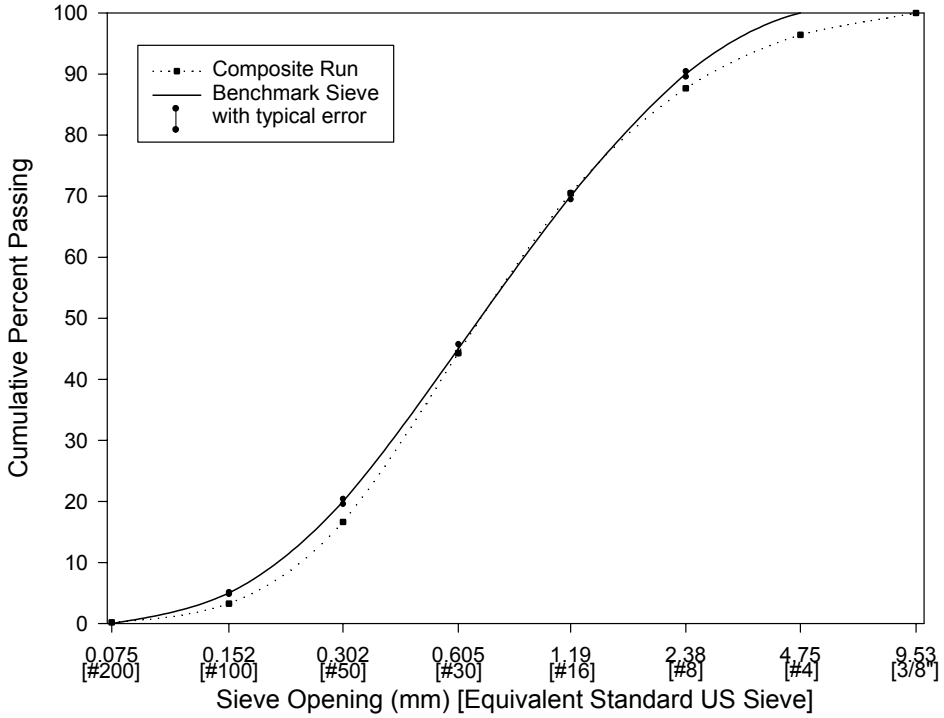

Sample: TX-F-STD Test Machine: PSDA

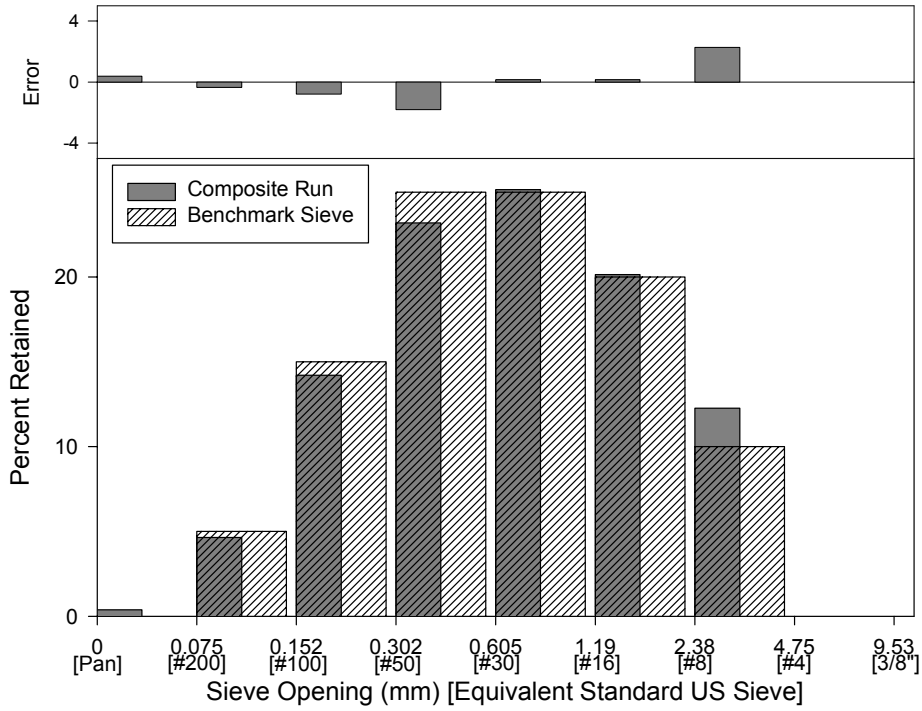

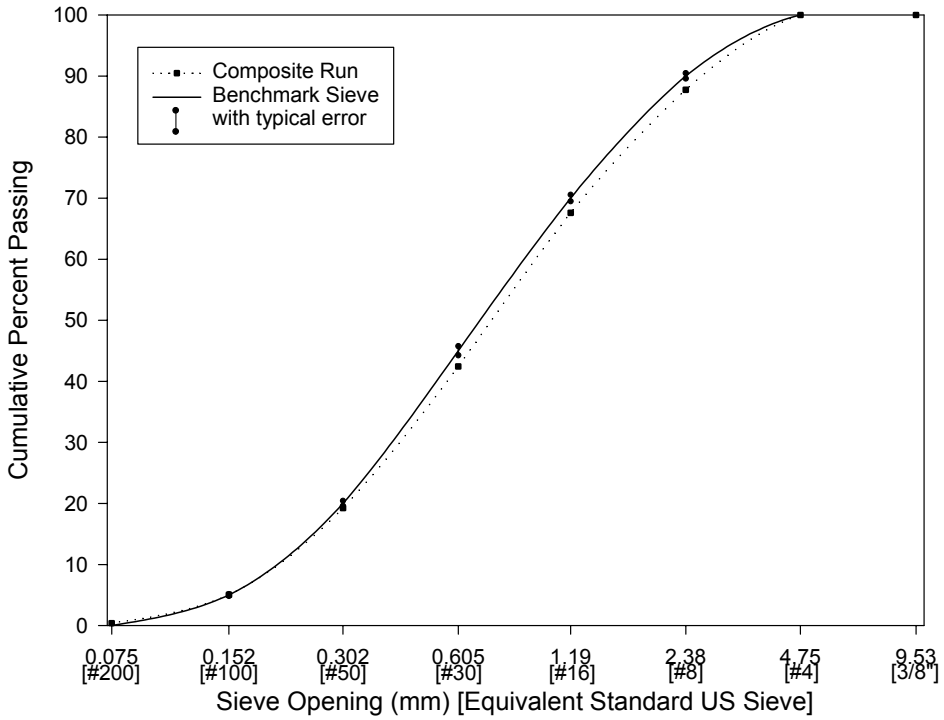

Sample: VA-F-STD	Test Machine: PSDA

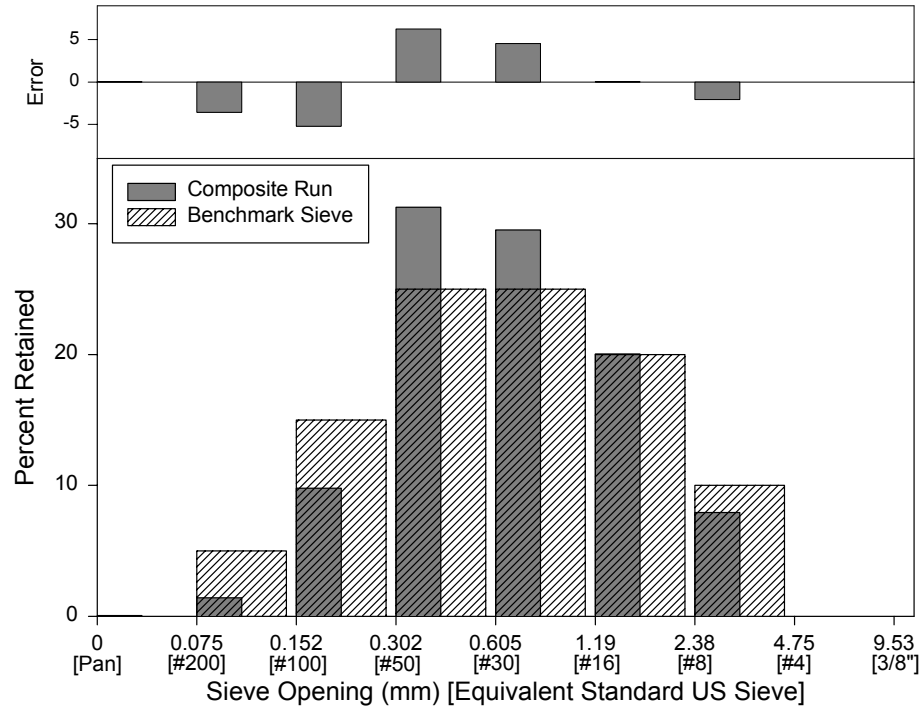

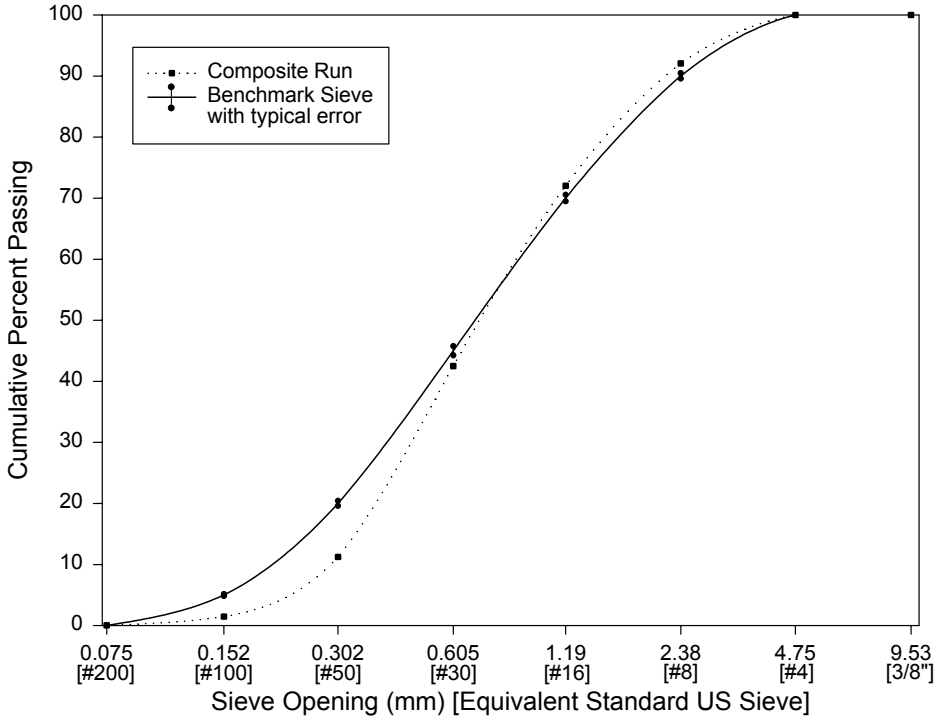

Bibliography

AASHTO - American Association of Highway and Transportation Officials (1995). "Size of Aggregate for Road and Bridge Construction." Designation: M 43-88. AASHTO, Washington, D.C.

Aljassar, A. H. (1993). "Automation of Aggregate Size-Gradation Analysis." PhD thesis, University of Waterloo, Ottawa, Canada

Ang, A. H-S., Tang, W.H. (1975). *Probability Concepts in Engineering Planning and Design: Volume 1 - Basic Principles*. Wiley, New York.

ASTM - American Society for Testing and Materials, (1995). "Standard Test Method for Flat Particles, Elongated Particles, or Flat and Elongated Particles in Coarse Aggregate, Designation" Designation: D 4791–95. *Annual Book of ASTM Standards*, ASTM, West Conshohocken, PA.

ASTM - American Society for Testing and Materials (1999). "Standard Test Method for Sieve Analysis of Fine and Coarse Aggregates." Designation: C136–96a, *Annual Book of ASTM Standards,* ASTM, West Conshohoken, PA.

Bourke, T.M., Lieber K.J., Browne I.B. (1997). "Non-Contact Measurement of Particulate Material Parameters Including Size and Shape." *Australian Journal of Mining,* February, pp. 54-56.

Broyles, D.A., Adel G.T., Rimmer H.W. (1994). "Rapid Shape Analysis of Crushed Stone by Computerized Image Processing", *Automation in the Aggregates Industry – The Key to Future Profitability, National Stone Association Automation Conf.*, Columbus, Ohio.

Brzezicki J.M., Kasperkiewicz J. (1999). "Automatic Image Analysis in Evaluation of Aggregate Shape." *Journal of Computing in Civil Engineering*, Vol. 13, No. 2, pp. 123-128.

Coakley, J.P., Syvitski, J.P.M. (1991). "SediGraph technique." *Principles, Methods, and Application of Particle Size Analysis*, Cambridge University Press, pp. 129-142.

Descantes, Y., Delalande, G., Mishellany, A. (2000) "Use of the VDG 40 Videograder as a Grading Control Device for French Highway Construction." *Proc., 8th Annual Symposium, ICAR,* Denver, Colorado, April.

Dumitru, I., Formosa, M., Browne, I., Lieber, K. (2000). "Measurement of Minus Three mm Particles." *Quarry (Australia, Malaysia & New Zealand)*, Vol. 10, No. 3, pp. 42-46.

Dillon, D. (2000). [Personal Communication]. Vice-President of Design, John B. Long Company, Knoxville, TN, July 20.

Fernlund, J. M. R. (1998). "The Effect of Particle Form on Sieve Analysis: A Test by Image Analysis." *Engineering Geology*, Vol. 50, No. 1-2, pp. 111-124.

Gilbert, Robert B. (2000). "Class Notes – Decision, Risk, & Reliability" The University of Texas, Austin, Texas, December 6.

Kemeny, J.M., Devgan, A., Hagaman, R.M., and Wu, X. (1993). "Analysis of rock Fragmentation Using Digital Image Processing." *Journal of Geotechnical Engineering*, Vol. 119, No. 7, pp. 1144-1160.

Kennedy, S.K., and Mazzullo, J. (1991). "Image Analysis Method of Grain Size Measurement." *Principles, Methods, and Application of Particle Size Analysis*, Cambridge University Press, pp. 76-87.

Kennedy, T.W., Huber, G.A., Harrigan, E.T., Cominsky, R. J., Hughes, C.S., Harold, V.Q., and Moulthrop, J.S. (1994). "Superior Performing Asphalt Pavements (Superpave): The Product of the SHRP Asphalt Research Program." SHRP-A-410, Strategic Highway Research Program, National Research Council, Washington, D.C.

Kim, H., Browne, C.R., Rauch, A.F., Haas, C.T. (2000). "Technical Aspects of Implementing Rapid Aggregate Gradation." *Proc., 8th Annual Symposium, ICAR,* Denver, Colorado, April.

Kim, H., Browne, C.R., Rauch, A.F., Haas, C.T. (2001). "A Prototype Laser Scanner for Characterizing Size and Shape Parameters in Aggregates." *Proc., 9th Annual Symposium, ICAR,* Austin, Texas, April.

Kuo, C.-Y., Frost, J.D., Lai, J.S., Wang, L. (1996). "Three-dimensional image Analysis of Aggregate Particles from Orthogonal Projections." *Emerging Technologies in Geotechnical Engineering, Transportation Research Record No. 1526*, Transportation Research Board, Washington, D.C.

Kuo, C.-Y., Rollings, R.S., Lynch, L.N. (1998). "Morphological Study of Coarse Aggregates Using Image Analysis." *Journal of Materials in Civil Engineering*, Vol. 10, No. 3, pp. 135-142.

Kuo, C.-Y., Freeman, R. B. (2000). "Imaging Indices for Quantification of Shape, Angularity, and Surface Texture of Aggregates." *79th Annual Meeting, Transportation Research Board*, Washington, D.C.

Laboratoire Central des Ponts et Chaussees (1994). "Aggregates: Granulometric Analysis, Flattening and Elongation Video-granulometer Test." French Norm P18-566 (Translation), Paris, France, May.

Maerz, N.H. (1999). "Online Fragmentation Analysis: Achievements in the Mining Industry." *Proc., 7th Annual Symposium, ICAR,* Austin, Texas, April.

Maerz, N.H., Zhou, W. (1999). "Flat and Elongated: Advances Using Digital Image Analysis." *Proc., 7th Annual Symposium, ICAR,* Austin, Texas, April.

Mora,C.F., Kwan,A.K.H., Chan,H.C. (1998). "Particle Size Distribution Analysis of Coarse Aggregate Using Digital Image Processing." Cement and Concrete Research, Vol. 28, No. 6, pp. 921-932.

Penumadu, D. (2001). [Personal Communication]. Associate Professor, Clarkson University, Potsdam, NY, January 23.

Prowell, B.D., Weingart, R. (1999). "Precision of Flat and Elongated Particle Tests: ASTM 4791 and VDG-40 Videograder." Transportation Research Board, *78th Annual Meeting,* Washington, D.C., January 10-14.

Rao, C., Tutumluer, E., (2000). "A New Image Analysis Approach for Determination of Volume of Aggregates." Transportation Research Board, *79th Annual Meeting,* Washington, D.C., January 9-13.

Rauch, A.F., Haas, C.T, Kim, H., Browne, C., (2000). "Rapid Test to Establish Grading of Unbound Aggregate Products." International Center for Aggregates Research (ICAR), Interim Report 503-1*,* Austin, TX, February.

Reckart, T. A. (2001). [Personal Communication]. CPA Product Manager, W. S. Tyler, Mentor, OH, January 18.

Split Engineering (2001). http://www.spliteng.com/, accessed February 7.

Strickland, M. L. (2000). [Personal Communication]. OptiSizer Product Manager, Micromeritics Corporation, Norcross, GA, July 10.

Tyler, W.S. (2001). "Particle Size and Shape Analyzers (CPA)", Product Brochure, Mentor, OH.

WipWare Inc. (2001). http://wipware.com/, accessed February 14.